UAB
Universitat Autònoma de Barcelona

FUNCTIONAL EVOLUTION AND REGULATION OF AQUAPORIN TRAFFICKING IN MARINE FISH OOCYTES

Alba Ferré García

Ph.D. Thesis in aquaculture

FUNCTIONAL EVOLUTION AND REGULATION OF AQUAPORIN TRAFFICKING IN MARINE FISH OOCYTES

Alba Ferré García

Directors: Dr. Joan Cerdà Luque

Dr. François Chauvigné

Tutor: Dra. Nerea Roher Armentia

Departments: Animal Biology, Plant Biology and Ecology; Cellular Biology, Physiology and Immunology; Animal and food Science

Faculty of Biosciences

Universitat Autónoma de Barcelona

Universitat de Barcelona

2024

FUNCTIONAL EVOLUTION AND REGULATION OF AQUAPORIN TRAFFICKING IN MARINE FISH OOCYTES

Memory presented by:

Alba Ferré García

For the degree of Doctor by the Universitat Autónoma de Barcelona and Universitat de Barcelona

Thesis supervised by Dr. Joan Cerdà Luque from *Institut de Recerca i Tecnologia Agroalimentàries* (IRTA), and Dr. François Chauvigné from *Consejo Superior de Investigaciones Científicas* (CSIC)

Barcelona, 2024

Per a tu, Maria.

“The beautiful thing about learning is
nobody can take it away from you”
-B.B. King

“Les coses importants
són les que no ho semblen”
-Mercè Rodoreda

Table of Contents

Acknowledgements

Esto se acaba, así que me gustaría agradecer a diferentes personas y/o entidades que han ayudado, apoyado y hecho posible cerrar este gran capítulo.

Primer de tot, agrair al Dr. Joan Cerdà, y donar-me la oportunitat de realitzar la tesis doctoral sota la teva supervisió. Gràcies per la teva passió y per fer-me créixer.

Deuxièmement et non moins important, Dr. François Chauvigné, merci beaucoup pour tant de choses. Merci de votre encadrement, d'être toujours prêt à aider et de votre compréhension. Merci pour tous ces fous rires et ces *afterworks*. Ceci est votre deuxième thèse.

To Dr. Roderick Nigel Finn, thank you very much for all your work, your contribution, your patience. Special thanks to you, Tanja and Oskar for opening the doors of your house and making me feel like one of the family.

A la Dra. Nerea Roher, per tutoritzar-me la tesis i estar sempre disponible per contestar les mil preguntes. Moltes gràcies.

Al Departament de Biologia Animal, Biologia Vegetal i Ecologia de la UAB, especialment al coordinador, el Dr. Lluís Tort, i a la María José Calejo, gràcies per facilitar-me tota la informació demanada.

To University of Bergen, Department of Biology at Bergen High Technology Center, and to Matre Research Station at Institute of Marine Research, for allowing me to be part of the research, and for using your facilities, *takk skal du ha*. Thanks to all the people who helped me both in the laboratory and outside of it, especially to Dr. Ozlem Yilmaz to make the stay more easy, *teşekkür ederim*.

Thanks to Institute of Oceanology Polish Academy of Sciences, at Department of Genetics and Marine Biotechnology, to Dr. Ewa Kulczykowska for allowing me to be part of the research, and for using your facilities. To lab partners Dr. Hanna Kalamarz-Kubiak, Dr. Ewa

Sokołowska, Dr. Konrad Pomianowski and obviously, Dr. Magdalena Gozdowska, *dziękuję za traktowanie mnie jak jeszcze jednego w laboratorium i poza nim*.

Y finalmente, para todos aquellos amigos que han formado parte de esto.

A la Dra. Cinta Zapater, a la Dra. Mónica Boj, al Dr. Marc Català, a la Dra. Judith Ollé, a la Dra. Júlia Castro i a la Carla Ducat, per tota la ajuda oferta, per tots els riures, per tots els plors, per totes les cerveses, per tots el sopar... Tots heu estat un gran suport, mil gràcies.

Al Dr. Víctor Sánchez porque cada vez que necesitaba que alguien me recordara el porqué estaba haciendo un doctorado, ahí estabas. Muchísimas gracias por todo el apoyo durante todos estos años, y por los que quedan.

A la futura Dra. Carla Gilabert (no tinc cap dubte) per tot l'amor que m'has donat, per totes les trucades, per haver-te creuat en la meva vida... gràcies.

A todos esos amigos pesados que han estado preguntado, "¿Cómo va la tesis?", Vane, Mireia, Laia, Taty, Jordi, Molina, gracias por seguir estando.

A mis padres, Esther y Javi, por darme todo el apoyo del mundo para cumplir mis sueños. Os quiero.

En especial a Carlos, gracias por aguantarme y acompañarme en esta locura. Te quiero.

Prologue

This thesis was carried out at the Group of Comparative Molecular Physiology of the Institut de Recerca i Tecnologia Agroalimentàries (IRTA) in the Institute of Biotechnology and Biomedicine (IBB) from Autonomous University of Barcelona (UAB), and supervised by Dr. Joan Cerdà Luque and Dr. François Chauvigné, during the period 2019 to 2024. The objective of this thesis was to study the molecular mechanisms involved in the regulation of the intracellular trafficking of the teleost specific aquaporins (Aqp1aa, Aqp1ab1 and Aqp1ab2) in oocytes of marine teleosts. These mechanisms are fundamental to control the function of the channels, and therefore knowing these mechanisms is essential to understand the molecular basis of the viability of marine fish gametes under aquaculture conditions. The results of the thesis uncover for the first time the major structural domains and binding proteins involved in the control of Aqp1aa, Aqp1ab1 and Aqp1ab2 trafficking in oocytes, as well as the endocrine regulation of these processes.

The thesis presented is structured in three chapters, corresponding to three scientific papers:

CHAPTER I: Ferré A, Chauvigné F, Vlasova A, Norberg B, Bargelloni L, Guigó R, Finn RN, Cerdà J. 2023. **Functional evolution of clustered aquaporin genes reveals insights into the oceanic success of teleost eggs.** *Molecular Biology and Evolution*. 40(4):msad071. doi: 10.1093/molbev/msad071.

CHAPTER II: Ferré A, Chauvigné F, Gozdowska M, Kulczykowska E, Finn RN, Cerdà J. 2023. **Neurohypophysial and paracrine vasopressinergic signaling regulates aquaporin trafficking to hydrate marine teleost oocytes.** *Frontiers in Endocrinology (Lausanne)*. 14:1222724. doi: 10.3389/fendo.2023.1222724.

CHAPTER III: Ferré A, Chauvigné F, Zapater C, Finn RN, Cerdà J. 2023. **Aquaporin splice variation differentially modulates channel function during marine teleost egg hydration.** *PLoS ONE*. 18(11):e0294814. doi: 10.1371/journal.pone.0294814.

In addition, during the completion of this thesis, an additional scientific article has been published, Chauvigné F, Ferré A, Cerdà J. 2021. The Xenopus Oocyte as an Expression System for Functional Analyses of Fish Aquaporins. *Methods in Molecular Biology*.

2218:11-28. doi: 10.1007/978-1-0716-0970-5_2, and the results have been presented in different international scientific meetings, such as the 11th International Congress of Andrology (Copenhagen, Denmark, May 2017), the 6th International Workshop on the biology of fish gametes, (Ceske Budejovice, Czech Republic, September 2017; the participation in this conference resulted in a prize for the best poster presentation), and the XIIIth International Symposium on Spermatology (Stockholm, Sweden, May 2018).

During the thesis two shorts research stays of two month each were carried out in the University of Bergen (Norway), under the supervision of Dr. Roderick Nigel Finn, and in the Institute of Oceanology Polish Academy of Sciences (Poland) under the supervision of Dr. Ewa Kulczykowska.

The thesis project was funded by the Spanish *Ministerio de Economía Industria y Competitividad* (MINECO), through a predoctoral fellowship (BES-2014-068745), and grants for predoctoral mobility for short stays in R&D centres (EBB-I-17-12047 and EBB-I-18-12896).

Abbreviation

17,20β-P, 17α,20β-dihydroxy-4- pregnen-3-one
17-P, 17α-hydroxyprogesterone
Ab, antibody
ANOVA, Analysis of variance
ANS, anisomycin
AP, alkaline phosphatase
AQP, aquaporin
ar/R, aromatic residue/arginine constriction region
AVP/Avp, arginine vasopressin
Avpr, arginine vasopressin receptor
Bb, Balbiani body
BF, bright field
Bim-II, bisindolylmaleimide II
BSA, bovine serum albumin
cAMP, cyclic adenosine monophosphate
Cbr1, 20β-hydroxysteroid dehydrogenase/carbonyl reductase-like
CDS, coding sequence
cGMP, cyclic guanine monophosphate
ChIP, chromatin immunoprecipitation
CHO, Chinese Hamster Ovary
Co-IP, co-immunoprecipitaiton
cRNA, complimentary ribonucleic acid
CT/Ct, carboxyl terminal peptide
Cyp17a2, cytochrome P450c17 polypeptide II
DAPI, 4',6-diamidino-2-phenylindole
DMEM, Dulbecco's Modified Eagle Medium
DMSO, dimethyl sulfoxide
dNTPs, deoxynucleotide triphosphates
E2, 17β-estradiol
ELISA, Enzyme-Linked ImmunoSorbent Assay
ER, endoplasmic reticulum
FAA, free amino acids
Fsh, follicle-stimulating hormone
FSK, forskolin
FW, freshwater
Glp, aquaglyceroporins
GnRHa, gonadotropin- releasing hormone analogs
Gs, G protein
GSCs, germline stem cells
Gsdf, gonadal soma-derived growth factor
GVBD, germinal vesicle breakdown
HA, human influenza hemagglutinin
HBSS, Hank's Balanced Salt Solution
HEK293T, human embryonic kidney cells 293T
HRP, horseradish peroxidase
IBMX, 3-Isobutyl-1-methylanxthine
Ig, immunoglobulin
Igf-I, insulin-like growth factor-I
IP, immunoprecipitation
ISH, *in situ* hybridization

LAMP-1, lysosomal-associated membrane protein 1
Lh, luteinizing hormone
LvH, lipovitellin heavy chain
LvL, lipovitellin light chain
MCF-7, human breast cancer cell line
MCMC, Markov chain Monte Carlo
MIP, major intrinsic protein
MPF, maturation-promoting factor
mPgr, membrane progestin receptors
mRNA, messenger RNA
mRNP, mRNA-protein
MS-222, Ethyl 3-aminobenzoate methanesulfonate salt
mya, millions years ago
NGS, normal goat serum
NPA, asparagine-proline-alanine motif
nt, nucleotides
Oxt, oxytocin
OXTR, oxitocin receptor
p38 MAPK, p38 mitogen-activated protein kinase
PBS, phosphate buffered saline
PBST, PBS-Tween
PCR, polymerase chain reaction
PDI, protein disulfide isomerase
P_f, coefficient of water osmotic permeability
PFA, paraformaldehyde
PGCs, primordial germ cells
nPgr, nuclear progestin receptor
Pi, inorganic phosphorus
PKA, protein kinase A
PKC, protein kinase C
PLC, phospholipase C
PM, plasma membrane
PMA, phorbol 12-myristate 13-acetate
polyA$^+$, polyadenylation
pp, posterior probability
RA, retinoic acid
RIPA, radioimmunoprecipitation assay
RNA, ribonucleic acid
ROS, reactive oxygen species
RPKM, reads per kilo base per million mapped reads
rps18, 18S ribosomal RNA
RT-PCR, reverse transcription-PCR
SDS, sodium dodecyl sulfate
SDS-PAGE, sodium dodecyl sulfate polyacrylamide gel electrophoresis
SEM, standard error of means
SW, seawater
TBS, tris buffered saline
TBST, TBS-Tween
TEA, tetraethylammonium
TM, total membrane
TMB, tetramethylbenzidine
TMDs, transmembrane domains
TNF, tumour necrosis factor
TPE, transposable element.
TSA1C, teleost-specific aquaporin-1 cluster
Tuba, α-tubulin
Vtg/Vgs, vitellogenins
WGA, wheat germ agglutinin
WGD, whole genome duplication

WGS, whole genome shotgun

Ywhaz-like (14-3-3ζ-like), Tyrosine 3-Monooxygenase/Tryptophan 5-Monooxygenase Activation Protein Zeta-like

ZP, zona pellucida

β-Gal, β-Galactosidase

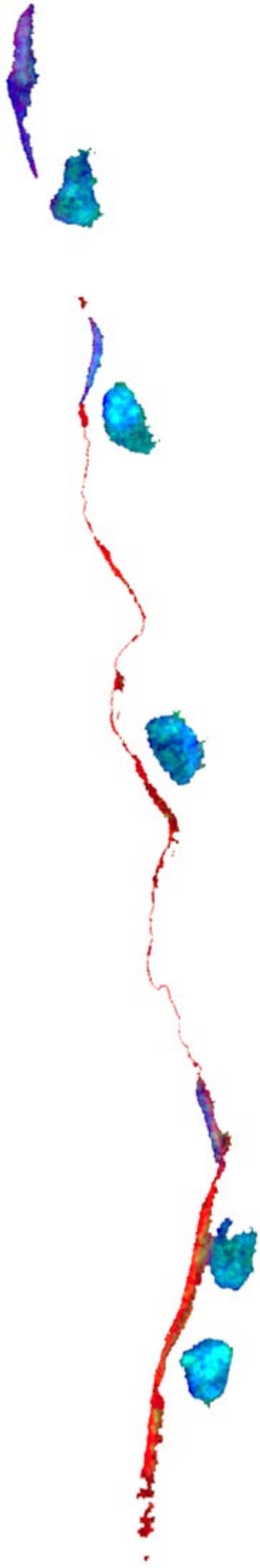

INTRODUCTION

The high demand for fish protein during the last years has made aquaculture one of the fastest growing industries on the planet (Froehlich *et al*., 2017). In addition to meet the food demand around the world, aquaculture production now outstrips the capture fisheries and has a positive impact on socioeconomic factors, and human health (Theuerkauf *et al*., 2019). However, the development of a sustainable aquaculture industry for fish, and particularly for marine species, still faces important bottlenecks, such as the availability of good quality fry, the establishment of new/emerging finfish species with high economical potential, the control of diseases, or the obtention of high flesh quality (Abdelrahman *et al*., 2017; Schrama *et al*., 2018). An essential aspect to solve some of these obstacles is the development of efficient methods to control the reproduction of cultured fish in order to obtain good quality eggs and larvae for the mass production of fry.

1.1. Reproduction and Egg Quality in Cultured Teleosts

The control of reproductive processes in fish is one of the most challenging aspects in aquaculture since the production of high-quality eggs (and sperm) from domesticated broodstock is a prerequisite for the sustainable expansion of aquaculture (Mylonas *et al*., 2017; de Siqueira-Silva *et al*., 2018; Yoshida, 2020). In captivity, the control of reproduction begins with the manipulation of the environment in order to provide the necessary conditions (photoperiod, temperature, and sometimes the spawning substrate) to stimulate the fish to undergo gametogenesis, maturation and spawning (Mylonas *et al*., 2017). However, in many commercially produced species, there are important reproductive dysfunctions, such as the failure to mature, ovulate or spawn the eggs (Mylonas *et al*., 2010), that hinder the efficient and reliable production of fertilized eggs.

To overcome these reproductive dysfunctions hormonal manipulations are usually employed. The hormones that are used include gonadotropins of mammalian origin, and gonadotropin-releasing hormone analogs (GnRHa), which are administered by injections or controlled-release delivery systems (Mylonas *et al*., 2010). Using biotechnology approaches, species-specific recombinant gonadotropins have been recently employed with promising results (Mazón *et al*., 2015; Chauvigné *et al*., 2017 and 2018). However, poor egg quality is a common limiting factor in many cultured species, particularly in marine fish, which hormone treatments cannot improve.

The quality of eggs includes a variety of biochemical and morphological features that ultimately condition the ability of the egg to be fertilized and develop into a normal embryo and larvae (Bobe *et al*., 2015). Different parameters, such as the egg diameter, morphology, yolk composition and the fertilization rates, have been used as quality markers (Lahnsteiner *et al*., 2009). However, the most used parameter to evaluate egg quality in cultured marine teleosts is the ability of eggs to float in seawater (egg buoyancy). This feature is acquired by the massive hydration of the oocyte during the formation of the egg in the ovary of females and is critical for the survival of early embryos (see below). Nevertheless, predictive molecular biomarkers determining egg quality, including the hydration process, remain to be identified (Yilmaz *et al*., 2017). These markers would be of great interest for the monitoring of the reproductive status of cultured populations, as well as for selective breeding programs. Therefore, it is essential to increase the basic knowledge on the physiological and molecular mechanisms involved in the formation of good quality eggs in fishes.

1.2. Teleost Oogenesis

The process of oogenesis in fish and other lower vertebrates starts when oogonia enter into meiosis to become primary oocytes, which are subsequently surrounded by somatic cells to form a follicle. Further growth of the follicle-enclosed oocyte mainly by the accumulation of yolk (vitellogenesis), its "maturation" (meiosis resumption) and hydration in marine species, and its further release from the enveloping layer of somatic cells (ovulation), results in the production of a fertilizable egg (Cerdà, 2018).

The physiological processes occurring during oogenesis are controlled by the pituitary gonadotropins, follicle-stimulating (Fsh) and luteinizing (Lh) hormones, which act in the ovarian follicle through their cognate receptors on the surface of the follicle cells (Levavi-Sivan *et al*., 2010). The general established model is that Fsh is the major regulator of oocyte growth through the stimulation of 17β-estradiol (E2) production by the follicular granulosa cells, which in turn triggers hepatic vitellogenin synthesis and release, and subsequent uptake by the oocyte (see below). In contrast, Lh is the hormone signal that activates the synthesis of the maturation-inducing progestins, such as the 17α,20β-dihydroxy-4- pregnen-3-one (17,20βP), which activate the maturation-promoting factor (MPF) in the oocyte to resume

meiosis (Nagahama and Yamashita, 2008). Lh is also involved in the control of ovulation through the synthesis of arachidonic acid and prostaglandins (Takahashi *et al*., 2019).

In teleosts, the process of oogenesis can be divided into six phases: oogonia differentiation from primordial germ cells (PGCs) and proliferation, primary oocyte growth, secondary growth, vitellogenesis, maturation and hydration, and ovulation (Lubzens *et al*., 2010). The major biological processes occurring during these phases are depicted in figure 1 and summarized below.

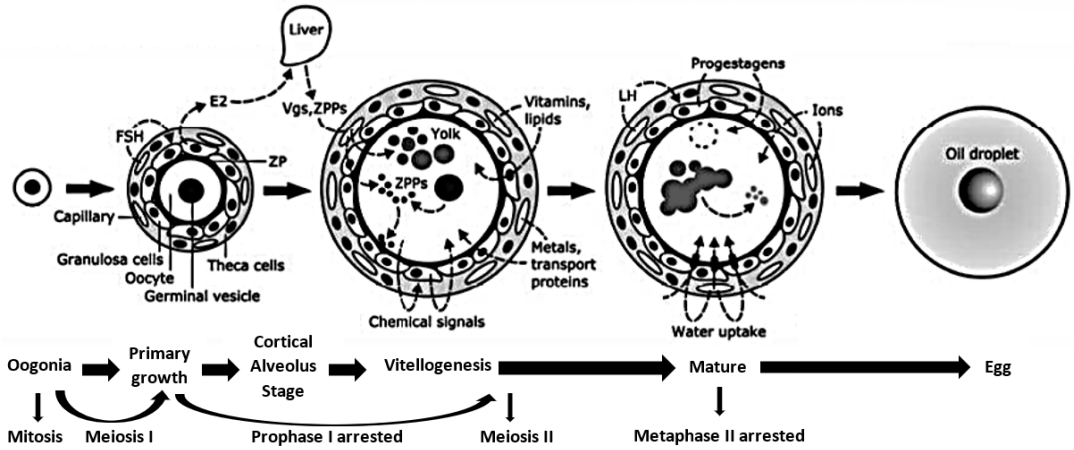

Figure 1. Stage of oocyte development in teleosts. From left to right: oogonia, oocyte growth, vitellogenesis, mature oocytes and egg. Oogonia differentiate and proliferate mitotically, and starts meiosis up to the prophase of the first meiotic division to form primary growth ovarian follicles. During vitellogenesis, the follicle (granulosa) cells are stimulated by Fsh to produce E2 which triggers the synthesis of vitellogenins (Vgs) from the liver, which in turn are taken by the growing oocyte and stored as yolk proteins. Further hormonal stimulation by Lh triggers the synthesis of progestogens by the granulosa cells, which will induce meiosis resumption up to metaphase of the second meiotic division in the oocyte (oocyte maturation). During this process, the hydrolysis of stored yolk proteins increases the osmotic pressure in the oocyte and drives massive hydration. Abbreviations: E2, 17β-estradiol; Fsh, follicle-stimulating hormone; Lh, luteinizing hormone; Vgs, vitellogenins; ZP, zona pellucida; ZPPs, zona pellucida proteins. Modified from Cerdà, 2008.

1.2.1. Oogonia Differentiation and Proliferation

PGCs are undifferentiated bipotential cells capable of evolving into oogonia or spermatogonia. The PGCs are diploid and they are initially formed at extragonadal locations, and later they migrate to the genital crest where they differentiate into the gametes (Wylie, 2000). The PGCs show cytosolic features as the "*nuage*", the electron-dense material (aggregation of RNAs and proteins) associated with germ cells and germ plasm material. The *nuage* is also found in oogonia, oocytes, spermatogonia, spermatocytes and spermatids and has an important role in germ line development and differentation (Eddy, 1975; Williamson and Lehmann, 1996). In zebrafish (*Danio rerio*), the migration process of PGCs

is controlled by different chemokines, which are recognized by the PGCs by the expression of specific receptors (Knaut and Schier, 2008).

During the process of oogonia differentiation, the PGCs give rise to germline stem cells (GSCs), which reside in a lateral, anterior-posterior band at the ovary periphery termed the germinal zone where meiotic oocytes are generated (Elkouby and Mullins, 2017). The mechanisms through which the GSCs differentiate into mitotic oogonia, the precursor cells of meiotic oocytes, are still poorly known. Differentiated oogonia undergo several mitotic divisions to increase their number in teleost females, and they are enclosed in germinal cradles or nests. In the Japanese medaka (*Oryzias latipe*s), the germinal cradles contain isolated germ cells surrounded by somatic cells, clusters of germ cells that form cysts, and early-stage oocytes already detained in prophase I of meiosis due to the perinuclear location of the *nuage* (Aoki *et al*., 2008; Lubzens *et al*., 2010; Nakamura *et al*., 2010). Within the cysts, oogonia initiate meiosis and form primary oocytes, which are arrested in the prophase of the first meiotic division (prophase I) and are connected to somatic cells for the formation of the ovarian follicle. This transition breaks the cysts releasing oocytes with pre-follicular cells that will form the granulosa cells (Cerdà *et al*., 2007).

In teleosts, the hormonal control of oogonia differentiation and proliferation is not well known. However, it has been suggested that pituitary gonadotropins, especially Fsh, can increase oogonial proliferation, as well as other steroids such E2 and growth factors such as the gonadal soma-derived growth factor (Gsdf) (Lubzens *et al*., 2010). The hormonal signals triggering meiosis in oogonia are also not well known, although retinoic acid (RA) signaling, progestin 17,20βP, and insulin-like growth factor-I (Igf-I) have been implicated in this process (Lubzens *et al*., 2010; Elkouby and Mullins, 2017).

1.2.2. Primary Growth

In the primary growth stage, Fsh and growth factors stimulate oocyte growth, and this stage is characterized by the accumulation of RNA in the oocyte, the increase of the volume of the cytoplasm, the formation of the vitelline envelope between the granulosa cells and the oocyte and of the Balbiani body (Bb) in the oocyte, and the initiation of chemical communication between the oocyte and granulosa cells (Lubzens *et al*., 2010; Grier, 2012; Johnson and Grier, 2018).

Prior to entry into meiosis, the oocyte is enveloped by follicle cells. Folliculogenesis is linked with the formation of the follicle cells, granulosa and theca cells, and the contact between oocyte and granulosa cells (Cerdà *et al*., 1999; Grier, 2012). When the oocyte is surrounded by the somatic cells, microvilli extend out from the cell membrane of the oocyte to reach and contact the plasma membrane of the granulosa cells, which may facilitate cell adhesion and the passage of small molecules (Lyman-Gingerich and Pelegrí, 2007).

The oocyte chromosomes now decondense and meiosis progresses until prophase I, while nucleoli appear and accumulate in the germinal vesicle of the oocyte. Coincident with this chromosomal disassembly, the oocytes begin to increase their rates of maternal mRNAs production (Wallace and Selman, 1990; Lyman-Gingerich and Pelegrí, 2007). The transcripts produced will be involved in further embryo development, but others will be required at later stages of oogenesis, such as during organelle formation and yolk and lipid incorporation (Luckenbach *et al*., 2008).

A rather prominent feature during the differentiation of the primary oocyte is the formation of the Bb, which is an aggregate of mRNA-protein (mRNP) and mitochondria that localizes to the oocyte cortex (Elkouby and Mullins, 2017). This structure forms the pathway for the delivery of mRNPs granules to the vegetal pole of the oocyte, while other mRNAs are recruited later to such defined vegetal pole (Escobar-Aguirre *et al*., 2017).

1.2.3. Secondary Growth

During the secondary growth, or cortical alveoli stage, the oocyte prepares to begin vitellogenesis, and several structural and hormonal changes occur. Bound vesicles appear and the cortical alveoli will become anchored at the oocyte cortex (Lyman-Gingerich and Pelegrí, 2007). Cortical alveoli first appear proximal to the Golgi complex where their contents are synthesized, and later they increase their size until filling the cytoplasm (Selman *et al*., 1993). In zebrafish, the accumulation of cortical alveoli is associated with the increase of aromatase mRNA expression and E2 production (Kwok *et al*., 2005). In salmonids, an increase of Fsh plasma levels during the transition from primary to secondary oocyte has been observed (Luckenbach *et al*., 2008), and experiments in vitro show that E2 and 11-ketotestosterone increase in secondary growth. Also, Fsh regulates steroidogenesis and dynamically controls the expression of several genes in early secondary oocyte growth, prior

to the onset of vitellogenesis (Luckenbach *et al*., 2008). These finding therefore suggest that Fsh may play a role in the formation of secondary growth oocytes in teleosts.

1.2.4. Vitellogenesis

In teleosts, the vitellogenic stage can last from one day in medaka to 1-2 weeks in tilapia (*Oreochromis niloticus*), or several months in salmonids (Jalabert *et al*., 2005). During this stage, the oocyte remains arrested in prophase I and incorporates different vitellogenin (Vtg) molecules, lipids and vitamins from the blood, so at the end of this stage the oocyte has stored all the nutritional components necessary for further embryo development, and becomes competent for fertilization (Menn *et al*., 2007; Lubzens *et al*., 2010 and 2017). During vitellogenesis, the vitelline envelope between the granulosa cells and oocyte totally develops, and intercellular communication between both cell types is formed through different cell-cell interaction structures, including gap junctions (Cerdà *et al*., 1999; Menn *et al*., 2007).

The process of vitellogenesis is controlled by the Fsh, which activates specific Fsh receptors in the granulosa cells to stimulate the synthesis of E2 (Lubzens *et al*., 2010). Estrogens are then released into the blood to trigger Vtg (VtgAa, VtgAb and VtgC) synthesis in the liver, which will then be incorporated in the oocyte by receptor-mediated endocytosis (Finn and Kristoffersen, 2007; Finn, 2007). The Vtgs are subsequently cleaved in a multi-step acidification process, mediated by proteases such as the aspartic protease cathepsin D, into yolk proteins (Finn, 2007; Cerdà *et al*., 2007). The yolk proteins are further stored in the oocyte in membrane-bound yolk globules throughout the growth period.

1.2.5. Oocyte Maturation and Ovulation

At the end of the vitellogenic phase, a surge of Lh triggers the meiosis resumption of the oocyte or “oocyte maturation” (i.e. completion of the first meiotic division followed by progression to metaphase II) followed by the ovulation process. The maturation phase is accompanied by several changes in the nucleus, such as the breakdown of the germinal vesicle (GVBD), chromosome condensation, assembly of the meiotic spindle and formation of the first polar body, where lipid coalescence and partial or complete disassembly and fusion of yolk globules are the major changes occurring in the cytoplasm (Cerdà, 2009). In

most oviparous marine teleosts, a marked increase in the oocyte volume (up to eightfold) also takes place during maturation as a result of a massive water uptake (see below).

The maturation of the oocyte is followed by the ovulation of the oocyte, during which the follicular envelope breaks forming a "hole", by which the oocyte will be expelled. During this process, the microvillar connections between the granulosa cell layer and the oocyte dissolve, allowing the detachment of the oocyte from the vitelline envelope and its expulsion from the follicle (Lubzens *et al*., 2010). This mechanism is mediated by the action of different proteolytic enzymes, cell death events, and muscular and microfilamentous contractile systems in the follicle cells (Schroeder and Pendergrass, 1976; Szöllösi *et al*., 1978; Schroeder and Talbot, 1985).

1.2.5.1. Endocrine Regulation

The meiotic resumption of the oocyte is mediated by maturation-inducing progestins, such as 17,20βP, which are secreted by the granulosa cells in response to Lh. These progestins activate a G protein-coupled membrane receptor on the oocyte surface, triggering the formation and activation of the MPF in the ooplasm, the final inducer of oocyte maturation (Yamashita, 1998; Thomas *et al*., 2004). The mechanism by which Lh stimulates the synthesis of progestins is possibly related to the steroidogenic shift from E2 to progestin production in the granulosa cells induced by the gonadotropin at the time of oocyte maturation (Nagahama and Yamashita, 2008). This shift occurs through the upregulation of the enzyme activities of the cytochrome P450c17 polypeptide II (Cyp17a2), which has only 17α-hydroxylase activity and can produce only 17α-hydroxyprogesterone (17-P), and the 20β-hydroxysteroid dehydrogenase/carbonyl reductase-like (Cbr1), which converts 17-P into progestins (Zhou *et al*., 2007a and b).

In contrast to the meiotic maturation process, the ovulatory mechanism requires Lh-induced transcriptional activity in follicle cells (Pinter and Thomas, 1999; Jalabert *et al*., 2005). Thus, at ovulation Lh stimulates the proteolysis and the expression of tumour necrosis factors (TNFs), which are involved in follicular cell death (Crespo *et al*., 2010 and 2015), as well as the production of prostaglandins, progestins, eicosanoids, catecholamines and vasoactive peptides (Thibault, 1999; Jalabert *et al*., 2005; Suwa and Yamashita, 2007). Other glycoproteins, such as osteopontin, are up-regulated in granulosa cells and seem to

participate in macrophage invasion and T-cell activation (Bobe and Goetz *et al*., 2001). Some of the actions of Lh during ovulation are mediated by the nuclear progestin receptor in granulosa cells (Hagiwara *et al*., 2014; Wu *et al*., 2020).

Recent studies in the primitive freshwater teleost stinging catfish (*Heteropneustes fossilis*) suggest that the basic neurohypophyseal nonapeptide arginine vasotocin (Avt), the ortholog of mammalian arginine vasopressin (AVP) which is known to be involved in osmoregulation, also plays a role during oocyte maturation and ovulation (Joy and Chaube, 2015). In this species, oocytes partially hydrate during meiotic maturation, although benthic eggs are produced (Singh and Joy, 2010). Transcripts encoding both Avt and its specific receptor subtypes (Avt1r and Avt2r) have been detected in catfish follicle cells, which shows seasonal expression and preovulatory changes in the ovary. In addition, follicular Avt secretion stimulated by progestins triggers prostaglandin secretion, GVBD, oocyte hydration and ovulation (Joy and Chaube, 2015; Singh *et al*., 2021). Interestingly, it has been suggested that Avt acts through the Avt1r to stimulate GVBD and ovulation, whereas the Avt2r type may be involved in the stimulation of oocyte hydration (Joy and Chaube, 2015).

1.2.5.2. The Oocyte Hydration Process

The mechanism of oocyte hydration occurring during meiosis resumption is a critical process in marine teleosts that assures the further survival of the embryo in the ocean. Oocyte hydration is more pronounced in marine species producing buoyant eggs in sea water (pelagophil), where water typically contributes >90% of the final egg weight, whereas the egg water content is lower (up to 85% in weight) in species that produce benthic, non-buoyant eggs (benthophil) (Cerdà *et al*., 2007; Finn and Kristoffersen, 2007; figure 2). This mechanism provides a water reservoir for the embryo to compensate for the passive water efflux in the hyperosmotic seawater until osmoregulatory organs develop (Finn and Kristoffersen, 2007). The high water content of marine pelagic eggs also causes them to float thus giving rise to their pelagic nature, which increases the survival of developing embryos by allowing more efficient oxygen exchange and their dispersal in the ocean (Craik and Harvey, 1987; Finn and Kristoffersen, 2007).

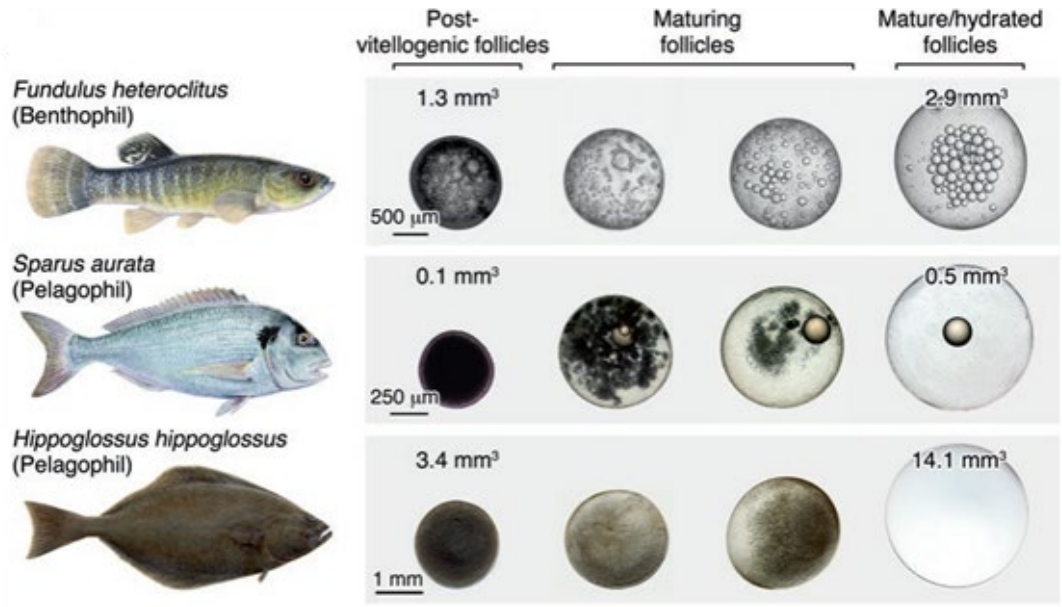

Figure 2. Oocyte hydration in marine teleosts. Follicle-enclosed oocytes from the benthophil common mummichog (*Fundulus heteroclitus*), and the pelagophil gilthead seabream (*Sparus aurata*) and Atlantic halibut (*Hippoglossus hippoglossus*), undergoing meiotic maturation and hydration. The volume of oocytes before and after hydration is indicated for each species. Taken from Cerdà *et al*., 2017.

In pelagophil teleosts, it is well established that oocyte hydration correlates with the proteolysis of yolk proteins stored in the oocyte, with the resulting organic osmolyte pool of free amino acids (FAA) providing much of the osmotic driving force for water influx into the oocyte (Cerdà *et al*., 2007; Finn and Fyhn, 2010). In benthophil species, where oocyte hydration is more modest than in pelagophil, limited proteolysis of yolk proteins occurs, resulting in the liberation of a small pool of FAAs (Cerdà *et al*., 2007; Finn and Fyhn, 2010). The linear arrangement of the complete Vtg protein consists of five sub-domains corresponding to the different yolk proteins stored in growing oocytes: a lipovitellin heavy chain (LvH), a phosphorylated serine-rich phosvitin, a lipovitellin light chain (LvL), and two Cys-rich C-terminal coding regions (β′ and Ct), which are homologous to the mammalian von Willebrand factor type D domain (Finn, 2007). During oocyte maturation, the VtgAa LvH, LvL and phosvitin are differentially cleaved by specific proteases such as cathepsins whereas the VtgAb remains predominantly intact as the major yolk protein for embryonic development (Matsubara *et al*., 2003; Finn, 2007; Kristofersen *et al*., 2009). However, while in most pelagophil teleosts the VtgAa LvH is extensively degraded, this molecule is only partially hydrolysed in benthophil species (Finn and Kristoffersen, 2007; Yilmaz *et al*., 2017). Thus, the FAAs resulting from these proteolytic mechanisms, together with the specific accumulation of inorganic ions such as K^+, Cl^-, NH_4^+ during oocyte maturation, as

well as of Pi arising from the dephosphorylation of phosvitins, represent the primary osmotic effectors in pelagophils, while inorganic ions such as Na^+ and K^+ seem to be the major osmolytes in benthophils (Cerdà *et al*., 2007; Finn *et al*., 2002; Sawaguchi *et al*., 2006; Kristoffersen and Finn, 2008).

The hydrolysis of yolk proteins during meiotic maturation is possibly activated by Lh through the action of cathepsins, although the specific molecular mechanisms involved are not well understood. In addition, the cellular mechanisms that allow water transport into the maturing oocyte remained long ignored, since water influx in oocytes was believed to occur passively. However, different studies during the last decade have uncovered the role of a novel molecular water channel (aquaporin) specific to teleosts as the facilitator of water permeation and resultant swelling of fish oocytes (Cerdà *et al.,* 2008; Cerdà *et al*., 2017). This discovery has provided an important insight into the molecular basis of the production of viable eggs in marine fish.

1.3. Phylogeny, Structure and Physiology of Vertebrate Aquaporin Water Channels

1.3.1. Phylogeny of Vertebrate Aquaporins

In the 80s a new protein family was identified, containing the bovine lens Major Intrinsic Proteins (MIP) (Pao *et al*., 1991) and the CHIP28 protein which was isolated in different human tissues (Preston and Agre, 1991). Both proteins had similar sequence and length (256-281 amino acids) and six predicted transmembrane domains, which suggested their possible function as a channel. Their function was discovered by measuring the osmotic water permeability (Pf) following microinjection and expression of the CHIP28 cRNA in *Xenopus laevis* oocytes. The results demonstrated the high-water transport capacity of these channels (Preston *et al*., 1992; Agre *et al*., 1993), which were subsequently defined by the term "aquaporins" (Preston and Agre, 1991). Thus, the MIP of the bovine lens fiber was called AQP0 and the CHIP28 was renamed AQP1 (Nielsen and Agre, 1995).

Following the discovery of AQP0 and -1 and with the rise of genomic techniques, many aquaporins were isolated, and these proteins are found in all Kingdoms of life: Animalia, Plantae, Fungi, Protista, Archaea, Viruses and Bacteria (Zardoya, 2005; Gazzarrini *et al*., 2006), which suggests the existence of a positive selection for these

proteins (Lorente-Martínez *et al*., 2018). Thus, aquaporins may have originated in Archaea or Bacteria, both of which have four grades of channel: AqpZ, AqpN, AqpM and GlpF (Finn *et al*., 2014). In animals, four phylogenetically distinct grades of aquaporins are also present: classical water channels (AQPs), AQP8-type channels, aquaglyceroporins (Glps), and unorthodox AQPs, all different in permeability properties and physiological function (Ishibashi *et al*., 2013; Almasalmeh *et al*., 2014; Finn *et al*., 2014; Ishibashi *et al*., 2017).

The classical aquaporins consist of eight paralogs: AQP0, -1, -2, -4, -5, -6, -14 and -15, while aquaglyceroporins include AQP3, -7, -9, -10 and -13 (Finn *et al*., 2014; Finn and Cerdà, 2018; Chauvigné *et al*., 2019). The unorthodox AQP11 and -12 have lower conserved amino acid sequences (Li and Wang, 2017). Finally, in the AQP8-type channels are represented by the AQP8 and –16 paralogs (Finn *et al*., 2014; Finn and Cerdà, 2015; Finn and Cerdà, 2018). However, in the Sauropsids (reptiles and birds) additional aquaporin genes were discovered, as in amphibia in which the relationship between paralogs and subfamilies is more divergent: three copies of AQP6 (AQP6ub, AQP6vs1, AQP6vs2), two copies of AQP5, and three copies of AQP4 (Finn *et al*., 2014; Suzuki *et al*., 2015). The placental mammalian aquaporins consist of the AQP0 to AQP12 subfamilies, but some studies revealed that the monotreme and marsupial mammals retain additional classes, AQP13 and AQP14 that are also present in amphibians; and in non-mammalian vertebrates (including sharks, frogs, alligators or turtles) two additional subfamilies AQP15 and AQP16 are known, so to date the vertebrate aquaporin superfamily finally consists of 17 subfamilies (Finn *et al*., 2014; Finn and Cerdà, 2015; Finn and Cerdà, 2018; figure 3).

1.3.2. Structure of Vertebrate Aquaporins

Aquaporins are a superfamily of small (25-34 kDa), hydrophobic, integral membrane channel proteins that facilitate rapid movement of water across bilaminar membranes following the osmotic gradient. Structural analysis of aquaporins has established that these protein channels share common structural features (Heymann and Engel, 2000). Functional aquaporins consists of a single polypeptide containing a water pore that are assembled in the membrane as homotetramer, but occasionally also as heterotetramers (Finn and Cerdà, 2015). The integral membrane region is composed of six transmembrane domains (TMDs), three extracellular (A, C, E) and two intracellular (B, D) loops, and two inverted hemihelices on loops B and E that project opposing Asp-Pro-Ala (NPA) motifs to regulate the single-file

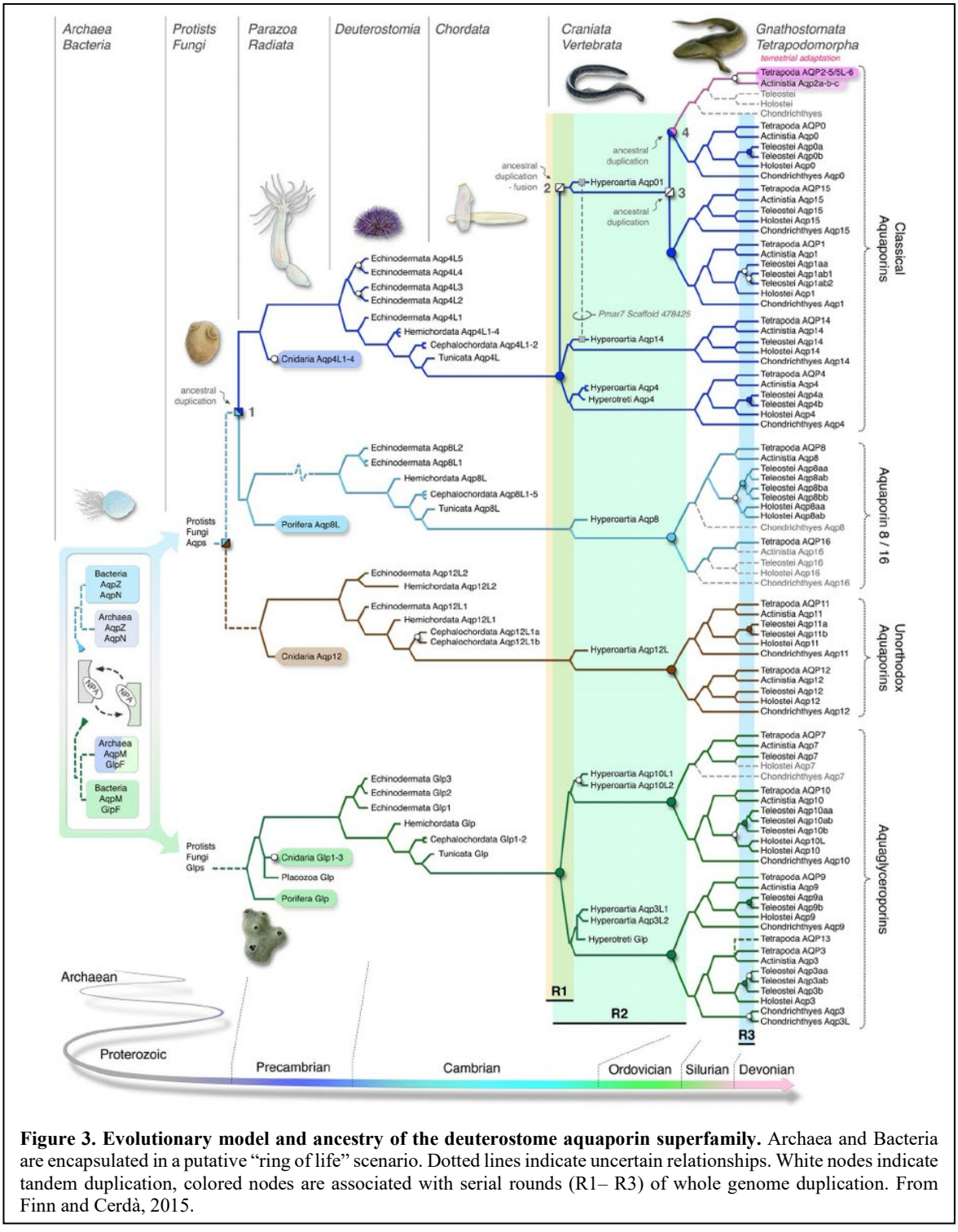

Figure 3. Evolutionary model and ancestry of the deuterostome aquaporin superfamily. Archaea and Bacteria are encapsulated in a putative "ring of life" scenario. Dotted lines indicate uncertain relationships. White nodes indicate tandem duplication, colored nodes are associated with serial rounds (R1– R3) of whole genome duplication. From Finn and Cerdà, 2015.

conductance of water, while simultaneously functioning as a cation and a proton excluding selectivity filter near the centre of the molecule (figure 4) (Finn and Cerdà, 2015). A second constriction that contributes to proton exclusion is located in the outer channel vestibule and typically consists of aromatic residues and an arginine (ar/R) to form the major selectivity filter determining which molecular permeant can traverse the pore (Finn and Cerdà, 2015).

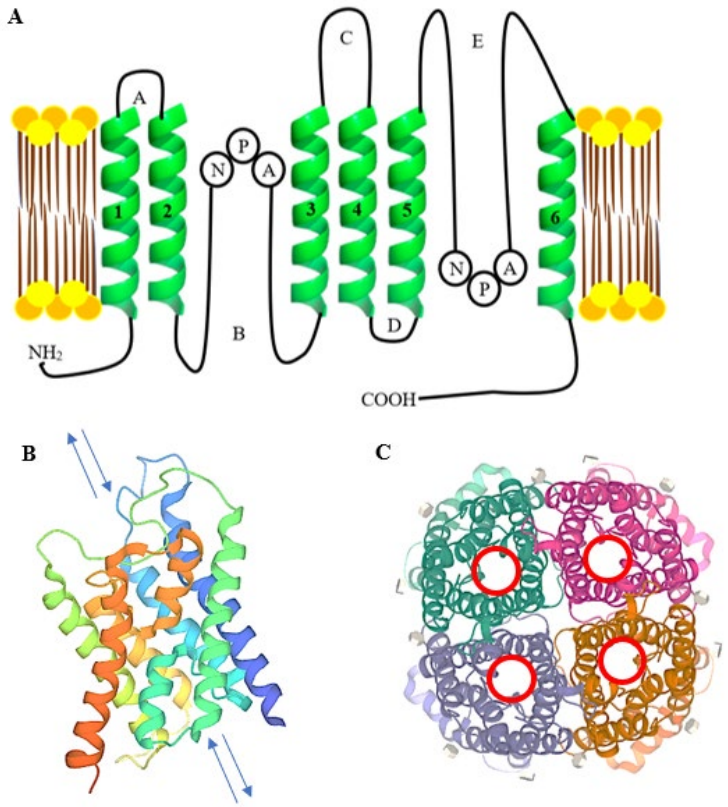

Figure 4. Aquaporin structure. (**A**) Secondary structure of the prototypical subunit of AQP1. It shows the bilaminar membrane (yellow/brown), the six α-helix domains (green); two NPA motifs between helix 2-3 and 5-6, five loops (A-E) and the intracellular N- and C-termini. (**B**) Three-dimensional reconstruction of the tertiary structure of AQP1, where the arrows simulate the flux of water. (**C**) Extracellular view of the quaternary structure of human AQP1 (Protein Data Bank 1J4N, Sui *et al*., 2001) showing cartoon renderings of the four monomers of water channels (in green, blue, pink and orange) where the red circle indicates the pores.

While some aquaporins are water-selective, others can also permeate uncharged solutes such as glycerol and urea and are then called aquaglyceroporins (Glps). *In silico* studies revealed that the arrangement of the ar/R residues correlates with the functional properties of the channel (Kitchen *et al*., 2019). Thus, classical water-selective aquaporins (such as AQP0, -1, -2, -4, or -5) typically display a tight ar/R cluster in which His-201 on TMD5 reduces the pore to between 1.5-3 Å wide, just slightly larger than the water molecule and thus excludes the passage of glycerol. Conversely, Glps (AQP3, -7, -9, –10, and -13) show a more open structure due to a longer polypeptide region in loop E and the tendency to display an uncharged constriction residue on TMD5 such that the pore is ~3.4 Å (Gonen and Walz, 2006; Tong *et al*., 2019). Channels such as AQP8 have also been termed aquaammoniaporins, as they are able to transport ammonia, or perixoporins, since they also facilitate the transport of hydrogen peroxide (H_2O_2), which is commonly generated as a biproduct of mitochondrial oxidative phosphorylation (Finn and Cerdà, 2015; Cerdà *et al*., 2017). The unorthodox aquaporins (AQP11 and -12), are channels that exhibit an

intracellular localization *in vivo*. The permeation properties of these channels are poorly defined, although some studies have shown that both water and glycerol can permeate the AQP11 pore (Ikeda *et al*., 2011; Yakata *et al*., 2011).

It is considered that aquaporins function only as homotetramer, but some reports suggest otherwise. For example, autosomal dominant neurohypophyseal diabetes insipidus is related to a heterotetramer including a wild-type and mutant AQP2, making it impossible for the protein to reach the membrane and thus causing diabetes (Sohara *et al*., 2006). Similarly, AQP1 can form mixed oligomers with mutant-AQP1 that inactivate it, which suggests that the vertical symmetry is necessary for residence of the protein in the lipid bilayer (Jung *et al*., 1994). Finally, AQP4 in the brain can form heterotetramers with a differentially spliced isoform of the protein (Lu *et al*., 1996), and in muscle, multimeric complexes formed by the full-length AQP4 and a truncated isoform can result in the attenuation of the expression of AQP4 and thus reducing the permeability of the plasma membrane (De Bellis *et al*., 2014). Consequently, the formation of heterotetramers may regulate the physiology of aquaporins.

1.3.3. Physiology and Regulation of Vertebrate Aquaporins

1.3.3.1. Classical Aquaporins

AQP0 is the most expressed protein in lens fiber cell membranes, and in addition to water transport, retains cell-to-cell adhesive properties to maintain the normal structure of the lens, which is critical to their integrity and transparency (Lo *et al*., 2014). AQP1 was the first water channel discovered (Preston *et al*., 1991; Preston *et al*., 1992) and the first aquaporin to also exhibit function as a gas channel, as it could enhance CO_2, NO, H_2O_2 and NH_3 permeability (Nakhoul *et al*., 1998; Prasad *et al*., 1998; Ripoche *et al*., 2006; Day *et al*., 2014; Finn and Cerdà, 2015; Li and Wang, 2017). AQP2 is AVP-regulated which plays an essential role in homeostatic response. The binding of AVP to its V2 receptor, induces the trafficking of AQP2 to the apical membrane of the principal cells of renal collecting ducts (antidiuresis) (Marples *et al*., 1995; Nielsen *et al*., 1993; Fenton *et al*., 2020).

AQP4 is highly expressed in the central nervous system where phosphorylation of its N-terminus induces gating of the pore resulting in a diminished water permeability (Gunnarson *et al*., 2004). AQP5 is involved in generation of saliva, tears and pulmonary

secretions as well as water conservation in birds (Song *et al*., 2002; Müller *et al*., 2006). It is permeable to water and CO_2 (Geyer *et al*., 2013). AQP6 is permeable to water, glycerol, urea, anions, NO_3^- , CO_2 and NH_3, and colocalizes with the H^+-ATPase in intracellular renal vesicles in mammals. In response to acid-base changes H^+-ATPase a translocation from the vesicles to the apical plasma membrane occurs but not AQP6, indicating that AQP6 is exclusively at the intracellular sites (Beitz *et al*., 2006). In amphibians three paralogs of AQP6 (AQP6ub, AQP6vs1 and AQP6vs2) are directly involved in water conservation (Suzuki *et al*., 2015; Finn *et al*., 2014; Finn and Cerdà, 2018). Finally, the recently identified AQP14 has a non-canonical ar/R constriction and is a neuropeptide regulated polytransporter permeable to water, urea, ammonia, H_2O_2 and glycerol. This channel is found in the genomes of all vertebrate lineages except hagfishes and eutherian mammals, and may play a role in osmoregulation in fish (Chauvigné *et al*., 2019).

1.3.3.2. GLPs

The Glps are permeable to water and glycerol, as well as to other small, uncharged solutes, such as ammonia, urea and polyols (Li and Wang, 2017). AQP3 was the first mammalian Glp discovered (Ishibashi *et al*., 1994). It has a wide tissue distribution, although it is most abundant in skin, and plays an important role in cell migration, inflammation and cancer progression (Echevarria *et al*., 1994; Boury-Jamot *et al*., 2006; Hara-Chikuma *et al*., 2012 Almasalmeh *et al*., 2014; Hara-Chikuma *et al*., 2015; Satooka and Hara-Chikuma, 2016). AQP10 is also able to transport antimonite and arsenite when expressed in *Xenopus* oocytes (Ishibashi *et al*., 2002), and its function is related with obesity together with AQP7 (Laforenza *et al*., 2013), which is also abundant in adipose tissue (Geyer *et al*., 2013; Li and Wang, 2017). AQP9 is present in liver (Finn and Cerdà, 2015; Rojek *et al*., 2008) and also transports much larger substrates, such as lactate, purine and pyrimidine, probably due to a biggest pore size (Viadiu *et al*., 2007; Li and Wang, 2017). In the frog *X. laevis*, AQP13 is located in fat body, oocyte and kidney (Virkki *et al*., 2002). This Glp was also found in the genomes of monotreme mammals the platypus (*Ornithorhynchus anatinus*) and the echidna (*Tachyglossus aculeatus*) (Finn *et al*., 2014; Yilmaz *et al*., 2020).

1.3.3.3. Unorthodox Aquaporins

AQP11 and -12 may have a role in cellular differentiation, apoptosis, organogenesis, mating and intercellular communication (Ishibashi *et al*., 2017). The second NPA motif of AQP11 has a substitution of alanine to cysteine (NPC), which allows permeability to glycerol (Finn and Cerdà, 2015; Ishibashi *et al*., 2017). The first NPA motif of AQP12 shows a substitution of alanine to threonine (NPT), but to date AQP12 has not been characterized functionally. In mammals, AQP12 is specifically expressed in zymogen granules of pancreatic acinar cells (Itoh *et al*., 2005). Although its function is unclear, this channel seems to be upregulated in pancreatitis, and may be directly associated with cell proliferation, adhesion, migration and resistance to inflammation (Da Silva *et al*., 2020).

1.3.3.4. AQP8-like Channels

AQP8 can transport water, NH_3 and H_2O_2 (Soto *et al*., 2012; Chauvigné *et al*., 2015). In mice kidney, it is localized in the mitochondrial membrane, and plays a role in adaptative response of proximal tubule to acidosis (Soria *et al*., 2010). AQP16 are restricted to non-mammalian vertebrates and have not been studied so far (Finn *et al*., 2014).

1.3.4. Regulation of Aquaporin Expression and Function

After translation, proteins undergo post-translational modifications that can be reversible or irreversible. It includes the addition a functional complexity of the molecules, such as ubiquitination, phosphorylation of glycosylation, that may modulate localization, stability, activity and interaction with protein partners. These modifications depend on the nature of the covalent modification and the identity of the substrate that are specifically targeted by the chemical reaction to specific residues of the protein (Mateo Sánchez *et al*., 2016; Li and Wang, 2017).

Phosphorylation is the most studied post-translational modification of aquaporins. Many aquaporins appear to be phosphorylated *in vivo* and *in vitro*, but the AQP2 is amongst the best characterized (Nielsen *et al*., 1993; Eto *et al*., 2010; Moeller *et al*., 2014; Wong *et al*., 2020). The distribution and translocation to the membrane of AQP2 is regulated by AVP. The protein contains numerous putative phosphorylation sites for various proteins kinases based on bioinformatic analysis (Brown, 2003; Eto *et al*., 2010), and a complex regulation

by cAMP activation of PKA or cGMP-mediated mechanism is proposed to modulate AQP2 trafficking (Bouley *et al*., 2000; figure 5).

Phosphorylation is the most studied post-translational modification of aquaporins. Many aquaporins appear to be phosphorylated *in vivo* and *in vitro*, but the AQP2 is amongst the best characterized (Nielsen *et al*., 1993; Eto *et al*., 2010; Moeller *et al*., 2014; Wong *et al*., 2020). The distribution and translocation to the membrane of AQP2 is regulated by AVP. The protein contains numerous putative phosphorylation sites for various proteins kinases based on bioinformatic analysis (Brown, 2003; Eto *et al*., 2010), and a complex regulation by cAMP activation of PKA or cGMP-mediated mechanism is proposed to modulate AQP2 trafficking (Bouley *et al*., 2000; figure 5).

Transmembrane water flux can be altered either by trafficking of aquaporins or by gating (Finn and Cerdà, 2018). Post-translational modifications including phosphorylation and protonation are mechanisms that regulate the distribution and open/close the channel (Li and Wang, 2017).

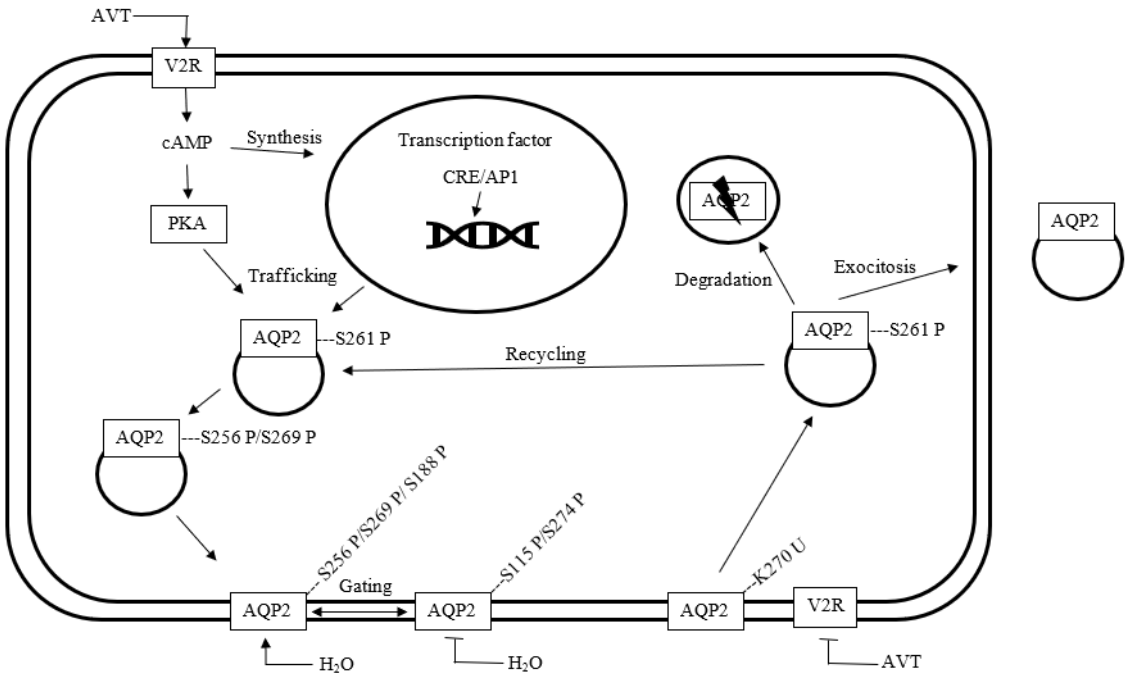

Figure 5. Pathway of AVP-regulation of AQP2. AVP binding to V2 receptor (V2R) increases intracellular cAMP, which activates PKA activity and AQP2 trafficking. The AQP2-S261 is dephosphorylated while S188, S256 and S269 are phosphorylated, which allows the trafficking of AQP2 to the plasma membrane. Also, gating occurs when S115 and S274 are phosphorylated. When isotonicity is restored AQP2 is ubiquitinated at the K270 and reinternalized. The S261 phosphorylation then causes AQP2 recycling, degradation or excretion. Based on Li and Wang, 2017.

Ubiquitination of AQP1 and -2 C-terminus when they locate at the plasma membrane results in their internalization, externalization and/or degradation (Leitch *et al*., 2001; Moeller *et al*., 2014; Fenton *et al*., 2020). Glutathionylation provides a protecting effect on cysteine residues against irreversible oxidation during redox imbalance. Also, reactive oxygen species (ROS) may influence the expression of AQP2 (Tamma *et al*., 2014).

The extracellular loops of aquaporins often contain a glycosylation site (Li and Wang, 2017). Glycosylation plays a role in the trafficking and translocation to plasma membrane, but it is not essential (Baumgarten *et al*., 1998) as site directed mutagenesis in AQP1 reveals that non-glycosylated AQP1 does not affect water permeability in *Xenopus* oocytes (Preston *et al*., 1993; Li and Wang, 2017). However, AQP2 glycosylation is involved in the secretion of the protein from the Golgi body (Hendriks *et al*., 2004).

Acetylation, carbamylation, oleylation, palmitoylation are other post-translational modification that can affect aquaporins. N-terminal acetylation, carbamylation and oleylation of AQP0 may modulate protein-protein interactions and thus the regulation of water permeability in the lens (Gutierrez *et al*., 2011). AQP4 can be modified with palmitic acid, which inhibits the formation of AQP4 square arrays in CHO (Chinese Hamster Ovary) cells (Suzuki *et al*., 2008).

Aquaporins are expressed in different tissues and are localized in different cellular compartments, and hence are regulated by various hormones such as AVP and insulin, by local molecules such as purines, prostaglandins and dopamine, or by environmental signals like pH or osmolality. (Zelenina *et al*., 2000; Umenishi *et al*., 2003; Zhang *et al*., 2015; Choi *et al*., 2015).

1.4. Fish Aquaporins

Teleosts are bony fishes that inhabit both marine and freshwater environments. They are thus exposed to opposing osmotic gradients. To avoid homeosmotic instability, they compensate for the gain or loss of water and ions through the control of osmoregulatory organs. Aquaporins facilitate the water transport in osmoregulatory organs (Madsen *et al*., 2015) and play important roles in gametes and embryos of oviparous teleosts that evolved molecular adaptations in germ cells to cope with the osmotic challenges. (Cerdà *et al*., 2017).

The teleost genomes experienced an additional whole genome duplication (third WGD) originated in early evolution of the lineage (Dong *et al*., 2016) and hence exhibit the largest repertoire of aquaporins in vertebrates (Tingaud-Sequeira *et al*., 2010; Finn and Cerdà, 2011). Copy numbers range from 18 to 26 depending upon the species that are distributed in four grades including classical aquaporins, Aqp8-like, Glps and unorthodox aquaporins (Tingaud-Sequeira *et al*., 2010; Finn *et al*., 2014; Finn and Cerdà, 2015). By contrast paleotetraploid fish that underwent a fourth round of WGD, such as carps and salmonids, retain the highest gene copy number, with between 38 to 48 paralogs including pseudogenes identified (Finn *et al*., 2014; Yilmaz *et al*., 2020). Teleost fishes may thus retain two or three duplicates of their aquaporins that are redundantly expressed in tissues. However, some paralogs such as AQP7 and -12 are only presents a single copy genes (Cerdà and Finn, 2010; Finn and Cerdà, 2015). Teleosts and other actinopterygian fishes do not possess the AQP2, -5, and -6-type orthologs of tetrapods, which are considered permissive for terrestrial adaptation (Finn *et al*., 2014). In addition to WGD, some genes copies emerged by tandem duplication, including *aqp1ab*, *aqp3ab*, *aqp8ab*, *aqp8bb*, *aqp10ab* and *aqp10bb* (Tingaud-Sequeira *et al*., 2010; Zapater *et al*., 2011; Finn *et al*., 2014; Yilmaz *et al*., 2020). Thus, the duplication and neofunctionalization of the teleost *aqp8* paralogs (*aqp8aa*, *-8ab*, *-8ba* and *-8bb*) has been explained on the basis of a combination of WGD and tandem replication (Cerdà and Finn, 2010; Finn *et al*., 2014).

The diversity of fish aquaporins is highlighted in a phylogenetic tree based on Bayesian inference, comparing the repertoire of common carp AQPs with that of zebrafish and European seabass (Cerdà *et al*., 2017; figure 6).

1.4.1. Role of Aquaporins during Fish Oocyte Hydration

The essential function of aquaporins in fish oocyte hydration was first discovered in the marine pelagophil gilthead seabream (*Sparus aurata*), which spawn highly hydrated eggs in seawater. In seabream, the complete hydrolysis of yolk proteins is a very accelerated process that lasts around 2 h. For a long time it was assumed that water influx into the oocyte occurred passively following the osmotic gradient caused by the cleavage of yolk proteins and the uptake of ions. However, an aquaporin ortholog of mammalian AQP1 was

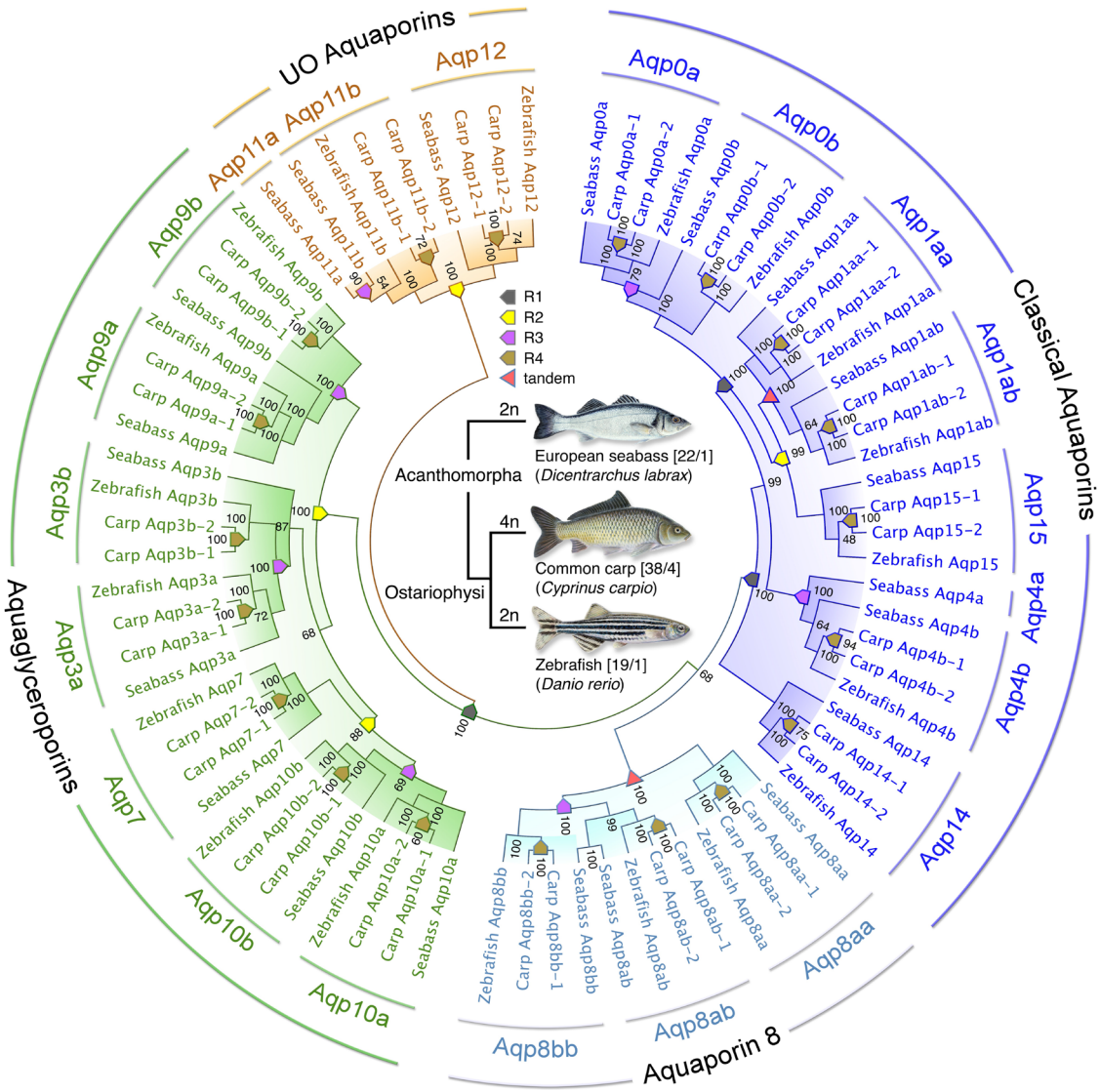

Figure 6. The aquaporin family of teleosts. The data are from European seabass, which is diploid (2n) and has 22 paralogs and 1 pseudogene; common carp, which is tetraploid (4n) and has 38 paralogs and 4 pseudogene; and zebrafish, which is diploid (2n) and has 19 paralogs and 1 pseudogene. Four rounds of WGD (R1, R2, R3 and R4) are respectively indicated in grey, yellow, purple and brown) next to tandem duplication (pink triangles). Bayesian posterior probabilities are shown at each node. Taken from Cerdà *et al*., 2017.

discovered to be highly expressed in the seabream ovary, and was termed Aqp1o (later renamed as Aqp1ab) (Fabra *et al*., 2005). Further functional studies showed that Aqp1o was a water channel facilitating the process of oocyte hydration mediated by the osmotic gradient created by yolk degradation and osmolyte accumulation during meiotic maturation (Fabra *et al*., 2005 and 2006; Cerdà, 2009; Lubzens *et al*., 2010; Cerdà *et al*., 2017).

More recent studies revealed that teleosts have two paralogous gene copies related to human AQP1, aqp1aa and aqp1ab, which originated by tandem duplication of the ancestral

aqp1aa gene, and hence the aqp1ab gene is teleost-specific. The teleost Aqp1aa channel remains more similar to the mammalian AQP1 ortholog (~86% identity in the amino acid sequence), and its mRNA is expressed ubiquitously, whereas Aqp1ab is more divergent, especially in the C-terminal domain of the channel (Tingaud-Sequeira *et al*., 2008; Finn and Cerdà, 2011). Interestingly, the *aqp1ab* transcripts are highly accumulated in the ovary of marine fish producing pelagophil eggs, such as the seabream, the Atlantic halibut (*Hippoglossus hippoglossus*), the Senegalese sole (*Solea senegalensis*) or the European eel (*Anguilla anguilla*), although this channel is also expressed in different osmoregulatory organs, such as the intestine and kidney (Fabra *et al*., 2006; Zapater *et al*., 2011; Tingaud-Sequeira *et al*., 2008; Kagawa *et al*., 2011). In contrast, in some freshwater fish species, such as the zebrafish, the expression of *aqp1ab* is not predominant in the ovary, while in others, such as the mummichog (*Fundulus heteroclitus*) or the Japanese medaka, this gene appears to be lost from the genome (Cerdà *et al*., 2017).

In the seabream ovary, *aqp1ab* transcription occurs in oocytes, but not in the surrounding granulosa or theca cells, and it is activated at the primary growth stage, when meiosis is arrested early in oogenesis (Zapater *et al*., 2013). Protein translation takes place at the same time, and when oocytes reach the secondary growth stage, Aqp1ab is highly accumulated in cytoplasmic vesicles, which slowly move towards the most cortical region of the cytoplasm throughout the vitellogenic period (Fabra *et al*., 2005 and 2006; figure 7). During meiotic maturation, shortly after GVBD, and before the hydrolysis of yolk proteins occurs, Aqp1ab is translocated further into the oocyte microvilli crossing the vitelline envelope, where it can transport water (Fabra *et al*., 2005 and 2006). The *aqp1ab* transcriptional activity decreases as vitellogenesis and maturation proceeds, which suggests

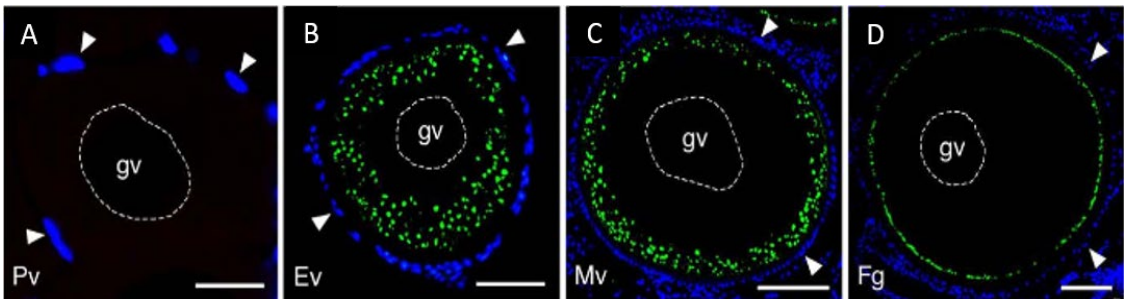

Figure 7. Aquaporin localization. Localization of seabream Aqp1ab during oocyte growth by immunofluorescence microscopy from paraffin ovary sections. Nucleus from somatic cells are in blue color (counterstained with Hoechst), and Aqp1ab are in green color by specific antibody for seabream Aqp1ab. The dashed round is the location of germinal vesicle (gv). The view shows follicles at previtellogenesis (Pv, **A**), early vitellogenesis (Ev, **B**), mid-vitellogenesis (Mv, **C**) and fully grown (Fg, **D**). Bars, 20µm (A), 50µm (B), 100µm (C and D). Modified from Fabra *et al*., 2006.

that the major regulatory pathways controlling Aqp1ab function in the seabream oocyte occur at the post-translational level (Fabra *et al*., 2006; Zapater *et al*., 2013). In the pelagophil Atlantic halibut *aqp1ab* mRNA expression and the protein synthesis seem to be upregulated during the hydration process, but a similar pattern of Aqp1ab trafficking to that observed in the seabream occurs during the hydration process (Zapater *et al*., 2011).

The essential function of Aqp1ab during oocyte hydration in pelagophil teleosts was inferred from early studies in which swelling of seabream oocytes during meiotic maturation in vitro was reduced by mercury, a typical inhibitor of aquaporin water conductance, or the quaternary ammonium cation tetraethylammonium (TEA), both of which can completely or partially block the permeability of Aqp1ab and mammalian AQP1 when expressed in *X. laevis* oocytes (Fabra *et al*., 2005 and 2006). More recently, however, more specific inhibition of the Aqp1ab has been obtained in Atlantic halibut oocytes by using Aqp1ab specific, affinity-purified antibodies, which indicate that the decrease of oocyte hydration of Atlantic halibut oocytes can be directly related to the loss of function of Aqp1ab (Zapater *et al*., 2011). These data thus provide functional evidence of the essential physiological role of this water channel in the hydration process of pelagic teleost eggs.

1.4.2. Molecular Regulation of Aqp1ab in Fish Oocytes

Previous studies in the seabream show that high levels of *aqp1ab* mRNAs and Aqp1ab proteins are stored in the oocytes before entering into the vitellogenic phase. Further transactivation experiments, incubations of ovarian explants *in vitro*, and chromatin immunoprecipitation (ChIP) assays show that the transcriptional activation of the *aqp1ab* gene in primary growth oocytes is dependent on the classical nuclear progestin receptor (Pgr), which is expressed in the cytoplasm of oogonia and the nucleus of primary oocytes and can bind to two different sites in the *aqp1ab* promoter region (Zapater *et al*., 2013). The Pgr is activated by the progestin 17,20ßP produced by primordial granulosa cells associated to primary oocytes in response to Fsh (Zapater *et al*., 2012). However, this mechanism can be potentially modulated by Sry-related high mobility group [HMG]-box (Sox) transcription factors, which can bind to specific sites upstream and downstream of the Pgr binding site in the 5′-flanking region of the seabream *aqp1ab* gene (Zapater *et al*., 2013). Thus, Sox3 and Sox8b, which are expressed in oogonia, elicit a synergic effect to enhance Pgr-mediated transcription in transactivation assays, whereas Sox9b, which is highly expressed in more

advanced oocytes, coinciding with a strong depletion of *aqp1ab* transcripts, represses *aqp1ab* transcription. These findings thus uncover a novel endocrine pathway for the *aqp1ab* transcriptional regulation in fish oocytes (Cerdà *et al*., 2017; figure 8).

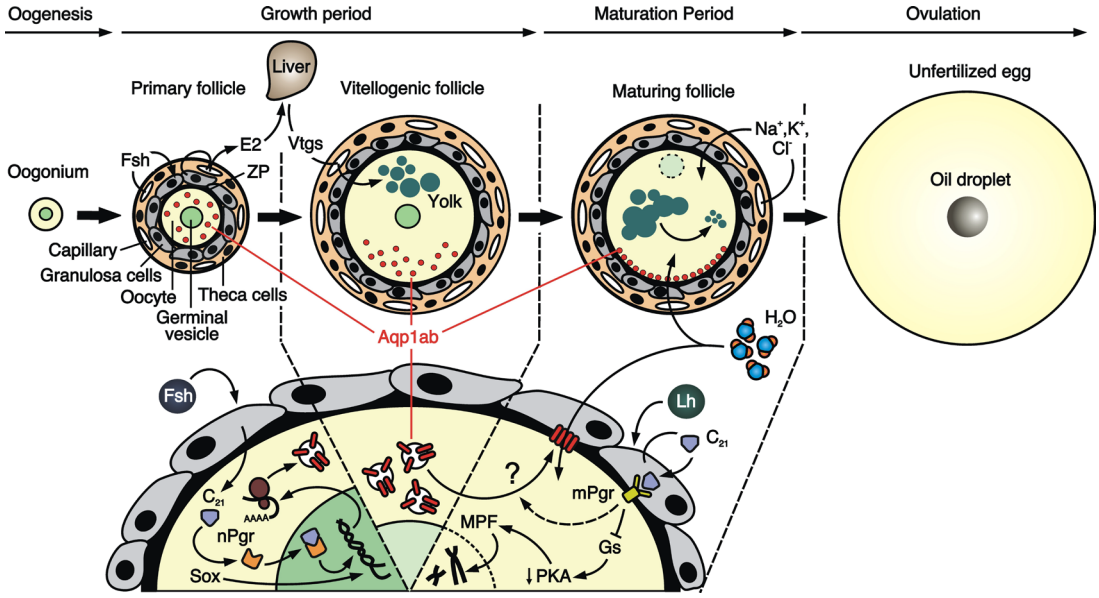

Figure 8. Current model of the regulatory pathways of Aqp1ab in the teleost oocyte. During oocyte differentiation and early growth, follicle cells surrounding the oocytes are presumably stimulated by Fsh to produce and release C21 steroids (17,20ßP), which activate the nuclear progestin receptor (nPgr) in the oocyte cytoplasm, triggering aqp1ab transcription and translation. Sox transcription factors can potentially modulate this mechanism. When oocytes enter into the growth period, vitellogenins (Vtgs) produced by the liver in response to estrogens are incorporated in the oocyte by receptor-mediated endocytosis and processed into yolk proteins that are stored in yolk globules. At the same time, Aqp1ab-containing vesicles are transported toward the oocyte cortex. When vitellogenesis resumes, maturation-inducing progestins synthesized by follicle cells in response to Lh activate G protein-coupled membrane progestin receptors (mPgr α and/or β) on the oocyte surface, repressing the stimulatory G protein (Gs) and causing a decrease in cAMP levels followed by the inactivation of protein kinase A (PKA). Decreased PKA activity leads to the activation of the maturation promoter factor (MPF), which triggers meiosis resumption. This process coincides with the proteolytic cleavage of yolk proteins, the accumulation of inorganic ions, and the translocation of Aqp1ab into the microvillar portion of the oocyte plasma membrane through an unknown mechanism. Taken from Cerdà *et al*., 2017.

In contrast to the *aqp1ab* transcriptional mechanisms, the post-translational regulatory pathways controlling the transport of Aqp1ab-containing vesicles toward the oocyte cortex and eventually into the microvillar portion of the oocyte plasma membrane remain largely unknown. Studies in seabream, Atlantic halibut, and stinging catfish, using frog oocytes as a heterologous expression system for wild-type or chimeric Aqp1ab constructs, suggest that the C-termini of these channels contain putative regulatory motifs that may control their intracellular trafficking. In the seabream, Ser^{254} at the cytoplasmic C-terminus, as well as a di-Leu motif located in the same domain, can mediate Aqp1ab recycling (Tingaud-Sequeira *et al*., 2008), but the mechanisms that enhance the insertion of the channel into the oocyte plasma membrane during hydration remain elusive. In addition, it has been found that the

trafficking of halibut Aqp1ab to the oocyte plasma membrane only occurs when it is ectopically expressed in native or piscine (e.g. zebrafish) oocytes, although membrane trafficking is rescued in *X. laevis* oocytes when the channel is co-expressed with polyA$^+$ mRNA purified from native post-vitellogenic ovarian follicles (Zapater *et al*., 2011). These surprising observations may suggest that Atlantic halibut Aqp1ab may have evolved more specialized mechanisms than the seabream ortholog for its intracellular transport in oocytes. However, immunological inhibition of Aqp1ab in halibut oocytes only halves the hydration (Zapater *et al*., 2011), which may indicate that another aquaporin, perhaps a yet unidentified Aqp1ab duplicate, might also be involved in oocyte hydration. Therefore, the establishment of the molecular pathways involved in Aqp1ab trafficking in fish oocytes require further investigation.

The potential endocrine regulation of Aqp1ab trafficking is also unknown. However, in the stinging catfish, cAMP can drive the sorting of Aqp1ab to the plasma membrane of *X. laevis* oocytes, presumably through PKA-mediated phosphorylation of Ser^{277} (Chaube *et al*., 2011). This observation is interesting since, as mentioned earlier, oocyte hydration in this species can be triggered by Avt, whose mammalian counterpart AVP initiates the intracellular transport of tetrapod AQP2 to the plasma membrane of renal epithelial cells through the cAMP/PKA pathway. Accordingly, the catfish oocyte expresses the Avtr2 which activates adenylate cyclase via Gs proteins to increase the intracellular levels of cAMP (Joy and Chaube, 2015). Therefore, although the stinging catfish is not a pelagophil species, it potentially offers the first model of an endocrine post-translational regulation of Aqp1ab in teleost oocytes (Cerdà *et al*., 2017). However, in more advanced euacanthomorph teleosts, including marine pelagophil species, it is unknown whether an intraovarian vasotocinergic system can regulate oocyte meiotic maturation and hydration as it occurs in the catfish. Thus, the investigation of this mechanism in the oocyte of these species may provide novel insights into the transductional pathways controlling Aqp1ab trafficking and insertion in the oocyte surface during meiotic maturation and hydration.

1.5. References

Abdelrahman H, ElHady M, Alcivar-Warren A, Allen S, Al-Tobasei R, Bao L, Beck B, Blackburn H, Bosworth B, Buchanan J, *et al*. 2017. Aquaculture genomics, genetics and breeding in the United States: current status, challenges, and priorities for future research. *BMC Genomics*. 18(1):191. doi: 10.1186/s12864-017-3557-1.

Agre P, Preston GM, Smith BL, Jung JS, Raina S, Moon C, Guggino WB, Nielsen S. 1993. Aquaporin CHIP: the archetypal molecular water channel. *Am J Physiol*. 265(4 Pt 2):F463-76. doi: 10.1152/ajprenal.1993.265.4.F463.

Almasalmeh A, Krenc D, Wu B, Beitz E. 2014. Structural determinants of the hydrogen peroxide permeability of aquaporins. *FEBS J*. 281(3):647-56. doi: 10.1111/febs.12653.

Aoki Y, Nagao I, Saito D, Ebe Y, Kinjo M, Tanaka M. 2008. Temporal and spatial localization of three germline-specific proteins in medaka. *Dev Dyn*. 237(3):800-7. doi: 10.1002/dvdy.21448.

Baumgarten R, Van De Pol MH, Wetzels JF, Van Os CH, Deen PM. 1998. Glycosylation is not essential for vasopressin-dependent routing of aquaporin-2 in transfected Madin-Darby canine kidney cells. *J Am Soc Nephrol*. 9(9):1553-9. doi: 10.1681/ASN.V991553.

Beitz E, Liu K, Ikeda M, Guggino WB, Agre P, Yasui M. 2006. Determinants of AQP6 trafficking to intracellular sites versus the plasma membrane in transfected mammalian cells. *Biol Cell*. 98(2):101-9. doi: 10.1042/BC20050025.

Bobe J, Goetz FW. 2001. A novel osteopontin-like protein is expressed in the trout ovary during ovulation. *FEBS Lett*. 489(2-3):119-24. doi: 10.1016/s0014-5793(01)02090-7.

Bobe J. 2015. Egg quality in fish: Present and future challenges. *Animal Front*. 5(1):66-72. doi:10.2527/af.2015-0010.

Bouley R, Breton S, Sun T, McLaughlin M, Nsumu NN, Lin HY, Ausiello DA, Brown D. 2000. Nitric oxide and atrial natriuretic factor stimulate cGMP-dependent membrane insertion of aquaporin 2 in renal epithelial cells. *J Clin Invest*. 106(9):1115-26. doi: 10.1172/JCI9594.

Boury-Jamot M, Sougrat R, Tailhardat M, Le Varlet B, Bonté F, Dumas M, Verbavatz JM. 2006. Expression and function of aquaporins in human skin: Is aquaporin-3 just a glycerol transporter? *Biochim Biophys Acta*. 1758(8):1034-42. doi: 10.1016/j.bbamem.2006.06.013.

Brown D. 2003. The ins and outs of aquaporin-2 trafficking. *Am J Physiol Renal Physiol*. 284(5):F893-901. doi: 10.1152/ajprenal.00387.2002.

Cerdà J, Chauvigné F, Finn RN. 2017. The physiological role and regulation of aquaporins in teleost germ cells. *Adv Exp Med Biol*. 969:149-171. doi: 10.1007/978-94-024-1057-0_10.

Cerdà J, Fabra M, Raldúa D. 2007. Physiological and molecular basis of fish oocyte hydration. In: Babin, P.J., Cerdà, J., Lubzens, E (eds). The Fish Oocyte. Springer. 349-396. doi: 10.1007/978-1-4020-6235-3_12.

Cerdà J, Finn RN. 2010. Piscine aquaporins: an overview of recent advances. *J Exp Zool A Ecol Genet Physiol*. 313(10):623-50. doi: 10.1002/jez.634.

Cerdà J, Reidenbach S, Prätzel S, Franke WW. 1999. Cadherin-catenin complexes during zebrafish oogenesis: heterotypic junctions between oocytes and follicle cells. *Biol Reprod*. 61(3):692-704. doi: 10.1095/biolreprod61.3.692.

Cerdà J. 2018. Oogenesis, Fish Amphibians. In: Skinner M (eds). Encyclopedia of Reproduction, 2nd Ed, Vol 6. Elsevier. 228-233. doi: 10.1016/B978-0-12-809633-8.20561-X.

Cerdà J. 2009. Molecular pathways during marine fish egg hydration: the role of aquaporins. *J Fish Biol*. 75(9):2175-96. doi: 10.1111/j.1095-8649.2009.02397.x.

Cerdà J., Bobe J., Babin P.J., Admon A., Lubzens E. 2008. Functional genomics and proteomic approaches for the study of gamete formation and viability in farmed finfish. *Fisheries Sciences*. 16:54-70. doi: 10.1080/10641260802324685.

Chaube R, Chauvigné F, Tingaud-Sequeira A, Joy KP, Acharjee A, Singh V, Cerdà J. 2011. Molecular and functional characterization of catfish (*Heteropneustes fossilis*) aquaporin-

1b: changes in expression during ovarian development and hormone-induced follicular maturation. *Gen Comp Endocrinol*. 170(1):162-71. doi: 10.1016/j.ygcen.2010.10.002.

Chauvigné F, Boj M, Finn RN, Cerdà J. 2015. Mitochondrial aquaporin-8-mediated hydrogen peroxide transport is essential for teleost spermatozoon motility. *Sci Rep*. 5:7789. doi: 10.1038/srep07789.

Chauvigné F, González W, Ramos S, Ducat C, Duncan N, Giménez I, Cerdà J. 2018. Seasonal-and dose-dependent effects of recombinant gonadotropins on sperm production and quality in the flatfish Solea senegalensis. *Comp Biochem Physiol A Mol Integr Physiol*. 225:59-64. doi: 10.1016/j.cbpa.2018.06.022.

Chauvigné F, Ollé J, González W, Duncan N, Giménez I, Cerdà J. 2017. Toward developing recombinant gonadotropin-based hormone therapies for increasing fertility in the flatfish *Senegalese sole*. *PLoS One*. 12(3):e0174387. doi: 10.1371/journal.pone.0174387.

Chauvigné F, Yilmaz O, Ferré A, Fjelldal PG, Finn RN, Cerdà J. 2019. The vertebrate Aqp14 water channel is a neuropeptide-regulated polytransporter. *Commun Biol*. 2:462. doi: 10.1038/s42003-019-0713-y.

Choi HJ, Jung HJ, Kwon TH. 2015. Extracellular pH affects phosphorylation and intracellular trafficking of AQP2 in inner medullary collecting duct cells. *Am J Physiol Renal Physiol*. 308(7):F737-48. doi: 10.1152/ajprenal.00376.2014.

Craik JCA, Harvey SM. 1987. The causes of buoyancy in eggs of marine teleosts. *J Mar Biol Ass UK*. 67(1) 169-182. doi:10.1017/S0025315400026436.

Crespo D, Bonnet E, Roher N, MacKenzie SA, Krasnov A, Goetz FW, Bobe J, Planas JV. 2010. Cellular and molecular evidence for a role of tumor necrosis factor alpha in the ovulatory mechanism of trout. *Reprod Biol Endocrinol*. 8:34. doi: 10.1186/1477-7827-8-34.

Crespo D, Goetz FW, Planas JV. 2015. Luteinizing hormone induces ovulation via tumor necrosis factor α-dependent increases in prostaglandin F2α in a nonmammalian vertebrate. *Sci Rep*. 5:14210. doi: 10.1038/srep14210.

da Silva IV, Cardoso C, Méndez-Giménez L, Camoes SP, Frühbeck G, Rodríguez A, Miranda JP, Soveral G. 2020. Aquaporin-7 and aquaporin-12 modulate the inflammatory phenotype of endocrine pancreatic beta-cells. *Arch Biochem Biophys*. 691:108481. doi: 10.1016/j.abb.2020.108481.

Day RE, Kitchen P, Owen DS, Bland C, Marshall L, Conner AC, Bill RM, Conner MT. 2014. Human aquaporins: regulators of transcellular water flow. *Biochim Biophys Acta*. 1840(5):1492-506. doi: 10.1016/j.bbagen.2013.09.033.

De Bellis M, Pisani F, Mola MG, Basco D, Catalano F, Nicchia GP, Svelto M, Frigeri A. 2014. A novel human aquaporin-4 splice variant exhibits a dominant-negative activity: a new mechanism to regulate water permeability. *Mol Biol Cell*. 25(4):470-80. doi: 10.1091/mbc.E13-06-0331.

de Siqueira-Silva DH, Saito T, Dos Santos-Silva AP, da Silva Costa R, Psenicka M, Yasui GS. 2018. Biotechnology applied to fish reproduction: tools for conservation. *Fish Physiol Biochem*. 44(6):1469-1485. doi: 10.1007/s10695-018-0506-0.

Dong C, Chen L, Feng J, Xu J, Mahboob S, Al-Ghanim K, Li X, Xu P. 2016. Genome wide identification, phylogeny, and expression of aquaporin genes in common carp (*Cyprinus carpio*). *PLoS One*. 11(12):e0166160. doi: 10.1371/journal.pone.0166160.

Echevarria M, Windhager EE, Tate SS, Frindt G. 1994. Cloning and expression of AQP3, a water channel from the medullary collecting duct of rat kidney. *Proc Natl Acad Sci U S A*. 91(23):10997-1001. doi: 10.1073/pnas.91.23.10997.

Eddy EM. 1975. Germ plasm and the differentiation of the germ cell line. *Int Rev Cytol*. 43:229-80. doi: 10.1016/s0074-7696(08)60070-4.

Elkouby YM, Mullins MC. 2017. Coordination of cellular differentiation, polarity, mitosis and meiosis - New findings from early vertebrate oogenesis. *Dev Biol*. 430(2):275-287. doi: 10.1016/j.ydbio.2017.06.029.

Escobar-Aguirre M, Elkouby YM, Mullins MC. 2017. Localization in Oogenesis of Maternal Regulators of Embryonic Development. *Adv Exp Med Biol*. 953:173-207. doi: 10.1007/978-3-319-46095-6_5.

Eto K, Noda Y, Horikawa S, Uchida S, Sasaki S. 2010. Phosphorylation of aquaporin-2 regulates its water permeability. *J Biol Chem*. 285(52):40777-84. doi: 10.1074/jbc.M110.151928.

Fabra M, Raldúa D, Bozzo MG, Deen PM, Lubzens E, Cerdà J. 2006. Yolk proteolysis and aquaporin-1o play essential roles to regulate fish oocyte hydration during meiosis resumption. *Dev Biol*. 295(1):250-62. doi: 10.1016/j.ydbio.2006.03.034.

Fabra M, Raldúa D, Power DM, Deen PM, Cerdà J. 2005. Marine fish egg hydration is aquaporin-mediated. Science. 307(5709):545. doi: 10.1126/science.1106305.

Fenton RA, Murali SK, Moeller HB. 2020. Advances in Aquaporin-2 trafficking mechanisms and their implications for treatment of water balance disorders. *Am J Physiol Cell Physiol*. 319:C1–C10. doi: 10.1152/ajpcell.00150.2020.

Finn RN. 2007. Vertebrate yolk complexes and the functional implications of phosvitins and other subdomains in vitellogenins. *Biol Reprod*. 76:926–935. doi: 10.1095/biolreprod.106.059766

Finn RN, Cerdà J. 2011. Aquaporin evolution in fishes. *Front Physiol*. 2:44. doi: 10.3389/fphys.2011.00044.

Finn RN, Cerdà J. 2015. Evolution and functional diversity of aquaporins. *Biol Bull*. 229(1):6-23. doi: 10.1086/BBLv229n1p6.

Finn RN, Chauvigné F, Hlidberg JB, Cutler CP, Cerdà J. 2014. The lineage-specific evolution of aquaporin gene clusters facilitated tetrapod terrestrial adaptation. *PLoS One*. 9(11):e113686. doi: 10.1371/journal.pone.0113686.

Finn RN, Fyhn HJ. 2010. Requirement for aminoacids in ontogeny of fish. *Aquac Res*. 41:684–716. 10.1111/j.1365-2109.2009.02220.x.

Finn RN, Kristoffersen BA. 2007. Vertebrate vitellogenin gene duplication in relation to the "3R hypothesis": correlation to the pelagic egg and the oceanic radiation of teleosts. *PLoS One*. 2(1):e169. doi: 10.1371/journal.pone.0000169.

Finn RN, Østby GC, Norberg B, Fyhn HJ. 2002. *In vivo* oocyte hydration in Atlantic halibut (*Hippoglossus hippoglossus*); proteolytic liberation of free amino acids, and ion transport, are driving forces for osmotic water influx. *J Exp Biol*. 205(Pt 2):211-24. doi: 10.1242/jeb.205.2.211.

Finn RN, Cerdà J. 2018. Aquaporin. In: Choi S (eds). Encyclopedia of Signaling Molecules. Springer. 374–390. doi: 10.1007/978-3-319-67199-4_101692.

Froehlich HE, Gentry RR, Rust MB, Grimm D, Halpern BS. 2017. Public perceptions of aquaculture: Evaluating spatiotemporal patterns of sentiment around the world. *PLoS One*. 12(1):e0169281. doi: 10.1371/journal.pone.0169281.

Gazzarrini S, Kang M, Epimashko S, Van Etten JL, Dainty J, Thiel G, Moroni A. 2006. Chlorella virus MT325 encodes water and potassium channels that interact synergistically. *Proc Natl Acad Sci U S A*. 103(14):5355-60. doi: 10.1073/pnas.0600848103.

Geyer RR, Musa-Aziz R, Qin X, Boron WF. 2013. Relative $CO_{(2)}/NH_{(3)}$ selectivities of mammalian aquaporins 0-9. *Am J Physiol Cell Physiol*. 304(10):C985-94. doi: 10.1152/ajpcell.00033.2013.

Gonen T, Walz T. 2006. The structure of aquaporins. *Q Rev Biophys*. 39(4):361-96. doi: 10.1017/S0033583506004458.

Grier HJ. 2012. Development of the follicle complex and oocyte staging in red drum, Sciaenops ocellatus Linnaeus, 1776 (Perciformes, Sciaenidae). *J Morphol*. 273(8):801-29. doi: 10.1002/jmor.20034.

Gunnarson E, Zelenina M, Aperia A. 2004. Regulation of brain aquaporins. *Neuroscience*. 129(4):947-55. doi: 10.1016/j.neuroscience.2004.08.022.

Gutierrez DB, Garland D, Schey KL. 2011. Spatial analysis of human lens aquaporin-0 post-translational modifications by MALDI mass spectrometry tissue profiling. *Exp Eye Res*. 93(6):912-20. doi: 10.1016/j.exer.2011.10.007.

Hagiwara A, Ogiwara K, Katsu Y, Takahashi T. 2014. Luteinizing hormone-induced expression of Ptger4b, a prostaglandin E2 receptor indispensable for ovulation of the

medaka Oryzias latipes, is regulated by a genomic mechanism involving nuclear progestin receptor. *Biol Reprod*. 90(6):126. doi: 10.1095/biolreprod.113.115485.

Hara-Chikuma M, Chikuma S, Sugiyama Y, Kabashima K, Verkman AS, Inoue S, Miyachi Y. 2012. Chemokine-dependent T cell migration requires aquaporin-3-mediated hydrogen peroxide uptake. *J Exp Med*. 209(10):1743-52. doi: 10.1084/jem.20112398.

Hara-Chikuma M, Satooka H, Watanabe S, Honda T, Miyachi Y, Watanabe T, Verkman AS. 2015. Aquaporin-3-mediated hydrogen peroxide transport is required for NF-κB signalling in keratinocytes and development of psoriasis. *Nat Commun*. 6:7454. doi: 10.1038/ncomms8454.

Hendriks G, Koudijs M, van Balkom BW, Oorschot V, Klumperman J, Deen PM, van der Sluijs P. 2004. Glycosylation is important for cell surface expression of the water channel aquaporin-2 but is not essential for tetramerization in the endoplasmic reticulum. *J Biol Chem*. 279(4):2975-83. doi: 10.1074/jbc.M310767200.

Heymann JB, Engel A. 2000. Structural clues in the sequences of the aquaporins. *J Mol Biol*. 295(4):1039-53. doi: 10.1006/jmbi.1999.3413.

Ikeda M, Andoo A, Shimono M, Takamatsu N, Taki A, Muta K, Matsushita W, Uechi T, Matsuzaki T, Kenmochi N, *et al*. 2011. The NPC motif of aquaporin-11, unlike the NPA motif of known aquaporins, is essential for full expression of molecular function. *J Biol Chem*. 286(5):3342-50. doi: 10.1074/jbc.M110.180968.

Ishibashi K, Morinaga T, Kuwahara M, Sasaki S, Imai M. 2002. Cloning and identification of a new member of water channel (AQP10) as an aquaglyceroporin. *Biochim Biophys Acta*. 1576(3):335-40. doi: 10.1016/s0167-4781(02)00393-7.

Ishibashi K, Morishita Y, Tanaka Y. 2017. The evolutionary aspects of aquaporin family. *Adv Exp Med Biol*. 969:35-50. doi: 10.1007/978-94-024-1057-0_2.

Ishibashi K, Tanaka Y, Morishita Y. 2014. The role of mammalian superaquaporins inside the cell. *Biochim Biophys Acta*. 1840(5):1507-12. doi: 10.1016/j.bbagen.2013.10.039.

Ishibashi K. 1996. Aquaporin water channels. *Nihon Rinsho*. 54(3):685-91. Japanese.

Itoh T, Rai T, Kuwahara M, Ko SB, Uchida S, Sasaki S, Ishibashi K. 2005. Identification of a novel aquaporin, AQP12, expressed in pancreatic acinar cells. *Biochem Biophys Res Commun*. 330(3):832-8. doi: 10.1016/j.bbrc.2005.03.046.

Jalabert B. 2005. Particularities of reproduction and oogenesis in teleost fish compared to mammals. *Reprod Nutr Dev*. 2005. 45(3):261-79. doi: 10.1051/rnd:2005019.

Johnson AK, Grier HJ. 2018. Ovarian germinal epithelium, oocyte development and the secretory epithelium in monkfish (Lophius americanus Valenciennes). *J Morphol*. 279(12):1887-1896. doi: 10.1002/jmor.20910.

Joy KP, Chaube R. 2015. Vasotocin--A new player in the control of oocyte maturation and ovulation in fish. *Gen Comp Endocrinol*. 221:54-63. doi: 10.1016/j.ygcen.2015.02.013.

Jung JS, Preston GM, Smith BL, Guggino WB, Agre P. 1994. Molecular structure of the water channel through aquaporin CHIP. The hourglass model. *J Biol Chem*. 269(20):14648-54.

Kagawa H, Kishi T, Gen K, Kazeto Y, Tosaka R, Matsubara H, Matsubara T, Sawaguchi S. 2011. Expression and localization of aquaporin 1b during oocyte development in the Japanese eel (*Anguilla japonica*). *Reprod Biol Endocrinol*. 9:71. doi: 10.1186/1477-7827-9-71.

Kitchen P, Salman MM, Pickel SU, Jennings J, Törnroth-Horsefield S, Conner MT, Bill RM, Conner AC. 2019. Water channel pore size determines exclusion properties but not solute selectivity. *Sci Rep*. 9(1):20369. doi: 10.1038/s41598-019-56814-z.

Knaut H, Schier AF. 2008. Clearing the path for germ cells. *Cell*. 132(3):337-9. doi: 10.1016/j.cell.2008.01.023.

Kristofersen BA, Nerland A, Nilsen F, Kolarevic J, Finn RN. 2009. Genomic and proteomic analyses reveal nonneofunctionalized vitellogenins in a basal clupeocephalan, the Atlantic herring, and point to the origin of maturational yolk proteolysis in marine teleosts. *Mol Biol Evol*. 26(5):1029-44. doi: 10.1093/molbev/msp014.

Kristoffersen BA, Finn RN. 2008. Major osmolyte changes during oocyte hydration of a clupeocephalan marine benthophil: Atlantic herring (*Clupea harengus*). *Mar Biol*. 154:683–692. doi: 10.1007/s00227-008-0961-8.

Kwok HF, So WK, Wang Y, Ge W. 2005. Zebrafish gonadotropins and their receptors: I. Cloning and characterization of zebrafish follicle-stimulating hormone and luteinizing hormone receptors--evidence for their distinct functions in follicle development. *Biol Reprod*. 72(6):1370-81. doi: 10.1095/biolreprod.104.038190.

Laforenza U, Scaffino MF, Gastaldi G. 2013. Aquaporin-10 represents an alternative pathway for glycerol efflux from human adipocytes. *PLoS One*. 8(1):e54474. doi: 10.1371/journal.pone.0054474.

Lahnsteiner F, Soares F, Ribeiro L, Dinis MT. 2009. Egg quality determination in teleost fish. In: Cabrita E, Robles V, Herraez P (eds). Methods in Reproductive Aquaculture, Marine and Freshwater Species. CRC Press. 149–173. doi: 10.1201/9780849380549.ch4.

Leitch V, Agre P, King LS. 2001. Altered ubiquitination and stability of aquaporin-1 in hypertonic stress. *Proc Natl Acad Sci U S A*. 98(5):2894-8. doi: 10.1073/pnas.041616498.

Levavi-Sivan B, Bogerd J, Mananos EL, Gomez A, Lareyre JJ. 2010. Perspectives on fish gonadotropins and their receptors. *Gen Comp Endocrinol*. 165:412-437. doi: 10.1016/j.ygcen.2009.07.019.

Li C, Wang W. 2017. Molecular biology of aquaporins. *Adv Exp Med Biol*. 969:1-34. doi: 10.1007/978-94-024-1057-0_1.

Lo WK, Biswas SK, Brako L, Shiels A, Gu S, Jiang JX. 2014. Aquaporin-0 targets interlocking domains to control the integrity and transparency of the eye lens. *Invest Ophthalmol Vis Sci*. 55(3):1202-12. doi: 10.1167/iovs.13-13379.

Lorente-Martínez H, Agorreta A, Torres-Sánchez M, San Mauro D. 2018. Evidence of positive selection suggests possible role of aquaporins in the water-to-land transition of mudskippers. *Org Divers Evol*. 18, 499–514. doi: 10.1007/s13127-018-0382-6.

Lu M, Lee MD, Smith BL, Jung JS, Agre P, Verdijk MA, Merkx G, Rijss JP, Deen PM. 1996. The human AQP4 gene: definition of the locus encoding two water channel

polypeptides in brain. *Proc Natl Acad Sci U S A*. 93(20):10908-12. doi: 10.1073/pnas.93.20.10908.

Lubzens E, Bobe J, Young G, Sullivan C. 2017. Maternal investment in fish oocytes and eggs: The molecular cargo and its contributions to fertility and early development. *Aquaculture*. 472,107-143. doi:10.1016/j.aquaculture.2016.10.029

Lubzens E, Young G, Bobe J, Cerdà J. 2010. Oogenesis in teleosts: how eggs are formed. *Gen Comp Endocrinol*. 165(3):367-89. doi: 10.1016/j.ygcen.2009.05.022.

Luckenbach JA, Iliev DB, Goetz FW, Swanson P. 2008. Identification of differentially expressed ovarian genes during primary and early secondary oocyte growth in coho salmon, *Oncorhynchus kisutch*. *Reprod Biol Endocrinol*. 6:2. doi: 10.1186/1477-7827-6-2.

Lyman-Gingerich J, Pelegrí F. 2007. Material factors in fish oogenesis and embryonic development. In: Babin PJ, Cerdà J, Lubzens E (eds). The Fish Oocyte. Springer. 141-174. doi: 10.1007/978-1-4020-6235-3_6.

Madsen SS, Engelund MB, Cutler CP. 2015. Water transport and functional dynamics of aquaporins in osmoregulatory organs of fishes. *Biol Bull*. 229(1):70-92. doi: 10.1086/BBLv229n1p70.

Marples D, Knepper MA, Christensen EI, Nielsen S. 1995. Redistribution of aquaporin-2 water channels induced by vasopressin in rat kidney inner medullary collecting duct. *Am J Physiol*. 269(3 Pt 1):C655-64. doi: 10.1152/ajpcell.1995.269.3.C655.

Mateo Sánchez S, Freeman SD, Delacroix L, Malgrange B. 2016. The role of post-translational modifications in hearing and deafness. *Cell Mol Life Sci*. 73(18):3521-33. doi: 10.1007/s00018-016-2257-3.

Matsubara T, Nagae M, Ohkubo N, Andoh T, Sawaguchi S, Hiramatsu N, Sullivan CV, Hara A. 2003. Multiple vitellogenins and their unique roles in marine teleosts. *Fish Physiol Biochem*. 28:295–299. doi: 10.1023/B:FISH.0000030559.71954.37

Mazón MJ, Molés G, Rocha A, Crespo B, Lan-Chow-Wing O, Espigares F, Muñoz I, Felip A, Carrillo M, Zanuy S, Gómez A. 2015. Gonadotropins in European sea bass: Endocrine

roles and biotechnological applications. *Gen Comp Endocrinol*. 221:31-41. doi: 10.1016/j.ygcen.2015.05.002.

Menn FL, Cerdà J, Babin PJ. 2007. Ultrastructural aspects of the ontogeny and differentiation of ray-finned fish ovarian follicles. In: Babin PJ, Cerdà J, Lubzens E (eds). The Fish Oocyte. Springer. 1-38. doi: 10.1007/978-1-4020-6235-3_1.

Moeller HB, Aroankins TS, Slengerik-Hansen J, Pisitkun T, Fenton RA. 2014. Phosphorylation and ubiquitylation are opposing processes that regulate endocytosis of the water channel aquaporin-2. *J Cell Sci*. 127(Pt 14):3174-83. doi: 10.1242/jcs.150680.

Müller C, Sendler M, Hildebrandt JP. 2006. Downregulation of aquaporins 1 and 5 in nasal gland by osmotic stress in ducklings, Anas platyrhynchos: implications for the production of hypertonic fluid. *J Exp Biol*. 209(Pt 20):4067-76. doi: 10.1242/jeb.02491.

Mylonas CC, Duncan NJ, Asturiano JF. 2017. Hormonal manipulations for the enhancement of sperm production in cultured fish and evaluation of sperm quality. *Aquaculture*. 472: 21–44. doi: 10.1016/j.aquaculture.2016.04.021.

Mylonas, C.C., Fostier, A., Zanuy, S., 2010. Broodstock management and hormonal manipulations of fish reproduction. *Gen Comp Endocrinol*. 165, 516–534. doi: 10.1016/j.ygcen.2009.03.007.

Nagahama Y, Yamashita M. 2008. Regulation of oocyte maturation in fish. *Dev Growth Differ*. 50:S195-S219. doi: 10.1111/j.1440-169X.2008.01019.x.

Nakamura S, Kobayashi K, Nishimura T, Higashijima S, Tanaka M. 2010. Identification of germline stem cells in the ovary of the teleost medaka. *Science*. 328(5985):1561-3. doi: 10.1126/science.1185473.

Nakhoul NL, Davis BA, Romero MF, Boron WF. 1998. Effect of expressing the water channel aquaporin-1 on the CO_2 permeability of *Xenopus* oocytes. *Am J Physiol*. 274(2):C543-8. doi: 10.1152/ajpcell.1998.274.2.C543.

Nielsen S, Agre P. 1995. The aquaporin family of water channels in kidney. *Kidney Int*. 48(4):1057-68. doi: 10.1038/ki.1995.389.

Nielsen S, DiGiovanni SR, Christensen EI, Knepper MA, Harris HW. 1993. Cellular and subcellular immunolocalization of vasopressin-regulated water channel in rat kidney. *Proc Natl Acad Sci U S A*. 90(24):11663-7. doi: 10.1073/pnas.90.24.11663.

Pao GM, Wu LF, Johnson KD, Höfte H, Chrispeels MJ, Sweet G, Sandal NN, Saier MH Jr. 1991. Evolution of the MIP family of integral membrane transport proteins. *Mol Microbiol*. 5(1):33-7. doi: 10.1111/j.1365-2958.1991.tb01823.x.

Pinter J, Thomas P. 1999. Induction of ovulation of mature oocytes by the maturation-inducing steroid 17,20beta,21-trihydroxy-4-pregnen-3-one in the spotted seatrout. *Gen Comp Endocrinol*. 115(2):200-9. doi: 10.1006/gcen.1999.7312.

Prasad GV, Coury LA, Finn F, Zeidel ML. 1998. Reconstituted aquaporin 1 water channels transport CO_2 across membranes. *J Biol Chem*. 273(50):33123-6. doi: 10.1074/jbc.273.50.33123.

Preston GM, Agre P. 1991. Isolation of the cDNA for erythrocyte integral membrane protein of 28 kilodaltons: member of an ancient channel family. *Proc Natl Acad Sci U S A*. 88(24):11110-4. doi: 10.1073/pnas.88.24.11110.

Preston GM, Carroll TP, Guggino WB, Agre P. 1992. Appearance of water channels in *Xenopus* oocytes expressing red cell CHIP28 protein. *Science*. 256(5055):385-7. doi: 10.1126/science.256.5055.385.

Preston GM, Jung JS, Guggino WB, Agre P. 1993. The mercury-sensitive residue at cysteine 189 in the CHIP28 water channel. *J Biol Chem*. 268(1):17-20. doi: 10.1016/S0021-9258(18)54108-9.

Ripoche P, Goossens D, Devuyst O, Gane P, Colin Y, Verkman AS, Cartron JP. 2006. Role of RhAG and AQP1 in NH_3 and CO_2 gas transport in red cell ghosts: a stopped-flow analysis. *Transfus Clin Biol*. 13(1-2):117-22. doi: 10.1016/j.tracli.2006.03.004.

Rojek A, Praetorius J, Frøkiaer J, Nielsen S, Fenton RA. 2008. A current view of the mammalian aquaglyceroporins. *Annu Rev Physiol*. 70:301-27. doi: 10.1146/annurev.physiol.70.113006.100452.

Satooka H, Hara-Chikuma M. 2016. Aquaporin-3 controls breast cancer cell migration by regulating hydrogen peroxide transport and its downstream cell signaling. *Mol Cell Biol*. 36(7):1206-18. doi: 10.1128/MCB.00971-15.

Sawaguchi S, Ohkubo N, Matsubara T. 2006. Identification of two forms of vitellogenin-derived phosvitin and elucidation of their fate and roles during oocyte maturation in the barfin flounder, *Verasper moseri*. *Zool Sci*. 23:1021–1029. doi: 10.2108/zsj.23.1021.

Schrama D, Cerqueira M, Raposo CS, Rosa da Costa AM, Wulff T, Gonçalves A, Camacho C, Colen R, Fonseca F, Rodrigues PM. 2018. Dietary creatine supplementation in gilthead seabream (*Sparus aurata*): Comparative proteomics analysis on fish allergens, muscle quality, and liver. *Front Physiol*. 9:1844. doi: 10.3389/fphys.2018.01844.

Schroeder PC, Pendergrass P. 1976. The inhibition of in-vitro ovulation from follicles of the teleost, *Oryzias latipes*, by cytochalasin B. *J Reprod Fertil*. 48(2):327-30. doi: 10.1530/jrf.0.0480327.

Schroeder PC, Talbot P. 1985. Ovulation in the animal kingdom: a review with an emphasis on the role of contractile processes. *Gamete Res*. 11, 191–221. doi: 10.1002/mrd.1120110209.

Selman K, Wallace RA, Sarka A, Qi X. 1993. Stages of oocyte development in the zebrafish, Brachydanio rerio. *J Morphol*. 218(2):203-224. doi: 10.1002/jmor.1052180209.

Singh V, Chaube R, Joy KP. 2021. Vasotocin stimulates maturation-inducing hormone, oocyte maturation and ovulation in the catfish Heteropneustes fossilis: Evidence for a preferential calcium involvement. *Theriogenology*. 167:51-60. doi: 10.1016/j.theriogenology.2021.03.001.

Singh V, Joy KP. 2010. An involvement of vasotocin in oocyte hydration in the catfish *Heteropneustes fossilis*: A comparison with effects of isotocin and hCG. *Gen Comp Endocrinol*. 166(3):504-12. doi: 10.1016/j.ygcen.2010.02.020.

Sohara E, Rai T, Yang SS, Uchida K, Nitta K, Horita S, Ohno M, Harada A, Sasaki S, Uchida S. 2006. Pathogenesis and treatment of autosomal-dominant nephrogenic diabetes

insipidus caused by an aquaporin 2 mutation. *Proc Natl Acad Sci U S A*. 103(38):14217-22. doi: 10.1073/pnas.0602331103.

Song Y, Sonawane N, Verkman AS. 2002. Localization of aquaporin-5 in sweat glands and functional analysis using knockout mice. *J Physiol*. 541(Pt 2):561-8. doi: 10.1113/jphysiol.2001.020180.

Soria LR, Fanelli E, Altamura N, Svelto M, Marinelli RA, Calamita G. 2010. Aquaporin-8-facilitated mitochondrial ammonia transport. *Biochem Biophys Res Commun*. 393(2):217-21. doi: 10.1016/j.bbrc.2010.01.104.

Soto G, Alleva K, Amodeo G, Muschietti J, Ayub ND. 2012. New insight into the evolution of aquaporins from flowering plants and vertebrates: orthologous identification and functional transfer is possible. *Gene*. 503(1):165-76. doi: 10.1016/j.gene.2012.04.021.

Sui H, Han BG, Lee JK, Walian P, Jap BK. 2001. Structural basis of water-specific transport through the AQP1 water channel. Nature. 414(6866):872-8. doi: 10.1038/414872a.

Suwa K, Yamashita M. Regulatory. 2007. Mechanisms of oocyte maturation and ovulation. In: Babin PJ, Cerdà J, Lubzens E (eds). The Fish Oocyte. Springer. 323-348. doi: 10.1007/978-1-4020-6235-3_11.

Suzuki H, Nishikawa K, Hiroaki Y, Fujiyoshi Y. 2008. Formation of aquaporin-4 arrays is inhibited by palmitoylation of N-terminal cysteine residues. *Biochim Biophys Acta*. 1778(4):1181-9. doi: 10.1016/j.bbamem.2007.12.007.

Suzuki M, Shibata Y, Ogushi Y, Okada R. 2015. Molecular machinery for vasotocin-dependent transepithelial water movement in amphibians: aquaporins and evolution. *Biol Bull*. 229(1):109-19. doi: 10.1086/BBLv229n1p109.

Szöllösi D, Jalabert B, Breton B. 1978. Postovulatory changes in the theca folliculi of the trout. *Ann Biol Anim*. 18, 883–891. doi: 10.1051/rnd:19780520.

Takahashi T, Hagiwara A, Ogiwara K. 2019. Follicle rupture during ovulation with an emphasis on recent progress in fish models. *Reproduction*. 157(1):R1-R13. doi: 10.1530/REP-18-0251.

Tamma G, Ranieri M, Di Mise A, Centrone M, Svelto M, Valenti G. 2014. Glutathionylation of the aquaporin-2 water channel: a novel post-translational modification modulated by the oxidative stress. *J Biol Chem*. 289(40):27807-13. doi: 10.1074/jbc.M114.586024.

Theuerkauf SJ, Morris JA Jr, Waters TJ, Wickliffe LC, Alleway HK, Jones RC. 2019. A global spatial analysis reveals where marine aquaculture can benefit nature and people. *PLoS One*. 14(10):e0222282. doi: 10.1371/journal.pone.0222282.

Thibault C. 1999. Ovulation. *Contracept Fertil Sex*. 27(9):605-13. French.

Thomas P, Pang Y, Zhu Y, Detweiler C, Doughty K. 2004. Multiple rapid progestin actions and progestin membrane receptor subtypes in fish. *Steroids*. 69, 567–573. doi: 10.1016/j.steroids.2004.05.004.

Tingaud-Sequeira A, Calusinska M, Finn RN, Chauvigné F, Lozano J, Cerdà J. 2010. The zebrafish genome encodes the largest vertebrate repertoire of functional aquaporins with dual paralogy and substrate specificities similar to mammals. *BMC Evol Biol*. 10:38. doi: 10.1186/1471-2148-10-38.

Tingaud-Sequeira A, Chauvigné F, Fabra M, Lozano J, Raldúa D, Cerdà J. 2008. Structural and functional divergence of two fish aquaporin-1 water channels following teleost-specific gene duplication. *BMC Evol Biol*. 8:259. doi: 10.1186/1471-2148-8-259.

Tong H, Hu Q, Zhu L, Dong X. 2019. Prokaryotic aquaporins. *Cells*. 8(11):1316. doi: 10.3390/cells8111316.

Umenishi F, Schrier RW. 2003. Hypertonicity-induced aquaporin-1 (AQP1) expression is mediated by the activation of MAPK pathways and hypertonicity-responsive element in the AQP1 gene. *J Biol Chem*. 278(18):15765-70. doi: 10.1074/jbc.M209980200.

Viadiu H, Gonen T, Walz T. 2007. Projection map of aquaporin-9 at 7 A resolution. *J Mol Biol*. 367(1):80-8. doi: 10.1016/j.jmb.2006.12.042.

Virkki LV, Franke C, Somieski P, Boron WF. 2002. Cloning and functional characterization of a novel aquaporin from *Xenopus laevis* oocytes. *J Biol Chem*. 277(43):40610-6. doi: 10.1074/jbc.M206157200.

Wallace RA, Selman K. 1990. Ultrastructural aspects of oogenesis and oocyte growth in fish and amphibians. *J Electron Microsc Tech*. 16(3):175-201. doi: 10.1002/jemt.1060160302.

Williamson A, Lehmann R. 1996. Germ cell development in Drosophila. *Annu Rev Cell Dev Biol*. 12:365-91. doi: 10.1146/annurev.cellbio.12.1.365.

Wong KY, Wang WL, Su SH, Liu CF, Yu MJ. 2020. Intracellular location of aquaporin-2 serine 269 phosphorylation and dephosphorylation in kidney collecting duct cells. *Am J Physiol Renal Physiol*. 319(4):F592-F602. doi: 10.1152/ajprenal.00205.2020.

Wu XJ, Liu DT, Chen S, Hong W, Zhu Y. 2020. Impaired oocyte maturation and ovulation in membrane progestin receptor (mPR) knockouts in zebrafish. *Mol Cell Endocrinol*. 511:110856. doi: 10.1016/j.mce.2020.110856.

Wylie C. 2000. Germ cells. *Curr Opin Genet Dev*. 10(4):410-3. doi: 10.1016/s0959-437x(00)00105-2.

Yakata K, Tani K, Fujiyoshi Y. 2011. Water permeability and characterization of aquaporin-11. *J Struct Biol*. 174(2):315-20. doi: 10.1016/j.jsb.2011.01.003.

Yamashita M. 1998. Molecular mechanisms of meiotic maturation and arrest in fish and amphibian oocytes. *Semin Cell Dev Biol*. 9(5):569-79. doi: 10.1006/scdb.1998.0251.

Yilmaz O, Chauvigné F, Ferré A, Nilsen F, Fjelldal PG, Cerdà J, Finn RN. 2020. Unravelling the complex duplication history of deuterostome glycerol transporters. *Cells*. 9(7):1663. doi: 10.3390/cells9071663.

Yilmaz O, Patinote A, Nguyen TV, Com E, Lavigne R, Pineau C, Sullivan CV, Bobe J. 2017. Scrambled eggs: Proteomic portraits and novel biomarkers of egg quality in zebrafish (*Danio rerio*). *PLoS One*. 12(11):e0188084. doi: 10.1371/journal.pone.0188084.

Yoshida M. 2020. Overview: reproductive systems in aquatic animals. In: Yoshiba M, Asturiano JF (eds). Reproduction in Aquatic Animals. From Basic Biology to Aquaculture Technology. Springer. 13-24. doi: 10.1007/978-981-15-2290-1_2

Zapater C, Chauvigné F, Norberg B, Finn RN, Cerdà J. 2011. Dual neofunctionalization of a rapidly evolving aquaporin-1 paralog resulted in constrained and relaxed traits controlling channel function during meiosis resumption in teleosts. *Mol Biol Evol*. 28(11):3151-69. doi: 10.1093/molbev/msr146.

Zapater C, Chauvigné F, Scott AP, Gómez A, Katsiadaki I, Cerdà J. 2012. Piscine follicle-stimulating hormone triggers progestin production in gilthead seabream primary ovarian follicles. *Biol Reprod*. 87(5):111. doi: 10.1095/biolreprod.112.102533.

Zapater C, Chauvigné F, Tingaud-Sequeira A, Finn RN, Cerdà J. 2013. Primary oocyte transcriptional activation of Aqp1ab by the nuclear progestin receptor determines the pelagic egg phenotype of marine teleosts. *Dev Biol*. 377(2):345-62. doi: 10.1016/j.ydbio.2013.03.001.

Zardoya R. 2005. Phylogeny and evolution of the major intrinsic protein family. *Biol Cell*. 97(6):397-414. doi: 10.1042/BC20040134.

Zelenina M, Christensen BM, Palmér J, Nairn AC, Nielsen S, Aperia A. 2000. Prostaglandin E(2) interaction with AVP: effects on AQP2 phosphorylation and distribution. *Am J Physiol Renal Physiol*. 278(3):F388-94. doi: 10.1152/ajprenal.2000.278.3.F388.

Zhang Y, Peti-Peterdi J, Müller CE, Carlson NG, Baqi Y, Strasburg DL, Heiney KM, Villanueva K, Kohan DE, Kishore BK. 2015. P2Y12 receptor localizes in the renal collecting duct and its blockade augments arginine vasopressin action and alleviates nephrogenic diabetes insipidus. *J Am Soc Nephrol*. 26(12):2978-87. doi: 10.1681/ASN.2014010118.

Zhou LY, Wang DS, Kobayashi T, Yano A, Paul-Prasanth B, Suzuki A, Sakai F, Nagahama Y. 2007a. A novel type of P450c17 lacking the lyase activity is responsible for C21-steroid biosynthesis in the fish ovary and head kidney. *Endocrinology*. 148:4282-4291. doi: 10.1210/en.2007-0487.

Zhou LY, Wang DS, Shibata Y, Paul-Prasanth B, Suzuki A, Nagahama Y. 2007b. Characterization, expression and transcriptional regulation of P450c17-I and -II in the medaka, Oryzias latipes. *Biochem Biophys Res Comm*. 362:619-624. doi: 10.1016/j.bbrc.2007.08.044.

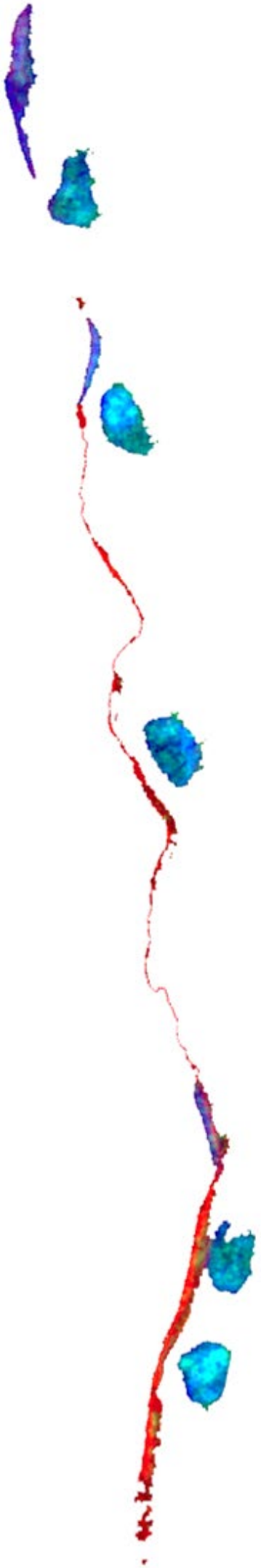

OBJECTIVES

In teleosts, two genes related to mammalian *AQP1* have been found and termed *aqp1aa* and *aqp1ab*. The latter *aqp1ab* gene arose by tandem duplication rather than whole genomic duplication. The Aqp1ab protein is a water-selective channel that plays an essential role in oocyte hydration of marine species that spawn pelagic eggs (pelagophils). The Aqp1ab channel is temporarily inserted into the oocyte plasma membrane during meiosis resumption to facilitate the hydration mechanism and thus assures a water reservoir when the single-celled eggs are released into the hyperosmotic seawater. This process confers the phenotypic nature of the pelagic egg (buoyancy), which not only provides the early embryos with a vital pool of water until osmoregulatory systems develop, but also results in their geodispersal in the oceanic environment. The Aqp1ab-mediated oocyte hydration mechanism is thus a highly critical event in the reproduction of marine teleosts, and represents one of the key factors that determines the survival and hence quality of female gametes in farmed marine fish.

Previous studies in the pelagophil gilthead seabream have uncovered the endocrine pathway for the transcriptional regulation of the *aqp1ab* gene in primary growth oocytes. However, the specific regulatory mechanisms that control the intracellular trafficking of Aqp1ab during vitellogenesis and oocyte maturation, resulting in the transport of the channel toward the oocyte cortex, and eventually into the microvillar portion of the oocyte plasma membrane, are not known. In addition, studies on the flatfish pelagophil Atlantic halibut surprisingly uncovered a unique trafficking regulation of the Aqp1ab channel of this species that seems to be different to that of the seabream. Such a trafficking regulation appears to be teleost-specific since it could not be replicated in amphibian oocytes. These findings suggest that alternative regulatory pathways may control the trafficking of teleost Aqp1ab, or that two Aqp1ab-related channels might coexist in teleosts, which may be differentially regulated.

It is well known that the intracellular transport of some mammalian AQPs, such as AQP2 in the kidney, is controlled by AVP through the cAMP/PKA signalling pathway. In teleosts, there is evidence that osmoregulatory adaptations, which are mainly regulated by the pituitary neuropeptide hormones Avt and It, respective orthologs of mammalian AVP and oxytocin, are associated with changes in the expression of AQP paralogs in the intestine. In addition, an ovarian vasotocinergic system has been proposed as an important

player in oocyte maturation and hydration in primitive teleosts, such as the stinging catfish. However, it is not known whether the same paracrine signalling pathway is present in modern acanthomorph pelagophil teleosts, such as the seabream, which may regulate Aqp1ab trafficking in the oocyte.

Finally, recent studies in mammals have reported the expression of multiple splice variants of AQP4 and AQP8. These alternative forms may represent new regulatory mechanisms through which the cell-surface expression and activity of AQPs can be physiologically modulated. Therefore, we propose to investigate whether an alternative splicing of *aqp1ab* mRNAs may exist in fish as an additional mechanism to control Aqp1ab function in the oocyte.

In the present thesis, three objectives have been established to investigate the three hypotheses proposed above. These objectives are as follows.

Objective 1: To investigate the possible existence of a second *aqp1ab* gene in teleosts, establish its phylogenetic and syntenic relationships with other piscine Aqp1-type genes, and study the diversity of the post-translational regulatory mechanisms for this group of channels (Chapter I).

Objective 2: To examine the existence of a vasotocinergic and isotocinergic paracrine system in the seabream ovary and its role in the regulation of Aqp1ab trafficking in the oocyte during hydration (Chapter II).

Objective 3: To identify alternative forms of *aqp1ab* genes in teleosts and study their potential implications in the regulation of Aqp1ab function in the oocyte (Chapter III).

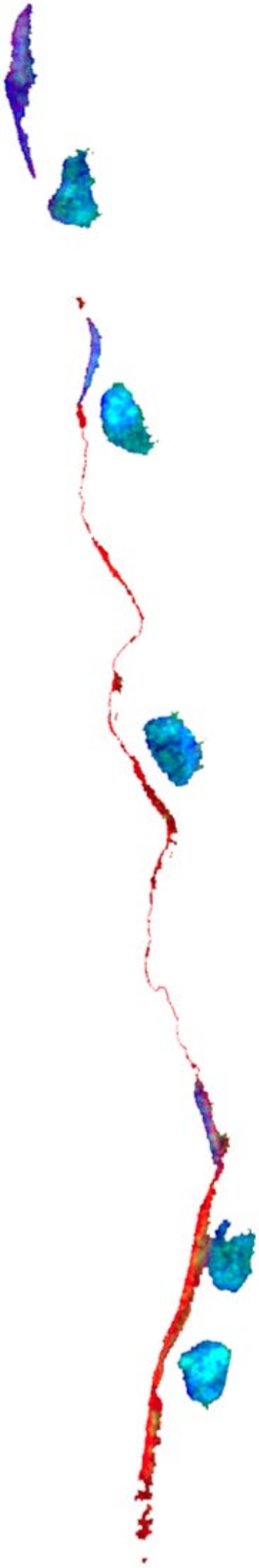

PUBLICATIONS

CHAPTER I:

Functional Evolution of Clustered Aquaporin Genes Reveals Insights into the Oceanic Success of Teleost Eggs

Alba Ferré [1], François Chauvigné [2], Anna Vlasova [3], Birgitta Norberg [4], Luca Bargelloni [5], Roderic Guigó [3 6], Roderick Nigel Finn [1 7], Joan Cerdà [1]

[1]Institute of Agrifood Research and Technology (IRTA)-Institute of Biotechnology and Biomedicine (IBB), Universitat Autònoma de Barcelona, Barcelona, Spain.
[2]Institute of Marine Sciences, Spanish National Research Council (CSIC), Barcelona, Spain.
[3]Centre for Genomic Regulation (CRG), The Barcelona Institute of Science and Technology, Barcelona, Spain.
[4]Institute of Marine Research, Austevoll Research Station, Storebø, Norway.
[5]Department of Comparative Biomedicine and Food Science (BCA), University of Padova, Legnaro, PD, Italy.
[6]Universitat Pompeu Fabra (UPF), Barcelona, Spain.
[7]Department of Biology, Bergen High Technology Centre, University of Bergen, Bergen, Norway.

Molecular Biology and Evolution. 40(4):msad071.
doi: 10.1093/molbev/msad071.

3.1.1. Abstract

Aquaporin-mediated oocyte hydration is considered important for the evolution of pelagic eggs and the radiative success of marine teleosts. However, the molecular regulatory mechanisms controlling this vital process are not fully understood. Here, we analyzed >400 piscine genomes to uncover a previously unknown teleost-specific aquaporin-1 cluster (TSA1C) comprised of tandemly arranged *aqp1aa-aqp1ab2-aqp1ab1* genes. Functional evolutionary analysis of the TSA1C reveals a ~300-million-year history of downstream *aqp1ab*-type gene loss, neofunctionalization and subfunctionalization, but with marine species that spawn highly hydrated pelagic eggs almost exclusively retaining at least one of the downstream paralogs. Unexpectedly, one third of the modern marine euacanthomorph teleosts selectively retain both *aqp1ab*-type channels, and co-evolved protein kinase-mediated phosphorylation sites in the intracellular subdomains together with teleost-specific Ywhaz-like (14-3-3ζ-like) binding proteins for co-operative membrane trafficking regulation. To understand the selective evolutionary advantages of these mechanisms, we show that a two-step regulated channel shunt avoids competitive occupancy of the same plasma membrane space in the oocyte and accelerates hydration. These data suggest that the evolution of the adaptive molecular regulatory features of the TSA1C facilitated the rise of pelagic eggs and their subsequent geodispersal in the oceanic currents.

Keywords: Functional evolution, teleosts, aquaporin, trafficking, 14-3-3 proteins, oocyte hydration

3.1.2. Introduction

The most dramatic evolutionary radiation in vertebrate history occurred amongst the true spiny ray-finned fishes (Euacanthomorphacea) in the late Cretaceous and early Eocene (Maissey, 1996; Friedman, 2010). Fossil evidence revealed that this unprecedented radiation transpired predominantly in marine environments in a fraction of the time it took for birds and mammals to achieve such diversity (Maissey, 1996; Friedman, 2010). The sudden appearance of the myriad of adult forms pertaining to hundreds of new families found in fossil sites around the world suggests that key traits associated with the adaptive marine radiation of euacanthomorph teleosts were also likely associated with an efficient mechanism of dispersal. In this regard, a key reproductive trait that may have independently evolved for the first time in the Triassic in marine elopomorph teleosts (the ancestors of extant eels, bonefishes, and tarpons) was the pelagic egg, which passively drifts in the oceanic currents (Finn and Kristoffersen, 2007). Upon fertilization, these free-floating, single-celled orbs of life become the caretakers of the genome, which holds the past, present, and future of the lineage. However, they are devoid of any of the organ systems or avoidance behaviors that develop in the juveniles and adults, yet must equally survive in the hyperosmotic oceanic environment to ensure its continuance. Despite the lack of parental care, the selective success of this reproductive trait certainly became manifest in the euacanthomorph marine teleosts, the majority of which regardless of their systematic affinities, demersal or pelagic habitats, coastal or oceanic distribution, or tropical or boreal ranges, spawn pelagic eggs (Ahlstrom and Moser, 1981; Kendall *et al*., 1984). Understanding the molecular adaptations associated with the evolution of such traits could therefore shed light on how teleosts came to dominate the oceans.

The pelagic nature of marine teleost eggs is considered to have arisen as an exaptation to the recolonization of seawater by freshwater ancestors (Fyhn *et al*., 1999; Finn *et al*., 2000; Finn and Kristoffersen, 2007). In this regard, it has been shown that the oocytes of oviparous marine teleosts that freely broadcast their eggs at spawning undergo substantial hydration during the phase of meiotic maturation (Finn and Fyhn, 2010; Cerdà *et al*., 2017). Since the yolk osmolality is the same as the body fluids of the adults and thus strongly hypoosmotic to seawater, the hydration provides the embryos with a vital pool of water until osmoregulatory cells and organs develop (Finn *et al*., 2002). The level of oocyte hydration is related to the degree of proteolysis of vitellogenin-derived yolk proteins and is most

pronounced in pelagic eggs, typically resulting in water contents of >90% of the egg mass, thus reducing the specific gravity below that of the ambient seawater and causing them to float (Finn, 2007; Sullivan and Yilmaz, 2018).

A facilitated pathway for water entry into the oocyte was discovered almost two decades ago as a teleost-specific, water-selective aquaporin (Aqp1o - now termed Aqp1ab) (Fabra *et al*., 2005). This channel is temporally inserted into the oocyte plasma membrane during meiotic maturation and maximal yolk proteolysis, and it is thus essential for the development of the pelagic egg phenotype (Fabra *et al*., 2006; Zapater *et al*., 2011 and 2013). The Aqp1ab channel is now known to belong to a broader superfamily of aquaporins (Agre *et al*., 1993), which in jawed vertebrates currently comprise 17 subfamilies (Aqp0-16) (Finn *et al*., 2014; Chauvigné *et al*., 2019). Teleosts, however, retain an even larger repertoire of aquaporins, in part due to independent whole genome duplications, but also due to more ancestral and lineage-specific tandem duplications (Tingaud-Sequeira *et al*., 2008 and 2010; Cerdà and Finn, 2010; Finn and Cerdà, 2011; Finn *et al*., 2014; Yilmaz *et al*., 2020). As a result, aquaporin gene clusters became more prevalent in the actinopterygian lineage with up to seven identified to date (i.e. *aqp1aa-1ab*; *aqp3a1-3a2*; *aqp3b1-3b2*; *aqp8aa-8ab*; *aqp8ba-8bb*; *aqp10aa-10ab*; and *aqp10ba-10bb*) compared to two in the sarcopterygian lineage (*AQP3-7* and *AQP2-5-6* type clusters) (Finn *et al*., 2014; Yilmaz *et al*., 2020). The actinopterygian *aqp1ab* gene thus evolved and neofunctionalized as a downstream tandem duplicate of the *aqp1aa* paralog, which retains a more conserved protein structure to tetrapod AQP1 (Tingaud-Sequeira *et al*., 2008; Zapater *et al*., 2011).

The *aqp1aa-1ab* binary cluster has so far been detected in all teleosts studied to date, including members of the elopomorph (e.g. eels), ostariophysan (e.g. zebrafishes, carps and catfishes), and euteleostean lineages such as protacanthopterygians (e.g. salmons) and euacanthomorphaceans (e.g. seabreams, seabasses, cichlids, flatfishes and pufferfishes) (Cerdà *et al*., 2017; Zhang *et al*., 2021). In two of these studies, however, a second *aqp1ab*-type gene was noted in the gilthead seabream (*Sparus aurata*) and African cichlids (Zapater *et al*., 2013; Finn *et al*., 2014). In the seabream, what appeared to be exon ghosts in the 5′-promoter region of *aqp1ab* indicated that a duplicated *aqp1ab*-type pseudogene existed in this locus (Zapater *et al*., 2013), while in the African cichlids, each species studied retained a tetra-exon copy of the *aqp1ab* gene in the same upstream locus (Finn *et al*., 2014).

To decipher whether the *aqp1ab* upstream genes in teleosts were the result of lineage-specific duplications or were inherited from a common ancestor, here we initially conducted a gene-walking experiment in the seabream. This revealed a complete tetra-exon *aqp1ab*-type gene, but when ectopically expressed in amphibian (*Xenopus laevis*) oocytes, the translated protein was not trafficked to the plasma membrane. Surprisingly, however, phylogenetic analyses revealed that the novel seabream *aqp1ab-type* coding sequence (CDS) was more closely related to the African cichlid upstream *aqp1ab* CDS, as well as the previously studied Atlantic halibut (*Hippoglossus hippoglossus*) *aqp1ab* CDS, which was only functional in native or teleost oocytes, but not when expressed in frog oocytes (Zapater *et al*., 2011). These observations suggested that the upstream *aqp1ab*-type gene was likely derived from a common ancestral duplication, and that a trafficking factor present in teleost oocytes was missing in amphibian oocytes. We therefore conducted a systematic phylogenetic survey amongst > 400 piscine genomes to uncover the ancient origin of a hitherto unknown teleost-specific *aqp1* cluster (TSA1C), comprised of *aqp1aa* and two *aqp1ab*-type genes. To understand the functional evolution of the channels in the TSA1C, we selected distantly related teleosts as models that retain one or both of the downstream *aqp1ab*-type genes. Using comparative transcriptomics and functional experiments, we reveal how the intracellular subdomains of the TSA1C channels co-evolved with teleost-specific Ywhaz-like regulatory proteins (Tyrosine 3-Monooxygenase/Tryptophan 5-Monooxygenase Activation proteins or 14-3-3ζ-like) together with protein kinase-mediated phosphorylation pathways to differentially regulate their membrane trafficking. The findings provide new insight into the molecular adaptations facilitating the success of teleost eggs in the oceans.

3.1.3. Materials and Methods

3.1.3.1. Animals and Reagents

Fish were obtained from different aquaculture stations in Spain and Norway, whereas adult *X. laevis* were purchased from the Centre de Ressources Biologiques Xénopes (University of Rennes, France). Details relating to the care and use of fish and frogs are described in (supplementary text S1, see Annexes, page 262). All reagents were purchased from Merck unless indicated otherwise. The commercial and custom made antibodies employed are described in (supplementary table S3, see Annexes, page 258).

3.1.3.2. Phylogenetic, Syntenic and Structural Analyses

Sequences were assembled from open-source databases, aligned and converted to codons prior to analysis via Bayesian inference, with *in silico* sequence analyses performed as described in (supplementary text S1, see Annexes, page 262). A list of aquaporin type, spawning habitat and egg type according to fishbase (https://www.fishbase.in/) is provided in (supplementary table S1, see Annexes, page 256). The syntenic analyses of the aquaporin genes were conducted via tblastn searches of WGS databases. Scaled sequence logos illustrating the relative conservation of resides in the aquaporin loop D and CT-subdomains were generated with Geneious v9.1.8 (Biomatters Ltd, New Zealand).

3.1.3.3. Transcriptome Shotgun Sequencing

Illumina RNA-seq library construction and HiSeq2500 sequencing were carried out to sequence the transcriptome of Atlantic halibut and *X. laevis* postvitellogenic ovarian follicles. The complete methods for *the novo* assembly of the transcriptomes and the identification of YWHA orthologs are described in (supplementary text S1, see Annexes, page 262).

3.1.3.4. Expression Constructs and Site-Directed Mutagenesis

The teleost aquaporin and YwhazL cDNAs employed in this study, and their GenBank accession numbers, are indicated in (supplementary text S1, see Annexes, page 262). The cDNAs were subcloned into the pT7Ts (Deen *et al*., 1994) or pcDNA3 (Invitrogen) expression vectors, and in most cases fused with an HA or Flag epitope tag at the N- or C-terminus of the encoded proteins by using PCR. Mutations into the loop D or C-terminal amino acid sequence of aquaporins were introduced by using the QuikChange Lightning Kit (Agilent Technologies; 210518) following the manufacturer's instructions. Substitution of the Aqp1ab1 or -1ab2 complete C-terminus for that of Aqp1aa was carried out by PCR as previously described (Tingaud-Sequeira *et al*., 2008). All constructs were verified by DNA Sanger sequencing to confirm that only the desired chimeras or mutations were produced.

3.1.3.5. Expression *in X. laevis* Oocytes and Swelling Assays

The cRNAs corresponding to the different constructs were synthesized in vitro with T7 RNA polymerase from *Xba*I-digested pT7Ts vector containing the cDNAs. The isolation and

microinjection of oocytes (0.5-15 ng of cRNA depending on the construct), as well as the swelling assays, was carried out as previously described (Deen *et al*., 1994; Chauvigné *et al*., 2011). The effect of PKC or PKA activation on the oocyte P_f was tested by preincubating the oocytes with 100 nM PMA for 30 min, or with 100 µM IBMX for 1 h and subsequently with 100 µM FSK for 30 min, before determination of oocyte swelling or protein extraction. The effect of p38 MAPK activation was tested using 100 µM ANS. Control oocytes were treated with 0.1% of the drug vehicle dimethyl sulfoxide (DMSO).

3.1.3.6. *In Vitro* Incubation of Seabream Ovarian Follicles and Water Uptake Assays

Ovarian follicles at different developmental stage were collected from naturally spawning seabream females and the P_f of follicles at each stage was determined under hypertonic conditions as previously described (Fabra *et al*., 2006; Zapater *et al*., 2011). For *in vitro* incubations, groups of 10 postvitellogenic follicles were placed in 75% Leivovitz L-15 culture medium with L-glutamine and treated with 100 µM IBMX and 100 µM FSK for 1 h at 18ºC, or with 0.1% DMSO (controls). After incubation, follicles were fixed for immunofluorescence microscopy or used for water uptake assays. For this, follicles were transferred to 200 µl ultra-pure water containing 10 µCi [^{3}H] water (1 mCi/ml) (American Radiolabeled Chemicals Inc., ART 0194A) for 20 min at room temperature. Follicles were washed twice in distilled water, dissolved in 400 µl of 10% sodium dodecyl sulfate (SDS) for 1 h, mixed with 4 ml of liquid scintillation cocktail (Perkin Elmer LLC Ultima Gold; LLC6013326), and counted using a Beckman Coulter scintillation counter. Some follicles were exposed to [^{3}H] water for 1 min and immediately washed in water for the subtraction of the background signal from externally bound solute.

3.1.3.7. Protein Extraction and Immunoblotting

The total and plasma membrane fractions of *X. laevis* oocytes (n = 10) and seabream ovarian follicles (n = 50) were isolated as described previously (Kamsteeg and Deen, 2001). For the seabream follicles, the final pellet was resuspended in 1 × Laemmli sample buffer supplemented with 1 mM NaF, 1 mM Na_3VO_4 and protease inhibitors. In some experiments, whole protein extracts from seabream follicles were obtained by homogenization in 500 µl of radioimmunoprecipitation assay (RIPA) buffer (150 mM NaCl, 50 mM Tris pH 8.0, 1.0% Triton X-100, 0.5% sodium deoxycholate, 0.1% SDS, supplemented with 1 mM NaF, 1 mM

Na_3VO_4, protease inhibitors, and 80 U benzonase) using a glass douncer, and further incubation on ice for 15 min. The samples were then centrifuged at 14000 × *g* at 4ºC for 1 min, and the supernatant mixed with 2 × Laemmli sample buffer and heated at 95ºC for 10 min. In some cases, lysates were digested with calf intestine alkaline phosphatase (New England Biolabs Inc.; M0525) for 1 h at 37ºC prior to Laemmli sample buffer addition. Immunoblotting was subsequently carried out as previously described (Zapater *et al*., 2011).

3.1.3.8. Co-Immunoprecipitation

X. laevis oocytes and seabream follicles were homogenized in the lysis buffer from the Pierce™ Crosslink Magnetic IP/Co-IP Kit (Pierce; 88805) with a bouncer on ice, and centrifuged at 14000 × *g* for 1 min. An aliquot (10%) of the protein extract was collected as the input of the IP and mixed with 2 × Laemmli sample buffer, whereas the remaining extract was incubated overnight at 4°C under constant agitation with magnetic beads previously coated with anti-HA, anti-SaAqp1ab1 or anti-SaAqp1ab2 antibodies. For rabbit primary antibodies, the IP was carried out using the kit indicated above, and final eluted proteins in 50 µl of elution buffer were mixed with 4 × Laemmli sample buffer supplemented with protease and phosphatase inhibitors. For chicken antibodies, the IP was performed using Dynabeads™ M-280 Tosylactivated (Invitrogen; 14203) following the manufacturer's instructions. The input and immunoprecipitated samples were immunoblotted as indicated above.

3.1.3.9. Immunofluorescence Microscopy and Quantification

Samples were processed and immunostained as previously described (Chauvigné *et al*., 2018). Control sections were incubated without primary antibodies (when using commercial antibodies) or with antibodies preincubated with the corresponding peptides used for immunization (for custom made antibodies). Double immunostaining using rabbit antibodies against seabream Aqp1ab1 and either YwhaLa/b or -zLb were performed by staining first for YwhaLa/b or -zLb as described above using an anti-rabbit Cy3-coupled secondary antibody. After fixing with 4% paraformaldehyde (PFA) for 1 h, slides were incubated with the Aqp1ab1 antibody previously labeled with Zenon™ Rabbit IgG Alexa Fluor™ 488 Labeling Kit (Invitrogen, Z25302) following manufacturer instructions. After 1 h, sections were washed and fixed again with PFA for 15 min, incubated with 4',6-diamidino-2-phenylindole (DAPI; 1:10000), and mounted with Fluoromount™ Aqueous Mounting

Medium (F4680). Immunofluorescence was observed and documented with a Zeiss Axio Imager Z1/Apotome fluorescent microscope (Carl Zeiss Corp.). Changes in Aqp1ab1, -1ab2, YwhazLa/b and -zLb abundance in the plasma membrane of seabream oocytes were evaluated by measuring the fluorescence intensity of the microvilli crossing the vitelline envelope with respect to the total fluorescence (plasma membrane plus cytoplasm) using the ImageJ software v.1.52o (https://imagej.nih.gov/ij/). For all treatments or developmental stage, the images were acquired with the same fluorescence exposure and similar orientation, so that the area of the plasma membrane and cytoplasm was equivalent.

3.1.3.10. Statistics

Comparisons between two independent groups were made by the two-tailed unpaired Student's *t*-test. The statistical significance among multiple groups was analysed by one-way ANOVA, followed by the Tukey's multiple comparison test, or by the non-parametric Kruskal-Wallis test and further Dunn's test for nonparametric post hoc comparisons. Percentages were square root transformed previous analyses. Differences between proportions were tested via the critical z-value approach. Statistical analyses were carried out using the GraphPad Prism v9.1.2 (226) (GraphPad Software). In all cases, statistical significance was defined as $P < 0.05$ (*), $P < 0.01$ (**), or $P < 0.001$ (***).

3.1.4. Results

3.1.4.1. Phylogenomics Uncovers an Ancient *aqp1*-type Cluster in Teleosts

An initial gene walking experiment using gilthead seabream genomic DNA uncovered four aquaporin-like exons 219 nucleotides (nt) upstream of the previously identified *aqp1ab* channel, and 8,144 nt downstream of the encoded *aqp1aa* gene (Fabra *et al*., 2005 and 2006; figure 1A). The deduced primary structure and initial phylogenetic analysis in relation to 263 *aqp1*-type piscine CDS assembled from 94 genomes and 42 transcriptomes revealed that an additional *aqp1ab*-type channel exists in this locus (figure 1B and supplementary figure S1, see Annexes, page 222). Bayesian inference indicated that non-teleost species such as cartilaginous, chondrostean and holostean fishes encode a single *aqp1* channel, while all teleosts have at least one *aqp1aa* gene, and different species have one or two copies of *aqp1ab* genes, which co-cluster on a separate branch to the *aqp1aa* genes. In line with the convention of aquaporin nomenclature, which names genes in accordance with the

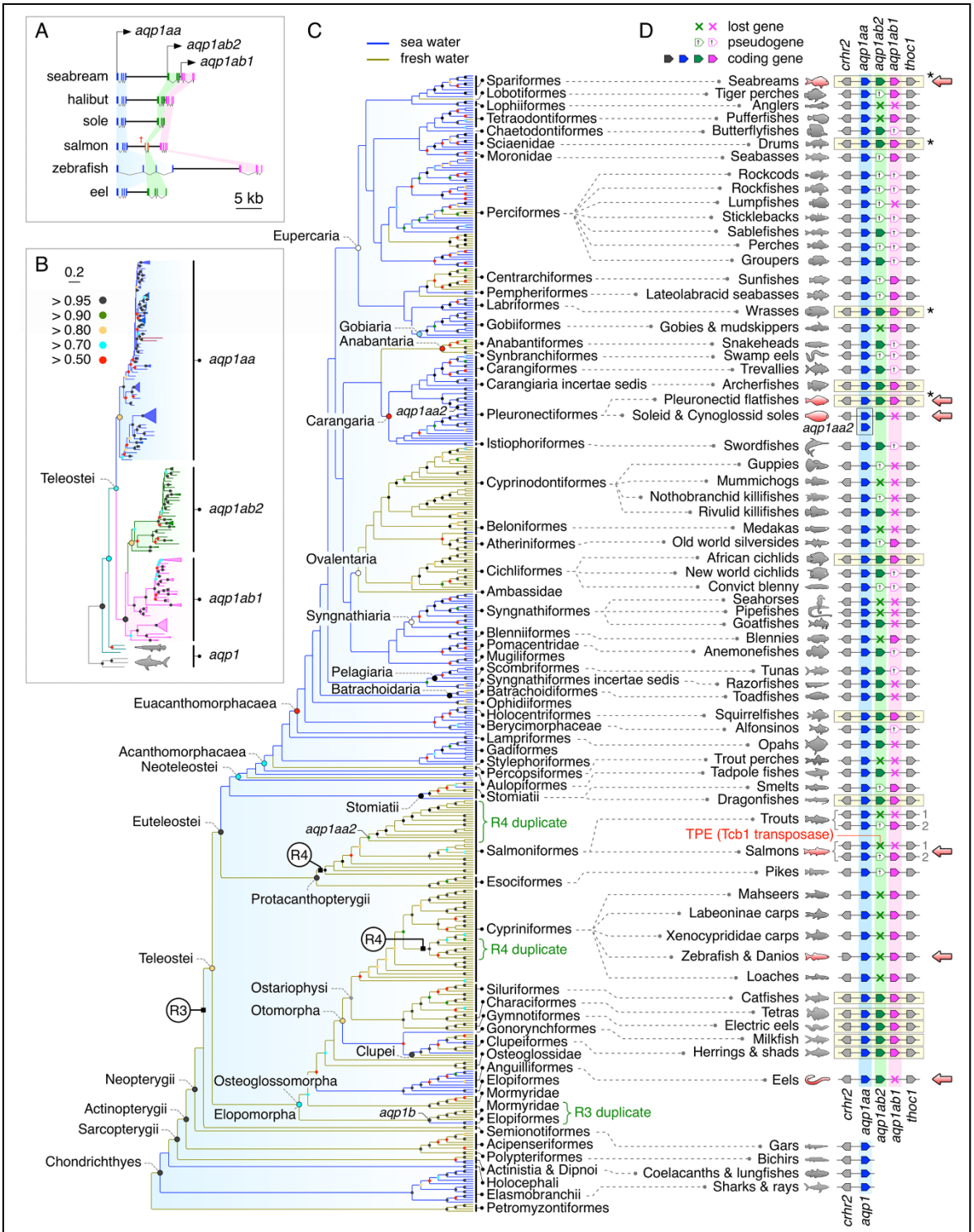

Figure 1. The origin of the teleost-specific aquaporin-1 cluster (TSA1C). (**A**) Genomic organization of the TSA1C in distantly related teleosts drawn to scale. Canonical *aqp1aa*, *-1ab2* and *-1ab1* genes consist of four exons (blue, green and magenta bars, respectively), while pseudogenes vary from premature stop codons to highly degraded fragments (e.g. salmon, red bars†). In cypriniform teleosts (e.g. zebrafish) *aqp1ab2* is absent, while in anguilliform teleosts (e.g. eel) *aqp1ab1* is absent. (**B**) Bayesian majority rule consensus tree of the TSA1C coding sequences rooted with chondrichthyan *aqp1*. The tree is inferred from 20 million MCMC generations (nucmodel = 4by4, nst = 2, rates = gamma) of 239,282 aligned nucleotide sites aligned by codon. Support values shown at each node (colored dots) are Bayesian posterior probability ranges shown in the key. The scale bar indicates the expected rate of substitutions per site. (**C**) Bayesian majority rule consensus tree of piscine *aqp1* orthologs rooted with hyperoartian *aqp01*. The tree is initially inferred from 100 million MCMC generations (nucmodel = 4by4, nst = 2, rates = gamma) of 399,429 aligned nucleotide sites aligned by codon (N = 494 taxa), with the Acanthomorphata segment of the tree re-inferred from a

further 100 million MCMC generations (nucmodel = 4by4, nst = 2, rates = gamma) of 235,624 aligned nucleotide sites aligned by codon (N = 301 taxa). Whole genome duplication events (R3, R4) are indicated at relevant nodes. Support values and scale bar as in (B). (**D**) Syntenic arrangement of the TSA1C in selected fishes illustrating full (yellow backgrounds), partial (presence of pseudogenes) or no conservation of the cluster (both *aqp1ab*-type paralogs lost). Gene coding direction is indicated by the pointed end of each symbol with pseudogenes indicated by a white X on the symbol. Lost genes are indicated with an X. Both paralogons are shown for paleotetraploid salmonids. Asterisks indicate that some species within the group have *aqp1ab*-type pseudogenes. Red arrows highlight species selected for experimental studies. TPE: transposable element.

chronology of their discovery, we named the second seabream *aqp1ab*-type channel and its orthologs in other species *aqp1ab2*, and renamed the original seabream *aqp1ab* channel (Fabra *et al*., 2005 and 2006) and its orthologs in other species *aqp1ab1*. These analyses thus uncover a novel ternary TSA1C comprised of *aqp1aa-aqp1ab2-aqp1ab1*, in which the *aqp1ab2* and *aqp1ab1* genes, when present in teleost genomes, are closely juxtaposed downstream of the *aqp1aa* gene (figure 1A).

The above analyses also revealed that some species of teleost harbor a second type of *aqp1aa* gene, including soleid and cynoglossid flatfishes, salmonids and some cyprinids. In each case, however, the second *aqp1aa* gene, which we term *aqp1aa2*, co-clusters within these specific lineages, and can thus be explained on the basis of lineage-specific duplication. Thus *aqp1aa2* in salmonids is consistent with a fourth round (R4) of autotetraploidization, while that of selected cyprinids is consistent with an independent R4 allotetraploidization event (Berthalot *et al*., 2014; MacQueen & Johnston, 2014; Xu *et al*., 2019). Conversely, the *aqp1aa2* gene in soleid and cynoglossid flatfishes is not found in the genomes of all other families (n = 7) of flatfish searched, but evolved in the absence of the *aqp1ab1* gene, which is present in the genomes of pleuronectid, paralichthyid, scophthalmid and bothid flatfishes (figure 1A and B and supplementary figure S1, see Annexes, page 222). In tongue sole (*Cynoglossus semilaevis*), *aqp1aa2* is located on chromosome 15 (GenLoc 271 kb), and is not syntenic to the extant *aqp1aa-aqp1ab2* cluster, which is located on chromosome 20 (GenLoc 8,758 kb). From this, we surmise that the *aqp1aa2* gene of soleid and cynoglossid flatfishes is not an integral member of the TSA1C in these lineages.

Interestingly, the initial phylogenetic analysis (figure 1B) indicated that the absence of the *aqp1ab1* gene is not restricted to certain families of flatfishes, but it is also absent from the genomes of other species, such as elopomorph eels, rivulid killifishes, and perciform sticklebacks, or exists as a pseudogene in scombrid tunas and perciform rockfishes (supplementary figure S1, see Annexes, page 222). Conversely, *aqp1ab2* is absent from the genomes of cyprinid fishes, including zebrafish (*Danio rerio*), gobiid mudskippers and

tetraodontiform pufferfishes, or exists as a pseudogene in the genomes of some pleuronectid, labrid, moronid and perciform teleosts (supplementary figure S1, see Annexes, page 222). However, intact *aqp1ab2* and *aqp1ab1* genes are found in the genomes of clupeid, characiform, siluriform, cichliform and pleuronectiform teleosts, suggesting that the TSA1C could have arisen in the common ancestor of all clupeocephalan teleosts (Otomorpha and Euteleosteomorpha). Since recent studies have revealed that aquaporin tandem duplicates of *aqp3*, *aqp8* and *aqp10* evolved in pre-teleostean lineages (Cerdà and Finn, 2010; Finn *et al*., 2014; Yilmaz *et al*., 2020), we conducted a separate phylogenetic analysis of *aqp1*-type genes and their syntenic loci assembled from the genomes of non-teleost fishes in relation to those of the elopomorph, osteoglossomorph and clupeid teleosts.

The results confirmed that lampreys retain a single fused ortholog (*aqp01*) (Finn *et al*., 2014), while cartilaginous, sarcopterygian and actinopterygian cladistian and holostean fishes retain a single *aqp1*-type ortholog (supplementary figure S3, see Annexes, page 222). However, two orthologs were detected in the chondrostean sturgeons and paddlefishes, and four orthologs including one or two pseudogenes were identified in osteoglossomorph teleosts such as the Aba (*Gymnarchus niloticus*) or mormyrid elephantfishes (Mormyridae). Conversely, three intact orthologs were identified in elopomorph and clupeid teleosts. The phylogenetic topology of the chondrostean duplicates shows that they form a binary cluster (posterior probability [pp] = 1.0) on a sister branch to the single cladistian orthologs (pp = 1.0; supplementary figure S3A, see Annexes, page 222), and are located on separate chromosomes (supplementary figure S3B, see Annexes, page 222). This is consistent with the expected taxonomic position of Chondrostei, and an independent paleopolyploidy events in the lineage (Crow *et al*., 2012; Du *et al*., 2020). We therefore concluded that the chondrostean paralogs are not associated with the TSA1C, and named them *aqp1c1* and *aqp1c2*.

The phylogenetic topology of the teleost orthologs also reveals that one of the CDS assembled from the elopomorph and osteoglossomorph genomes clusters on a sister branch to the *aqp1aa* paralogs (pp = 0.8; supplementary figure S3A, see Annexes, page 222), yet each gene is located on a separate linkage group to the *aqp1aa-aqp1ab2-aqp1ab1* paralogs, which are all tandemly arranged in the TSA1C (supplementary figure S3B, see Annexes, page 222). Based upon the semi-conserved synteny, we concluded that this novel *aqp1*-type ortholog found in elopomorph and osteoglossomorph teleosts represents the previously

undetected ohnolog (i.e. originating from R3, the teleost-specific whole genome duplication, Amores *et al*., 2011; Gasanov *et al*., 2021), and we therefore named it *aqp1b*. This ohnolog was not found in any of the clupeocephalan genomes searched (n = 365), suggesting that it is probably lost in the vast majority (93%) of extant teleost families.

The above analyses revealed that the genomes of elopomorph teleosts such as bonefishes, tarpons and deep-sea eels retain the *aqp1b* ohnolog together with a binary cluster of *aqp1aa-aqp1ab2* paralogs. However, although catadromous anguillimorph eels also retain the *aqp1aa-aqp1ab2* cluster, the *aqp1b* ohnolog was not found in their genomes and all elopomorph teleosts have seemingly lost the downstream *aqp1ab1* tandem duplicate. Interestingly, identification of a Tcb1-type transposase in the putative *aqp1ab1* locus suggests that gene deactivation and loss may have been associated with paleotransposon activity. Conversely, with the exception of the Aba, which appears to have a complete form of *aqp1ab2*, the genomes of most osteoglossomorph teleosts still encode intact *aqp1b* and *aqp1aa* ohnologs, but have fragmented pseudogenes of the *aqp1ab2* and *aqp1ab1* tandem duplicates (supplementary figure S3, see Annexes, page 222). Amongst clupeid teleosts, the three extant *aqp1*-type genes are all tandemly located as a ternary cluster that forms the TSA1C, with each of the *aqp1aa*, *aqp1ab2* and *aqp1ab1* paralogs phylogenetically clustering with the same topology and high pp as shown in figure 1B. The only pseudogene detected was identified as a fragmented *aqp1ab1* gene in the denticle herring (*Denticeps clupeoides*).

Taken together, the above analyses reveal that the TSA1C likely evolved at the root of the crown clade of Teleostei (figure 2), in the near aftermath of the R3 event ~300 Ma (Amores *et al*., 2011). The TSA1C is thus ancient, but has until now been masked due to differential gene loss in various lineages. To determine whether a retention bias of either the *aqp1ab2* or *aqp1ab1* genes occurred during teleost evolution, we conducted a systematic phylogenetic analysis of the *aqp1*-type genes (figure 1C and supplementary figures S2 and S4, see Annexes, page 222) and their syntenic loci (figure 1D) assembled from >400 piscine genomes. Bayesian inference of the *aqp1aa*, *aqp1b* and non-teleost *aqp1* CDS, recovered the major groupings of piscine diversity, including the majority (85%) of teleost orders (Hughes *et al*., 2018), and confirmed the asymmetric retention of the *aqp1aa* gene in all teleosts, but only the *aqp1b* ohnolog in osteoglossomorph and elopomorph species. The tree further recovered the topology of the R4 duplicates in salmonids and selected cyprinids and

the *aqp1aa2* duplicates in soleid and cynoglossid flatfishes. By contrast, a high number of pseudogenes of either *aqp1ab2* (n = 105; supplementary figure S4A, see Annexes, page 222) or *aqp1ab1* (n = 72; supplementary figure S4B, see Annexes, page 222) were identified, with no evidence of either paralog in 41 species. The loss or fragmentation of *aqp1ab*-type genes is thus not related with the systematic affinities of teleosts, but appears to have occurred stochastically throughout teleost evolution either in association with paleotransposon activity in salmonids and eels, or through mutation load in other species. Nevertheless, 59 species from 16 orders of teleosts still retain both of the *aqp1ab*2 and *aqp1ab1* paralogs within the TSA1C. Since the biological significance of clusters of retained genes remains unclear (Albalat and Cañestro, 2016), we investigated whether *aqp1ab*-type gene retention could be related to the previously established vital function of oocyte hydration and the formation of pelagic eggs (Fabra *et al*., 2005; 2006; Kagawa *et al*., 2011; Zapater *et al*., 2011 and 2013).

3.1.4.2. Selective Retention and Expression of *aqp1ab* Genes in Marine Pelagophil Teleosts

Data on the spawning habitat (seawater, SW, or freshwater, FW) and type of egg spawned, i.e. pelagic, benthic or internal, were compiled for 425 species of teleosts (supplementary table S1, see Annexes, page 256). Pelagic eggs were defined as eggs that float freely without external buoyancy aids such as bubble nests or egg rafts. Benthic eggs included all eggs that sink in a non-lotic environment, including those that are spawned on, or are attached to substrate, egg rafts, bubble nests or are collected by mouth brooders. Internal eggs were defined as those that are not exposed to the external environment, including those of ovoviviparous and viviparous species, as well as species that incubate their eggs in brood pouches (e.g. seahorses and pipefishes). The compiled data set reveals that approximately half (51%) of the species spawn in SW, and half (49%) spawn in FW. However, as evident in figure 1C, there is a systematic bias, where the more basal lineages of the non-euacanthomorph teleosts mostly (79%) spawn in FW, while the majority (65%) of the modern euacanthomorph teleosts spawn in SW. An intriguing observation emerges when examining the euacanthomorph species (n = 217) in relation to the type of egg spawned and retention of *aqp1ab*-type genes. A higher proportion (60%) of the marine species from this group spawn pelagic eggs (pelagophils) as opposed to benthic (benthophils) (26%) or internally incubated eggs (14%) (supplementary figure S5A, see Annexes, page 225).

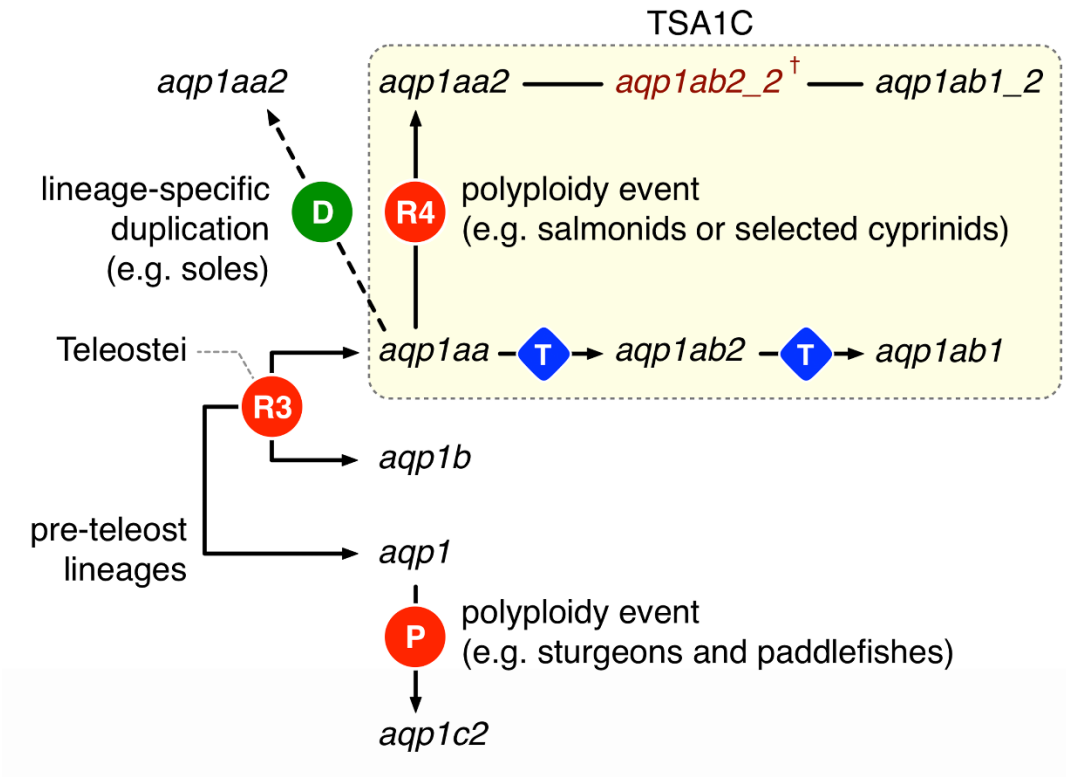

Figure 2. The origins of multiple aquaporin-1 orthologs in fishes. Whole genome duplication (polyploidy) events (R3, R4, and P) respectively generated *aqp1b* ohnologues in teleosts, a paralogous TSA1C in paleotetraploid salmonids and allotetraploid cyprinids and *aqp1c2* in chondrostean sturgeons and paddlefishes. Tandem duplication (T) gave rise to the teleost *aqp1ab2* and *aqp1ab1* paralogs. Conversely, lineage-specific duplication (D) generated the *aqp1aa2* paralogs in soleid and cynoglossid flatfishes.

Conversely, a greater fraction (81%) of the FW species are benthophils as opposed to pelagophils (1%), and there is no significant difference between the proportions of species in SW (14%) or FW (18%) with internal egg development. Most striking is that nearly all of the pelagophils (95%) retain at least one of the *aqp1ab2* or the *aqp1ab1* genes, with a third of the species (33%) retaining both paralogs (supplementary figure S5B, see Annexes, page 225). This level of gene retention is much higher when compared to that of the benthophils (57% retain 1 paralog; 12% retain both paralogs), and greatly exceeds that of species that incubate their eggs internally, where no species retains both paralogs, and 91% no longer possess the TSA1C. Quantitative analyses of the mRNA expression levels in different adult tissues further revealed that *aqp1ab*-type transcripts are highly enriched in the ovaries of marine pelagophil species, such as pleuronectids, soleids and sparids, but not those of freshwater benthophils such as salmonids and cyprinids (Tingaud-Sequiera *et al.*, 2008; supplementary figure S6, see Annexes, page 226).

3.1.4.3. Intracellular Trafficking of the TSA1C is Differentially Regulated

To better understand the evolutionary basis of the above observations and to investigate how species that retain both *aqp1ab1* and *aqp1ab2* paralogs can avoid expression redundancy of their channel products, we functionally characterized each channel in the TSA1C from distantly related marine and FW teleosts. These species included those that retain one of the downstream *aqp1ab*-type genes, such as the elopomorph European eel (*Anguilla anguilla*), the ostariophysan zebrafish and stinging catfish (*Heteropneustes fossilis*), the protacanthopterygian Atlantic salmon (*Salmo salar*) and the euacanthomorph Senegalese sole (*Solea senegalensis*), and two euacanthomorph marine teleosts that retain both *aqp1ab*-type genes, the Atlantic halibut and the gilthead seabream. These species also spawn different types of eggs with zebrafish, salmon and catfish producing benthic eggs, while sole, seabream and halibut produce highly hydrated pelagic eggs.

To determine whether the TSA1C paralogs from each model species encode functional water channels, we used oocytes from *X. laevis* as standard surrogate experimental systems for the fish oocytes (Chauvigné *et al*., 2021). Oocytes were injected with the corresponding cRNAs, synthesized from non-tagged or human influenza hemagglutinin (HA)-tagged cDNAs, or with water as negative controls, and subsequently submitted to swelling assays (figure 3). Oocytes expressing Aqp1aa from zebrafish (DrAqp1aa), European eel (AaAqp1aa), Atlantic salmon (SsaAqp1aa), gilthead seabream (SaAqp1aa), Atlantic halibut (HhAqp1aa), or Senegalese sole (SseAqp1aa) showed a 6 to 11-fold increase in osmotic water permeability (P_f) with respect to the control oocytes after a hypoosmotic challenge, whereas oocytes injected with SseAqp1aa2 showed a P_f increment of ~3 times (figure 3A). However, with respect to the controls, oocytes expressing DrAqp1ab1, SsAqp1ab1, SaAqp1ab1 or HhAqp1ab1 only showed ~4-fold increase in P_f, while those expressing AaAqp1ab2, SaAqp1ab2, HhAqp1ab2, SseAqp1ab2 or Aqp1ab2 from the stinging catfish (HfAqp1ab2), displayed even less swelling with ~1-fold increase in P_f (figures 3B and C and supplementary figure S7A and B, see Annexes, page 227).

To investigate the intracellular trafficking to the *X. laevis* oocyte plasma membrane of the TSAC1channels, we employed immunoblotting and immunofluorescence microscopy using paralog-specific or anti-HA antibodies. These experiments revealed that teleost

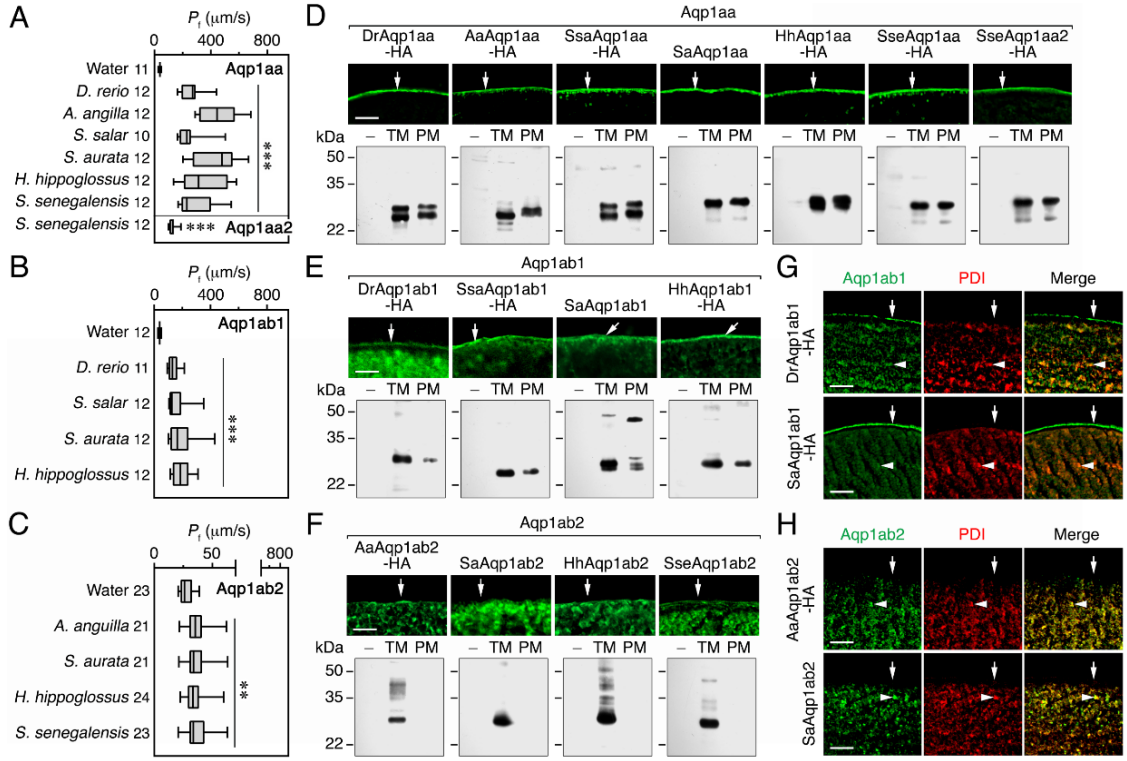

Figure 3. Functional characterization of Aqp1-like channels in teleosts. (**A-C**) Osmotic water permeability (P_f) of *X. laevis* oocytes injected with water (controls) or expressing wild-type Aqp1aa, -1ab1 or -1ab2 paralogs from different teleosts. All data points are presented as box and whisker plots/scatter dots with horizontal line (inside box) indicating median and outliers. The number of oocytes in each group is indicated on the left of each plot. Data were statistically analyzed by an unpaired Student's *t*-test (**, $P < 0.01$; ***, $P < 0.001$; with respect to controls). (**D-F**) Immunolocalization (upper panels) and immunoblot (lower panels) of the different intact or HA-tagged channels (as indicated) in oocytes. Proteins were detected by using an anti-HA commercial antibody or paralog-specific antibodies. Molecular mass markers (kDa) are on the left. TM, total membrane; PM, plasma membrane. (**G**, **H**) Double immunostaining of oocytes expressing zebrafish or seabream Aqp1ab1, or European eel or seabream Aqp1ab2, and the endoplasmic reticulum (ER) marker protein disulfide isomerase (PDI). The PM of oocytes is indicated by arrows (D-H), whereas the arrowheads (G and H) indicate colocalization of the channels with the PDI. Scale bars, 25 µm.

Aqp1aa polypeptides were constitutively expressed at the plasma membrane (figure 3D). In contrast, the Aqp1ab1 and -1ab2 channels were differentially retained in the cytoplasm (figure 3E and F), thus explaining the lower P_f of oocytes expressing these paralogs compared to those injected with Aqp1aa. Double immunostaining of Aqp1ab1 or -1ab2 with the endoplasmic reticulum (ER) marker protein disulfide isomerase (PDI) further revealed that both channels colocalized with the PDI (figure 3G and H and supplementary figure S7C and D, see Annexes, page 227), suggesting an impaired sorting of these aquaporins from the ER to the frog oocyte plasma membrane. Transient expression of Flag-tagged Aqp1aa, -1ab1 or -1ab2 from different teleosts in the human breast cancer cell line MCF-7 confirmed the constitutive expression of teleost Aqp1aa in the plasma membrane, as well as the differential retention of Aqp1ab1 and -1ab2 in the ER (supplementary figure S8A-C, see Annexes, page

228). However, these trials also showed a stronger colocalization of Aqp1ab2 with the lysosomal-associated membrane protein 1 (LAMP-1) compared to that of Aqp1ab1 (supplementary figure S8D and E, see Annexes, page 228), indicating that the Aqp1ab2 channels are also rapidly redirected to lysosomal degradation.

3.1.4.4. Protein Kinases Regulate the Intracellular Trafficking of the TSA1C Channels

Since intracellular trafficking of aquaporins is often regulated by protein kinase-mediated phosphorylation of subdomain-specific residues (Nesverova and Törnroth-Horsefield, 2019), we initially tested whether protein kinase A (PKA) and C (PKC) activators, forskolin (FSK) and phorbol 12-myristate 13-acetate (PMA), respectively, could regulate the trafficking of Aqp1aa, -1ab1 or -1ab2 from each model teleost species in *X. laevis* oocytes (supplementary figure S9, see Annexes, page 230). Subsequently, to identify the potential amino acid residues involved, we conducted *in silico* searches for putative PKA- or PKC-mediated phosphorylation sites in the intracellular loop D and C-termini of the channels, followed by site-directed mutagenesis experiments (supplementary figure S10, see Annexes, page 232). The data confirmed that PKC positively regulates plasma membrane trafficking of human AQP1, as well as the Aqp1aa orthologs from elopomorph and cyprinid teleosts (AaAqp1aa and DrAqp1aa) through phosphorylation of conserved Thr residues in loop D. In contrast, in modern euteleost lineages (SaAqp1aa, SseAqp1aa and SseAqp1aa2), this mechanism switches to negative regulation of Aqp1aa trafficking due to substitution of the upstream Thr by a Val residue. These experiments also revealed that PKA mediates positive membrane trafficking of Aqp1aa orthologs from elopomorph and cyprinid teleosts through phosphorylation of conserved C-terminal Ser residues, but not in euacanthomorph species (SaAqp1aa and SseAqp1aa2). By contrast, the trafficking of the Aqp1ab1 paralog was negatively regulated by PKC in the cyprinid and salmonid teleosts (DrAqp1ab1 and SsaAqp1ab1), which surprisingly appeared to be linked to the presence of two Thr-Thr residues in loop D, whereas that of Aqp1ab2 was stimulated by PKC but only in the elopomorph European eel (AaAqp1ab2). Activation of PKA promoted Aqp1ab1 plasma membrane trafficking in all the teleost species tested, however the involved phosphorylation sites could not be determined using current prediction algorithms. The same positive effect of PKA on channel trafficking was only conserved in Aqp1ab2 from species that retain only this paralog, such as European eel and sole. Interestingly, we also identified p38 MAPK

putative phosphorylation sites conserved in the Aqp1ab1 C-termini of most (74%) of the euteleost species examined (supplementary figure S10F, see Annexes, page 232), which reduce plasma membrane trafficking (Tingaud-Sequeira *et al*., 2008). Such p38 MAPK sites are not found in the otophysan lineages of siluriform and clupeiform teleosts that also retain intact *aqp1ab1* genes. These data thus suggest that the intracellular trafficking of the TSA1C is differentially regulated by PKA and PKC, and also by p38 MAPK in the case of Aqp1ab1, but that the specific residues involved in these regulations appear to have changed with the evolution of the different lineages.

3.1.4.5. Novel Teleost Ywhaz-like Binding Proteins Regulate Aqp1ab1 and -1ab2 Trafficking

Although the previous experiments could not determine the specific mechanisms involved in the trafficking regulation of Aqp1ab1 and -1ab2 in some teleosts, experiments using chimeric proteins indicated that the Aqp1ab1 and -1ab2 C-termini are mechanistically associated with the cytoplasmic retention of the channels in amphibian oocytes (supplementary figure S11, see Annexes, page 236). Further *in silico* analysis of the C-termini of teleost Aqp1ab1 and -1ab2 revealed the presence of potential binding motifs for YWHA (14-3-3) regulatory proteins (supplementary figure S10*F* and *J*, see Annexes, page 232), which can bind membrane proteins in a PKA-mediated Ser/Thr phosphorylation-dependent manner to regulate their function and subcellular sorting (Fu *et al*., 2000; Moeller *et al*., 2016; Prado *et al*., 2019). The YWHA interaction motif in the target protein usually contains an Arg residue that increases binding affinity (Rajan *et al*., 2002; Shikano *et al*., 2005). Therefore, to investigate whether YWHA proteins could regulate teleost Aqp1ab1 and -1ab2 trafficking, as well to establish which specific residues could be involved in these mechanisms, we conducted a mutagenesis screen in which the C-terminal Arg within the predicted YWHA motif was substituted by Ala, and all potential phosphorylation sites in this subdomain were separately replaced by Asp to mimic a constitutive phosphorylation state (supplementary figure S12, see Annexes, page 237). The results of these experiments for the Aqp1ab1 channels appeared to be puzzling among species, but the data did suggest that binding of Aqp1ab2 to a teleost-specific YWHA carrier protein might be involved in the regulation of channel trafficking.

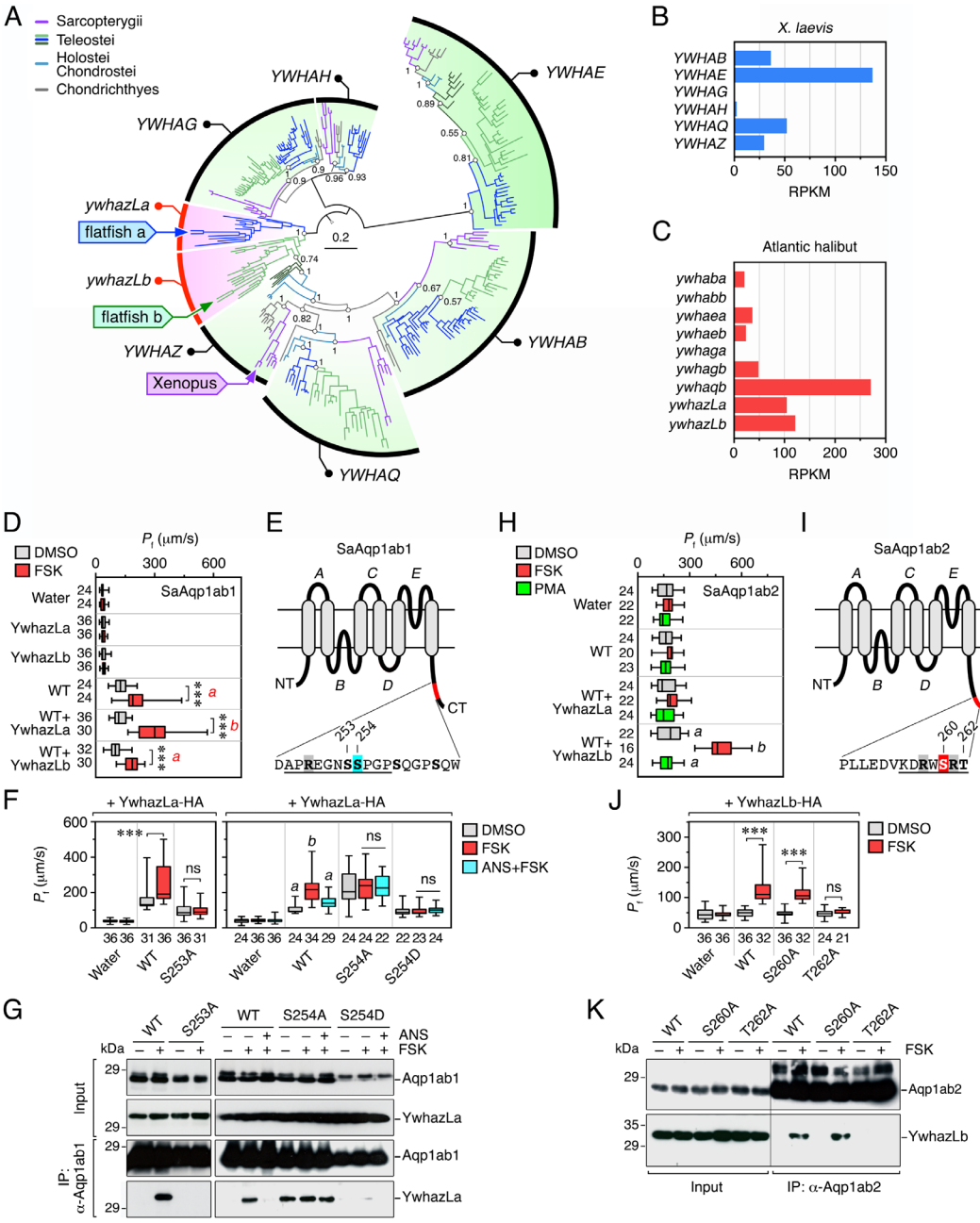

Figure 4. Identification of teleost-specific YWHA proteins and regulation of Aqp1ab1 and -1ab2 trafficking. (**A**) Bayesian majority rule mid-point rooted consensus tree (3 million MCMC generations inferred from 278,404 nucleotide sites) from 337 gnathostome *YWHA* coding sequences. Posterior probabilities are shown at selected nodes (see supplementary figures S13 and S14, Annexes, page 240 for fully annotated trees). *X. laevis YWHAZ* and flatfish *ywhazLa* and *-zLb* branches are respectively indicated. (**B-C**) Expression levels assessed as reads per kilo base per million mapped reads (RPKM) of transcripts encoding YWHA proteins in the *X. laevis* and Atlantic halibut ovarian follicle transcriptomes. (**D**, **H**) P_f of *X. laevis* oocytes injected with water or expressing wild-type (WT) SaAqp1ab1 (D) or SaAqp1ab2 (H), with or without co-injection of HA-tagged seabream YwhazLa or -zLb, respectively, and treated with DMSO, FSK (PKA activator) or PMA (PKC activator). (**E**, **I**) Schematic representation of SaAqp1ab1 and -1ab2 monomers showing the six transmembrane domains, the five connecting loops (A-E), and the predicted YWHA binding regions (underlined) in the C-termini (see also supplementary figure S10, Annexes, page 232). Residues shaded in blue and red indicate putative PKA and p38 MAPK phosphorylation sites, respectively. (**F**, **J**) P_f of oocytes injected with water or expressing WT SaAqp1ab1 (F) or WT SaAqp1ab2 (J), or mutant channels at specifi c residues potentially involved in YwhazL binding, and treated with FSK alone or in the presence of the p38 MAPK activator anisomycin (ANS). Control and aquaporin expressing oocytes were also co-injected with YwhazLa-HA or –zLb-HA as above. (**G**, **K**) Co-immunoprecipitation of Aqp1ab1 and YwhazLa (G), or Aqp1ab2 and YwhazLb (K), in oocytes treated as in F and J, respectively. The immunoprecipitated (IP) products using an anti-HA or anti-

SaAqp1ab1 and -1ab2 specific antibodies (in G and K, respectively) were immunoblotted with appropriate antibodies (as indicated). Molecular mass markers (kDa) are on the left. In D, H, H and J, data are presented as box and whisker plots with the number of oocytes in each group indicated on the left or below of each plot. Data were analyzed by the unpaired Student's *t*-test (*, $P < 0.05$; **, $P < 0.01$; ***, $P < 0.001$; as indicated in brackets). In D and H, letters indicate significant differences in one-way ANOVA ($P < 0.05$). ns, statistically not significant.

To identify teleost-specific Ywha paralogs that could facilitate Aqp1ab1 and -1ab2 membrane trafficking, we conducted a comparative transcriptomic analysis of Atlantic halibut postvitellogenic and *X. laevis* stage IV ovarian follicles by RNA sequencing (supplementary table S2, see Annexes, page 257). In parallel, we further constructed a phylogenetic tree of the vertebrate YWHA binding proteins with a view to finding teleost-specific duplicates that display long branch lengths and thus potential neofunctionalization in relation to the amphibian orthologs. Bayesian inference of the CDS of the YWHA-encoding transcripts shows that teleosts and amphibians have orthologs of the mammalian *YWHAB*, *YWHAE*, *YWHAG*, *YWHAH*, *YWHAQ* and *YWHAZ* subfamilies (figure 4A, and supplementary figure S13, see Annexes, page 240). Teleost duplicates were identified in each subfamily, except *YWHAH*, with the longest branch lengths in relation to the single *X. laevis* orthologs noted for *YWHAQ* and *YWHAZ*. The *YWHAQ* cluster recovered the expected interrelationships of Chondrichthyes, Actinopterygii and Sarcopterygii, however, the duplicated *ywhaqa* and *ywhaqb* orthologs were restricted to non-euacanthomorph species, with only the *ywhaqb* gene found in the Euacanthomorphacea. By contrast, both of the teleost duplicates within the *YWHAZ* cluster are found in the Euacanthomorphacea, but formed more distantly related clusters external to the non-teleost actinopterygian, chondrichthyan and sarcopterygian CDS. We therefore named these novel teleost-specific duplicates Ywhaz-like-a (*ywhazLa*) and Ywhaz-like-b (*ywhazLb*). Using this initial analysis as a framework, we searched the halibut and *X. laevis* transcriptomes to establish which of the YWHA genes are expressed in the respective ovarian follicles. The orthology of each identified transcript was confirmed by Bayesian inference (supplementary figure S14A-E, see Annexes, page 240), and revealed that the *YWHAB*, *YWHAE*, *YWHAQ* and *YWHAZ* paralogs are each expressed in the *X. laevis* follicle with *YWHAE* showing the highest expression (figure 4B). In the halibut follicle, the *ywhaqb*, *ywhazLa* and *ywhazLb* transcripts showed the highest expression, whereas *ywhaba*, *ywhaea*, *ywhaeb* and *ywhagb* were expressed at relatively lower levels (figure 4C).

The above results highlighted YwhazLa and -zLb as candidate binding proteins that could have duplicated and neofunctionalized to a degree that is specific to modern euacanthomorph teleosts. Thus, although *X. laevis* oocytes express orthologous YWHA proteins that can facilitate the heterologous membrane trafficking of the teleost Aqp1aa and -1ab1 paralogs, amphibian YWHA proteins may no longer possess the specificity required for trafficking the Aqp1ab2 channel. To test this hypothesis, we conducted further experiments using site-directed mutagenesis and co-immunoprecipitation to detect aquaporin-YwhazL interactions, where seabream YwhazLa and -zLb cRNAs were co-expressed with those of Aqp1ab1 and -1ab2 of distantly related teleosts in *X. laevis* oocytes. The results suggested that plasma membrane trafficking of teleost Aqp1ab1 channels (DrAqp1ab1, SsaAqp1ab1, SaAqp1ab1 and HhAqp1ab1) in response to PKA phosphorylation can be regulated by endogenous frog YWHA proteins, but that this mechanism is more efficiently controlled by the binding to the teleost-specific YwhazLa paralogs (figure 4D and supplementary figures S15A-F and S17A, see Annexes, page 241 and 248). In the cyprinid zebrafish, the data confirmed the presence of two PKA mechanisms regulating Aqp1ab1 trafficking, one dependent on the phosphorylation status of Ser^{261} in the C-terminus of the channel for YwhazLa binding, and another independent of YwhazLa interaction and controlled by Ser^{263} phosphorylation (supplementary figures S12A and S15G and H, see Annexes, page 237 and 241). In contrast, in the marine euacanthomorph teleost seabream (SaAqp1ab1; figure 4E-G), as well as in salmonids (SsaAqp1ab1; supplementary figures S17B, see Annexes, page 248), apparently only one mechanism based on PKA phosphorylation of C-terminal Ser^{253} and Ser^{258}, respectively, regulates the YwhazLa interaction and channel trafficking. These data indicate that although salmonids only retain the Aqp1ab1 paralog as do cyprinids, the salmonid Aqp1ab1s have lost the second YwhazLa-independent PKA regulatory mechanism for channel trafficking. We further observed that the p38 MAPK-mediated phosphorylation sites within the Ywha binding domain in the Aqp1ab1 C-termini of salmonid and euacanthomorph teleosts (Ser^{252}-Ser^{253} and Ser^{254} in salmon and seabream, respectively) prevent the YwhazLa interaction resulting in recycling of the channel (figure 4E-G and supplementary figure S17B and C, see Annexes, page 248).

For Aqp1ab2, we found that in the elopomorph eel trafficking of the channel is preferentially regulated by PKA-mediated YwhazLa binding, through phosphorylation of C-

terminal Ser^{241} (supplementary figure S16A, C, E and G, see Annexes, page 246), as observed for DrAqp1ab1. However, eel AaAqp1ab2 also retains a YwhazLa-independent mechanism for channel trafficking, which is mediated by dual PKC phosphorylation of Ser^{255} in the C-terminus (supplementary figure S16G, see Annexes, page 246) and of Thr^{148} in loop D (supplementary figures S10J and K, see Annexes, page 232). In contrast, in all the euacanthomorph marine teleosts investigated, Aqp1ab2 trafficking is specifically (SaAqp1ab2 and HhAqp1ab2) or partially (SseAqp1ab2) dependent on YwhazLb interaction (figure 4H and supplementary figure S16B, D and F, and S17D, see Annexes, page 246 and 248). Thus, in seabream, halibut and sole, the interaction depends on PKA phosphorylation of Thr^{262}, Ser^{241}-Ser^{242}, and Ser^{242}, respectively (figure 4I and J and supplementary figure S17E and F, see Annexes, page 248). Plasma membrane targeting of SseAqp1ab2 is also regulated by PKA phosphorylation of Thr^{233} outside of the predicted YWHA interacting region, but this mechanism still depends on YwhazLa or -zLb binding, since inhibition of this interaction prevents PKA-mediated trafficking of the channel to the plasma membrane (supplementary figure S17F, see Annexes, page 248).

The above observations suggest that Aqp1ab-type trafficking regulation evolved from a relatively relaxed, low-specificity YWHA-binding requirement that has been maintained in species that retain only one of the channels, albeit with a slight binding preference of Aqp1ab1 to YwhazLa. However, a highly constrained binding requirement of Aqp1ab2 to YwhazLb evolved in euacanthomorph species that retain both of the Aqp1ab-type channels. In addition the pre-euteleost Aqp1ab1 channels evolved YWHA-independent phosphorylation mechanisms for trafficking to the plasma membrane, while the euteleost channels evolved recycling mechanisms mediated by p38 MAPK-phosphorylation.

3.1.4.6. *In vivo* Aqp1ab1 and -1ab2 Plasma Membrane Trafficking and YwhazL Binding is Regulated to Facilitate Oocyte Hydration During Meiosis Resumption

To investigate the physiological significance of YwhazL regulation of the TSA1C trafficking, we determined the *in vivo* dynamics of the subcellular localization of endogenous Aqp1aa, -1ab1 and -1ab2, and their interactions with YwhazLa and -zLb proteins, during teleost oocyte hydration. For this, we employed the seabream as a model organism for

marine euacanthomorph teleosts (supplementary figure S19, see Annexes, page 250) and paralog-specific antisera (supplementary figure S20A and B, see Annexes, page 252).

Immunofluorescence microscopy showed that the expression of Aqp1aa was restricted to the theca cells surrounding vitellogenic ovarian follicles, and this localization did not change during oocyte hydration (supplementary figure S21A, see Annexes, page 254). In contrast, both Aqp1ab1 and -1ab2 were localized in the most cortical region of the ooplasm, while Aqp1ab2 was also detected in the granulosa and theca cells (figure 5A). During oocyte hydration, Aqp1ab1 almost disappeared from the oocyte cortical cytoplasm and accumulated in the most distal part of the microvilli crossing the vitelline envelope, whereas Aqp1ab2 became localized in a more basal region of the microvilli (figure 5B and D). In hydrated mature oocytes, Aqp1ab1 and -1ab2 signals were no longer observed in the microvilli or were greatly reduced, respectively (figure 5C). Immunoblotting and double immunolocalization experiments using seabream YwhazLa/b- or -zLb specific antibodies showed the colocalization of Aqp1ab1 and YwhazLa/b signals in the oocyte, as well as of those of Aqp1ab2 and YwhazLb (figure 5A-C), with their abundance in the plasma membrane increasing during the hydration process (figure 5E). Concomitantly, increased phosphorylation of Aqp1ab1 and -1ab2 was only observed in follicles enclosing hydrating oocytes (supplementary figure S19C and D, see Annexes, page 250). However, co-immunoprecipitation revealed that Aqp1ab1 already interacts with YwhazLa and -zLb in vitellogenic follicles, with the interaction being maintained during oocyte hydration and terminated in mature follicles (figure 5F), whereas Aqp1ab2 only binds to YwhazLb in follicles containing hydrating oocytes (figure 5G).

To confirm that PKA activation triggers Aqp1ab1 and -1ab2 phosphorylation and the YwhazL interactions in oocytes, we incubated isolated seabream vitellogenic ovarian follicles *in vitro* in the presence or absence of FSK. These experiments showed that FSK triggered the translocation of Aqp1ab1 and -1ab2 to the distal and proximal regions of the oocyte microvilli, respectively (figure 5H and supplementary figure S22, see Annexes, page 255), as observed in the *in vivo* hydrating oocytes, and increased water permeability with respect to DMSO-treated (control) follicles (figure 5I). Co-immunoprecipitation confirmed that in control follicles Aqp1ab1 was already phosphorylated and bound to both YwhazLa and -zLb (figure 5J), without the channel trafficking to the distal region of the oocyte microvilli. However, when such distal membrane trafficking is activated by FSK, Aqp1ab1

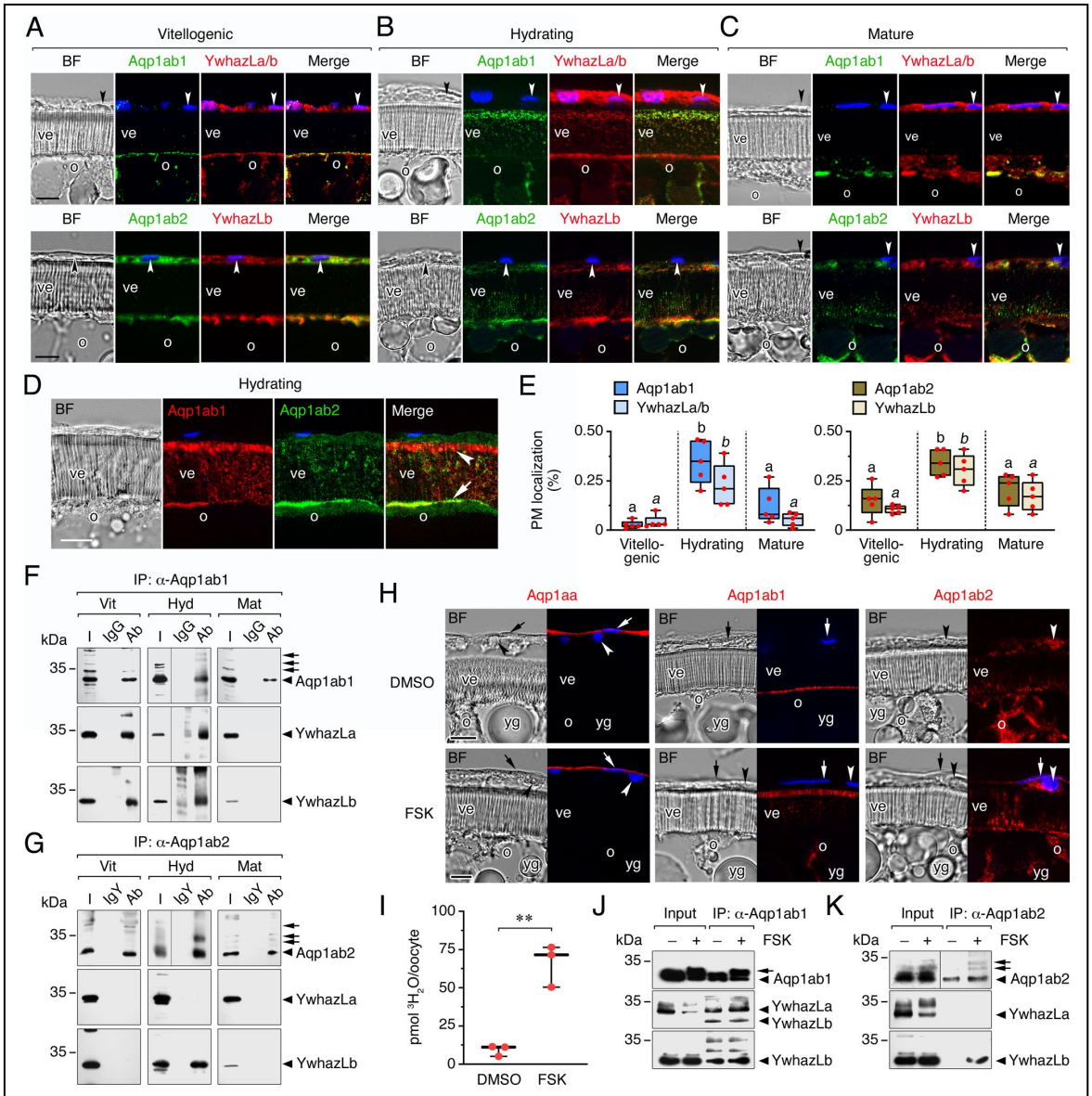

Figure 5. Aqp1ab1 and -1ab2 plasma membrane trafficking and YwhazL interaction is regulated during seabream oocyte hydration *in vivo* and *vitro*. (**A-C**) Double immunostaining of Aqp1ab1 (green) and YwhazLa/b (red), and Aqp1ab2 (green) and YwhazLb (red), in ovarian follicles enclosing vitellogenic (Vit; A), hydrating (Hyd; B) or mature (Mat; C) oocytes. The granulosa (arrowheads) and theca (arrows) cells are counterstained with DAPI (blue). Abbreviations: ve, vitelline envelope; o, oocyte; yg, yolk globule. Control sections are shown in supplementary figure S21B (see Annexes, page 254). Scale bars, 10 µm. (**D**) Double immunostaining of Aqp1ab1 (red; arrowhead) and -1ab2 (green; arrow) in hydrating oocytes. Scale bars and abbreviations as in A-C. (**E**) Fluorescence quantitative estimation of the amount of Aqp1ab1, -1ab2, YwhazLa/b and -zLb in the plasma membrane of oocytes during hydration. (**F**, **G**) Co-immunoprecipitation of Aqp1ab1 (F) or -1ab2 (G) and YwhazLa and -zLb in Vit, Hyd and Mat follicles. The immunoprecipitated products (IP) using seabream Aqp1ab1 and -1ab2 specific antibodies (in F and G, respectively) were immunoblotted with appropriate antibodies as indicated. Phosphorylated forms of the channels are indicated by arrows, whereas aquaporin and YwhazL monomers are indicated by arrowheads. I, input; IgG or IgY, immunoglobulin G or Y; Ab, immunoprecipitating antibody. In F-G and J-K, molecular mass markers (kDa) are on the left. (**H**) Immunostaining of Aqp1aa, -1ab1 and -1ab2 in post-vitellogenic ovarian follicles treated with DMSO (control) or FSK in vitro. Labels as in A-C. Scale bar, 10 µm. (**I**) Uptake of 3H2O by follicle- enclosed oocytes treated with DMSO or IBMX/FSK. (**J**, **K**) Co-immunoprecipitation of Aqp1ab1 (J) or -1ab2 (K) and YwhazLa and -zLb in postvitellogenic follicles treated or not with IBMX/FSK. Labels as in F-G. Data in E and I are presented as box and whisker plots with the number of follicles (E) or pools of 10 follicles (I) analyzed indicated by dots, and were analyzed by ANOVA ($P < 0.05$; different letters indicate significant differences for each protein) or an unpaired Student's t-test (**, $P < 0.01$), respectively.

becomes more phosphorylated, while maintaining the interaction with YwhazLa and -zLb (figure 5J). Phosphorylation of Aqp1ab2 was also increased after FSK stimulation, but in this case the YwhazLb interaction was only detected in the presence of FSK, when the channel is translocated to the basal region of oocyte microvilli (figure 5K).

3.1.4.7. Dual Phosphorylation Generates a Two-Step Regulation of Aqp1ab1 Trafficking to Avoid Competitive Plasma Membrane Occupancy During Oocyte Hydration

The previous data suggested that Aqp1ab1 and -1ab2 phosphorylation in seabream oocytes mediates the YwhazL interaction to facilitate channel trafficking to the plasma membrane. However, the binding of Aqp1ab1 to YwhazL proteins apparently does not induce channel shuttling to the distal region of the oocyte microvilli. Rather, this mechanism appears to be associated with an additional phosphorylation of Aqp1ab1, indicating that a second PKA-mediated phosphorylation event of Aqp1ab1 may have evolved in pelagophil euacanthomorph teleosts. To investigate this hypothesis, we re-examined the role of the two predicted PKA phosphorylation sites in loop D of seabream Aqp1ab1 (Ser^{151} and Ser^{156}) in channel trafficking (figure 6A), either of which are conserved in >95% of marine euacanthomorphs that spawn pelagic eggs such as Atlantic halibut (supplementary figure S10F, see Annexes, page 232). Experiments using *X. laevis* oocytes showed that the increment of the P_f of FSK-treated oocytes co-expressing SaAqp1ab1-S151A or -S156A plus YwhazLa was reduced when compared to oocytes injected with wild-type SaAqp1ab1 and YwhazLa, the reduction being more prominent in the S156A mutant-expressing oocytes (figure 6B). Co-immunoprecipitation and immunoblotting corroborated that none of the mutants prevented the YwhazLa interaction (figure 6C and D), but the relative amount of the S156A mutant in the oocyte plasma membrane was lower than that of the wild-type (figure 6C). Immunostaining of intact *X. laevis* ovarian follicles expressing YwhazL proteins and SaAqp1ab2, together with wild-type SaAqp1ab1 or the S156A mutant, and exposed to FSK, revealed that wild-type SaAqp1ab1 was trafficked to the most distal region of the oocyte microvilli traversing the vitelline envelope, whereas the S156A mutant remained retained in the microvillar proximal region (figure 6E). In contrast, SaAqp1ab2 was accumulated in the proximal region of the microvilli in response to FSK, regardless of the co-expression with the wild-type SaAqp1ab1 or the S156A mutant (figure *6*E). These data therefore suggest that when Aqp1ab1 is bound to YwhazLa or -zLb, a second PKA-mediated

phosphorylation of a loop D Ser is the mechanism by which the channel is shuttled to the distal region of the oocyte microvilli, thus avoiding competitive plasma membrane spatial occupancy with Aqp1ab2 during oocyte hydration.

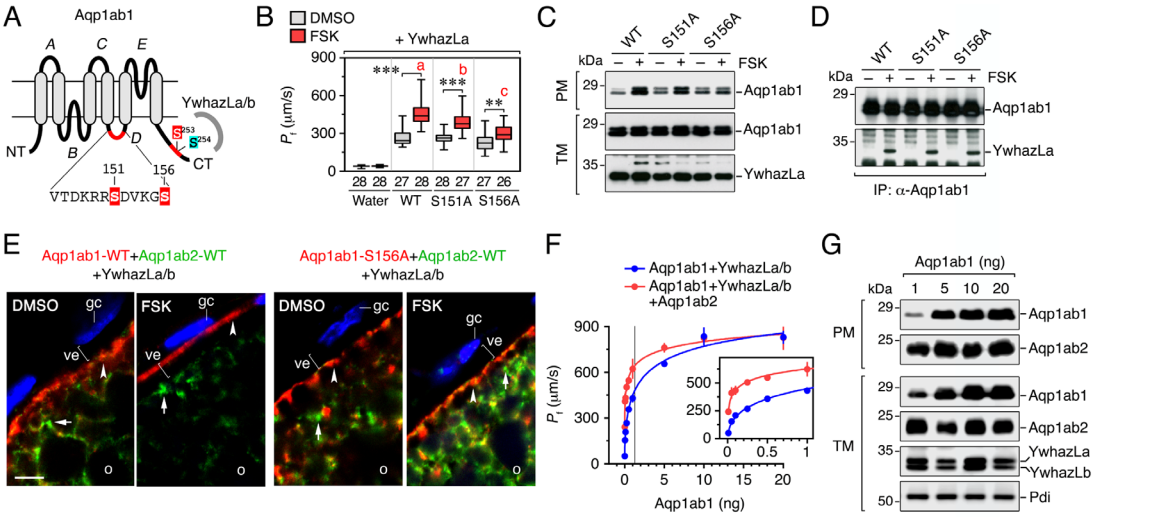

Figure 6. Seabream Aqp1ab1 trafficking is regulated by dual phosphorylation of the cytoplasmic loop D and C-terminus of the channel. (**A**) Schematic representation of the SaAqp1ab1 monomer showing the C-terminus regulatory sites for YwhazLa or -zLb binding (S^{253} and S^{254}), and the amino acid sequence of loop D with the two predicted PKA phosphorylation sites shaded in red. (**B**) P_f of *X. laevis* oocytes injected with water or expressing SaAqp1ab1-WT or mutant channels in loop D (S151A and S156A), and treated with DMSO (control) or FSK. All oocytes were co-injected with YwhazLa-HA. Data are presented as box and whisker plots with the number of oocytes in each group indicated below the plot. For each construct, data were analyzed by the unpaired Student's *t*-test (**, $P < 0.01$: *** $P < 0.001$; as indicated in brackets). Data from oocytes exposed to FSK were separately analyzed by one-way ANOVA ($P < 0.05$; different letters in red color indicate significant differences). (**C-D**) Immunoblot of Aqp1ab1 and YwhazLa in protein extracts of total (TM) and plasma (PM) membrane from oocytes treated as in A (C), and of Aqp1ab1 co-immunoprecipitates (D). (**E**) Double immunostaining of Aqp1ab1 (red) and Aqp1ab2 (green) in *X. laevis* follicle-enclosed oocytes expressing WT Aqp1ab1 (red) or Aqp1ab1-S156A (red), and Aqp1ab2 (green), YwhazLa and -zLb, and treated with DMSO or FSK. gc, granulosa cells; ve, vitelline envelope; o, oocyte. Scale bar, 5 µm. (**F**) P_f of oocytes expressing increasing amounts of Aqp1ab1 cRNA (0.05-20 ng) and fixed amounts of YwhazLa and -zLb (15 ng), in the presence or absence of Aqp1ab2 (20 ng) expression, and treated with FSK. The insert shows the P_f of oocytes injected from 0.05 up to 1 ng Aqp1a1 cRNA. (**G**) Immunoblot of Aqp1ab1, -1ab2, YwhazLa and -zLb in TM and PM protein extracts from oocytes treated as in F. In C,D and G, molecular mass markers are on the left.

To finally investigate the physiological relevance of non-competitive membrane space occupancy of Aqp1ab channels during oocyte hydration, *X. laevis* oocytes were injected with increasing amounts of SaAqp1ab1 cRNA and fixed amounts of YwhazLa and -zLb, in the presence or absence of a constant dose of SaAqp1ab2, followed by P_f determination and immunoblot analysis after FSK treatment. At low doses of SaAqp1ab1 cRNA, the P_f of oocytes correlated well with the protein expression levels and the accumulation of the channel in the oocyte plasma membrane, whereas at high doses of SaAqp1ab1 the P_f and the expression levels reached a plateau (figure 6F and G), possibly indicating the saturation of the oocyte translation machinery. However, co-expression of SaAqp1ab2 with low doses of SaAqp1ab1 resulted in an increased oocyte P_f, which was no longer observed when high doses of SaAqp1ab1 were injected in the oocytes (figure 6F). These data indicate that

expression of Aqp1ab1 and -1ab2 in different regions of the oocyte plasma membrane augments the bulk rate of aquaporin-mediated water flow.

3.1.4.8. A Model for the Regulation of Aqp1ab1 and -1ab2 Intracellular Trafficking During Oocyte Hydration in Marine Euacanthomorph Teleosts

By integrating the functional data obtained in this study for the seabream, a new model for the molecular regulation of Aqp1ab1 and -1ab2 intracellular trafficking during oocyte hydration in marine euacanthomorph teleosts that retain both paralogs can be proposed (figure 7). During vitellogenesis, Aqp1ab1 is phosphorylated at Ser^{253} by PKA to bind YwhazLa and -zLb, and the complex is transported to the oocyte cortical region, where it is retained just below the oocyte plasma membrane. At this stage, Aqp1ab2 is not bound to YwhazLb and remains in the cytoplasm. When oocyte meiosis resumption and yolk hydrolysis are activated by hormonal signals (Fabra *et al*., 2006), the Aqp1ab1 channel complexed with YwhazLa or -zLb is further phosphorylated by PKA at Ser^{156} in loop D, which further shuttles Aqp1ab1 to the most distal region of the oocyte microvilli. Activation of PKA also phosphorylates Thr^{262} in Aqp1ab2, which drives the YwhazLb interaction and the trafficking of the channel to the proximal region of the oocyte microvilli. After hydration, Aqp1ab1 is probably phosphorylated by p38 MAPK at Ser^{254}, which prevents the YwhazL interaction needed for continued trafficking, while also likely decreasing Aqp1ab1 half-life Simultaneously, the interaction of Aqp1ab2 with YwhazLb is also terminated by a yet unknown mechanism that dissociates YwhazLb binding, or due to a decreased synthesis of YwhazLb in the oocyte, such that this paralog also ceases its trafficking to the plasma membrane. The model shows how marine euacanthomorph teleosts that retain a complete so that the channel is directed into the degradation pathway (Moeller *et al*., 2016). TSA1C evolved subfunctionalized mechanisms involving protein kinases and specific YwhazL proteins for the regulation of the trafficking of the downstream Aqp1ab-type paralogs such that competitive plasma membrane spatial occupancy is avoided and the bulk water flow is augmented during oocyte hydration.

3.1.5. Discussion

The origin of the extraordinary diversity of modern marine euacanthomorph teleosts has yet to be fully explained. Since the earliest teleosts are estimated to have arisen towards the end

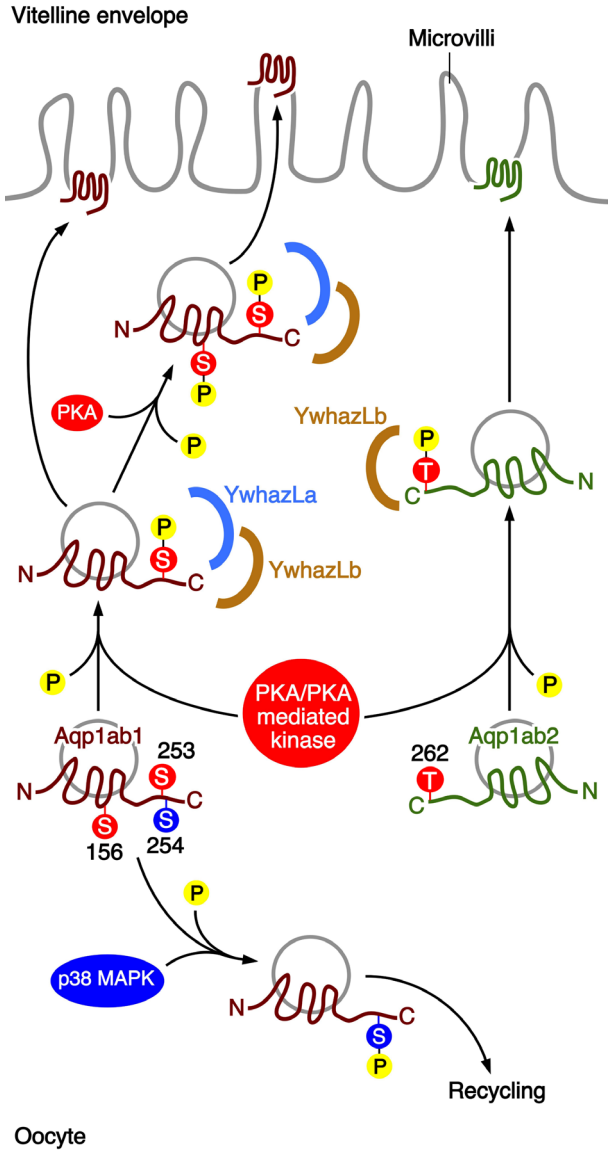

Figure 7. Proposed model for the regulatory pathways controlling Aqp1ab1 and -1ab2 intracellular trafficking during oocyte hydration in the marine euacanthomorph teleost gilthead seabream. During vitellogenesis, Aqp1ab1 is phosphorylated at Ser^{253} by PKA (or by another kinase activated by PKA) to bind YwhazLa and -zLb, and the complex is transported to the oocyte cortical region, where it is retained just below the oocyte plasma membrane. At this stage, Aqp1ab2 is not bound to YwhazLb and remains in the cytoplasm. When meiosis resumption and yolk hydrolysis are activated in oocytes by hormonal signals, the Aqp1ab1 channel complexed with YwhazLa or -zLb is phosphorylated again by PKA at Ser^{156} in loop D, which further shuttles Aqp1ab1 to the most distal region of the oocyte microvilli. At this time, Aqp1ab2 is also phosphorylated by PKA at Thr^{262}, which drives the YwhazLb interaction and the trafficking of the channel to the proximal region of the oocyte microvilli. This model may explain how marine euacanthomorph teleosts that retain a complete TSA1C evolved subfunctionalized mechanisms involving protein kinases and specific YwhazL proteins for the trafficking regulation of the downstream Aqp1ab-type paralogs, such that competitive plasma membrane spatial occupancy is avoided and the bulk water flow is augmented during oocyte hydration.

of the Paleozoic Era ~300 mya in the aftermath of an R3 whole genome duplication (Hurley *et al*., 2007; Amores *et al*., 2011; Near *et al*., 2012; Hughes *et al*., 2018), it has been suggested that the additional gene repertoires and their subsequent neo-/sub-functionalization could have provided the genetic material for the radiative success (Hoegg

et al., 2004; Postlethwait *et al*., 2004). However, the large chronological gap (~245 million years) between the R3 event and the explosive radiation of the Euacanthomorphacea in marine environments ~55 Ma, together with the rediploidization of the genomes (Lien *et al*., 2016; Van de Peer *et al*., 2017) are considered problematic for single causal events such as R3 (Santini *et al*., 2009). Indeed, a similar uncoupling between WGD events and adaptation potential has been noted for plants (Schranz *et al*., 2012). In the present work, we uncover an ancient TSA1C together with novel molecular regulatory mechanisms that co-evolved to provide the majority of marine euacanthomorph embryos with the water of life when no osmoregulatory systems exist. The process of oocyte hydration, which occurs during the final meiotic maturation stages of oogenesis, is so efficient that the spawned eggs typically achieve water contents of >90%, so that they float pelagically for dispersal in the oceanic currents. In contrast to previous studies (Fabra *et al*., 2005; 2006; Kagawa *et al*., 2009; Zapater *et al*., 2011), we show here that the mechanism of oocyte hydration involves in fact two tandemly duplicated *aqp1ab*-type genes that are selectively retained in species that spawn pelagic eggs. The phylogenetic and synteny analyses of piscine *aqp1*-type genes revealed that two of the three main lineages of extant teleosts (Elopomorpha and Osteoglossomorpha) still encode the R3 ohnologs (*aqp1aa* and *aqp1b*), and that the teleost-specific *aqp1ab*-type genes only duplicated downstream of the *aqp1aa* paralog to form the TSA1C. Since we did not find traces of the *aqp1ab*-type genes in the genomes of the pre-teleost actinopterygian lineages, yet observe that the osteoglossomorph teleosts still retain pseudogene remnants of *aqp1ab1* and *-1ab2*, the tandem duplication event likely occurred soon after R3 and was thus ancient and specific for teleosts.

The consequences of gene duplication have been widely recognized, with stochastic silencing and loss occurring as the most prevalent outcome within a few million years (Lynch and Conery, 2000). This type of outcome fits the evolution of the *aqp1b* ohnologs, which are seemingly extinct in all clupeocephalan teleosts. Conversely, gene preservation is associated with the acquisition of novel (neo-) or split (sub-) functions (Force *et al*., 1999). In the present context, we find that all three processes have continued to impact the trajectories of *aqp1ab*-type genes throughout ~300 million years of teleost evolution. The data show that many lineages have lost or only retain fragmented pseudogenes of both paralogs, while others have lost either the *aqp1ab1* or *-1ab2* gene, yet many species still retain both of the tandem duplicates. An overwhelming majority (95%) of species that spawn

pelagic eggs in marine environments retain at least one of the duplicates, with a third of the species still harboring complete copies of both paralogs. Conversely, much higher levels of gene loss are seen in species that spawn benthic eggs (43%) or incubate their eggs internally (91%). In marine benthic eggs, oocytes hydrate to a significantly lower degree than pelagic eggs, reaching water contents of 68-82% of egg wet mass (Finn *et al*., 2002a and 2002b; Cerdà *et al*., 2007), while the eggs of seahorses and pipefishes, which are incubated in the male brood pouch that remains hyposmotic to seawater (Ripley, 2009), do not hydrate (Finn, unpublished data).

Although some species of FW teleosts also retain the TSA1C, with *aqp1ab*-type gene expression occurring in extraovarian tissues (Cerdà and Finn, 2010; Engelund and Madsen, 2014; Cerdà *et al*., 2017), our present and previous data (Tingaud-Sequeira *et al*., 2008; Zapater *et al*., 2011) show that *aqp1ab1* and *-1ab2* transcript enrichment within the ovaries of marine pelagophil species are orders of magnitude higher than in the somatic tissues, and that both channels are localized in the same plasma membrane of hydrating oocytes. Such a co-localization of closely related water-selective channels is unexpected, since it may imply redundant membrane space occupancy. This observation, together with the absence of membrane trafficking when Aqp1ab2 was heterologously expressed in amphibian oocytes, prompted us to investigate the intracellular trafficking regulation of the TSA1C channels.

By comparing the subdomains of the teleost TSA1C channels to the Aqp1 orthologs of non-teleost vertebrates, it became evident that the regulatory sites in the Aqp1 and Aqp1aa orthologs have remained relatively fixed through time, while those of the Aqp1ab1 and -1ab2 channels have selectively changed during teleost evolution (figure 8). For example, PKC positively regulates the membrane trafficking of the Aqp1/Aqp1aa orthologs through phosphorylation of a conserved Thr in loop D in most vertebrate groups except some amphibians, Polypteriformes, Siluriformes and Euteleostei, which encode a Val or Ala. The Thr/Val substitution in Euteleostei resulted in the loss of the positive PKC-mediated regulation and the emergence of a negative PKC-mediated regulation. Further, in contrast to Chondrichthyes and Sarcopterygii, many actinopterygian fishes evolved a C-terminal Ser for positive regulation via PKA-mediated phosphorylation. Nevertheless, even in euacanthomorph species in which the Aqp1aa C-terminal PKA site is conserved, as in Senegalese sole, an alternative negative PKC-mediated regulation still exists, while the positive PKA-mediated regulation of the older lineages is also maintained.

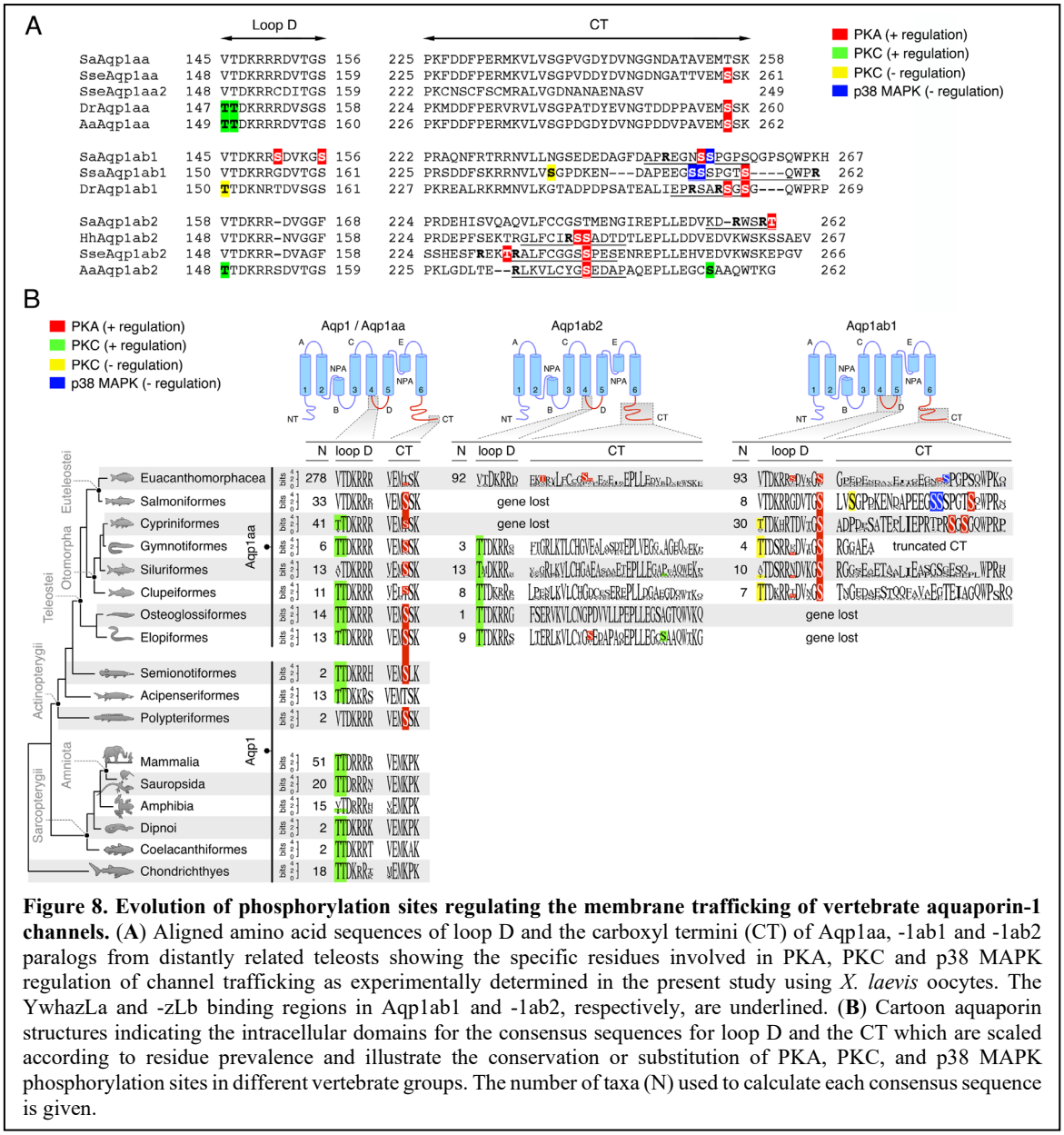

Figure 8. Evolution of phosphorylation sites regulating the membrane trafficking of vertebrate aquaporin-1 channels. (**A**) Aligned amino acid sequences of loop D and the carboxyl termini (CT) of Aqp1aa, -1ab1 and -1ab2 paralogs from distantly related teleosts showing the specific residues involved in PKA, PKC and p38 MAPK regulation of channel trafficking as experimentally determined in the present study using *X. laevis* oocytes. The YwhazLa and -zLb binding regions in Aqp1ab1 and -1ab2, respectively, are underlined. (**B**) Cartoon aquaporin structures indicating the intracellular domains for the consensus sequences for loop D and the CT which are scaled according to residue prevalence and illustrate the conservation or substitution of PKA, PKC, and p38 MAPK phosphorylation sites in different vertebrate groups. The number of taxa (N) used to calculate each consensus sequence is given.

In contrast to the Aqp1/Aqp1aa, the two Aqp1ab-type channels evolved PKA, PKC and p38 MAPK regulatory sites that are both dependent and independent of the teleost-specific YwhazL binding proteins (figure 8). The identification of the novel YwhazLa and -zLb paralogs in the present study extend recent findings reporting that ostariophysan teleosts encode duplicated *ywhaz* genes of the mammalian *YWHAZ* ortholog (Zhang *et al.*, 2021). In the present context, however, we note that the *ywhazLa* gene synteny is only conserved between Otophysi and osteoglossomorph teleosts, while the *ywhazLb* gene is only syntenic within the Ostariophysi (e.g. zebrafish and catfishes). The novel *ywhazLa* and *-zLb* genes identified here cluster within the vertebrate *ywhaz* clade, but are polyphyletic and are not

syntenic between euacanthomorph and the more basal teleost lineages. Their neofunctionalization can be inferred from the longer branch lengths, and the mutagenesis experiments show their specific functional requirement for plasma membrane trafficking of the Aqp1ab-type channels. For example, in the basal cohort of elopomorph teleosts, such as the European eel, which spawn pelagic eggs and only retain the Aqp1ab2 paralog, PKA-mediated positive regulation of membrane trafficking is dependent on C-terminal YwhazLa binding and two YwhazLa-independent PKC-regulated sites in loop D and the C-terminus, respectively (figure 8). In modern lineages of euacanthomorph species that retain both the Aqp1ab2 and -1ab1 paralogs, the PKC-mediated regulation of Aqp1ab2 is lost, and membrane trafficking became dependent on PKA-mediated phosphorylation of the same C-terminal Ser residues as in the elopomorph teleosts, but dependent on YwhazLb rather than YwhazLa binding.

A more intricate regulation of membrane trafficking evolved in the teleost Aqp1ab1 channels (figure 8). Amongst cyprinid species, such as zebrafish, PKA-mediated phosphorylation of different Ser residues in the C-terminus positively regulates membrane trafficking, on both YwhaLa-dependent and independent manner, while PKC-mediated phosphorylation in loop D recycles the channel. In salmonids, such as the Atlantic salmon, only the positive PKA-mediated regulation in the C-terminus that is dependent on YwhazLa binding is maintained, while new C-terminal recycling sites emerge that are regulated by PKC (outside of the YwhazLa binding domain) and p38 MAPK (within the YwhazLa binding site). The p38 MAPK negative regulatory site in the YwhazLa binding region is maintained in euacanthomorph teleosts, such as seabream, together with a positive PKA-mediated YwhazLa-dependent site. However, two additional positive PKA-mediated regulation sites appear in loop D of Aqp1ab1 that depend on the binding of the channel to YwhazLa. It is this latter two-step regulation that generates a membrane trafficking shunt of Aqp1ab1 to the distal region of the microvilli, and thus the avoidance of competitive occupancy of the same membrane space as the Aqp1ab2 channel. In contrast, Aqp1ab2 is dependent on YwhazLb binding, and lacks the loop D regulatory step, and thus remains in the proximal region of the plasma membrane. Our *ex vivo* experimental data also show that the Aqp1ab1 membrane shunt can be recapitulated in the surrogate *X. laevis* oocytes co-expressing Aqp1ab1, -1ab2 and the YwhaL binding proteins, resulting in an increase in the bulk rate of water transport.

The combined findings thus shed new light on the molecular adaptations facilitating the success of teleost eggs in the oceans. To survive in the harsh hyperosmotic saline environment, teleosts evolved adaptive solutions that provide their hyposmotic marine embryos with the water of life prior to the development of homeosmotic regulatory systems. The process involved the selective retention of duplicated *aqp1ab*-type water channel genes that are tandemly arranged in an ancient ternary cluster, the TSA1C. Each channel co-evolved with specific YwhazL regulatory proteins and PKA-, PKC- and p38 MAPK-mediated phosphorylation pathways to regulate hydration of the oocytes. The most intricate solutions evolved in the highly diverse marine euacanthomorph teleosts that retain both of the Aqp1ab1 and -1ab2 channels. In such species, an innovative membrane shunt evolved that avoids competitive space occupancy in the oocyte plasma membrane and an increase in the rate of bulk water influx during hydration. The hydration process is terminated though the evolution of p38 MAPK-mediated phosphorylation sites in the YwhazLa binding region of Aqp1ab1, which dissociates the interaction with YwhazLa, and through a different mechanism also resulting in the release of the YwhazLb from Aqp1ab2. Both mechanisms consequently induce the recycling of the two Aqp1ab-type channels from the plasma membrane, so that >90% of the egg water content remains locked within the yolk cell due to the reduction in the oocyte permeability. When fertilized, the water-endowed eggs with a recombined allelic potential have a lower specific gravity than the surrounding seawater and they thus float as passive pelagic passengers in the oceanic currents, which geodisperse them to new horizons.

Acknowledgements: We thank Michael Dondrup (University of Bergen, Norway) and Per Gunnar Fjelldal (Institute of Marine Research, Norway) for assistance in bioinformatic analysis and collection of biological samples from Atlantic salmon, respectively. This work was supported by the Spanish Ministry of Science and Innovation (MCIN/AEI/ 10.13039/501100011033), the European Regional Development Fund (ERDF) “A way of making Europe” (European Union), Grant no. AGL2016-76802-R (to J.C.), and the Norwegian Research Council (RCN) Grant no. 294768/E40 (to R.N.F). F.C. and A.F. were supported, respectively, by the “Ramon y Cajal” programe (RYC-2015-17103) and a predoctoral (BES-2014-068745) contract from Spanish MCIN. R.N.F. was also supported by the University of Bergen (Norway).

Author Contributions: J.C. and R.N.F. designed the study. B.N. and L.B. provided biological samples and genomic sequences. R.N.F. and J.C. carried out the phylogenetic and *in silico* analyses. A.F., F.C. and M.C. performed wet laboratory experiments and collected data. A.V., R.G. and R.N.F. carried out RNA-seq analysis. A.F., F.C., R.N.F. and J.C. interpreted the results. J.C. acquired the funding and supervised the work. J.C. and R.N.F. wrote the manuscript. All authors approved the final version of the manuscript.

Conflict of interest: The authors declare that they have no competing interests.

3.1.6. References

Agre P, Sasaki S, Chrispeels MJ. 1993. Aquaporins: a family of water channel proteins. *Am J Physiol.* 265(3 Pt 2):F461. doi: 10.1152/ajprenal.1993.265.3.F461.

Ahlstrom EH, Moser HG. 1981. Systematics and development of early life history stages of marine fishes: Achievements during the past century, present status and suggestions for the future. *Rapp P-v Réun Cons int Explor Mer*.178**:**541-546.

Albalat R, Cañestro C. 2016. Evolution by gene loss. *Nature Rev Genet.* 17(7):379-91. doi: 10.1038/nrg.2016.39.

Amores A, Catchen J, Ferrara A, Fontenot Q, Postlethwait JH. 2011. Genome evolution and meiotic maps by massively parallel DNA sequencing: Spotted gar, an outgroup for the teleost genome duplication. *Genetics*. 188(4):799-808. doi: 10.1534/genetics.111.127324.

Berthelot C, Brunet F, Chalopin M, Juanchich A, Bernard M, Noel B, Bento P, Da Silva C, Labadie K, Alberti A, *et al*. 2014. The rainbow trout genome provides novel insights into evolution after whole-genome duplication in vertebrates. *Nat Commun.* 5:3657. doi: 10.1038/ncomms4657.

Cerdà J, Fabra M, Raldúa D. 2007. Physiological and molecular basis of fish oocyte hydration. In: Babin, P.J., Cerdà, J., Lubzens, E (eds). The Fish Oocyte. Springer. 349-396. doi: 10.1007/978-1-4020-6235-3_12.

Cerdà J, Finn RN. 2010. Piscine aquaporins: an overview of recent advances. *J Exp Zool A Ecol Genet Physiol*. 313(10):623-50. doi: 10.1002/jez.634.

Cerdà J, Chauvigné F, Finn RN. 2017. The physiological role and regulation of aquaporins in teleost germ cells. *Adv Exp Med Biol*. 969:149-171. doi: 10.1007/978-94-024-1057-0_10.

Chauvigné F, Lubzens E, Cerdà J. 2011. Design and characterization of genetically engineered zebrafish aquaporin-3 mutants highly permeable to the cryoprotectant ethylene glycol. *BMC Biotechnol*. 11:34. doi: 10.1186/1472-6750-11-34.

Chauvigné F, Boj M, Vilella S, Finn RN, Cerdà J. 2013. Subcellular localization of selectively permeable aquaporins in the male germ line of a marine teleost reveals spatial redistribution in activated spermatozoa. *Biol Reprod*. 89(2):37. doi: 10.1095/biolreprod.113.110783.

Chauvigné F, Parhi J, Ducat C, Ollé J, Finn RN, Cerdà J. 2018. The cellular localization and redistribution of multiple aquaporin paralogs in the spermatic duct epithelium of a maturing marine teleost. *J Anat*. 233(2):177-192. doi: 10.1111/joa.12829.

Chauvigné F, Yilmaz O, Ferré A, Fjelldal PG, Finn RN, Cerdà J. 2019. The vertebrate Aqp14 water channel is a neuropeptide-regulated polytransporter. *Comm Biol*. 2:462. doi: 10.1038/s42003-019-0713-y.

Chauvigné F, Ferré A, Cerdà J. 2021. The *Xenopus* oocyte as an expression system for functional analyses of fish aquaporins. *Methods Mol Biol*. 2218:11-28. doi: 10.1007/978-1-0716-0970-5_2.

Crow KD, Smith CD, Cheng JF, Wagner GP, Amemiya CT. 2012. An independent genome duplication inferred from Hox paralogs in the American paddlefish - A representative basal ray-finned fish and important comparative reference. *Genome Biol Evol*. 4(9):937-53. doi: 10.1093/gbe/evs067.

Deen PM, Verdijk MA, Knoers NV, Wieringa B, Monnens LA, van Os CH, van Oost BA. 1994. Requirement of human renal water channel aquaporin-2 for vasopressin-dependent concentration of urine. *Science*. 264(5155):92-5. doi: 10.1126/science.8140421.

Du K, Stöck M, Kneitz S, Klopp C, Woltering JM, Adolfi MC, Feron R, Prokopov D, Makunin A, Kichigin I, *et al*. 2020. The sterlet sturgeon genome sequence and the

mechanisms of segmental rediploidization. *Nature Ecol Evol*. 4(6):841-852. doi: 10.1038/s41559-020-1166-x.

Engelund MB, Madsen SS. 2014. Tubular localization and expressional dynamics of aquaporins in the kidney of seawater-challenged Atlantic salmon. *J Comp Physiol B*. 185(2):207-23. doi: 10.1007/s00360-014-0878-0.

Fabra M, Raldúa D, Power DM, Deen PM, Cerdà J. 2005. Marine fish egg hydration is aquaporin-mediated. Science. 307(5709):545. doi: 10.1126/science.1106305.

Fabra M, Raldúa D, Bozzo MG, Deen PM, Lubzens E, Cerdà J. 2006. Yolk proteolysis and aquaporin-1o play essential roles to regulate fish oocyte hydration during meiosis resumption. *Dev Biol*. 295(1):250-62. doi: 10.1016/j.ydbio.2006.03.034.

Finn RN, Fyhn HJ, Norberg B, Munholland J, Reith M. 2000. Oocyte hydration as a key feature in the adaptive evolution of teleost fishes to seawater. In: Norberg B, Kjesbu OS., Taranger GL, Anderson E, Stefansson SO, (eds). Proc. 6th Int. Symp. *Reprod. Physiol. Fish*. Inst Mar Res and Univ Bergen. p 289-291.

Finn RN, Østby G, Norberg B, Fyhn HJ. 2002a. *In vivo* oocyte hydration in Atlantic halibut (*Hippoglossus hippoglossus*); Proteolytic liberation of free amino acids, and ion transport are driving forces for osmotic water influx. *J Exp Biol*. 205(Pt 2):211-24. doi: 10.1242/jeb.205.2.211.

Finn RN, Wamboldt M, Fyhn HJ. 2002b. Differential processing of yolk proteins during oocyte hydration in fishes (Labridae) that spawn benthic and pelagic eggs. *Mar Ecol Prog Ser*. 237: 217-226. doi:10.3354/meps237217.

Finn RN. 2007. The maturational disassembly and differential proteolysis of paralogous vitellogenins in a marine pelagophil teleost: A conserved mechanism of oocyte hydration. *Biol Reprod*. 76(6):936-48. doi: 10.1095/biolreprod.106.055772.

Finn RN, Kristoffersen BA. 2007. Vertebrate vitellogenin gene duplication in relation to the ‘‘3R Hypothesis’’: Correlation to the pelagic egg and the oceanic radiation of teleosts. *PLoS One*. 2(1):e169. doi: 10.1371/journal.pone.0000169.

Finn RN, Fyhn HJ. 2010. Requirement for amino acids in ontogeny of fish. *Aquacult Res*. 41(5):684 - 716. doi: 10.1111/j.1365-2109.2009.02220.x.

Finn RN, Cerdà J. 2011. Aquaporin evolution in fishes. *Front Physiol*. 2:44. doi: 10.3389/fphys.2011.00044.

Finn RN, Chauvigné F, Hlidberg JB, Cutler CP, Cerdà J. 2014. The lineage-specific evolution of aquaporin gene clusters facilitated tetrapod terrestrial adaptation. *PLoS One*. 9(11):e113686. doi: 10.1371/journal.pone.0113686.

Finn RN, Cerdà J. 2015. Evolution and functional diversity of aquaporins. *Biol Bull*. 229(1):6-23. doi: 10.1086/BBLv229n1p6.

Force A, Lynch M, Pickett FB, Amores A, Yan YL, Postlethwait J. 1999. Preservation of duplicate genes by complementary, degenerative mutations. *Genetics.* 151(4):1531-45. doi: 10.1093/genetics/151.4.1531.

Friedman M. 2010. Explosive morphological diversification of spiny-finned teleost fishes in the aftermath of the end-Cretaceous extinction. *Proc Biol Sci.* 277(1688):1675-83. doi: 10.1098/rspb.2009.2177.

Fu H, Subramanian RR, Masters SC. 2000. 14-3-3 proteins: Structure, function, and regulation. *Annu Rev Pharmacol Toxicol*. 40:617-47. doi: 10.1146/annurev.pharmtox.40.1.617.

Fyhn HJ, Finn RN, Reith M, Norberg B. 1999. Yolk protein hydrolysis and oocyte free amino acids as key features in the adaptive evolution of teleost fishes to seawater. *Sarsia*. 84:5-6, 451-456. doi: 10.1080/00364827.1999.10807350.

Gasanov EV, Jedrychowska J, Kuznicki J, Korzh V. 2021. Evolutionary context can clarify gene names: Teleosts as a case study. *BioEssays*. 43(6):e2000258. doi: 10.1002/bies.202000258.

Hoegg S, Brinkmann H, Taylor JS, Meyer A. 2004. Phylogenetic timing of the fish-specific genome duplication correlates with the diversification of teleost fish. *J Mol Evol*. 59(2):190-203. doi: 10.1007/s00239-004-2613-z.

Hughes LC, Orti G, Huang Y, Sun Y, Baldwin CC, Thompson AW, Arcila D, Betancur-R, Rli C, Becker L, *et al*. 2018. Comprehensive phylogeny of ray-finned fishes (Actinopterygii) based on transcriptomic and genomic data. *Proc Natl Acad Sci USA*. 115(24):6249-6254. doi: 10.1073/pnas.1719358115.

Hurley IA, Mueller RL, Dunn KA, Schmidt EJ, Friedman M, Ho RK, Prince VE, Yang Z, Thomas MG, Coates MI. 2007. A new time-scale for ray-finned fish evolution. *Proc Royal Soc*. 274(1609):489-98. doi: 10.1098/rspb.2006.3749.

Kagawa H, Horiuchi Y, Kasuga Y, Kishi T. 2009. Oocyte hydration in the Japanese eel (*Anguilla japonica*) during meiosis resumption and ovulation. *J Exp Zool*. 311(10):752-62. doi: 10.1002/jez.560.

Kamsteeg EJ, Deen PM. 2001. Detection of aquaporin-2 in the plasma membranes of oocytes: a novel isolation method with improved yield and purity. *Biochem Biophys Res Commun*. 282(3):683-90. doi: 10.1006/bbrc.2001.4629.

Kendall AW, Ahlstrom EH, Moser HG. 1984. Early life history stages of fishes and their characters. In: Moser HG, editor. Ontogeny and systematics of fishes. Am Soc Ichthyol Herpetol Special publ 1. p. 11-22.

Lien S, Koop BF, Sandve SR, Miller JR, Kent MP, Nome T, Hvidsten TR, Leong JS, Minkley DR, Zimin A, *et al*. 2016. The Atlantic salmon genome provides insights into rediploidization. *Nature.* 533(7602):200-5. doi: 10.1038/nature17164.

Lynch M, Conery JS. 2000. The Evolutionary fate and consequences of duplicate genes. *Science*. 290(5494):1151-5. doi: 10.1126/science.290.5494.1151

MacQueen DJ, Johnston I. 2014. A well-constrained estimate for the timing of the salmonid whole genome duplication reveals major decoupling from species diversification. *Proc R Soc B Biol Sci*. 281(1778):20132881. doi: 10.1098/rspb.2013.2881.

Maissey JG. 1996. Discovering fossil fishes. New York: Westview Press.

Moeller HB, Slengerik-Hansen J, Aroankins T, Assentoft M, MacAulay N, Moestrup SK, Bhalla V, Fenton RA. 2016. Regulation of the Water Channel Aquaporin-2 via 14-3-3θ and -ζ. *J Biol Chem*. 291(5):2469-84. doi: 10.1074/jbc.M115.691121..

Near TJ, Eytan RI, Domburg A, Kristen KL, Moore JA, Davis MP, Wainwright PC, Friedman M, Smith WL. 2012. Resolution of ray-finned fish phylogeny and timing of diversification. *Proc Natl Acad Sci USA.* 109(34):13698-703. doi: 10.1073/pnas.1206625109.

Nesverova V, Törnroth-Horsefield S. 2019. Phosphorylation-dependent regulation of mammalian aquaporins. *Cells*. 8(2):82. doi: 10.3390/cells8020082.

Postlethwait J, Amores A, Cresko W, Singer A, Yan YL. 2004. Subfunction partitioning, the teleost radiation and the annotation of the human genome. *Trends Genet*. 20(10):481-90. doi: 10.1016/j.tig.2004.08.001.

Prado K, Cotelle V, Li G, Bellati J, Tang N, Tournaire-Roux C, Martinière A, Santoni V, Maurel C. 2019. Oscillating aquaporin phosphorylation and 14-3-3 proteins mediate the circadian regulation of leaf hydraulics. *Plant Cell*. 31(2):417-429. doi: 10.1105/tpc.18.00804.

Rajan S, Preisig-Müller R, Wischmeyer E, Nehring R, Hanley PJ, Renigunta V, Musset B, Schlichthörl G, Derst C, Karschin A, Daut J. 2002. Interaction with 14-3-3 proteins promotes functional expression of the potassium channels TASK-1 and TASK-3. *J Physiol*. 545(1):13-26. doi: 10.1113/jphysiol.2002.027052.

Ripley JL. 2009. Osmoregulatory role of the paternal brood pouch for two Sygnathus species. *Comp Biochem Physiol.* 154(1):98-104. doi: 10.1016/j.cbpa.2009.05.003.

Santini F, Harmon LJ, Carnevale G, Alfaro ME. 2009. Did genome duplication drive the origin of teleosts? A comparative study of diversification in ray-finned fishes. *BMC Evol Biol*. 9:194. doi: 10.1186/1471-2148-9-194.

Shikano S, Coblitz B, Sun H, Li M. 2005. Genetic isolation of transport signals directing cell surface expression. *Nat Cell Biol*. 7(10):985-92. doi: 10.1038/ncb1297.

Schranz ME, Mohammadin S, Edger PP. 2012. Ancient whole genome duplications, novelty and diversification: the WGD Radiation Lag-Time Model. *Curr Opin Plant Biol*. 15(2):147-53. doi: 10.1016/j.pbi.2012.03.011.

Sullivan CV, Yilmaz O. 2018. Vitellogenesis and Yolk Proteins, Fish. Encyclopedia of Reproduction, 2nd Ed. Elsevier Inc, p 1-11.

Tingaud-Sequeira A, Chauvigné F, Fabra M, Lozano J, Raldúa D, Cerdà J. 2008. Structural and functional divergence of two fish aquaporin-1 water channels following teleost-specific gene duplication. *BMC Evol Biol*. 8:259. doi: 10.1186/1471-2148-8-259.

Van de Peer Y, Mizrachi E, Marchal K. 2017. The evolutionary significance of polyploidy. *Nature Rev Genetics*. 18(7):411-424. doi: 10.1038/nrg.2017.26.

Xu P, Xu J, Liu G-J, Chen L, Zhou Z, Peng W, Jiang Y, Zhao Z, Jia Z, Sun Y, *et al*. 2019. The allotetraploid origin and asymmetrical genome evolution of the common carp *Cyprinus carpio*. *Nat Commun*. 10(1):4625. doi: 10.1038/s41467-019-12644-1.

Yilmaz O, Chauvigné F, Ferré A, Nilsen F, Fjelldal PG, Cerdà J, Finn RN. 2020. Unravelling the Complex Duplication History of Deuterostome Glycerol Transporters. *Cells*. 9(7):1663. doi: 10.3390/cells9071663.

Zapater C, Chauvigné F, Norberg B, Finn RN, Cerdà J. 2011. Dual neofunctionalization of a rapidly evolving aquaporin-1 paralog resulted in constrained and relaxed traits controlling channel function during meiosis resumption in teleosts. *Mol Biol Evol*. 28(11):3151-69. doi: 10.1093/molbev/msr146.

Zapater C, Chauvigné F, Tingaud-Sequeira A, Finn RN, Cerdà J. 2013. Primary oocyte transcriptional activation of Aqp1ab by the nuclear progestin receptor determines the pelagic egg phenotype of marine teleosts. *Dev Biol*. 377(2):345-62. doi: 10.1016/j.ydbio.2013.03.001.

Zhang X, Yu p, Wen H, Qi X, Tian Y, Zhang K, Fu Q, Li Y, Li C. 2021. Genome-wide characterization of aquaporins (aqps) in *Lateolabrax maculatus*: Evolution and expression patterns during freshwater acclimation. *Mar Biotechnol*. 23(5):696-709. doi: 10.1007/s10126-021-10057-0.

CHAPTER II:

Neurohypophysial and paracrine vasopressinergic signaling regulates aquaporin trafficking to hydrate marine teleost oocytes

Alba Ferré[1], François Chauvigné[2], Magdalena Gozdowska[3], Ewa Kulczykowska[3], Roderick Nigel Finn[1,4] and Joan Cerdà[1]

[1]Institute of Agrifood Research and Technology (IRTA)-Institute of Biotechnology and Biomedicine (IBB), Universitat Autònoma de Barcelona, Barcelona, Spain.
[2]Institute of Marine Sciences, Spanish National Research Council (CSIC), Barcelona, Spain. [3]Department of Genetics and Marine Biotechnology, Institute of Oceanology, Polish Academy of Sciences, Sopot, Poland.
[4]Department of Biological Sciences, University of Bergen, Bergen, Norway.

Frontiers in Endocrinology (Lausanne). 14:1222724. 2023.
doi: 10.3389/fendo.2023.1222724.

3.2.1. Abstract

The dual aquaporin (Aqp1ab1/Aqp1ab2)-mediated hydration of marine teleost eggs, which occurs during oocyte meiosis resumption (maturation), is considered a key adaptation underpinning their evolutionary success in the oceans. However, the endocrine signals controlling this mechanism are almost unknown. Here, we investigated whether the nonapeptides arginine vasopressin (Avp, formerly vasotocin) and oxytocin (Oxt, formerly isotocin) are involved in marine teleost oocyte hydration using the gilthead seabream (*Sparus aurata*) as a model. We show that concomitant with an increased systemic production of Avp and Oxt, the nonapeptides are also produced and accumulated locally in the ovarian follicles during oocyte maturation and hydration. Functional characterization of representative Avp and Oxt receptor subtypes indicates that Avpr1aa and Oxtrb, expressed in the postvitellogenic oocyte, activate phospholipase C and protein kinase C pathways, while Avpr2aa, which is highly expressed in the oocyte and in the follicular theca and granulosa cells, activates the cAMP-protein kinase A (PKA) cascade. Using *ex vivo, in vitro* and mutagenesis approaches, we determined that Avpr2aa plays a major role in the PKA-mediated phosphorylation of the aquaporin subdomains driving membrane insertion of Aqp1ab2 in the theca and granulosa cells, and of Aqp1ab1 and Aqp1ab2 in the distal and proximal regions of the oocyte microvilli, respectively. The data further indicate that luteinizing hormone, which surges during oocyte maturation, induces the synthesis of Avp in the granulosa cells via progestin production and the nuclear progestin receptor. Collectively, our data suggest that both the neurohypophysial and paracrine vasopressinergic systems integrate to differentially regulate the trafficking of the Aqp1ab-type paralogs via a common Avp-Avpr2aa-PKA pathway to avoid competitive occupancy of the same plasma membrane space and maximize water influx during oocyte hydration.

Keywords: Aquaporin, trafficking, vasopressin, oxytocin, progestin, oocyte hydration, teleost

3.2.2. Introduction

Water transport during vertebrate oogenesis determines the phenotypic nature of antral follicles in mammals and the pelagic (floating) eggs of marine teleosts (Huang *et al*., 2006; Cerdà *et al*., 2017). In both cases, aquaporins are recognized as the primary channels of transmembrane water flux resulting in the fluid-driven expansion of the follicles (Cerdà *et al*., 2017; McConnell *et al*., 2002). However, little is known of the endocrine signals regulating their follicular trafficking. Aquaporins belong to a large family of integral membrane proteins that evolved to facilitate the flux of water and other small molecules through their central pores (Agre *et al*., 1993). They function in tetrameric assemblages, with each aquaporin monomer that forms a water pore comprised of six transmembrane domains, two hemi-helices bearing conserved Asn-Pro-Asp (NPA) motifs, three extracellular loops (A, C, E), two intracellular loops (B, D), and intracellular N- and C-terminal domains of varying lengths (King *et al*., 2004). Up to 15 subfamilies (AQP0-14) are recognized in egg-laying mammals, but due to gene loss, only 13 subfamilies (AQP0-12) remain in placental mammals (Finn *et al*., 2014). Conversely, although a similar number of orthologous subfamilies have been identified in teleost fishes, the gene copy numbers are higher (19-26 in diploids, 38-48 in paleotetraploids) due to extra rounds of whole genome duplications combined with cladal- and lineage-level tandem duplications and gene losses (Finn *et al*., 2014; Tingaud-Sequeira *et al*., 2010; Cerdà and Finn, 2010; Finn and Cerdà, 2011, 2015; Yilmaz *et al*., 2020; Ferré *et al*., 2023).

In mammalian follicles AQP1, -5, -7, -8 and -9 are thought to mediate water transport via the granulosa cells to form the extracellular antrum (McConnell *et al*., 2002; Skowronski *et al*., 2009; Wang *et al.*, 2018). In contrast, in marine teleosts water flows intracellularly into the oocyte across the plasma membrane via tandemly duplicated orthologs of mammalian AQP1 (Aqp1ab1 and/or Aqp1ab2) (Ferré *et al*., 2023; Fabra *et al*., 2005, 2006; Kagawa *et al*., 2011; Zapater *et al*., 2011). The Aqp1ab-type paralogs are encoded in an ancient teleost-specific aquaporin-1 cluster (TSA1C: *aqp1aa-aqp1ab2-aqp1ab1*) that evolved ~300 Ma with the emergence of the clade (Ferré *et al*., 2023). The *aqp1ab*-type genes of the TSA1C are highly selectively retained in marine species that spawn pelagic eggs, and their loop D and C-terminal subdomains co-evolved together with protein kinase (PKA) pathways and 14-3-3ζ-like (YwhazL) binding proteins to establish a

two-step regulated trafficking mechanism that avoids competitive occupancy of the same oocyte membrane space (Ferré *et al*., 2023). This preovulatory process occurs during the maturational break down of the germinal vesicle (GVBD) and meiosis resumption to form highly hydrated pelagic eggs (>90% H_2O) that are subsequently dispersed in the oceanic currents (Ferré *et al*., 2023; Cerdà *et al*., 2007).

With the exception of a study showing that teleost *aqp1ab1* transcription is activated by the nuclear progestin receptor (nPgr) (Zapater *et al*., 2013), very little is known of the endocrine regulation of water transport in marine teleost oocytes during meiosis resumption. Studies in the freshwater stinging catfish (*Heteropneusteus fossilis*), which spawns partially hydrated benthic eggs (Singh *et al*., 2010), have, however, suggested that vasotocinergic mechanisms acting through distinct arginine vasotocin receptors (Avtr1 and Avtr2) could differentially regulate GVBD and ovulation, and aquaporin-mediated oocyte hydration, respectively (Acharjee *et al*., 2011; Chaube *et al*., 2011; Joy and Chaube, 2015). Such receptors are now termed arginine vasopressin receptors (Avpr) that bind vasopressin (formerly vasotocin), which diverged early in vertebrate evolution to form Avpr1, Avpr2 and oxytocin (Oxt, formerly isotocin) receptor (Oxtr) subtypes (Mayasich *et al*., 2016; Odekunle and Elphick, 2021; Daza *et al*., 2022; Mennigen *et al*., 2022; Yamaguchi *et al*., 2023). In mammals, the AVPR1 and OXTR subtypes activate phospholipase C (PLC) for calcium signaling and protein kinase (PKC) activation, while the AVPR2 subtype activates the cAMP-PKA-mediated transduction mechanism (Birnbaumer, 2000; Maybauer *et al*., 2008). The orthologous teleost Avpr and Oxtr are more numerous than the four paralogs present in mammals due in part to a specific whole genome duplication at the root of the crown clade (Mennigen *et al*., 2022). Despite only a few studies being conducted to characterize which receptor-mediated pathways are induced, the available evidence indicates that the teleost Avpr1, Avpr2 and Oxtr subtypes regulate the same signal transduction cascades as in mammals (Mahlmann *et al*., 1994; Hausmann *et al*., 1995; Warne, 2001; Konno *et al*., 2010). More recently, two studies using the *Xenopus laevis* oocyte expression system have shown that the Avp-Avpr2aa (formerly Avp2r)-cAMP-PKA axis can regulate the intracellular trafficking of teleost Aqp1ab1 and Aqp14 channels, while Oxt acting through the Oxtrb (formerly Itr) and a PKC-mediated mechanism can regulate the trafficking of Aqp1aa (Martos-sitcha *et al*., 2015; Chauvigné *et al*., 2019).

In the stinging catfish, in addition to the neuroendocrine/reproductive centers of the

brain (Mennigen *et al*., 2022), an intraovarian vasopressinergic system has been described that could also be involved in the paracrine regulation of oocyte hydration (Acharjee *et al*., 2011; Chaube *et al*., 2011; Joy and Chaube, 2015; Rawat *et al*., 2019). However, although the Aqp1ab2 channel has been implicated in this mechanism (Chaube *et al*., 2011), no study has yet demonstrated its subcellular localization or indeed that of the Aqp1aa and Aqp1ab1 channels, which are also encoded in the TSA1C of catfishes (Ferré *et al*., 2023). In contrast to freshwater fishes in which only ~1% produce semi-buoyant eggs, the great majority of modern euacanthomorph marine teleosts, such as the gilthead seabream (*Sparus aurata*), produce highly hydrated pelagic eggs (Cerdà *et al*., 2017; Ferré *et al*., 2023; Finn and Kristoffersen, 2007), yet the ovarian production of Avp or Oxt has not been reported. Since we have recently observed that PKA- and PKC-mediated signal transduction pathways stimulate relocation of each of the TSA1C channels (Aqp1aa, Aqp1ab1 and Aqp1ab2) in surrogate amphibian oocytes (Ferré *et al*., 2023), here we investigated the potential roles of the Avp-Avpr and Oxt-Oxtr axes in the regulation of aquaporin trafficking that facilitates oocyte hydration in the seabream.

3.2.3. Materials and Methods

3.2.3.1. Experimental Animals and Sampling

Adult gilthead seabream were obtained from the Institut de Recerca i Tecnologia Agroalimentàries (IRTA) aquaculture facilities (Tarragona, Spain) and transported to the facilities in Institut de Ciències del Mar (Barcelona, Spain). Fish were maintained under natural conditions of photoperiod and temperature and fed three times a week with dry pellets (Seabream Alterna AE, Skretting) and squid *ad libitum*. Samples of blood and gonads were collected throughout the year from sacrificed females as previously described (Zapater *et al*., 2013), frozen in liquid nitrogen and stored at -80ºC. The stage of ovarian development in each female was determined by standard histological analysis as described previously (Zapater *et al*., 2012).

Adult *X. laevis* were purchased from the Centre de Ressources Biologiques Xénopes (University of Rennes, France) and maintained at the AQUAB facilities of the Universitat Autònoma de Barcelona (UAB, Spain). Frogs were kept in tanks with filtrated freshwater at 18ºC, under a 12-h light-dark cycle, and fed two days a week with beef heart or pellets

(*Xenopus* Sticks, AQUA Schwarz GmbH, Göttingen, Germany). Oocytes were collected by surgical laparotomy from anesthetized females.

3.2.3.2. Ligand and Receptor Nomenclature

The nomenclature used for the seabream vasopressin and oxytocin nonapeptides and corresponding cognate receptors is adopted according to the Human Genome Nomenclature Committee (HGNC) (www.genenames.org), the zebrafish information network (ZFIN) (www.zfin.org) and Ensembl (v109) (www.ensembl.org), according to that previously described (Mennigen *et al*., 2022). The specific nomenclature of the gilthead seabream Avprs and Oxtrs was established through Bayesian inference of two million MCMC generations (aamodel = mixed; burnin = 25%) of a ClustalX amino acid alignment of the seabream Avprs and Oxtrs in relation to 88 actinopterygian orthologs downloaded from Ensembl (v109) (supplementary figure S1, see Annexes, page 272). The resultant tree topology matches that computed by maximum likelihood by Daza *et al*., 2022, with the exception that the zebrafish Avpr2ba and Avpr2bb receptors are named in accordance with the Ensembl (v109) nomenclature.

3.2.3.3. Antibodies and Reagents

Affinity-purified rabbit or chicken polyclonal antibodies specific for seabream Aqp1aa, -1ab1 and -1ab2 have been described elsewhere (Ferré *et al*., 2023; Raldúa *et al*., 2008). Antisera against Avp and Oxt were generously provided by Prof. Olivier Kah (INSERM-Université de Rennes 1, France). The HA tag rabbit antibody was from Thermo Fisher Scientific (Invitrogen, #PA1-985), whereas anti-YWHAZ antibodies were purchased from GeneTex (#GTX101075) and Signalway Antibody LLC (#SAB40525), which specificity for seabream YwhazLa and/or YwhazLb has been validated elsewhere (Ferré *et al*., 2023). Synthetic Avp (CYIQNCPRG-NH_2) and Oxt (CYISNCPIG-NH_2) were obtained from PeptideSynthetics (Peptide Protein Research Ltd.). All other reagents were purchased from Merck unless indicated otherwise.

3.2.3.4. HPLC Determination of Avp and Oxt Content in Plasma and Ovary

Ovarian and plasma levels of Avp and Oxt *in vivo* were determined using HPLC with fluorescence detection preceded by solid-phase extraction (SPE). Pieces of ovary (150-350 mg) previously frozen and stored at -80ºC were sonicated in 1 ml of Milli-Q water, acidified with 3 µl of glacial acetic acid and incubated in a boiling water bath during 3.5 min. The samples were centrifuged (30 min, 4°C, 10,000 × *g*). Plasma samples (1.5-2 ml each) were acidified with 1 M HCl (100 µl) and centrifuged at 6000·× *g* for 20 min at 4 °C. In both cases, the supernatants were loaded onto previously equilibrated SPE columns (Strata-X, 30 mg/ml; Phenomenex, Torrance, USA) and eluted in 80% acetonitrile. Eluates were evaporated to dryness using TurboVap LVTM (Caliper Life Sciences, PerkinElmer, Inc.), and frozen and stored at -20ºC until HPLC analysis. Before quantitative analysis, the dried samples were reconstituted with 0.1 ml of 4% acetic acid and divided into two aliquots for duplicate analysis. For plasma, samples were redissolved in 0.1 ml of acetonitrile:H_2O (2:1). For pre-column derivatization, 50 µl of sample and 50 µl of 0.05 M borate buffer (pH 8) were mixed, and then 3 µl of NBD-F (4-fluoro-7-nitro-2,1,3-benzoxadiazole; 30 mg/ml of acetonitrile) was added. The solution was heated at 40˚C for 10 min, cooled on ice, and acidified with 5 µl of 1 M HCl. Chromatographic analysis was achieved using Agilent 1200 Series Quaternary HPLC System (Agilent Technology, USA). Peptide separations were performed on a Kinetex C18 column (4.6 x 150 mm, 5 µm, Phenomenex, USA). A gradient elution system was applied for separation of derivatized peptides. The mobile phase consisted of solvent A (0.1% TFA in H_2O) and solvent B (0.1% TFA in 3:1 acetonitrile:H_2O). A linear gradient was 40-65% of eluent B in 20 min. Flow rate was set at 1 ml/min and the column temperature was set to 20˚C. Fluorescence detection was carried out at 530 nm with excitation at 470 nm.

3.2.3.5. Expression Constructs

Full-length cDNAs encoding seabream Aqp1aa, Aqp1ab1, Aqp1ab2, YwhazLa and -zLb have been previously isolated (GenBank accession numbers AY626939, AY626938, MW960021, OK572451 and OK572452, respectively). Mutated Aqp1aa, Aqp1ab1 and Aqp1ab2 constructs in PKA and PKC phosphorylation sites were previously produced

(Ferré *et al*., 2023). Full-length cDNAs encoding seabream Avpr1aa, Avpr2aa and Oxtrb were isolated by RT-PCR using intestine or rectum total RNA as previously described (Zapater *et al*., 2011) and oligonucleotide primers designed based on publicly available sequences (GenBank accession numbers KC195974, KC960488 and KC195973, respectively; supplementary table S1, see Annexes, page 270). The cDNAs were subcloned into the pT7Ts (Deen *et al*., 1994) or pcDNA3 (Invitrogen) expression vectors, and fused with an HA epitope tag (YPYDVPDYA) in the C-terminus before the stop codon by using PCR. The final clones were Sanger sequenced to confirm that the constructs were correct.

3.2.3.6. Pharmacological Avp and Oxt Receptor Characterization

Seabream Avp and Oxt receptor cDNA constructs in pcDNA3 were transiently expressed in HEK293T cells (ATCC # CRL-11268). The cells were grown in 24 wells plates in DMEM supplemented with penicillin/streptomycin, 2 mM glutamine, and 10% fetal bovine serum (FBS) (Life Technologies) and were incubated at 37ºC in 5% CO_2. Receptor activation was measured using luciferase reporter gene assays and intracellular Ca^{2+} levels. At approximately 50-60% confluence, cells were transfected using Lipofectamine 3000 (Invitrogen) with empty pcDNA3 or Avpr1aa (5 ng), Avpr2aa (5 ng), or Oxtrb (50 ng) cDNAs, 50 ng of pCRE-luc (Agilent Technologies) or 200 ng of pSRE-luc (BD Biosciences Clontech), and 5 ng or 50 ng of β-Gal plasmid (Promega Corp.) to normalize the transfection efficiency. The transfected cells were grown for 36 h at 37°C in an air/CO_2 [95:5 (v/v)] atmosphere before starvation for 16 h by replacing the DMEM by serum-free DMEM medium. The cells were then incubated in triplicate with different concentrations of Avp or Oxt (from 10^{-5} M to 10^{-12} M), or sterile dimethyl sulfoxide (DMSO) vehicle (0.01% final concentration), for 3 h. In some experiments, the cells were incubated with increasing concentrations (from 10^{-12} to 10^{-5} M) of different AVP (SR49059, Merck #S5701; TLV, Merck #T7455) and OXT (L-371,257, Tocris #2410) receptor antagonists for 1 h prior to stimulation with 10^{-8} M Avp or Oxt. After incubation, the cells were harvested in lysis buffer (25 mM Tris-phosphate, pH 7.8, 2 mM DTT, 10% glycerol, 1% triton X-100), frozen at -80ºC for 16-24 h and centrifuged at 14,000 × *g* for 1 min. To determine the luciferase activity, 20 µl of the supernatant was mixed with 100 µl of reconstituted Luciferin (BioThema) in a 96-well plate (Nunc F96 MicroWell Black and White Polystyrene Plate, Thermo Fisher Scientific), and the luminescence measured in an

Orion II microplate luminometer (Titertek-Berthold). Luciferase activity was normalized to β-Gal activity measured by colorimetric detection using an Infinite M200 microplate reader (Tecan Group Ltd.). The data was finally expressed as fold-change of luciferase activity with respect to control cells exposed to DMSO only.

To determine the intracellular Ca^{2+} levels after receptor activation we used the cell permeant Fluo-4-AM vital dye (Life technologies #F14201). For this, HEK293T cells were transfected as above with 2.5 µg of Avpr1aa, Avpr2aa or Oxtrb cDNAs in 6-well plates (Thermo Scientific). After 16 h, the cells were transferred to a black 96-well microplate and incubated 24 h at 37°C in an air/CO_2 [95:5 (v/v)] atmosphere. Fluo-4 AM was diluted in Hank's Balanced Salt Solution (HBSS) supplemented with glucose, containing 8% NP-40 and 20% DMSO, and added to the cells at 5 µM final concentration. Cells were incubated for 1 h at 37°C in an air/CO_2 [95:5 (v/v)] atmosphere, and subsequently exposed in triplicate to the nonapeptides, in the presence of absence of inhibitors, as described above. After washing twice with fresh DMEM, fluorescence intensity was measured at excitation and emission wavelengths of 494 and 506 nm, respectively, using an Infinite M200 microplate reader (Tecan Group Ltd.). The background signal of cells incubated with HBSS without Fluo-4 AM was subtracted from each value.

3.2.3.7. Gene expression Analyses

For RT-PCR, total RNA was extracted from different adult tissues, including pituitary, kidney, ovary and isolated ovarian follicles, using the RNeasy Minikit (Qiagen) and DNAse I treatment, following the manufacturer's instructions. Total RNA (5 µg) was reverse transcribed using 0.5 µg oligo$(dT)_{17}$ primer, 1 mM deoxynucleotide triphosphates (dNTPs), 40 IU RNAse out (Life Technologies Corp.), and 10 IU SuperScript II Reverse Transcriptase enzyme (Life Technologies Corp.) for 1.5 h at 42ºC. The PCR was carried out with 1 µl of the RT reaction in a final volume of 50 µl containing PCR buffer with Mg^{2+}, 0.2 mM dNTPs, 1 IU of Taq polymerase (Roche), and 0.2 µM of forward and reverse oligonucleotide primers specific for seabream *pro-avp*, *pro-oxt*, *avpr1aa*, *avpr2aa* and *oxtrb* (supplementary table S1, see Annexes, page 270). Reactions were amplified using one cycle at 95ºC for 2 min; 35 cycles at 95ºC for 30 sec, 60-62ºC (depending on primer Tm) for 30 sec, and 1 min at 72ºC; and 7 min for final elongation at 72ºC. The 18S

ribosomal RNA (*rps18*) was used as reference gene. The PCR products were run on 1% agarose gels and photographed.

Cellular localization of *pro-avp*, *pro-oxt*, *avpr1aa*, *avpr2aa* and *oxtrb* expression in ovarian follicles was carried out by ISH using digoxigenin-labelled gene-specific riboprobes as described previously (Cerdà *et al*., 2008). The sense and antisense riboprobes were synthesized using T7- or SP6-RNA polymerases from a PCR-amplified template using specific oligonucleotide primers (supplementary table S1, see Annexes, page 270). The *pro-avp* and *pro-oxt* probes corresponded to the C-terminal end and part of the 3´UTR, or the proximal 3´UTR, respectively. For the receptors, the probes spanned ~300 bp from the middle of the *avpr2aa* cDNA sequence, and ~200 bp of the *avpr1aa and oxtrb* cDNAs including the C-terminus and a portion of the 3´UTR.

3.2.3.8. Functional Expression in *X. laevis* Oocytes and Swelling Assays

The cRNAs corresponding to the different constructs were synthesized *in vitro* with T7 RNA polymerase from *Xba*I-digested pT7Ts vector containing the cDNAs. The isolation and microinjection of oocytes, and subsequent swelling assays, were carried out as previously described (Chauvigné *et al*., 2021). Oocytes were injected with 50 nl of water alone (controls) or containing 15 ng of Avpr1aa, Avpr2aa or Oxtrb cRNAs. Oocytes expressing the receptors were also injected with wild-type or mutant Aqp1aa (0.1 ng), Aqp1ab1 (0.5 ng) or Aqp1ab2 (25 ng) plus YwhazLb (25 ng). In some experiments, oocytes expressing Avpr2aa and Aqp1ab1 constructs were also injected with YwhazLa (25 ng). The oocyte P_f was determined after 3 h incubation with 10 µM Avp or Oxt (depending on the type of receptor expressed in oocytes). The role of PKA or PKC on the oocyte P_f was tested by preincubating the oocytes with 10 µM of H89 or Bim-II for 1 h prior to the addition of the hormones. Oocytes expressing Avpr1aa or Oxtrb together with Aqp1ab2 plus YwhazLb were treated with 10 µM FSK as previously described (Ferré *et al*., 2023). Control oocytes were treated with 0.1% DMSO.

3.2.3.9. *In Vitro* Incubation of Ovarian Explants and Isolated Ovarian Follicles

Pieces of the ovary at the vitellogenic stage (400-500 mg) were dissected from naturally spawning seabream females and placed in Petri dishes containing 75% Leivovitz L-15 culture medium with L-glutamine and 100 µg/ml gentamicin at pH 7.5. The explants were treated with 100 ng/ml of sea bass (*Dicentrarchus labrax*) rFsh or rLh (Molés *et al*., 2011), which activate the seabream Fsh and Lh receptors, respectively (Zapater *et al*., 2012), 0.1 µg/ml 17,20βP, in the presence or absence of 100 µM of RU486 (Merck M8046), or with 10 µM of OD 02-0 (Axon Medchem, 13258-85-0), for ~20 h at 18ºC in a temperature-controlled incubator. Control groups were treated with an equivalent volume of the cell culture medium used for rLh and rFsh production, or with 0.5% ethanol. After incubation, explants were frozen and stored at -80ºC until Avp extraction and determination by ELISA.

In other experiments, groups of fully-grown postvitellogenic ovarian follicles (n = 10), manually isolated from the ovary, were incubated with 10 µM Avp in the same culture medium as above, in the presence or absence of 10 µM of the receptor antagonist TLV, or with 0.1% DMSO (controls) for 6 h at 18ºC. After incubation, follicles were fixed for immunofluorescence microscopy, frozen in liquid nitrogen and stored at -80ºC for further protein extraction, or processed for water uptake assays using radiolabeled water as previously described (Ferré *et al*., 2023).

3.2.3.10. ELISA Determination of Avp in Treated Ovarian Explants *In Vitro*

To determine the Avp levels in ovarian explants incubated *in vitro*, a competitive ELISA was developed using the specific anti-Avp antiserum and the synthetic Avp to create the standard curve (supplementary figure S2, see Annexes, page 274). For this, polystyrene ELISA microtiter plates (F96 Maxisorp Nunc Immuno Plates; Nunc) were coated with 100 µl/well of 50 ng Avp/ml carbonate buffer (50 mM sodium carbonate, pH 9.6) and incubated overnight at 4ºC. For the blank and the non-specific binding, two wells were either not coated or coated with 100 µl/well of 50 ng BSA/ml carbonate buffer, respectively. Ovarian explants were homogenized on ice with a glass dounce tissue

homogenizer in water containing 0.25% glacial acetic acid in a proportion of 500 µl/100 mg tissue. After incubation of the homogenate at 100ºC for 5 min, the samples were centrifuged a 10,000 × *g* for 5 min at 4ºC, and the supernatant recovered in a new tube. The standards (0.01-500 ng Avp/ml) and experimental samples were diluted in PBST (PBS plus 0.05% Tween 20) with 0.5% normal goat serum (NGS), containing the Avp antibody diluted at 1:15,000, and were pre-incubated overnight at 4ºC. Displacement curves for ovarian samples were obtained by serial dilutions from 1:2 to 1:16 to confirm the parallelism with the standard curves. For the measurement of the experimental samples a 1:4 dilution was applied, and to evaluate the cross-reactivity of the assay with Oxt, the same standard curve as for Avp was created (0.01-500 ng/ml). All standards and samples were processed in duplicate. After coating, the plates were washed 3 times with 200 µl/well of PBST, and blocked with 200 µl/well of PBST buffer containing 2% NGS for 1 h at room temperature. Then, 100 µl of samples and standards preincubated with the antibody were added to each well, and plates were incubated at 4ºC for another 24 h. The plates were finally washed 3 times in PBST and each well was incubated with 100 µl/well of EIA grade affinity purified goat anti-rabbit IgG (H + L) HRP conjugated (Bio-rad Laboratories, Inc.) diluted 1:3000 in PBST plus 0.5% NGS for 2 h at room temperature. After washing, enzymatic color development was carried out by the addition of 100 µl/well of tetramethylbenzidine (TMB) peroxidase EIA substrate kit (Bio-rad Laboratories, Inc.) in darkness during 30 min, and the reaction was stopped with 100 µl/well of 1 N sulfuric acid. Absorbance was read at 450 nm with a VICTOR3™ Multilabel Plate Reader (PerkinElmer, Inc.). The amount of Avp was normalized to the wet weight of the ovarian explants. The intra-assay coefficient of variation was 4.64% (calculated by assaying eight replicates of an ovarian sample at 50% of maximum binding on the same plate), whereas the inter-assay coefficient of variation was 8.35%. The sensitivity of the assay for Avp was of 10 pg/ml, while its crossreaction with Oxt was calculated to be 8.43±1.72 %.

3.2.3.11. Immunofluorescence Microscopy

Isolated ovarian follicles were processed for immunofluorescence microscopy as previously described (Chauvigné *et al*., 2017 and 2018). Control sections were incubated with antibodies (1:400 dilution) preadsorbed with the corresponding peptides used for immunization (for aquaporin antibodies), or with the Avp or Oxt synthetic peptides.

Secondary antibodies were sheep anti-rabbit IgG Cy3 (Merck #C2306) or goat anti-chicken IgY Alexa Fluor 488 (Invitrogen #A11039) at a 1:1,000 dilution. Sections were counterstained with DAPI (1:10,000), and mounted with Fluoromount™ Aqueous Mounting Medium (Merck #F4680). Immunofluorescence was observed and documented with a Zeiss Axio Imager Z1/Apotome fluorescent microscope (Carl Zeiss Corp.). Changes in Aqp1ab1 and Aqp1ab2 in the oocyte plasma membrane after Avp treatment were evaluated using the ImageJ software v.1.52o (https://imagej.nih.gov/ij/) as previously described (Ferré *et al*., 2023).

3.2.3.12. Protein extraction and Immunoblotting

The total and plasma membrane fractions of *X. laevis* oocytes (n = 10), and total membrane fractions of seabream ovarian follicles (n = 50), were isolated as described previously (Ferré *et al*., 2023) and resuspended in Laemmli sample buffer. For immunoblotting, Laemmli-mixed protein samples were denatured at 95°C for 10 min and subjected to 12% sodium dodecyl sulfate polyacrylamide gel electrophoresis (SDS-PAGE) and blotted onto Immun-Blot nitrocellulose 0.2 µm membranes (Bio-Rad Laboratories, Inc.), as described previously (Chauvigné *et al*., 2013). Membranes were blocked with 5% nonfat dry milk in TBST (20 mM Tris, 140 mM NaCl, 0.1% Tween, pH 8) for 1 h at room temperature, and subsequently incubated overnight at 4ºC with the seabream-specific Aqp1aa, Aqp1ab1 or Aqp1ab2 antisera, or HA antibodies, diluted (1:1,000) in TBST with 5% milk. Bound antibodies were detected with horseradish peroxidase-coupled anti-rabbit (Bio-Rad Laboratories, Inc., #172-1019) or anti-chicken (Thermo Fisher Scientific, #A16054) secondary antibodies diluted 1:5000 as above, and reactive protein bands were revealed using ImmobilonTM Western chemiluminescent HRP substrate (Millipore, #WBKLS).

3.2.3.13. Co-Immunoprecipitation

X. laevis oocytes and seabream follicles (n = 10) were homogenized in the lysis buffer from the Pierce™ Crosslink Magnetic IP/Co-IP Kit (Pierce Thermo Fisher Scientific, #88805) with a bouncer on ice, and centrifuged at 14,000 × g for 1 min. An aliquot (10%) of the protein extract was collected as "input" and mixed with 2 × Laemmli sample buffer, whereas the remaining extract was incubated overnight at 4°C under constant agitation with magnetic beads previously coated with anti-Aqp1ab1 or anti-Aqp1ab2 antibodies. For

rabbit primary antibodies, the immunoprecipitation was carried out using the kit indicated above, and final eluted proteins in 50 µl of elution buffer were mixed with 4 × Laemmli sample buffer supplemented with protease and phosphatase inhibitors. For chicken antibodies, the immunoprecipitation was performed using Dynabeads™ M-280 Tosylactivated (Invitrogen Thermo Fisher Scientific, #14203) following the manufacturer's instructions. The input and immunoprecipitated samples were immunoblotted as indicated above.

3.2.3.14. Statistical Analyses

Comparisons between two independent groups were made by the two-tailed unpaired Student's *t*-test. The statistical significance among multiple groups was analyzed by one-way ANOVA, followed by the Tukey's multiple comparison test, or by the non-parametric Kruskal-Wallis test and further Dunn's test for nonparametric *post hoc* comparisons. Percentages were square root transformed previous analyses. Statistical analyses were carried out using the GraphPad Prism v9.1.2 (226) (GraphPad Software).

3.2.4. Results

3.2.4.1. A Paracrine Vasopressinergic and Oxytocinergic System is Present in the Seabream Ovary

To investigate whether teleost Avp and Oxt are produced locally in the seabream ovary, we initially determined the changes in the concentration of the nonapeptides both in the plasma and in the ovary of females showing different stages of ovarian follicle development (figure 1A) using high performance liquid chromatography (HPLC). Plasma and ovarian levels of Avp progressively increased in females with ovaries at the vitellogenic stage and undergoing meiotic maturation and hydration (figure 1B). However, in females with ovaries containing fully matured and hydrated follicle-enclosed oocytes and ovulated eggs, the ovarian Avp levels markedly dropped, while the plasma levels remained elevated (figure 1B). By contrast, the plasma Oxt levels in females were approximately three times higher than those of Avp and showed a cyclical pattern (figure 1C). Thus, circulating Oxt concentrations were higher during vitellogenesis and the fully mature and hydrated stages compared to other stages (figure 1C). However, the

intraovarian changes of Oxt during the reproductive cycle reflected those observed for Avp, with a precipitous drop during the maturation and hydration stage (figure 1C).

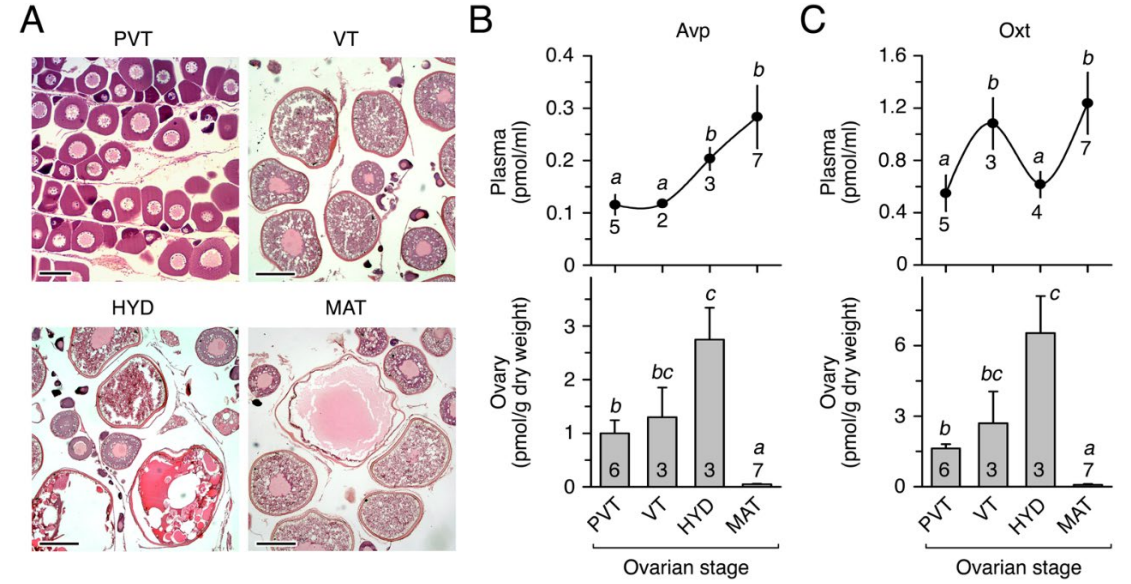

Figure 1. *In vivo* levels of arginine vasopressin (Avp) and oxytocin (Oxt) in seabream plasma and ovary during the natural reproductive cycle. (**A**) Representative photomicrographs of histological sections from ovaries containing ovarian follicle-enclosing oocytes at different developmental stages: previtellogenesis or primary growth stage (PVT), vitellogenesis (VT), oocytes undergoing meiosis resumption and hydration (HYD), and fully matured and hydrated oocytes and ovulated eggs (MAT). Scale bars, 100 µm (PVT), 400 µm (VT-MAT). (**B-C**) Levels of Avp (B) and Oxt (C) in plasma (upper panels) and ovary (lower panels) from females at the different reproductive stages as shown in A. In each panel, values (mean ± SEM) with different superscript are significantly (ANOVA, $P < 0.05$) different. The number of fish analyzed at each stage are indicated in each plot.

To rule out the possibility that intraovarian Avp and Oxt detected in our analysis were the result of their accumulation from circulating products, we investigated whether these peptides can also be produced within the seabream ovary, as reported for the stinging catfish (Rawat *et al*., 2019; Singh and Joy, 2008). For this, we first assessed the expression of *pro-avp* and *pro-oxt* genes in ovarian follicles by reverse transcription-polymerase chain reaction (RT-PCR) and *in situ* hybridization (ISH) using gene-specific oligonucleotide primers and riboprobes, respectively. The RT-PCR experiments indicated that *pro-avp* and *pro-oxt* mRNAs were expressed in the pituitary (as a positive control) and the ovary, whereas low but detectable transcripts from both genes were amplified in isolated vitellogenic ovarian follicles (figure 2A). The ISH performed with histological sections of ovaries at the primary growth and vitellogenic stages showed that primordial follicle cells adjacent to previtellogenic oocytes were strongly positive for *pro-avp*, whereas these cells were devoid of *pro-oxt* mRNAs (figure 2B). In vitellogenic ovarian follicles, in which

follicle cells are fully differentiated into cuboidal granulosa cells and enlarged and elongated theca cells, *pro-avp* transcripts were detected only in the granulosa cells, while both granulosa and theca cells appear to express *pro-oxt* mRNAs (figure 2B). In the cytoplasm of vitellogenic oocytes, some weak *pro-avp* and *pro-oxt* staining was also detected (figure 2B). For both transcripts, no extrafollicular expression (i.e., interstitial tissue) was noted in the ovarian stages examined, and control sections incubated with sense probes were negative (figure 2B).

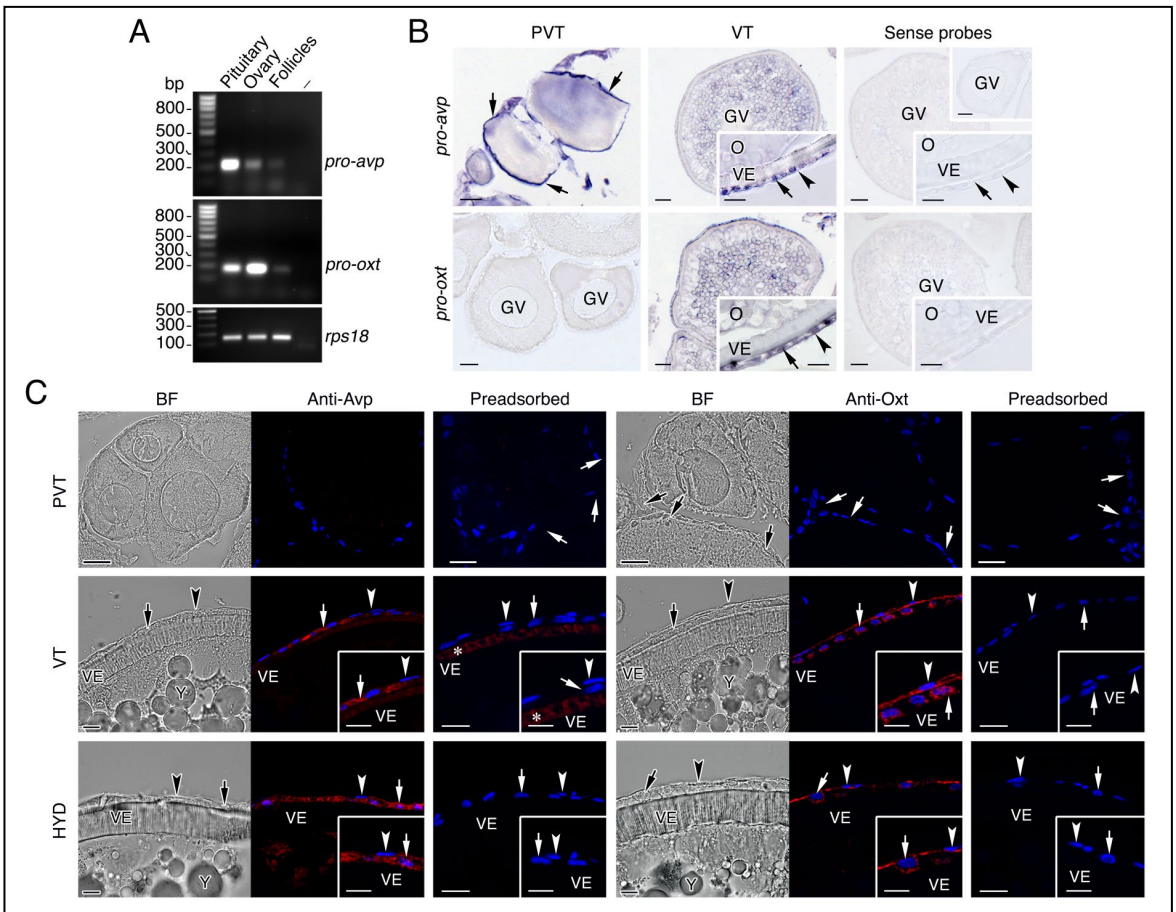

Figure 2. Identification of the cellular sites of Avp and Oxt production in seabream ovarian follicles. (**A**) Representative RT-PCR analysis of the expression of mRNAs encoding the Avp and Oxt pro-peptides (*pro-avp* and *pro-oxt*, respectively) in the seabream ovary and isolated vitellogenic ovarian folliclesand in the pituitary as positive control. The ribosomal protein S18 (*rps18*) was used as the reference. The minus indicates absence of RT during cDNA synthesis. The sizes (bp) of the molecular markers are indicated on the left. (**B**) Localization of *pro-avp* and *pro-oxt* transcripts in previtellogenic (PVT) and vitellogenic (VT) ovarian follicles. Paraffin sections were hybridized with antisense DIG-labeled riboprobes specific for *pro-avp* and *pro-oxt* or sense probes (rigth panels, negative controls). Scale bars: 10 µm (PVT), 20 µm and 8 µm insets (VT). (**C**) Immunostaining of Avp and Oxt peptides (red, right panels) in PVT and VT follicles, and in follicles undergoing meiosis resumption and hydration (HYD). The corresponding brightfield (BF) images are also shown (left panels). The reactions were visualized with Cy3-conjugated sheep anti-rabbit IgG and the nuclei were counterstained with 4',6-diamidino-2-phenylindole (DAPI; blue). Control sections were incubated with preabsorbed antiserum. In B and C, theca and granulosa cells are indicated by an arrowhead and arrow, respectively. Scale bars, 20 µm (PVT), 10 µm (VT and HYD). Abbreviations: GV, germinal vesicle; O, oocyte; VE, vitelline envelope.

The above observations were further confirmed by immunofluorescence microscopy using anti-Avp and anti-Oxt rabbit antisera, which were previously validated by immunostaining of the seabream posterior pituitary gland (supplementary figure S3, see Annexes, page 275). These experiments showed that primordial follicle cells associated to primary growth oocytes were negative for Avp or Oxt immunostaining, and confirmed that granulosa cells surrounding vitellogenic oocytes, as well as those surrounding oocytes undergoing meiotic maturation and hydration, synthesize Avp (figure 2C). In contrast, Oxt immunoreaction was observed in theca and granulosa cells in both follicular stages, in agreement with the ISH data (figure 2C). Preadsorption of the antisera with the corresponding Avp and Oxt peptides led to a complete absence of staining in all the follicular stages analyzed, except a cross-reaction of the Avp antiserum with the vitelline envelope in vitellogenic follicles (figure 2C), indicating the specificity of the signals in the follicular cells.

To assess whether Avprs and Oxtrs are also expressed in ovarian follicles we carried out RT-PCR and ISH using specific primers and riboprobes for two seabream Avpr subtypes, Avpr1aa and Avpr2aa (previously termed Avt1a2r and Avt2r, respectively), and one previously identified Oxtrb (formerly Itr) (Williams *et al*., 1995). These receptors were selected as representative Avprs and Oxtrs with a potential for different ligand specificities and the activation of different signal transduction pathways. The results of the RT-PCR assays, using kidney total RNA as a positive control, showed that both *avpr1aa* and *avpr2aa* transcripts could be amplified from the ovary and isolated follicles, while *oxtrb* expression was also noted in the ovary but not detected in follicles (figure 3A). The ISH data indicated that previtellogenic oocytes express *avpr2aa* and *oxtrb*, but not *avpr1aa*, whereas *oxtrb* mRNAs were also observed in the primordial follicle cells (figure 3B). During vitellogenesis, follicles start to express *avpr1aa*, but only in the oocyte and not in the follicle cells, whereas *avpr2aa* expression in oocytes is maintained and activated in the differentiated theca and granulosa cells (figure 3B). At this stage, the *oxtrb* transcripts in oocytes seemed to be slightly reduced and were no longer detected in the follicle cells (figure 3B). For the three transcripts sense probes gave negative results (figure 3B).

Altogether, the above data demonstrate the local production of Avp and Oxt nonapeptides in the seabream ovarian follicle, as well as the expression of their cognate receptors in the follicle cells and/or oocyte, which would be consistent with a role of a

vasopressinergic and oxytocinergic regulatory system controlling aquaporin intracellular trafficking and oocyte hydration

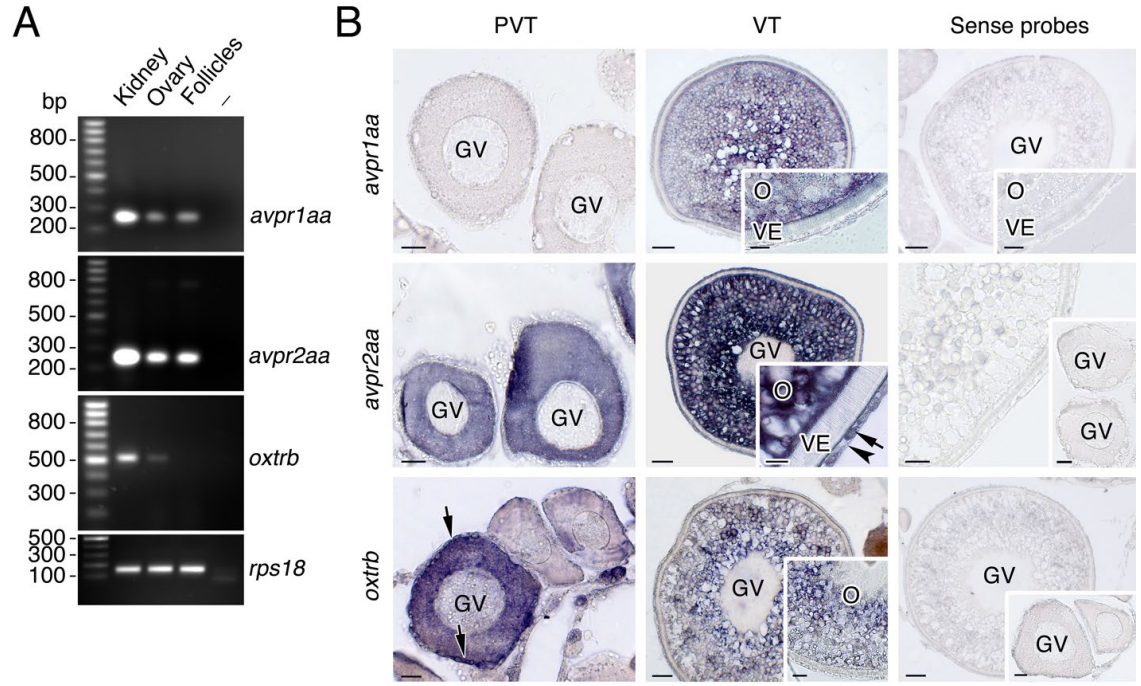

Figure 3. Localization of Avp and Oxt receptor mRNA expression in seabream ovarian follicles. (**A**) Representative RT-PCR analysis of the expression of *avpr1aa*, *avpr2aa* and *oxtrb* mRNAs in the seabream ovary and isolated ovarian follicles, and in kidney as positive control. The ribosomal protein S18 (*rps18*) was used as the reference. The minus indicates absence of RT during cDNA synthesis. The sizes (bp) of the molecular markers are indicated on the left. (**B**) Localization of *avpr1aa*, *avpr2aa* and *oxtrb* transcripts in previtellogenic (PVT) and vitellogenic (VT) ovarian follicles. Paraffin sections were hybridized with specific antisense DIG-labeled riboprobes or sense probes (rigth panels, negative controls). Theca and granulosa cells are indicated by an arrow and arrowhead, respectively. Scale bars, 10 µm (PVT), 20 µm (VT). Abbreviations: GV, germinal vesicle; O, oocyte; VE, vitelline envelope.

3.2.4.2. Pharmacological Characterization of Seabream Avpr1aa, Avpr2aa and Oxtrb Receptor Subtypes

Since the different Avprs and the Oxtrs are considered to trigger distinct PKA and PKC signaling cascades, and it has been shown that these kinases can regulate seabream Aqp1aa, -1ab1 and -1ab2 trafficking (Ferré *et al*., 2023; Martos-sitcha *et al.,* 2015), we next investigated the signaling pathways activated by seabream Avpr1aa, Avpr2aa and Oxtrb. For this, human embryonic kidney cells 293T (HEK293T) were transiently transfected with *avpr1aa*, *avpr2aa* or *oxtrb* full-length cDNAs, isolated from the seabream ovary based on publicly available data. Cells were transfected at the same time with β-Galactosidase (β-Gal) together with a cAMP-responsive reporter gene plasmid (pCRE-luc),

or a plasmid for activation of the phospholipase C (PLC)/PKC pathway (pSRE-luc), and exposed to increasing doses of the nonapeptides ranging from 10^{-12} to 10^{-5} M (figure 4). The receptor-induced increase in intracellular Ca^{2+} concentration ($[Ca^{2+}]_i$), as a second messenger in the PLC signal transduction pathway, was determined using Fluo-4 AM, a cell-permeable, fluorescent Ca^{2+} indicator.

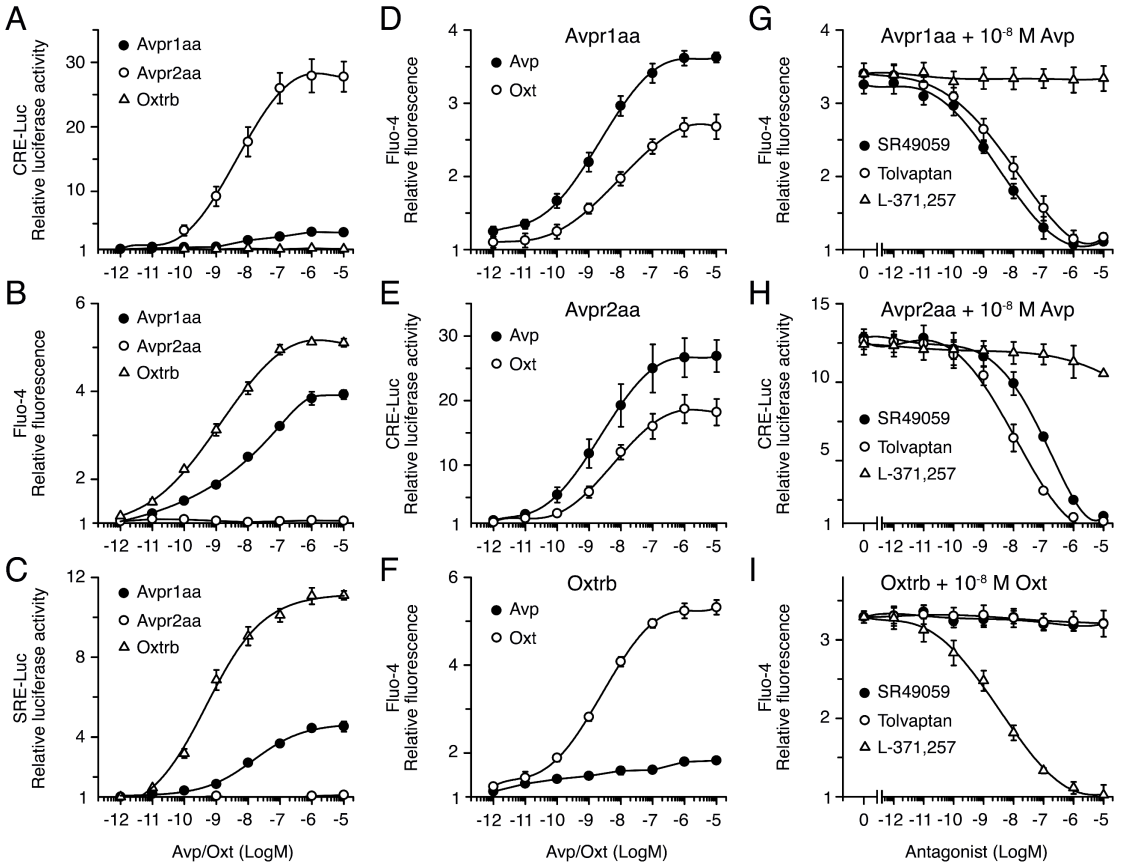

Figure 4. Functional characterization of seabream Avp and Oxt receptors in HEK293T cells. (**A-F**) Activation of the Avpr1aa, Avpr2aa and Oxtrb by graded concentrations of the corresponding ligands (A-C), and ligand selectivity (D-F) of each receptor. (**G-I**) Inhibition of the activation of the Avpr1aa, Avpr2aa and Oxtrb by 10^{-8} M of the corresponding ligands in the presence of increasing concentrations of vasopressin (SR49049 and Tolvaptan) and oxytocin (L-371 257) receptor antagonists. In all experiments, hormone-induced cAMP production and PKC activation were indirectly quantified by measuring the luciferase activity from the CRE-Luc and SRE-Luc reporter vectors, respectively, which were cotransfected with the receptor cDNA containing plasmids. Intracellular Ca^{2+} was determined by loading the cells with the Fluo-4 Ca^{2+}-sensitive dye before activation of the receptors. The data (mean ± SEM) from each plot are derived from three to six independent transfections.

In cells expressing the Avpr1aa or Oxtrb receptors, incubation with Avp or Oxt, respectively, resulted in a concentration-dependent increase of pSRE-induced luciferase activity and of $[Ca^{2+}]_i$, while it did not induce measurable increases in pCRE-mediated luciferase activity (figure 4A-C). However, the Avpr1aa was less affective at activating PKC or increasing the $[Ca^{2+}]_i$ than the Oxtrb, since the half-maximal effective

concentrations (EC_{50}) of Avp on its cognate receptor were ~10 times higher compared with those of Oxt on the Oxtrb (figures 4B, C). In contrast, in Avpr2aa expressing cells Avp induced a potent dose-dependent response in pCRE-induced luciferase activity, while PKC was not activated and the $[Ca^{2+}]_i$ was not affected (figure 4A-C). Receptor cross-activation experiments showed that both Avpr1aa and Avpr2aa could be activated by Avp and Oxt, although the EC_{50} for Oxt on these receptors was ~10 times higher with respect to that of Avp (figure 4D, E). On the contrary, the Oxtrb was more specific for Oxt, since only a slight increase of the $[Ca^{2+}]_i$ in response to Avp was noted in cells expressing this receptor (figure 4F).

To search for effective and selective inhibitors of seabream Avprs and Oxtrb, which could be used in further physiological experiments, we tested the effect of different non-peptide antagonists selective for mammalian AVPR1A (SR49059) (Serradeil-Le *et al*., 1993), AVPR2 (tolvaptan, TLV) (Kondo *et al*., 1999) and OXTR (L-371,257) (Williams *et al*., 1995). In these experiments, cells were transfected with Avpr1aa, Avpr2aa or Oxtrb and reporter plasmids as above, and preincubated with increasing doses (from 10^{-12} to 10^{-5} M) of the different receptor antagonists, and then subsequently treated with the approximate EC_{50} of Avp or Oxt on each cognate receptor (10^{-8} M). The results showed that activation of the Avpr1aa was equally inhibited by SR49059 and TLV, which showed half maximal inhibitory concentration (IC_{50}) of ~10^{-9} M, although the SR49059 was slightly more effective (figure 4G). Both SR49059 and TLV also inhibited the Avpr2aa, although in this case TLV was ~10 times more potent than SR49059 at blocking the receptor (figure 4H). In contrast, the L-371,257 antagonist had no effect on Avpr1aa or Avpr2aa activation (figure 4G, H). Finally, the Oxtrb was well blocked by L-371,257, showing an IC_{50} of ~10^{-9} M, while it was not affected by SR49059 or TLV (figure 4I). These data therefore indicate that TLV and L-371,257 are, respectively, potent and selective inhibitors of seabream Avpr and Oxtr receptor subtypes.

3.2.4.3. Avp and Oxt Differentially Regulate the Intracellular Trafficking of the Seabream TSA1C Channels

To investigate whether Avprs and Oxtrb can regulate the intracellular trafficking of Aqp1aa, -1ab1 or -1ab2, we initially employed oocytes from *X. laevis* as a surrogate experimental system (figure 5). Oocytes were injected with *avpr1aa*, *avpr2aa* or *oxtrb*

cRNAs, synthesized from human influenza hemagglutinin (HA)-tagged cDNAs, which drives the constitutive expression of the receptors in the oocyte plasma membrane (supplementary figure S4, see Annexes, page 276). To test the effect of receptor activation on the trafficking of the TSA1C channels, each receptor was coinjected with cRNAs encoding Aqp1aa, Aqp1ab1 or Aqp1ab2, or water as a negative control. Oocytes were exposed to Avp or Oxt, depending on the type of receptor expressed, or to the hormone vehicle dimethyl sulfoxide (DMSO) as control, and subsequently submitted to swelling assays to determine the osmotic water permeability (P_f). Since Aqp1ab2 can only traffic to the frog oocyte plasma membrane when it is bound to the teleost-specific YwhazLb protein in the presence of the intracellular cAMP activator forskolin (FSK) (Ferré *et al*., 2023), Aqp1ab2-injected oocytes were also coinjected with seabream YwhazLb cRNA and, in some experiments, exposed to FSK prior to nonapeptide treatment.

Oocytes expressing the Avpr1aa and Aqp1aa or Aqp1ab1 showed a 3-4-fold increase in P_f with respect to the control oocytes after a hypoosmotic challenge. However, Avp treatment reduced the P_f by 80% in oocytes expressing Aqp1aa, but not in those injected with Aqp1ab1 (figure 5A). In the case of oocytes expressing Avpr1aa plus Aqp1ab2, treatment with Avp did not affect the oocyte P_f triggered by FSK exposure (figure 5A). Preincubation of Avpr1aa+Aqp1aa oocytes with the PKC inhibitor bisindolylmaleimide II (Bim-II) prevented the Avp-induced inhibition of P_f (figure 5B), in agreement with the activation of the PLC/PKC signaling pathway by the Avpr1aa previously observed in HK293T cells. Immunoblotting of total and plasma membrane extracts of oocytes and immunofluorescence microscopy using Aqp1aa-specific antibodies revealed that the hormone-induced reduction in the oocyte P_f was due to the internalization of the channel in response to Avpr1aa activation, which was blocked in the presence of Bim-II (figure 5C, D). The same results were obtained in oocytes expressing the Oxtrb and Aqp1aa, Aqp1ab1 or Aqp1ab2 plus YwhazLb (figure 5I-L), indicating that activation of Avpr1aa or Oxtrb by their cognate ligands inhibit Aqp1aa trafficking to the oocyte surface through PKC signaling, while Aqp1ab1 and -1ab2 are not regulated by these receptors.

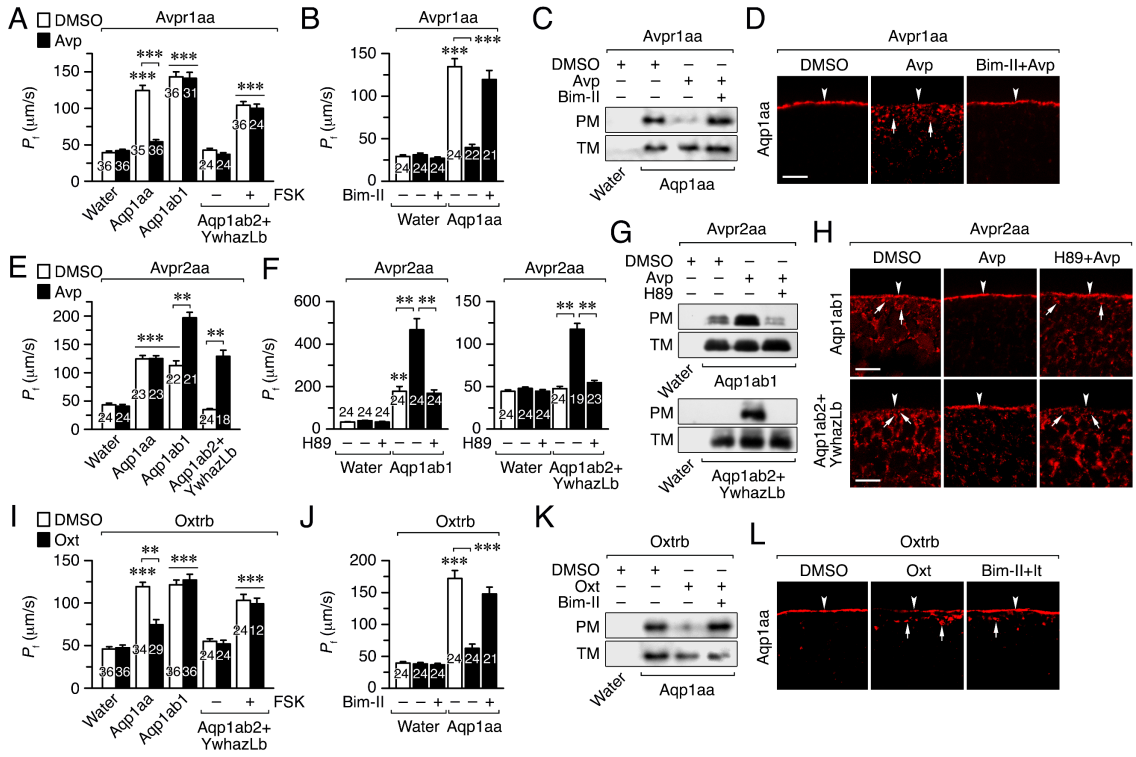

Figure 5. Avp and Oxt regulation of seabream Aqp1aa, Aqp1ab1 and Aqp1ab2 intracellular trafficking in *X. laevis* oocytes. (**A**, **B**, **E**, **F**, **I**, **J**) Osmotic water permeability (P_f) of oocytes expressing the seabream Avpr1aa (A, B), Avpr2aa (E, F) or Oxtrb (I, J), and injected with either water, wild-type Aqp1aa, Aqp1ab1 or Aqp1ab2 plus YwhazLb. Oocytes were treated with DMSO (controls) or 10 µM Avp or Oxt (A, E, I), in the presence or absence of 10 µM of PKC and PKA inhibitors (Bim-II and H89, respectively) (B, F, J). Oocytes injected with Aqp1ab2+ YwhazLb were also treated with or without 10 µM forskolin (FSK). Data are the mean ± SEM with the number of oocytes indicated in each bar. $^{**}P < 0.01$; $^{***}P < 0.001$ (unpaired Student's *t*-test), with respect to water-injected oocytes, or as indicated in brackets. (C, D, G, H, K, L) Representative immunoblot (**C**, **G**, **K**) of Aqp1aa, Aqp1ab1 and Aqp1ab2 in total (TM) and plasma (PM) membrane extracts from oocyes treated as above, and corresponding immunostaining (**D**, **H**, **L**), using paralog-specific antibodies. The arrowheads indicate the PM, whereas the arrows indicate aquaporin-containing intracellular vesicles. Scale bars, 10 µm.

In contrast, the P_f of oocytes expressing Avpr2aa and Aqp1ab1 or Aqp1ab2+YwhazLb (in the latter case without FSK pretreatment) was increased by ~2- and ~4-fold, respectively, after Avp exposure, whereas that of the oocytes co-expressing Avpr2aa and Aqp1aa did not change (figure 5E). The Avpr2aa-mediated increase in the P_f of oocytes expressing Aqp1ab1 or Aqp1ab2+YwhazLb occurred through the Avp-induced insertion of the channels into the oocyte plasma membrane as revealed by immunoblotting and immunolocalization experiments using paralog-specific antibodies (figure 5F-H). However, this trafficking was prevented by the PKA inhibitor H89 (figure 5F-H). These data thus show that Avpr2aa can positively regulate Aqp1ab1 and Aqp1ab2 trafficking to the plasma membrane through the PKA signaling cascade, which is activated in both oocytes and cultured cells.

3.2.4.4. Molecular Basis of the Nonapeptide Regulation of Aquaporin Trafficking

The above data are consistent with our recent study using direct pharmacological activation of PKC and PKA in *X. laevis* oocytes, which showed that in euacanthomorph teleosts, such as the seabream, PKC negatively regulates Aqp1aa trafficking to the plasma membrane, while PKA positively regulates this mechanism in Aqp1ab1 and Aqp1ab2 (Ferré *et al*., 2023). This latter study also identified the kinase phosphorylation sites involved in trafficking regulation of the different channels: Thr^{145} (loop D) in Aqp1aa, Ser^{156} and Ser^{253} (intracellular loop D and C-terminus, respectively) in Aqp1ab1, and Thr^{262} (C-terminus) in Aqp1ab2 (figure 6A, D, I). However, plasma membrane trafficking of Aqp1ab1 partially depends on channel binding to the teleost-specific YwhazLa, through PKA phosphorylation of Ser^{253} within the YWHA binding motif, while that of Aqp1ab2, as mentioned above, strictly relies on PKA-mediated Thr^{262} phosphorylation and the YwhazLb interaction (Ferré *et al*., 2023) (figure 6A, D, I). Therefore, in order to investigate whether Avp and Oxt control Aqp1aa, Aqp1ab1 and Aqp1ab2 trafficking through the same mechanisms, *X. laevis* oocytes were injected with cRNAs for *avpr1aa*, *avpr2aa* or *oxtrb* and wild-type TSA1C channels or mutant forms in which the PKA and PKC phosphorylation sites were replaced by non-phosphorylatable Ala residues (Ferré *et al*., 2023), together with HA-tagged YwhazLa or -zLb. The P_f of oocytes, the trafficking of the channels to the oocyte plasma membrane, and the interaction of Aqp1ab1 and Aqp1ab2 with YwhazLa or -zLb carrier proteins, respectively, in response to the nonapeptides, were then examined by using swelling assays, immunoblotting and co-immunoprecipitation using Aqp1ab1- and Aqp1ab2-specific antibodies.

The results of these experiments showed that the reduction of oocyte permeability and channel accumulation in the plasma membrane in response to Avp or Oxt, in oocytes expressing wild-type Aqp1aa plus Avpr1aa or Oxtrb, was completely reversed when oocytes expressed the Aqp1aa-V145T mutant instead of the wild-type (figure 6B, C), as observed when PKC is directly activated in Aqp1aa expressing oocytes (Ferré *et al*., 2023). In oocytes expressing wild-type Aqp1ab1, YwhazLa-HA and Avpr2aa, Avp triggered a more robust increment in the oocyte P_f and of the relative amount of the channel in the plasma membrane (figure 6E, F) than in oocytes without YwhazLa (figure 5E), which was

partially or completely prevented, respectively, in oocytes expressing the Aqp1ab1-S156A or -S253A mutants (figure 6E, F). However, the positive effect of Avp on plasma membrane trafficking of both wild-type Aqp1ab1 and Aqp1ab1-S156A channels was equally abolished in the presence of the H89 inhibitor (figure 6E, G). Co-immunoprecipitation experiments using the Aqp1ab1 antibody confirmed that Avp

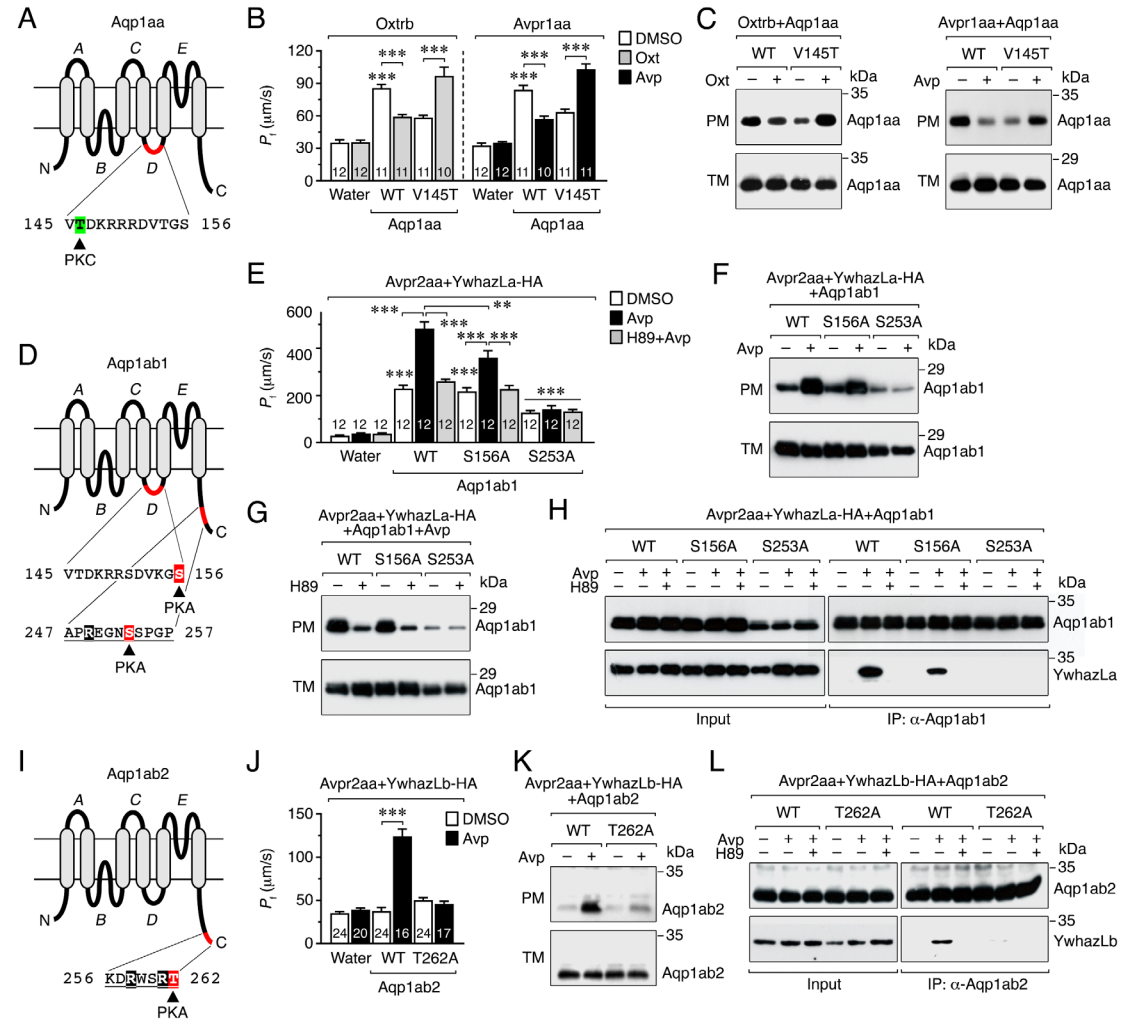

Figure 6. Molecular basis of the vasopressinergic and oxytocinergic regulation of Aqp1aa, Aqp1ab1 and Aqp1ab2 trafficking. (**A**, **D**, **I**) Schematic representation of seabream Aqp1aa, Aqp1ab1 and Aqp1ab2 monomers showing the six transmembrane domains, the five connecting loops (*A*-*E*), and the PKC and PKA phosphorylation sites involved in channel trafficking (12). The predicted YWHA-binding regions in the Aqp1ab1 and Aqp1ab2 C-termini are underlined. (**B**, **C**) Osmotic water permeability (P_f) (B) and immunoblots of total (TM) and plasma (PM) membrane extracts (C) of oocytes expressing the Oxtrb or Avpr1aa and wild-type (WT) Aqp1aa or the Aqp1aa-V145T mutant, and exposed to DMSO (controls) or 10 µM Avp or Oxt. (**E**-**G**) P_f of oocytes expressing the Avpr2aa and WT Aqp1ab1 or Aqp1ab1 mutants (S156A and S253A), together with HA-tagged YwhazLa (YwhazLa-HA), and treated with Avp in the presence or absence of 10 µm of H89. The corresponding immunoblots are shown in F and G. (**H**) Co-immunoprecipitation of WT and mutant Aqp1ab1 channels and YwhazLa-HA in the same oocytes using Aqp1ab1 and HA specific antibodies. (**J**, **K**) P_f (J) and immunoblot (K) of oocytes expressing the Avpr2aa and WT Aqp1ab2 or Aqp1ab2-T262A, together with YwhazLb-HA, and treated with Avp as above. (L) Co-immunoprecipitation of both channels in the same oocytes carried out as in H. Data in B, E and J are the mean ± SEM with the number of oocytes indicated in each bar. $^{**}P < 0.01$; $^{***}P < 0.001$ (unpaired Student's *t*-test), with respect to water-injected oocytes, or as indicated in brackets. In C, F-H, K and L, molecular mass markers (kDa) are on the right.

promoted the interaction of wild-type Aqp1ab1 and Aqp1ab1-S156A with YwhazLa, which was inhibited in both cases in the presence of H89 (figure 6H). However, the Aqp1ab1-S253A mutant, which did not traffic to the oocyte surface after Avp stimulation, was not able to interact with YwhazLa regardless of H89 treatment (figure 6H). These data agree with our previous study (Ferré *et al*., 2023) and suggest that Avp-mediated targeting of Aqp1ab1 to the plasma membrane depends on PKA phosphorylation of C-terminal Ser^{253}, which drives YwhazLa binding, and of loop D Ser^{156} once the complex Aqp1ab1-YwhazLa is formed. In contrast, oocytes expressing Aqp1ab2 and Avpr2aa, together with YwhazLb-HA, only showed a higher P_f, together with an increased channel expression in the oocyte plasma membrane and channel binding to YwhazLb, after Avp treatment, which were all blocked in oocytes expressing the Aqp1ab2-T262A mutant (figure 6J-L). These findings therefore indicate that the Avp-mediated regulation of Aqp1ab2 trafficking is specifically mediated by PKA phosphorylation of Thr^{262} in the C-terminus, allowing YwhazLb binding and further insertion of the channel into the plasma membrane.

3.2.4.5. Intraovarian Avp Production Is Regulated by Gonadotropin-Induced Progestin

The previous experiments show that seabream ovarian follicles can synthesize Avp, and that the ovarian levels of the nonapeptide *in vivo* increase during the stage of oocyte maturation and hydration. These observations would be compatible with a role of Avp regulating the intracellular trafficking of Aqp1ab1 and Aqp1ab2 in maturing oocytes, as observed in surrogate amphibian oocytes. However, our data also suggest that the local production of Avp may be under gonadotropic regulation, since a surge of the circulating luteinizing hormone (Lh) typically occurs in seabream females during the maturation stage (Gothilf *et al*., 1997; Meiri *et al*., 2002). To test this hypothesis, we carried out *in vitro* experiments in which the production of Avp by postvitellogenic ovarian explants in response to piscine single-chain recombinant Lh (rLh) was evaluated by a custom made Avp enzyme-linked immunosorbent assay (ELISA) (supplementary figure S2, see Annexes, page 274). To investigate the specificity of the rLh potential regulation, in these experiments we also tested the effect of single-chain recombinant follicle-stimulating hormone (rFsh). The results showed that rLh increased the concentration of Avp in the

explants by ~4-fold with respect to the water-exposed explants (controls), while the Avp levels in the rFsh-treated explants did not differ from the controls (figure 7A).

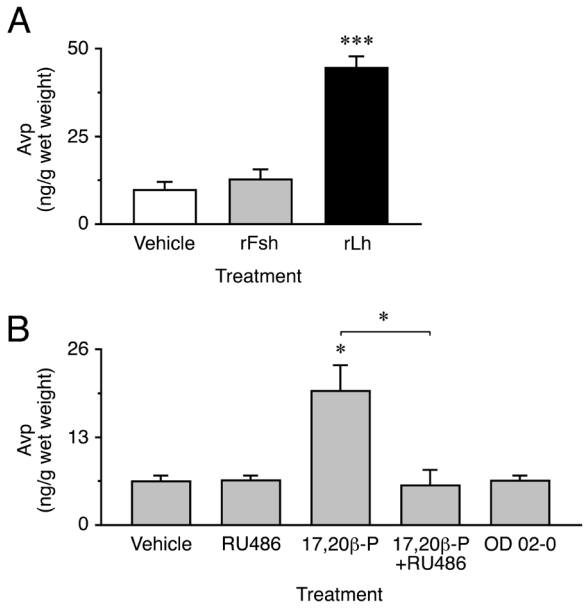

Figure 7. Gonadotropin and progestin induction of ovarian Avp production *in vitro*. (**A**) Amounts of Avp measured in ovarian extracts after ~20 h of exposure to 100 ng/ml of single-chain recombinant seabass Fsh or Lh (rFsh and rLh, respectively), or to the hormone vehicle (controls). Data are the mean ± SEM (n = 10 replicates compiled from two separated experiments on two females). (**B**) Avp content in ovarian explants incubated with 0.1 µg/ml 17,20β-P, 100 µM of the nuclear progesterone receptor inhibitor RU486, 17,20β-P+RU486, or to 10 µM of the membrane progestin receptor agonist OD 02-0. Controls were treated with 0.5% ethanol. Values are the mean ± SEM (n = 4 independent experiments on different females). *P < 0.05; ***P < 0.001 (unpaired Student's t-test), with respect to vehicle exposed explants, or as indicated in brackets.

Since the progestin 17α,20β-dihydroxypregn-4-en-3-one (17,20β-P) is known to be the maturation-inducing steroid secreted by granulosa cells in response to Lh in sparids (El Mohajer *et al*., 2022), we further investigated whether 17,20β-P could mediate the Lh induction of Avp synthesis in postvitellogenic ovarian explants. In addition, to examine the type of progestin receptor potentially involved in this mechanism, treatment with 17,20β-P was applied in the presence or absence of the nuclear progesterone receptor inhibitor RU486 (Zapater *el al*., 2013), while other explants were treated with the membrane progestin receptor agonist OD 02-0 (10- ethenyl-19-norprogesterone) (Nader *et al*., 2020) in the absence of 17,20β-P. The results of these trials confirmed that 17,20β-P induced a 3-fold increase in Avp synthesis in ovarian explants, comparable to that observed in response to rLh, which could be completely abolished by RU486, and not reproduced by OD 02-0 treatment (figure 7B). These data therefore suggest that the specific Lh induction of Avp

synthesis in the granulosa cells of seabream postvitellogenic follicles is mediated by a genomic mechanism through the nuclear progestin receptor.

3.2.4.6. The Avp-Avpr2aa-PKA Signaling Pathway Differentially Regulates Aqp1ab1 and Aqp1ab2 Trafficking in Postvitellogenic Seabream Oocytes

To investigate the physiological significance of the Avp regulation of the TSA1C channel trafficking in seabream oocytes, we determined the dynamics of the subcellular localization of endogenous Aqp1aa, Aqp1ab1, and Aqp1ab2, and their interactions with YwhazLa and -zLb proteins, after Avp treatment *in vitro*, using the Aqp1ab1- and Aqp1ab2-specific antisera and commercial mammalian YWHAZ antibodies specific for seabream YwhazLa/b or -zLb (Ferré *et al*., 2023). For this, we incubated isolated seabream vitellogenic ovarian follicles with Avp, in the presence or absence of the seabream Avpr1aa and Avpr2aa antagonist TLV or the PKA inhibitor H89, while control follicles were exposed to DMSO vehicle alone (figure 8).

The experiments showed that Avp did not induce meiotic maturation or oocyte hydration, in the latter case because the osmotic drive generated by yolk hydrolysis was not activated by the nonapeptide. Immunofluorescence microscopy indicated that Aqp1aa was localized to the epithelium surrounding the ovarian follicles, and not in the theca cell as previously reported (Ferré *et al*., 2023), and that this localization did not appear to change with Avp treatment (figure 8A, B). In contrast, both Aqp1ab1 and Aqp1ab2 were more accumulated in the most cortical cytoplasmic region of the oocytes, just below the plasma membrane, while Aqp1ab2 was also localized in the granulosa and theca cells (figure 8A, B). After Avp exposure, Aqp1ab1 immunoreactivity appeared more concentrated in the most distal part of the microvilli crossing the vitelline envelope, whereas the Aqp1ab2 channel became localized in a more basal region of the microvilli (figure 8A, B). The differential spatial localization of Aqp1ab1 and Aqp1ab2 in the oocyte microvilli in response to Avp mimics that observed in FSK-treated postvitellogenic follicles (Ferré *et al*., 2023). However, it was prevented in follicle-enclosed oocytes preincubated with TLV or H89 prior to Avp treatment (figure 8C, D). These observations were corroborated by Aqp1ab1 and Aqp1ab2 fluorescence quantification in the oocyte

plasma membrane (figure 8E), as well as by radiolabeled water uptake assays, which showed that water permeability of Avp-treated follicles was higher than that of follicles treated with DMSO alone and reduced in the presence of Avp plus the TLV or H89 inhibitors (figure 8F).

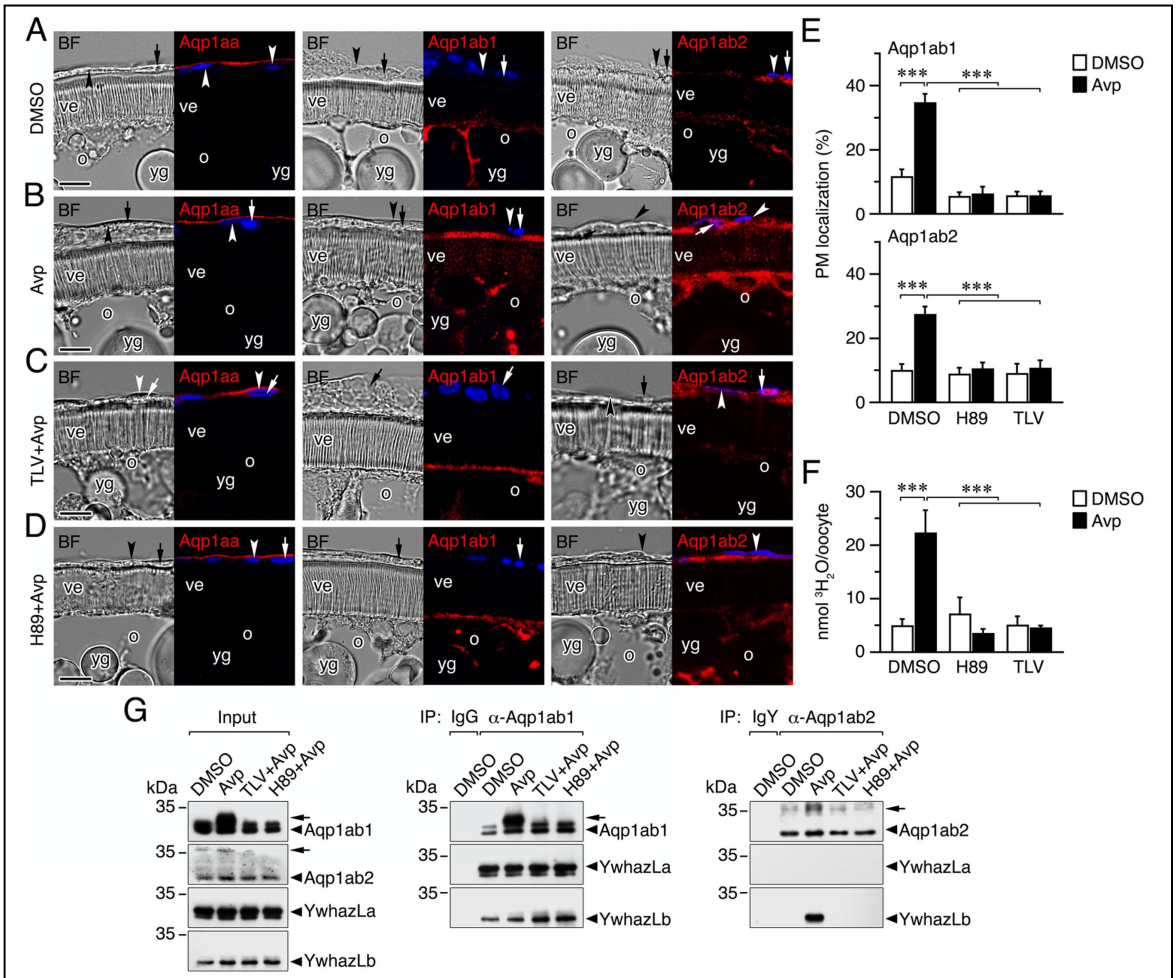

Figure 8. Avp regulation of aquaporin trafficking in seabream ovarian follicles *in vitro*. (**A-D**) Representative brightfield (BF, left panels) and immunostaining of Aqp1aa, Aqp1ab1 and Aqp1ab2 (red color, right panels) in follicles exposed to 10 µM Avp, in the presence or absence of 10 µM of the Avpr1aa and Avpr2aa antagonist Tolvaptan (TLV) or the PKA inhibitor H89. The immunostaining of follicles incubated with TLV or H89 alone are shown in supplementary figure S5 (see Annexes, page 277). The nuclei were counterstained with DAPI (blue color). The theca and granulosa cells are indicated by an arrowhead and arrow, respectively. ve, vitelline envelope; o, oocyte; yg, yolk globules. Scale bars, 10 µm. (**E**) Percentage (mean ± SEM; n = 5 follicles) of Aqp1ab1 and Aqp1ab2 in the oocyte plasma membrane (PM) after each treatment determined by image analysis. (**F**) Uptake (mean ± SEM; n = 3 pools of 10 oocytes) of ^3H_2O by follicle-enclosed oocytes treated with Avp as in E. ***P < 0.001 (unpaired Student's t-test) as indicated in brackets. (**G**) Co-immunoprecipitation of Aqp1ab1 and Aqp1ab2 with YwhazL proteins in ovarian follicles (n = 10) treated as in A-D. Left panel shows the immunoblotting of Aqp1ab1, Aqp1ab2, YwhazLa and YwhazLb in the input extracts before immunoprecipitation. The middle and right panels show co-immunoprecipitated YwhazLa and/or YwhazLb with Aqp1ab1 and Aqp1ab2. Controls were immunoprecipitated with IgG or IgY for the Aqp1ab1 and Aqp1ab2 antibodies, respectively. The arrowheads indicate phosphorylated forms of Aqp1ab1 and Aqp1ab2. Molecular mass markers (kDa) are on the left.

The potential changes in the phosphorylation state of Aqp1ab1 and Aqp1ab2 channels, and of their interactions with YwhazLa and -zLb carrier proteins, during Avp

treatment were subsequently investigated by co-immunoprecipitation and immunoblotting. These trials confirmed previous observations (Ferré *et al*., 2023; Fabra *el al*., 2006) indicating that in control postvitellogenic follicles, when Aqp1ab1 is held in the most cortical region of the oocyte and some inserted in the basal region of the microvilli, the channel is already phosphorylated and bound to both YwhazLa and -zLb (figure 8G). However, after Avp treatment Aqp1ab1 becomes more phosphorylated, while maintaining the interaction with YwhazLa and -zLb (figure 8G), which coincides with the secondary loop D Ser^{156} phosphorylation and trafficking of the channel to the most distal region of the oocyte microvilli. Phosphorylation of Aqp1ab2 was also increased after Avp stimulation, but in this case the YwhazLb interaction was only detected in the presence of the nonapeptide (figure 8G), when the channel is translocated to the basal region of the oocyte microvilli. The Avp-mediated increase in the phosphorylation of Aqp1ab1 and Aqp1ab2, as well as the binding of the latter channel to YwhazLb, was blocked by TLV and H89 (figure 8G), suggesting that the differential membrane trafficking regulation of the channels is regulated by the Avpr2aa-PKA transduction pathway.

3.2.5. Discussion

In this study we show for the first time that in addition to the hypophysial neuroendocrine system, a paracrine vasopressinergic and oxytocinergic signaling system exists in the ovary of a marine teleost. Since expression of Avp and/or Oxt precursor mRNAs or proteins are also expressed in the ovaries of freshwater catfishes (Joy and Chaube, 2015; Mennigen *et al*., 2022; Rawat *et al*., 2019; Singh and Joy, 2008), as well as in lampreys (Mayasich and Clarke, 2016), sharks (Gwee *et al*., 2009), birds (Saito and Grossmann, 1999), and mammals (Schaeffer *et al*., 1984; Sernia *et al*., 1994), it seems plausible that an ovarian vasopressinergic and/or oxytocinergic paracrine system existed prior to the emergence of vertebrates.

In the present context, we isolated paralogs from each of the major Avp and Oxt receptor subtypes (Avpr1aa, Avpr2aa and Oxtrb) and functionally characterized the signal transduction pathways they induce in order to determine how the systemic and paracrine systems might integrate to regulate aquaporin-mediated oocyte hydration. The data show that the Avpr1aa and Oxtrb subtypes activate PLC-PKC cascades while the Avpr2aa subtype activates the cAMP-PKA pathway. These results are consistent with the notion

that the functional pathway dichotomy between the Avpr1/Oxtr and Avpr2 subtypes may have emerged in the common ancestor of jawed vertebrates (Yamaguchi *et al*., 2023). However, since teleosts encode up to five copies of the Avpr2 subtype (supplementary figure S1, see Annexes, page 272), it will be important to validate the pathway specificity of each paralog to avoid expectation bias. For example, in related experiments, our ligand specificity analyses show that seabream Avpr1aa and Avpr2aa display some promiscuity for Avp and Oxt. By contrast, the Avpr1ab ortholog of the white sucker (*Catostomus commersoni*) is only activated by Avp (Mahlmann *et al*., 1994). Similarly, our data for the seabream Oxtrb show a high specificity for Oxt, while the white sucker Oxtra can also be activated by Avp, albeit with lower potency (Hausmann *et al*., 1995).

Since we had previously established that TSA1C channel trafficking is differentially regulated by the PKC-mediated phosphorylation of loop D sites in Aqp1aa and the PKA-mediated phosphorylation of loop D and C-terminal sites in Aqp1ab1 and the C-terminus of Aqp1ab2 (Ferré *et al*., 2023), we confirmed here that the same sites control the recycling of Aqp1aa and membrane insertion of the Aqp1ab-type channels when co-expressed with the Avpr1aa/Oxtrb and Avpr2aa subtypes, respectively. By further identifying the pituitary and follicular cell sources of Avp and Oxt together with the ovarian loci of their respective receptors, and monitoring the plasma and ovarian levels of each nonapeptide during oocyte growth and maturation, we can propose a model that is congruent with the suggestions for catfish (Joy and Chaube, 2015; Mennigen *et al*., 2022), to explain the neuroendocrine and paracrine regulation of aquaporin trafficking facilitating marine teleost oocyte hydration (figure 9).

In this model, neurohypophysial secretion of Avp throughout oocyte growth (vitellogenesis) arrives at the capillary beds of the thecal layer. From there it diffuses to activate the Avpr2aa receptor, which is expressed in the plasma membrane of the theca and granulosa cells, to induce the PKA-mediated phosphorylation of Thr^{262} in the C-terminus of Aqp1ab2. This results in the coupling of the YwhazLb binding protein and the trafficking of the channel to the cell surface of the theca and granulosa cells. Meanwhile, in the oocyte Aqp1ab1, which is already expressed since the primary growth stage (Zapater *et al*., 2013) and phosphorylated at the C-terminal Ser^{253} by a PKA-mediated mechanism (Ferré *et al*., 2023), preferentially couples with the YwhazLa binding protein and is trafficked close to the basal region of the oocyte microvilli during vitellogenesis. Some

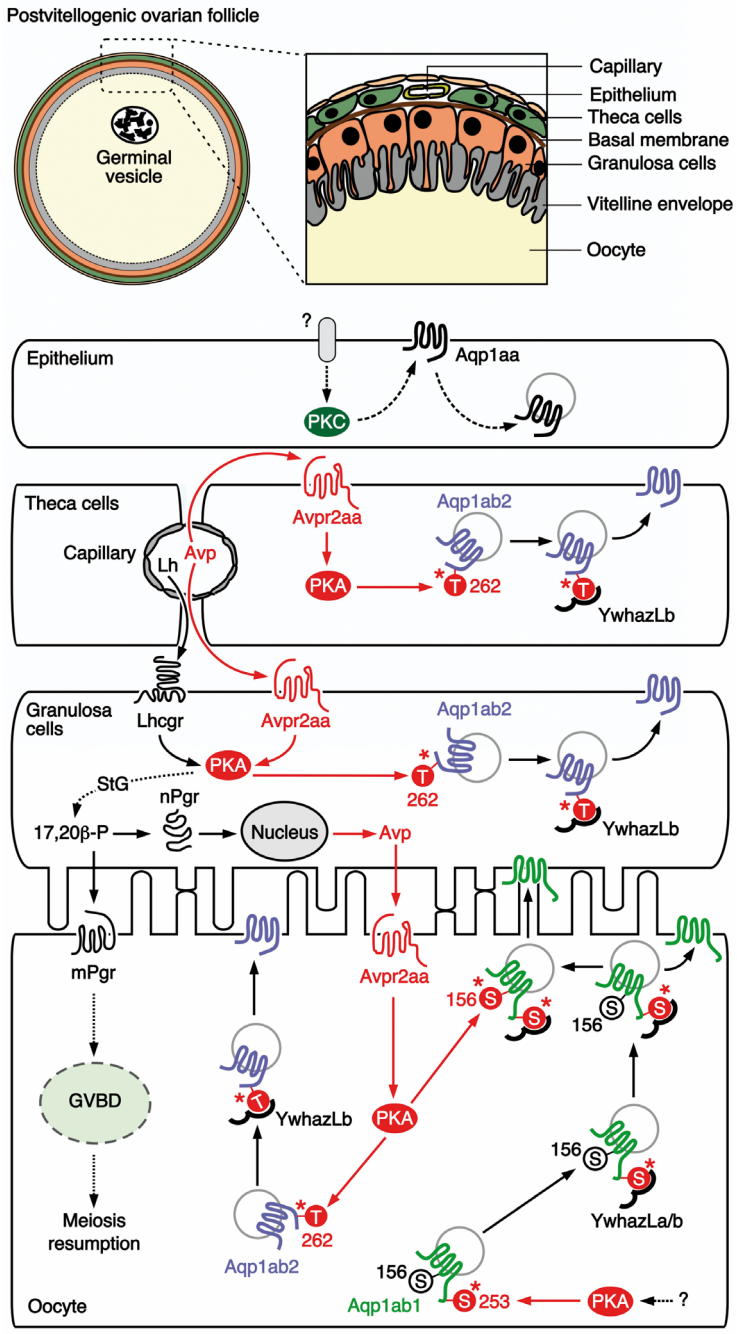

Figure 9. Proposed model for the vasopressinergic regulation of Aqp1ab1 and Aqp1ab2 function in seabream ovarian follicles during meiosis resumption and oocyte hydration. In primary growth oocytes, Aqp1ab1 is phosphorylated at Ser^{253} by protein kinase A (PKA), which is activated by a yet unknown signaling pathway, to bind YwhazLa and -zLb. The complex is then slowly transported to the oocyte cortical region during the vitellogenic period, where it is retained just below the oocyte plasma membrane in postvitellogenic oocytes, while some of Aqp1ab1 enters the basal region of the oocyte microvilli. The release of circulating hypohysial Avp and luteinizing hormone (Lh) from capillaries in the theca layer at the time of oocyte maturation activate the Avpr2aa in theca and granulosa cells, as well as the Lh/choriogonadotropin receptor (Lhcgr) in the granulosa cells. In the theca and granulosa, the Avp-stimulated Avpr2aa triggers PKA activation, which mediates the phosphorylation of Thr^{262} in Aqp1ab2 promoting the binding to YwhazLb and the trafficking of the channel to the plasma membrane of these cells. The activation of the Lhcgr-PKA pathway in granulosa cells drives the synthesis of the progestagen 17,20β-P, through a switch in the steroidogenic (StG) pathway from estrogen to progestagen production. The 17,20β-P, in turn stimulates the local synthesis of Avp through a genomic mechanism mediated by the nuclear progestin receptor (nPgr). The resulting release of Avp and 17,20β-P from the granulosa cells respectively activates the Avpr2aa and the membrane progestin receptor (mPgr) in the oocyte surface. The mPr triggers meiosis resumption (oocyte maturation), whereas the Avpr2aa-PKA signaling regulates the trafficking of Aqp1ab2 as in follicle cells, and a

secondary phosphorylation of Ser^{156} in the loop D of Aqp1ab1 channels already complexed with YwhazLa/b. The secondary phosphorylation of Aqp1ab1 further shuttles the channel to the most distal region of the oocyte microvilli. Finally, systemic (circulating) and/or local levels of Avp, or a possible Lh-mediated production of Oxt, may potentially activate the protein kinase C (PKC) signaling pathway in the epithelium, through a yet unidentified receptor, to induce the recycling of Aqp1aa. This model integrates both the systemic and paracrine vasopressinergic regulation of the intracellular trafficking of Aqp1ab-type paralogs in the seabream oocyte, such that competitive plasma membrane spatial occupancy by both channels is avoided and bulk water influx is augmented during oocyte hydration.

of Aqp1ab1 also enters the basal region of the oocyte microvilli (Ferré *et al*., 2023), potentially to mediate water homeostasis during the vitellogenic growth phase. Concomitant with the preovulatory surge of Lh (Gothilf *et al*., 1997; Meiri *et al*., 2002), our data show that the circulating and ovarian levels of Avp are increased during meiotic maturation and hydration of the oocytes. Such an elevated systemic Avp further enhances the PKA-mediated trafficking of Aqp1ab2 channels in the theca and granulosa cells. However, as in the catfish (Singh *et al*., 2021), the combined activation of Lh on Lhcgr and Avp on Avpr2aa could also multiply the action of the PKA-mediated Lh induction of the steroidogenic shift from estrogen production to the synthesis of the maturation-inducing progestin 17,20ß-P in granulosa cells (Lubzens *et al*., 2010). Thus, the 17,20ß-P could act as a master switch regulating the reciprocal genomic production of Avp via the nuclear progestin receptor in granulosa cells, and the non-genomic activation of GVBD and meiosis resumption via the membrane progestin receptor that is expressed in the oocyte plasma membrane (Nagahama *et al*., 2008). It is the former reciprocal genomic production of Avp that would provide the paracrine signal between the granulosa cells and the Avpr2aa in the oocyte plasma membrane, which now activates the PKA-mediated phosphorylation of Thr^{262} in the Aqp1ab2 C-terminus and Ser^{156} in loop D of Aqp1ab1. The Thr^{262} phosphorylation promotes the coupling of the YwhazLb binding protein and the trafficking of Aqp1ab2 to the basal region of the oocyte microvilli, while the secondary phosphorylation of loop D Ser^{156} in Aqp1ab1 relocalizes the channel to the distal portion of the oocyte microvilli. In this way, the two Aqp1ab-type paralogs are co-regulated by the same Avp-Avpr2aa-PKA pathway to cooperatively enhance water influx while avoiding competitive occupancy of the same membrane space.

Our proposed model does not yet explain the signal transduction mechanism that may activate PKC-mediated recycling of Aqp1aa in the follicular epithelium, which occurs when this channel is co-expressed with Avpr1aa or Oxtrb in *X. laevis* oocytes. Nevertheless, we did observe that in vitellogenic ovarian follicles, both the mRNA and protein of Oxt are accumulated in the theca and granulosa cells, while those of Avp are

only accumulated in the granulosa cells. These observations may suggest that trafficking of epithelial Aqp1aa could also be under Avp or Oxt regulation through receptors not characterized here, such as the Avpr1ab or the Oxtra, since in our study neither *avpr1aa* nor *oxtrb* mRNA expression could not be detected in the follicular epithelial layer. In any event, the potential recycling of the Aqp1aa channel in the follicular epithelium may provide an important mechanism for the flow of water into the hydrating oocyte. The water path originates with the seawater imbibed by the mother and is delivered to the follicles through the thecal capillary beds. By simultaneously recycling epithelial Aqp1aa and driving Aqp1ab2 to the membranes of the theca and granulosa cells, water is only free to flow in one direction toward the oocyte. The differential proteolysis of primarily vitellogenin-Aa (VtgAa) type yolk proteins (Finn and Kristoffersen, 2007; Finn, 2007; Kolarevic *et al*., 2008) generates the osmotic driving force that converts the oocyte into the water sink, which then enters via the vasopressinergic induction of the Aqp1ab1 and Aqp1ab2 channels to the distal and proximal regions of the microvilli. The water finally becomes trapped within the highly hydrated oocyte due to the precipitous drop in the ovarian levels of Avp, thus ending the paracrine regulation of the trafficking of the Aqp1ab-type channels, and their resultant internalization in the oocyte (Ferré *et al*., 2023). The subsequent cyclical increase in the level of circulating Oxt may thus prepare the oocytes for ovulation as in mammals (Gainer and Wray, 1994), leaving the eggs ready for fertilization and their future pelagic passage in the oceanic currents.

In conclusion, the present study uncovered a paracrine vasopressinergic and oxytocinergic system in the ovary of a modern euacanthomorph marine teleost, the gilthead seabream, which supports the notion that this mechanism may have existed prior to the emergence of vertebrates. In both the seabream and catfish, the ovarian vasopressinergic system is possibly activated via systemic neuroendocrine signaling to multiply the Lh induction of progestin which generates Avp for the paracrine signaling. In the seabream, however, by functionally characterizing the signal transduction pathways induced by each of the Avp and Oxt receptor subtypes and assaying their ligand specificities, it was possible to uncover the molecular basis of the nonapeptide regulated trafficking of the TSA1C channels. In this respect, the Avpr2aa paralog plays a vital role in the transduction of the paracrine signals and the co-ordinated trafficking of the Aqp1ab-type channels so that they avoid competitive occupancy of the same membrane space and

maximise the hydration of the oocyte. It remains to be seen if a similar neuroendocrine/paracrine regulation of aquaporin trafficking exists in older lineages of teleost that retain the Aqp1ab-type paralogs.

Ethics statement: Procedures relating to the care and use of fish and sample collection were approved by the Ethics Committee of IRTA, following the European Union Council Guidelines (86/609/EU). The procedure for surgical laparotomy of female frogs was approved by the Ethics Committee for Animal and Human Experimentation from UAB and the Catalan Government (Direcció General de Polítiques Ambientals i Medi Natural; Project no. 10985).

Author contributions: Conceptualization: JC. Investigation: AF, FC and MG. Formal Analysis: AF, FC, MG, EK, RNF and JC. Supervision: JC and EK. Funding Acquisition: JC and RNF. Visualization: JC. Writing-Original Draft Preparation: AF. Writing- Review & Editing: JC, RNF and EK. All authors approved the submitted version of the manuscript.

Funding: This work was supported by the Spanish Ministry of Science and Innovation (MCIN/AEI/ 10.13039/501100011033), the European Regional Development Fund (ERDF) "A way of making Europe" (European Union), Grant no. AGL2016-76802-R (to J.C.), and the Norwegian Research Council (RCN) Grant no. 294768/E40 (to R.N.F). A.F. was recipient of a predoctoral contract from Spanish MCIN (BES-2014-068745). R.N.F. was also supported by the University of Bergen (Norway).

***Conflict of interest*:** The authors declare that the research was conducted in the absence of any commercial or financial relationships that could be construed as a potential conflict of interest.

3.2.6. References

Acharjee A, Chaube R, Joy KP, Cerdà J. 2011. Hormonal regulation of aquaporin-1ab in *Heteropneustes fossilis in vitro*. *Indian J Sci Techol.* 4(8):165-66. doi: 10.17485/ijst/2011/v4is.95.

Agre P, Sasaki S, Chrispeels MJ. 1993. Aquaporins: a family of water channel proteins. *Am J Physiol.* 265(3 Pt 2):F461. doi: 10.1152/ajprenal.1993.265.3.F461.

Cerdà J, Chauvigne F, Agulleiro MJ, Marin E, Halm S, Martínez-Rodríguez G, Prat F. 2008. Molecular cloning of Senegalese sole (*Solea senegalensis*) follicle-stimulating hormone and luteinizing hormone subunits and expression pattern during spermatogenesis. *Gen Comp Endocrinol.* 156(3):470-81. doi: 10.1016/j.ygcen.2008.02.006.

Cerdà J, Chauvigné F, Finn RN. 2017. The physiological role and regulation of aquaporins in teleost germ cells. In: Yang B, (eds). Advances in Experimental Medicine and Biology vol 969, Aquaporins. Springer. p. 149-71. doi: 10.1007/978-94-024-1057-0_10.

Cerdà J, Fabra M, Raldúa D. 2007. Physiological and molecular basis of fish oocyte hydration. In: Babin P, Cerdà J, Lubzens E, (eds). The fish oocyte: from basic studies to biotechnological applications. Springer: Dordrecht. p. 349-96.

Cerdà J, Finn RN. 2010. Piscine aquaporins: an overview of recent advances. *J Exp Zool A Ecol Genet Physiol*. 313A:623-50. doi: 10.1002/jez.634.

Chaube R, Chauvigné F, Tingaud-Sequeira A, Joy KP, Acharjee A, Singh V, Cerdà J. 2011. Molecular and functional characterization of catfish (*Heteropneustes fossilis*) aquaporin-1b: changes in expression during ovarian development and hormone-induced follicular maturation. *Gen Comp Endocrinol.* 170:162-71. doi: 10.1016/j.ygcen.2010.10.002.

Chauvigné F, Boj M, Vilella S, Finn RN, Cerdà J. 2013. Subcellular localization of selectively permeable aquaporins in the male germ line of a marine teleost reveals spatial redistribution in activated spermatozoa. *Biol Reprod*. 89(2):37. doi: 10.1095/biolreprod.113.110783.

Chauvigné F, Ferré A, Cerdà J. 2021. The *Xenopus* oocyte as an expression system for functional analyses of fish aquaporins. *Methods Mol Biol.* 2218:11-28. doi: 10.1007/978-1-0716-0970-5_2.

Chauvigné F, Ollé J, González W, Duncan N, Giménez I, Cerdà J. 2017. Toward developing recombinant gonadotropin-based hormone therapies for increasing fertility in the flatfish Senegalese sole. *PLoS One.* 12(3):e0174387. doi: 10.1371/journal.pone.0174387.

Chauvigné F, Parhi J, Ducat C, Ollé J, Finn RN, Cerdà J. 2018. The cellular localization and redistribution of multiple aquaporin paralogs in the spermatic duct epithelium of a maturing marine teleost. *J Anat*. 233:177-92. doi: 10.1111/joa.12829.

Chauvigné F, Yilmaz O, Ferré A, Fjelldal PG, Finn RN, Cerdà J. 2019. The vertebrate Aqp14 water channel is a neuropeptide-regulated polytransporter. *Commun Biol.* 2:462. doi: 10.1038/s42003-019-0713-y.

Daza DO, Bergqvist CA, Larhammar D. 2022. The evolution of oxytocin and vasotocin receptor genes in jawed vertebrates: A clear case for gene duplications through ancestral whole-genome duplications. *Front Endocrinol.* 12:792644. doi: 10.3389/fendo.2021.792644.

Deen PM, Verdijk MA, Knoers NV, Wieringa B, Monnens LA, van Os CH, van Oost BA. 1994. Requirement of human renal water channel aquaporin-2 for vasopressin-dependent concentration of urine. *Science.* 264(5155):92-5. doi: 10.1126/science.8140421.

El Mohajer L, Bulteau R, Fontaine P, Milla S. 2022. Maturation inducing hormones in teleosts: Are progestogens always the first to be nominated? *Aquaculture*. 546:737315. doi: 10.1016/j.aquaculture.2021.737315.

Fabra M, Raldúa D, Bozzo MG, Deen PM, Lubzens E, Cerdà J. 2006. Yolk proteolysis and aquaporin-1o play essential roles to regulate fish oocyte hydration during meiosis resumption. *Dev Biol*. 295:250-62. doi: 10.1016/j.ydbio.2006.03.034.

Fabra M, Raldúa D, Power DM, Deen PM, Cerdà J. 2005. Marine fish egg hydration is aquaporin-mediated. *Science.* 307(5709):545. doi: 10.1126/science.1106305.

Ferré A, Chauvigné F, Vlasova A, Norberg B, Bargelloni L, Guigó R, Finn RN, Cerdà J. 2023. Functional evolution of clustered aquaporin genes reveals insights into the oceanic success of teleost eggs. *Mol Biol Evol.* msad071. doi: 10.1093/molbev/msad071.

Finn RN, Cerdà J. 2011. Aquaporin evolution in fishes. In: Madsen S, (eds). Aquaporins in fish: Expression, localization and functional dynamics. *Front Physiol*. 2:44. doi:

10.3389/fphys.2011.00044.

Finn RN, Cerdà J. 2015. Evolution and functional diversity of aquaporins. *Biol Bull.* 229(1):6-23. doi: 10.1086/BBLv229n1p6.

Finn RN, Chauvigné F, Hlidberg JB, Cutler CP, Cerdà J. 2014. The lineage-specific evolution of aquaporin gene clusters facilitated tetrapod terrestrial adaptation. *PLoS One*. 9(11):e113686. doi: 10.1371/journal.pone.0113686.

Finn RN, Kristoffersen BA. 2007. Vertebrate vitellogenin gene duplication in relation to the ‘‘3R Hypothesis’’: Correlation to the pelagic egg and the oceanic radiation of teleosts. *PLoS One*. 2(1):e169. doi: 10.1371/journal.pone.0000169..

Finn RN. 2007. The maturational disassembly and differential proteolysis of paralogous vitellogenins in a marine pelagophil teleost: A conserved mechanism of oocyte hydration. *Biol Reprod*. 76(6):936-48. doi: 10.1095/biolreprod.106.055772.

Gainer H, Wray S. 1994. Cellular and molecular biology of oxytocin and vasopressin. In: Knobil E, Neill JD, (eds). The Physiology of Reproduction. Vol 2. New York, Raven Press. p 1099-29.

Gothilf Y, Meiri I, Elizur A, Zohar Y. 1997. Preovulatory changes in the levels of three gonadotropin-releasing hormone-encoding messenger ribonucleic acids (mRNAs), gonadotropin beta-subunit mRNAs, plasma gonadotropin, and steroids in the female gilthead seabream, *Sparus aurata*. *Biol Reprod*. 57(5):1145-54. doi: 10.1095/biolreprod57.5.1145.

Gwee PC, Tay BH, Brenner S, Venkatesh B. 2009. Characterization of the neurohypophysial hormone gene loci in elephant shark and the Japanese lamprey: Origin of the vertebrate neurohypophysial hormone genes. *BMC Evol Biol.* 9:47. doi: 10.1186/1471-2148-9-47.

Hausmann H, Meyerhof W, Zwiers H, Lederis K, Richter D. 1995. Teleost isotocin receptor: Structure, functional expression, mRNA distribution and phylogeny. *FEBS Lett.* 370(3):227-30. doi: 10.1016/0014-5793(95)00832-t.

Huang HF, He RH, Sun CC, Zhang Y, Meng QX, Ma YY. 2006. Function of aquaporins in

female and male reproductive systems. *Human Reprod Update*. 12(6):785-95. doi: 10.1093/humupd/dml035.

Joy KP, Chaube R. 2015. Vasotocin – A new player in the control of oocyte maturation and ovulation in fish. *Gen Comp Endocrinol*. 221:54-63. doi: 10.1016/j.ygcen.2015.02.013.

Kagawa H, Kishi T, Gen K, Kazeto Y, Tosaka R, Matsubara H, Matsubara T, Sawaguchi S. 2011. Expression and localization of aquaporin 1b during oocyte development in the Japanese eel (*Anguilla japonica*). *Reprod Biol Endocrinol.* 9:71. doi: 10.1186/1477-7827-9-71.

King LS, Kozono D, Agre P. 2004. From structure to disease: The evolving tale of aquaporin biology. *Nature Reviews*. 5(9):687-98. doi: 10.1038/nrm1469.

Kolarevic J, Nerland A, Nilsen, F, Finn RN. 2008 Goldsinny wrasse (*Ctenolabrus rupestris*) is an extreme *vtgAa*-type pelagophil teleost. *Mol Reprod Dev*. 75(6):1011-20. doi: 10.1002/mrd.20845.

Kondo K, Ogawa H, Yamashita H, Miyamoto H, Tanaka M, Nakaya K, Kitano K, Yamamura Y, Nakamura S, Onogawa T, *et al*. 1999. 7-Chloro-5-hydroxy - 1 - [2 - methyl – 4 - (2 – methylbenzoyl - amino)benzoyl]- 2,3,4,5 - tetrahydro-1H-1-benzazepine (OPC-41061): a potent, orally active nonpeptide arginine vasopressin V2 receptor antagonist. *Bioorg Med Chem*. 7(8):1743-54. doi: 10.1016/s0968-0896(99)00101-7.

Konno N, Kurosawa M, Kaiya H, Miyazato M, Matsuda K, Uchiyama M. 2010. Molecular cloning and characterization of V2-type receptor in two ray-finned fish, gray bichir, *Polypterus senegalus* and medaka, *Oryzias latipes*. *Peptides.* 31(7):1273-9. doi: 10.1016/j.peptides.2010.04.014.

Lubzens E, Young G, Bobe J, Cerdà J. 2010. Oogenesis in teleosts: How eggs are formed. *Gen Comp Endocrinol.* 165(3):367-89. doi: 10.1016/j.ygcen.2009.05.022.

Mahlmann S, Meyerhof W, Hausmann H, Heierhorst J, Schönrock C, Zwiers H, Lederis K, Richter D. 1994. Structure, function, and phylogeny of [Arg^{8}]vasotocin receptors from

teleost fish and toad. *Proc Natl Acad Sci U S A.* 91(4):1342-5. doi: 10.1073/pnas.91.4.1342.

Martos-sitcha JA, Campinho MA, Mancera JM, Martínez-Rodríguez G, Fuentes J. 2015. Vasotocin and isotocin regulate aquaporin function in the seabream. *J Exp Biol*. 218(Pt 5):684-93. doi: 10.1242/jeb.114546.

Martos-Sitcha JA, Fuentes J, Mancera JM, Martínez-Rodríguez G. 2014. Variations in the expression of vasotocin and isotocin receptor genes in the gilthead sea bream *Sparus aurata* during different osmotic challenges. *Gen Comp Endocrinol.* 197:5-17. doi: 10.1016/j.ygcen.2013.11.026.

Mayasich SA, Clarke BL. 2016. The emergence of the vasopressin and oxytocin hormone receptor gene family lineage - Clues from the characterization of vasotocin receptors in the sea lamprey (*Petromyzon marinus*). *Gen Comp Endocrinol.* 226:88-101. doi: 10.1016/j.ygcen.2016.01.001.

Maybauer MO, Maybauer DM, Enkhbaatar P, Traber D. 2008. Physiology of the vasopressin receptors. *Best Pract Res Clin Anaesthesiol.* 22(2):253-63. doi: 10.1016/j.bpa.2008.03.003.

McConnell NA, Yunus RS, Gross SA, Bost KL, Clemens MG, Hughes Jr FM. 2002. Water permeability of an ovarian antral follicle is predominantly transcellular and mediated by aquaporins. *Endocrinology*. 143(8):2905-12. doi: 10.1210/endo.143.8.8953.

Meiri I, Gothilf Y, Zohar Y, Elizur A. 2002. Physiological changes in the spawning gilthead seabream, *Sparus aurata*, succeeding the removal of males. *J Exp Zool*. 292(6):555-64. doi: 10.1002/jez.10072.

Mennigen JA, Ramachandran D, Shaw K, Chaube R, Joy KP, Trudeau VL. 2022. Reproductive roles of the vasopressin/oxytocin neuropeptide family in teleost fishes. *Front Endocrinol (Lausanne)*. Oct 13;13:1005863. doi: 10.3389/fendo.2022.1005863.

Molés G, Zanuy S, Muñoz I, Crespo B, Martínez I, Mañanós E, Gómez A. 2011. Receptor specificity and functional comparison of recombinant sea bass (*Dicentrarchus labrax*) gonadotropins (FSH and LH) produced in different host systems. *Biol Reprod.*

84(6):1171-81. doi: 10.1095/biolreprod.110.086470.

Nader N, Dib M, Hodeify R, Courjaret R, Elmi A, Hammad AS, Dey R, Huang XY, Machaca K. 2020. Membrane progesterone receptor induces meiosis in *Xenopus* oocytes through endocytosis into signaling endosomes and interaction with APPL1 and Akt2. *PLoS Biol.* 18(11):e3000901. doi: 10.1371/journal.pbio.3000901.

Nagahama Y, Yamashita M. 2008. Regulation of oocyte maturation in fish. *Dev Growth Differ*. 1:S195-219. doi: 10.1111/j.1440-169X.2008.01019.x.

Ocampo Daza D, Bergqvist CA, Larhammar D. 2022The evolution of oxytocin and vasotocin receptor genes in jawed vertebrates: a clear case for gene duplications through ancestral whole-genome duplications. *Front Endocrinol (Lausanne)*. 12:792644. doi: 10.3389/fendo.2021.792644.

Odekunle EA, Elphick MR. 2021. Comparative and evolutionary physiology of vasopressin/ oxytocin-type neuropeptide signaling in invertebrates. *Front Endocrinol (Lausanne).* 11:225. doi: 10.3389/fendo.2020.00225.

Raldúa D, Otero D, Fabra M, Cerdà J. 2008. Differential localization and regulation of two aquaporin-1 homologs in the intestinal epithelia of the marine teleost *Sparus aurata*. *Am J Physiol Regul Integr Comp Physiol.* 294(3):R993-1003. doi: 10.1152/ajpregu.00695.2007.

Rawat A, Chaube R, Joy KP. 2019. In situ localization of vasotocin receptor gene transcripts in the brain-pituitary-gonadal axis of the catfish *Heteropneustes fossilis*: a morpho-functional study. *Fish Physiol Biochem*. 45(3):885-905. doi: 10.1007/s10695-018-0590-1.

Saito N, Grossmann R. 1999. Gene expression of arginine vasotocin in ovarian and uterine tissues of the chicken. *Asian-Aus J Anim Sci.* 12(5):695-701. doi: 10.5713/ajas.1999.695.

Schaeffer JM, Liu J, Hsueh AJW, Yen SSC. 1984. Presence of oxytocin and arginine vasopressin in human ovary, oviduct, and follicular fluid. *J Clin Endocrinol Metab.* 59(5):970-3. doi: 10.1210/jcem-59-5-970.

Sernia C, Bathgate RAD, Gemmell RT. 1994. Mesotocin and arginine vasopressin in the corpus luteum of an Australian marsupial, the brushtail possum (*Trichosurus vulpecula*). *Gen Comp Endocrinol*. 93(2):197-204. doi: 10.1006/gcen.1994.1023.

Serradeil-Le Gal C, Wagnon J, Garcia C, Lacour C, Guiraudou P, Christophe B, Villanova G, Nisato D, Maffrand JP, Le Fur G, *et al*. 1993. Biochemical and pharmacological properties of SR 49059, a new, potent, nonpeptide antagonist of rat and human vasopressin V1a receptors. *J Clin Invest*. 92(1):224-31. doi: 10.1172/JCI116554.

Singh V, Chaube R, Joy KP. 2021. Vasotocin stimulates maturation-inducing hormone, oocyte maturation and ovulation in the catfish *Heteropneustes fossilis*: Evidence for a preferential calcium involvement. *Theriogenology.* 167:51-60. doi: 10.1016/j.theriogenology.2021.03.001.

Singh V, Joy KP. 2008. Immunocytochemical localization, HPLC characterization, and seasonal dynamics of vasotocin in the brain, blood plasma and gonads of the catfish *Heteropneustes fossilis*. *Gen Comp Endocrinol.* 159(2-3):214-25. doi: 10.1016/j.ygcen.2008.09.003.

Singh V, Joy KP. 2010. An involvement of vasotocin in oocyte hydration in the catfish *Heteropneustes fossilis*: A comparison with effects of isotocin and hCG. *Gen Comp Endocrinol*. 166(3):504-12. doi: 10.1016/j.ygcen.2010.02.020.

Skowronski MT, Kwon TH, Nielsen S. 2009. Immunolocalization of aquaporin 1, 5, and 9 in the female pig reproductive system. *J Histochem Cytochem.* 57(1):61-7. doi: 10.1369/jhc.2008.952499.

Tingaud-Sequeira A, Calusinska M, Finn RN, Chauvigné F, Lozano J, Cerdà J. 2010. The zebrafish genome encodes the largest vertebrate repertoire of functional aquaporins with dual paralogy and substrate specificities similar to mammals. *BMC Evol Biol*. 10:38. doi: 10.1186/1471-2148-10-38.

Wang D, Di X, Wang J, Li M, Zhang D, Hou Y, Hu J, Zhang G, Zhang H, Sun M, Meng X, Sun B, Jiang C, Ma T, Su W. 2018. Increased formation of follicular antrum in aquaporin-8-deficient mice is due to defective proliferation and migration, and not steroidogenesis of granulosa cells. *Front Physiol.* 9:1193. doi:

10.3389/fphys.2018.01193.

Warne JM. 2001. Cloning and characterization of an arginine vasotocin receptor from the euryhaline flounder *Platichthys flesus*. *Gen Comp Endocrinol.* 122(3):312-9. doi: 10.1006/gcen.2001.7644.

Williams PD, Clineschmidt BV, Erb JM, Freidinger RM, Guidotti MT, Lis EV, Pawluczyk JM, Pettibone DJ, Reiss DR, Veber DF, *et al*. 1995. 1-(1-[4-[(N-acetyl-4-piperidinyl)oxy]-2-methoxybenzoyl]piperidin-4- yl)-4H-3,1-benzoxazin-2(1H)-one (L-371,257): a new, orally bioavailable, non-peptide oxytocin antagonist. *J Med Chem*. 38(23):4634-6. doi: 10.1021/jm00023a002.

Yamaguchi Y, Takagi W, Kaiya H, Konno N, Yoshida MA, Kuraku S, Hyodo S. 2023. Phylogenetic and functional properties of hagfish neurohypophysial hormone receptors distinct from their jawed vertebrate counterparts. *Gen Comp Endocrinol.* 336:114257. doi: 10.1016/j.ygcen.2023.114257.

Yilmaz O, Ferré A, Nilsen F, Fjelldal PG, Cerdà J, Finn RN. 2020. Unravelling the complex duplication history of deuterostome glycerol transporters. *Cells.* 9(7):1663. doi: 10.3390/cells9071663.

Zapater C, Chauvigné F, Norberg B, Finn RN, Cerdà J. 2011. Dual neofunctionalization of a rapidly evolving aquaporin-1 paralog resulted in constrained and relaxed traits controlling channel function during meiosis resumption in teleosts. *Mol Biol Evol*. 28(11):3151-69. doi: 10.1093/molbev/msr146.

Zapater C, Chauvigné F, Scott AP, Gómez A, Katsiadaki I, Cerdà J. 2012. Piscine follicle-stimulating hormone triggers progestin production in gilthead seabream primary ovarian follicles. *Biol Reprod*. 87(5):111. doi: 10.1095/biolreprod.112.102533.

Zapater C, Chauvigné F, Tingaud-Sequeira A, Finn RN, Cerdà J. 2013. Primary oocyte transcriptional activation of *aqp1ab* by the nuclear progestin receptor determines the pelagic egg phenotype of marine teleosts. *Dev Biol.* 377(2):345-62. doi: 10.1016/j.ydbio.2013.03.001.

CHAPTER III:

Aquaporin splice variation differentially modulates channel function during marine teleost egg hydration

Alba Ferré[1], François Chauvigné[2], Cinta Zapater[3], Roderick Nigel Finn[1,4], Joan Cerdà[1]

[1] Institute of Agrifood Research and Technology (IRTA)-Institute of Biotechnology and Biomedicine (IBB), Universitat Autònoma de Barcelona, Barcelona, Spain.

[2] Institute of Marine Sciences, Spanish National Research Council (CSIC), Barcelona, Spain.

[3] Institute of Aquaculture Torre de la Sal, Spanish National Research Council (CSIC), Castellón, Spain.

[4] Department of Biological Sciences, University of Bergen, Bergen, Norway.

PLoS ONE. 18(11):e0294814.

doi: 10.1371/journal.pone.0294814.

3.3.1. Abstract

Aquaporin-mediated oocyte hydration is a developmentally regulated adaptive mechanism that co-occurs with meiosis resumption in marine teleosts. It provides the early embryos with vital water until osmoregulatory systems develop, and in the majority of marine teleosts causes their eggs to float. Recent studies have shown that the subdomains of two water channels (Aqp1ab1 and Aqp1ab2) encoded in a teleost-specific aquaporin-1 cluster (TSA1C) co-evolved with duplicated Ywhaz-like (14-3-3ζ-like) binding proteins to differentially control their membrane trafficking for maximal egg hydration. Here, we report that in species that encode the full TSA1C, in-frame intronic splice variants of Aqp1ab1 result in truncated proteins that cause dominant-negative inhibition of the canonical channel trafficking to the plasma membrane. The inhibition likely occurs through hetero-oligomerization and retention in the endoplasmic reticulum (ER) and ultimate degradation. Conversely, in species that only encode the Aqp1ab2 channel we found an in-frame intronic splice variant that results in an intact protein with an extended extracellular loop E, and an out-of frame intronic splice variant with exon readthrough that results in a truncated protein. Both isoforms cause dominant-negative enhancement of the degradation pathway. However, the extended and truncated Aqp1ab2-type variants can also partially escape from the ER to reach the oocyte plasma membrane, where they dominantly-negatively inhibit water flux. The ovarian follicular expression ratios of the Aqp1ab2 isoforms in relation to the canonical channel are lowest during oocyte hydration, but subsequently highest when the canonical channel is recycled, thus leaving the eggs endowed with >90% water. These findings suggest that the expression of inhibitory isoforms of Aqp1ab1 and Aqp1ab2 may represent a new regulatory mechanism through which the cell-surface expression and the activity of the canonical channels can be physiologically modulated during oocyte hydration in marine teleosts.

Keywords: Aquaporin, splice forms, dominant-negative, oocyte hydration, teleost

3.3.2. Introduction

Massive water uptake during meiosis resumption of marine teleost oocytes is an adaptive mechanism that produces highly hydrated eggs that float when released in the hyperosmotic seawater. The mechanism is thought to have evolved as an exaptation that evolved to provide the hyposmotic embryos with life-supporting water until osmoregulatory systems developed (Fyhn *et al*., 1999). The hydration process involves the generation of an intracellular osmotic gradient via maturational yolk proteolysis and ion transport, and the coordinated temporal insertion of a water channel ortholog of mammalian AQP1 termed Aqp1ab in the oocyte plasma membrane (Finn *et* al., 2002; Fabra *et al*., 2005; Zapater *et al*., 2011; Cerdà *et al*., 2017). The teleost-specific Aqp1ab (previously termed Aqp1o or Aqp1b) is a water-selective integral membrane channel that evolved via tandem duplication of the *aqp1aa* gene (Fabra *et al*., 2006; Zapater *et al*., 2011; Tingaud-Sequeira *et al*., 2008; Finn and Cerdà, 2011; Cerdà *et al*., 2013).

Very recently, however, it has been shown that in fact two Aqp1ab-type channels (Aqp1ab1 and Aqp1ab2) evolved via tandem duplication within a teleost-specific aquaporin-1 cluster (TSA1C: aqp1aa-aqp1ab2-aqp1ab1) (Ferré *et al*., 2023a). The existence of the TSA1C was not previously noted due to differential aqp1ab-type gene loss in many lineages. For example, anguillid eels only retain the aqp1ab2 gene, while cyprinids, such as zebrafish, only retain the aqp1ab1 gene and the majority of species that incubate their eggs internally such as seahorses and guppies have either lost or inactivated both genes (Ferré *et al*., 2023a). Remarkably, however, functional forms of the Aqp1ab1 and -1ab2 channels are almost exclusively retained in marine species that spawn hydrated pelagic eggs (pelagophils), with a third of the highly diverse modern euacanthomorph teleosts retaining both copies (Ferré *et al*., 2023a). RNA tissue profiling revealed that in contrast to other members of the piscine aquaporin superfamily (Finn *et al*., 2014; Yilmaz *et al*., 2020), only the Aqp1ab-type channels are highly accumulated in the ovaries of marine pelagophil species (Tingaud-Sequeira *et al*., 2008; Ferré *et al*., 2023a). A recent study further showed that the Aqp1ab-type channel subdomains co-evolved with Ywhaz-like (14-3-3ζ-like) binding proteins to differentially regulate their trafficking to avoid competitive occupancy of the same plasma membrane space in the oocyte and accelerate bulk water influx for maximal egg hydration (Ferré *et al*., 2023a). In this regard, phosphorylation of C-terminal residues of Aqp1ab1 and -1ab2 promotes the binding of two teleost-specific proteins YwhazLa and YwhazLb, with

Aqp1ab2 showing exclusive specificity for YwhazLb, to facilitate trafficking to the proximal region of the plasma membrane microvilli. A second phosphorylation in loop D in Aqp1ab1 traffics the channel to the distal region of the microvilli, thus avoiding competitive membrane space occupancy. A separate study then revealed that both neurohypophysial and paracrine vasopressinergic signaling systems integrate to regulate the Aqp1ab-type membrane trafficking in the oocyte via a common arginine vasopressin (Avp)-Avpr2aa receptor mediated induction of the protein kinase A (PKA) pathway (Ferré *et al*., 2023b).

During the course of these earlier studies we also observed that some non-canonical Aqp1ab-type variants were expressed in the ovary of certain teleost species. The expression of aquaporin splice variants has previously been observed for mammalian AQP0 (Varadaraj *et al*., 2008) and AQP2 (Tajima *et al*., 2003; Sohara *et al*., 2006) in some cell types under pathophysiological conditions, but also for AQP4 (Moe *et al*., 2008; Sorani *et al*., 2008; De Bellis *et al*., 2014), AQP6 (Nagase *et al*., 2007) and AQP8 (Gao *et al*., 2014) in normal tissues. Similarly, aquaporin splice variants have also been described in crustaceans (Stavang *et al*., 2015; Catalán-García *et al*., 2021), insects (Tsujimoto *et al*., 2013), mollusks (Lind *et al*., 2017) and plants (Ampah-Korsah *et al*.,2016). In some cases, plant or animal aquaporin splice variants can result in modified proteins with altered permeability properties (Nagase *et al*., 2007; Ampah-Korsah *et al*.,2016). Conversely, various isoforms of mammalian AQP4 generated by alternative start codons or programmed translational readthrough can modulate supramolecular clustering in the plasma membrane and channel permeation (Bellis *et al*., 2017, Jorgacevski *et al*., 2020). In other cases, truncated proteins are produced which can result in dominant-negative impedance of membrane trafficking of the canonical channels (Varadaraj *et al*., 2008; De Bellis *et al*., 2014). Co-localization and functional studies with truncated AQP0-Δ213 and AQP4-Δ4 suggest that these isoforms gained dominant-negative repressive roles by trapping the canonical channels in the endoplasmic reticulum (ER) through hetero-oligomerization and altered conformation, thereby preventing their trafficking to the plasma membrane (Varadaraj *et al*., 2008; De Bellis *et al*., 2014).

In this context, in the present study we sought to investigate whether splice variation of the Aqp1ab-type channels harnesses homologous structure-function modulations, and whether such modulations could regulate oocyte hydration in marine pelagophil teleosts.

3.3.3. Materials and Methods

3.3.3.1. Animals and Sampling

Adult seabream and Atlantic halibut were obtained from aquaculture stations in Spain and Norway, respectively, and maintained as previously described (Zapater *et al*., 2011; Chauvigné *et al*., 2013). Two-year old adult Senegalese sole females were obtained from the commercial company Stolt Sea Farm S.A. (Spain), and transported and raised at the facilities of the Institute of Marine Sciences of Barcelona (Spanish Council for Scientific Research, CSIC, Spain). Fish were kept in 2000 l tanks under natural conditions of photoperiod and temperature, and fed with dry pellets (balanced diet, LE-7-Elite, Skretting) five days a week (Chauvigné *et al*., 2016). Tissue biopsies were collected from sacrificed fish during the natural spawning season for each species as previously described (Zapater *et al*., 2011; Chauvigné *et al*., 2013). For this, fish were sedated with 60 mg/l tricaine methanesulfonate (MS-222; Merck) and immediately sacrificed by decapitation. Tissue samples were frozen in liquid nitrogen and stored at -80˚C. To obtain ovarian follicles from sole females, the ovarian pieces were placed in Petri dishes containing 75% Leivovitz L-15 culture medium with L-glutamine and 100 µg/ml gentamicin at pH 7.5, and follicles at different developmental stages were manually isolated with watchmaker's forceps under an stereo microscope and frozen as above. Tissue biopsies from common sole were kindly provided by Dr. Marie-Laure Begout (IFREMER, France). The procedures relating to the care and use of fish and sacrifice were conducted in accordance with the protocols approved by the Ethics Committee (EC) of the Institut de Recerca i Tecnología Agroalimentàries (IRTA) following the European Union Council Guidelines (86/609/EU).

Frogs were purchased from the Centre de Ressources Biologiques Xénopes (University of Rennes, France) and maintained as previously described (Ferré *et al*., 2023a). Oocytes were collected by surgical laparotomy from anesthetized females following a procedure approved by the Ethics Committee for Animal and Human Experimentation (CEEAH) from Universitat Autònoma de Barcelona (Spain) and the Catalan Government (Direcció General de Polítiques Ambientals i Medi Natural; Project no. 10985).

3.3.3.2. Reagents and Antibodies

All reagents were purchased from Merck unless indicated otherwise. Antisera were raised in rabbits against synthetic peptides corresponding to the extracellular loop A of Senegalese sole Aqp1ab2 (GDRNNTYPDQEIKV), or to a specific amino acid sequence of the extracellular loop E of sole Aqp1ab2_v1 isoform (VSASRHSLTSRPSL) (Agrisera AB, Vännäs, Sweden). Antisera were affinity purified against the synthetic peptides. Previously characterized antibodies against gilthead seabream Aqp1ab1 (Ferré *et al*., 2023a), and commercial antibodies against α-tubulin (Merck #T9026), PDI (Merck #P7496), HA (Invitrogen #PA1-985) and FLAG (rabbit or mouse antibodies, Merck #F7425 and #F3165, respectively) were also employed.

3.3.3.3. Identification and Cloning of Aquaporin Splice Forms

To identify *aqp1ab1* and *-1ab2* isoforms in seabream, halibut and sole we carried out RT-PCR employing species-specific oligonucleotide primers based on previously deposited sequences in GenBank (supplementary table S1, see Annexes, page 278) (Ferré *et al*., 2023a). Total RNA was extracted from the ovary using the GenElute Total RNA Miniprep Kit and treated with Dnase I following the manufacturer instructions. The reverse transcription of RNA (5 µg) was performed with 0.5 µM oligo(dT)$_{12\text{-}18}$ (Thermo Fisher Scientific), 20 U of SuperScript II RT (Invitrogen), 5 × First-Strand Buffer (250 mM Tris-HCl, 375 mM KCl, 15 mM $MgCl_2$), 40 U of RNase OUT^{TM} (Thermo Fisher Scientific), and 1 mM dNTPs (Promega), for 1.5 h at 42ºC. The PCR reaction was carried out with 1 µl of cDNA containing 1 × PCR buffer with Mg^{2+}, 0.2 mM dNTPs, 1 U Taq polymerase, and 0.2 µM of the forward and reverse oligonucleotide primers, in a 50-µl final volume. Reactions were amplified using one cycle at 95ºC for 2 min; 35 cycles at 95ºC for 30 sec, 60ºC for 30 sec, and 1 min at 72ºC; and 7 min for final elongation at 72ºC. The PCR products were run in 2% agarose gel, cloned into the pGEM-T Easy vector (Promega) and DNA Sanger sequenced (Macrogen). The full-length cDNAs of the splice variants identified were finally amplified by RT-PCR as described above, using primers located in the 5'- and 3'-end UTR regions of each paralog and the Easy-A high-fidelity PCR cloning enzyme (Agilent), and Sanger sequenced.

3.3.3.4. Sequence and *In Silico* Structural Analyses of Aquaporin Isoforms

Multiple nucleotide and amino acid sequence alignments were carried out using Clustal Omega (https://www.ebi.ac.uk/Tools/msa/clustalo/9) (Sievers *et al*., 2011). The 3-dimensional structures of the WT and variant channels were inferred using the model leverage option in the Modeler server (modbase.compbio. ucsf.edu), based on auto-selected AQP0 (2b6pA), AQP4 (3gd8A) and AQP5 (3d9sA) templates. The best scoring models were selected using the slow (Seq-Prf, position–specific iterative-basic local alignment search tool) assignment method, and rendered with MacPymol (https://pymol.org/2/).

3.3.3.5. Microinjection of *X. laevis* Oocytes and Swelling Assays

The cDNAs coding for the WT and splice forms were subcloned into the pT7Ts expression vector (Deen *et al*., 1994), in some cases fused with an HA or FLAG epitope tag at the C-terminus of the encoded proteins by using PCR. The cRNAs were synthesized *in vitro* with T7 RNA polymerase from *Xba*I-digested pT7Ts. The isolation and microinjection of oocytes, as well as the swelling assays, were carried out as previously described (Chauvigné *et al*., 2021). The oocytes were injected with WT aquaporins (1 or 25 ng cRNA) or the different splice forms alone (25 or 50 ng cRNA), or with combinations of the WT with different amounts of the isoforms at ratios from 0.05 to 50 (for seabream and halibut Aqp1ab1) or from 0.004 to 1 (for sole Aqp1ab2). Oocytes expressing sole Aqp1ab2 and/or its isoforms were always coinjected with 25 ng of Atlantic halibut YwhazLb and treated with 100 µM FSK for 1 h prior to the swelling assays as previously described (Ferré *et al*., 2013a).

3.3.3.6. Protein Extraction

The total and plasma membrane fractions of *X. laevis* oocytes (n = 10) were isolated as described previously (Kamsteeg and Deen, 2001). Senegalese sole intact ovarian follicles or defolliculated oocytes (n = 50) were homogenized in RIPA buffer (150 mM NaCl, 50 mM Tris pH 8.0, 1.0% Triton X-100, 0.5% sodium deoxycholate, 0.1% SDS, supplemented with 1 mM NaF, 1 mM Na_3VO_4, EDTA-free protease inhibitors, and 80 U benzonase). Samples were centrifuged at 14,000 × g for 10 min at 4ºC, and the supernatant mixed with 2 × Laemmli sample buffer and heated at 95 °C for 10 min. For defolliculation, follicles were incubated with 0.05% trypsin, 10 µM HCl, in L-15 medium during 2 h, followed by exposure

to bovine serum albumin (BSA) diluted 1:500 in L-15 medium for 10 min, and a second treatment with 0.025% collagenase in L-15 for 30 min. Oocytes were subsequently washed with L-15, and stained with SYBR green to ensure total defolliculation.

3.3.3.7. Co-Immunoprecipitation

Frog oocytes expressing the different aquaporin constructs were homogenized in RIPA buffer as above, and an ~10% aliquot of the supernatant was collected as "input" and mixed with 2 × Laemmli sample buffer with protease inhibitors. The remaining supernatant was mixed with 50 µl of activated G-protein beads (PureProteome Protein A/G Mix Magnetic Beads, Millipore #LSKMAGAG), previously coupled to 5 µg of the corresponding primary antibody (either rabbit anti-seabream Aqp1ab1 or rabbit anti-FLAG), and incubated overnight with continuous mixing at 4ºC. After washing with PBS (137 mM NaCl, 2.7 mM KCl, 100 mM Na_2HPO_4, 2 mM KH_2PO_4, pH 7.4) with 0.05% Tween 20, the immunoprecipitate was eluted in 1 × Laemmli sample buffer, boiled at 95ºC for 10 min, and processed for immunoblotting.

3.3.3.8. Western Blotting

Laemmli-mixed protein extracts were subjected to 12% sodium dodecyl sulfate polyacrylamide gel electrophoresis (SDS-PAGE) and blotted onto Immuno-Blot nitrocellulose 0.2 µm membranes (Bio-Rad Laboratories, Inc.), as described previously (Chauvigné *et al*., 2013). The membranes were blocked for 1 h at room temperature in TBS (20 mM Tris, 140 mM NaCl, pH 7.6) with 0.1% Tween (TBST) containing 5% non-fat milk powder, and subsequently incubated with the primary antibodies (1:500 dilution) overnight at 4ºC. Bound antibodies were detected with horseradish peroxidase-coupled anti-rabbit IgG antibodies (Bio-Rad, #172-1019) for 1 h at room temperature. After washing in TBST, immunoreactive bands were revealed by the Immobilon™ Western chemiluminescent HRP substrate (Merck #WBKLS). In some extracts from sole ovarian follicles at different developmental stages, the intensity of the immunoreactive bands was scored by densitometry using the Quantity-One software (Bio-Rad Laboratories Inc.).

3.3.3.9. Histology

Senegalese sole ovary biopsies were fixed in Bouin's solution (75 ml saturated aqueous solution of picric acid, 25 ml formalin, and 5 ml glacial acetic acid) overnight at room temperature. Tissues were dehydrated and embedded in paraffin, and sections (8 µm) were attached to UltraStick/UltraFrost Adhesion slides (Electron Microscopy Sciences) and stained with hematoxylin and eosin, as previously described (Chauvigné *et al*., 2013).

3.3.3.10. Immunofluorescence Microscopy

X. laevis oocytes and sole ovarian pieces were fixed for 6 h with 4% paraformaldehyde paraformaldehyde (PFA), dehydrated and embedded in paraplast. Sections of 7 µm in thickness were further attached to UltraStick/UltraFrost Adhesion slides and rehydrated before permeabilization with 0.1% Triton X-100 in PBS for 20 min. Sections were then blocked with 5% goat serum and 0.1% BSA in PBST (PBS with 0.1% Tween 20) for 1 h, and subsequently incubated with the primary antibodies diluted at 1:400 in PBS overnight at 4°C in a humidified chamber. For the colocalization of the WT aquaporins and HA-tagged splice forms in *X. laevis* oocytes, SaAqp1ab1-WT was detected with a custom-made specific rabbit antibody (Ferré *et al*., 2023a), while FLAG-tagged HhAqp1ab1-WT and SseAqp1ab2-WT were detected with a rabbit or mouse anti-FLAG antibody. All the splice forms were detected with a goat anti-HA antibody. For the colocalization of the channels with PDI, we combined the previous antibodies with a rabbit anti-PDI. After washing with PBS, the sections were incubated with a sheep anti-rabbit IgG coupled with Cy3 (Merck #C2306), and with either goat anti-mouse IgG Alexa Fluor 488 (Invitrogen #A-11001) or donkey anti-goat IgG Alexa Fluor 488 (Invitrogen # A-11055), both diluted at 1:800 in PBS for 1 h. To colocalize PDI with SaAqpa1ab1-WT, we first performed PDI detection with the rabbit anti-PDI and the sheep anti-rabbit Cy3-coupled secondary antibody, and after fixing with PFA for 1 h, slides were incubated with the SaAqp1ab1 antibody previously labeled with Zenon™ Rabbit IgG Alexa Fluor™ 488 Labeling Kit (Invitrogen, #Z25302) following manufacturer instructions. After 1 h, sections were washed and fixed again with PFA for 15 min. In some experiments, the plasma membrane and nuclei were counterstained with WGA Alexa Fluor® 647 conjugate (Life Technologies Corp. #W32466, dilution 1: 10000) and DAPI (Merck #G8294, dilution 1: 5000), respectively. Control sections for the immunolocalization of Aqp1ab2 and Aqp1ab2_v1 in sole ovaries were incubated with

antibodies previously preadsorbed with 5-fold excess of their respective immunizing peptides for 1 h at 37ºC. Finally, all sections were mounted with fluoromount aqueous mounting medium (Merck #F4680), and immunofluorescence was observed and documented with a Zeiss Axio Imager Z1/ApoTome fluorescence microscope (CarlZeiss Corp.).

3.3.3.11. Statistics

All statistical analyses were performed with GraphPad Prism v10.0.2 (232) (GraphPad Software). Comparisons between two independent groups were made by the two-tailed unpaired Student's *t*-test, or by the nonparametric Mann Whitney U test in case of non-normal distribution. The statistical significance among multiple groups was analyzed by one-way ANOVA, followed by the Tukey's multiple comparison test, or by the non-parametric Kruskal-Wallis test and further Dunn's test for nonparametric *post hoc* comparisons. Statistical significance was accepted at $p \leq 0.05$. Data are expressed as mean ± standard error of means (SEM).

3.3.4. Results

3.3.4.1. Reverse-Transcriptase (RT)-PCR Reveals New mRNA Isoforms of Teleost Aqp1ab Channels

The *aqp1ab1* and *aqp1ab2* genes in the TSA1C are closely juxtaposed downstream of the *aqp1aa* gene and consist of four exons that in modern euacanthomorph species typically span 1.5-3 kb (figure 1A-C). To investigate whether teleosts express isoforms of these channels, we carried out a RT-PCR screening of selected adult tissues, including the ovary, in three representative marine pelagophil species, the spariform gilthead seabream (*Sparus aurata*), and the pleuronectiforms (flatfishes) Atlantic halibut (*Hippoglossus hippoglossus*) and Senegalese sole (*Solea senegalensis*), followed by DNA Sanger sequencing. For this analysis, we employed species- and paralog-specific oligonucleotide primers mapping to exon 2 and 3' UTR (*aqp1ab1*) or exon 2 and 4 (*aqp1ab2*) (figure 1A-C). In the seabream, the canonical *aqp1ab1* transcript and two other longer variants, designated as *aqp1ab1_v1* and *aqp1ab1_v2*, were amplified in the tissues tested, whereas only one mRNA corresponding to the canonical *aqp1ab2* was detected (figure 1D). The seabream

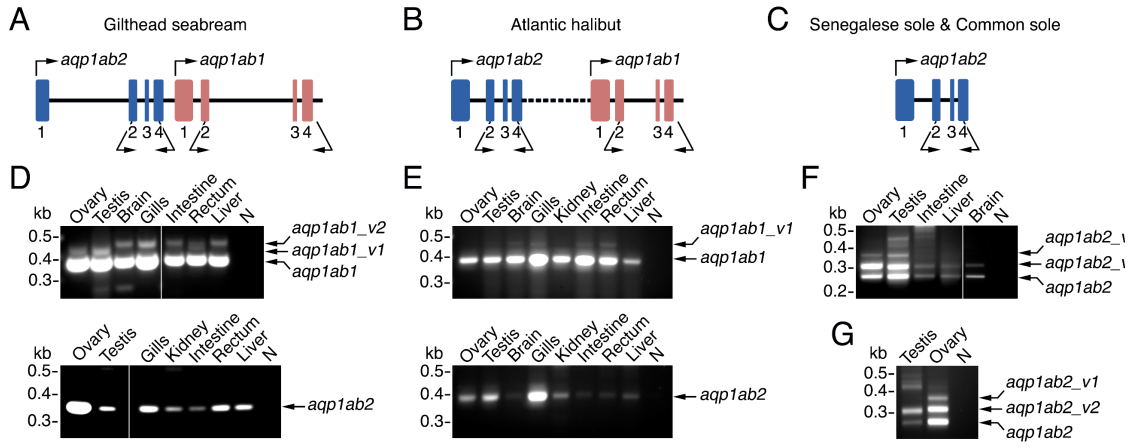

Figure 1. Identification of *aqp1ab1* and *aqp1ab2* alternative splicing in teleosts. (**A-C**) Genomic organization of tandemly arranged *aqp1ab2* and *aqp1ab1* genes in seabream (A) and Atlantic halibut (B), and of the single *aqp1ab2* gene in Senegalese sole and Common sole (C). The four exons (1-4) of both genes are represented by blue and red boxes, and the start codons are indicated by upper arrows. Lower arrows indicate the position of the oligonucleotide primers used for RT-PCR. (**D-E**) Representative RT-PCR analysis of *aqp1ab1* and *aqp1ab2* expression in different adult tissues from seabream (D) and halibut (E). A single *aqp1ab2* mRNA species is expressed in seabream and halibut, whereas two or one splice variants (*aqp1ab1_v1* and *aqp1ab1_v2*) in addition to *aqp1ab1* are detected, respectively, as indicated. (**F-G**) RT-PCR of *aqp1ab2* expression in Senegalese sole (F) and Common sole (G) where two splice forms (*aqp1ab2_v1* and *aqp1ab2 _v2*) in addition to *aqp1ab2* are amplified in the ovary and testis. In D-G, the sizes (kb) of molecular markers are indicated on the left.

aqp1ab1_v1 was detected in the ovary, testis and rectum, while the *aqp1ab1_v2* was present in the brain, gills, intestine, rectum and liver. In both cases, however, the expression levels of both transcript variants were much lower than those of the canonical transcript as judged by the relative intensities of the PCR products. Similarly, in Atlantic halibut, both canonical *aqp1ab1* and *aqp1ab2* transcripts could be amplified in all the tissues analyzed, while one additional *aqp1ab1_v1* longer mRNA was detected at low levels in the brain, gills, intestine and rectum (figure 1E). However, in the Senegalese sole, where *aqp1ab1* is absent in the TSA1C and a single *aqp1ab2* gene exists, two *aqp1ab2* mRNA variants longer that the canonical transcript were detected (figure 1F). One of these isoforms (*aqp1ab2_v1*) was less expressed than the canonical transcript and was specific to the ovary and testis, while the other (*aqp1ab2_v2*) was equally or more abundantly expressed than the canonical transcript, and was amplified in all the tissues analyzed. Interestingly, both *aqp1ab2* variants were also detected in the ovary of the congener common sole (*S. solea*) (figure 1G).

The full-length cloning and sequencing of the different aquaporin transcript variants revealed that seabream *aqp1b1_v1* and *aqp1ab1_v2* could potentially produce smaller Aqp1ab1 proteins (182 and 123 amino acids, respectively) than the canonical wild-type channel (SaAqp1ab1-WT, 267 amino acids), as a result of the in-frame addition of sequence fragments from intron 1 or 2, which introduce early stop codons and the production of

truncated proteins missing exons 3 and 4 (SaAqp1ab1_v1) or exons 2, 3 and 4 (SaAqp1ab1_v2) (figure 2A and D). Likewise, the Atlantic halibut *aqp1ab1_v1* mRNA includes an in-frame fragment of intron 3 after exon 3, resulting in the addition of a premature stop codon that would produce a shorter protein of 225 amino acids (HhAqp1ab1_v1), missing the complete exon 4, with respect to the HhAqp1ab1-WT (269 amino acids) (figure 2B and E). In contrast, the Senegalese sole *aqp1ab2_v1* mRNA showed an in-frame addition of a proximal sequence of intron 2 after exon 2, which results in a larger

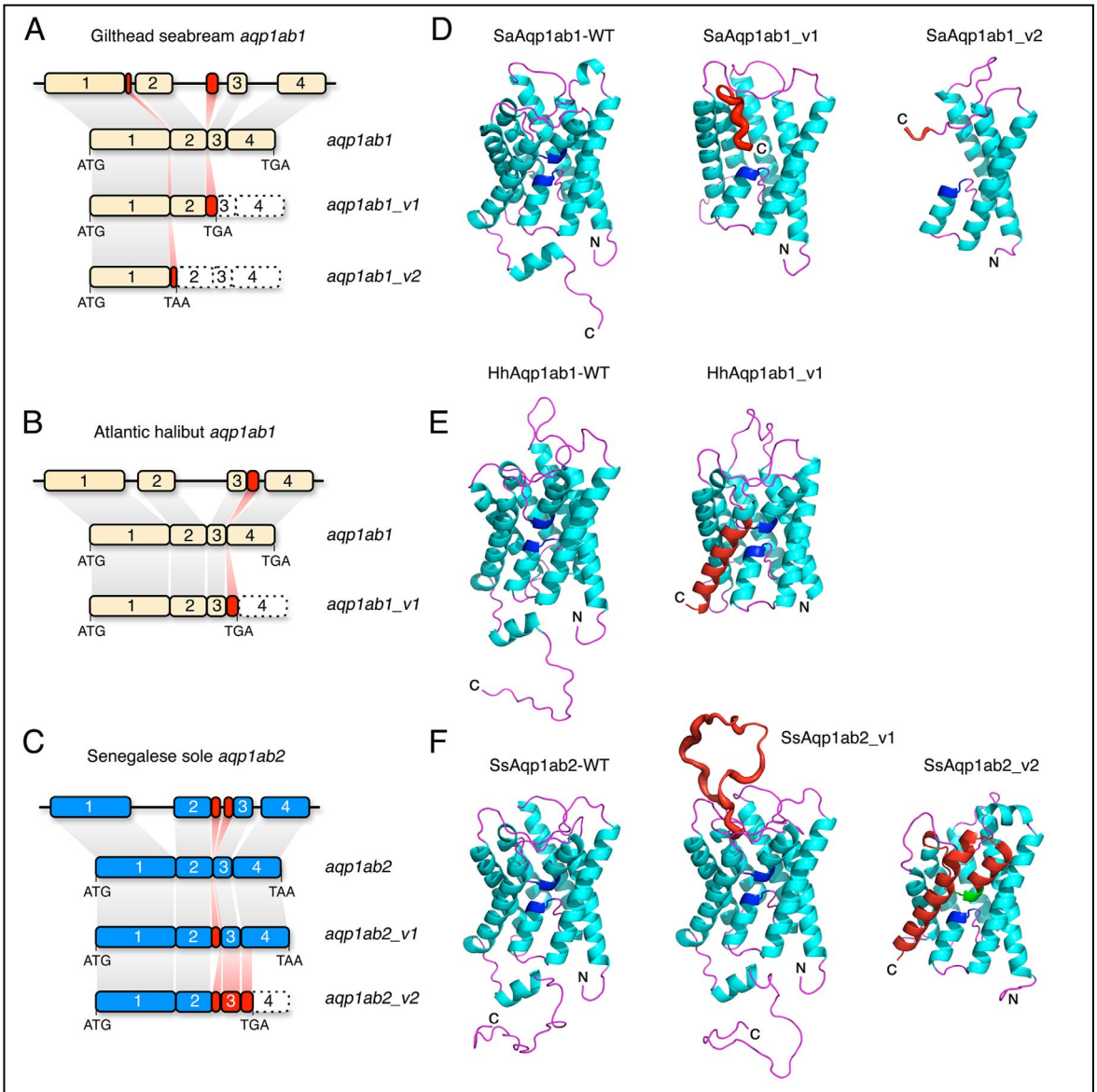

Figure 2. Model-based structure of teleost Aqp1ab1 and Aqp1ab2 and splice variants. (**A-C**) Schematic diagram of the seabream and halibut aqp1ab1 and sole aqp1ab2 genes, and the different emerging transcript variants identified in each species. The numbers represent the exons, and the initiation and stop codons in each mRNA are indicated. (**D-F**) Integral membrane views (cartoon renders) of the wild type and variant channels. Canonical transmembrane domains are shown in cyan, loops in magenta and the two conserved Asn-Pro-Ala (NPA) motifs in dark blue. Variant regions are shown in red. In sole Aqp1ab2_v2 (C and F), the splicing of the distal region of intron 2 causes out-of-frame readthrough of exon 3 and the spliced exon 4 resulting in a premature stop codon and the truncated protein.

protein with an extended extracellular loop E and four intact exons (SsAqp1ab2_v1) with respect to the SsAqp1ab2-WT (300 and 266 amino acids, respectively (figure 2C and F). The sole *aqp1ab2_v2* variant showed the addition of a distal sequence of intron 2 also after exon 2, but in this case there is a frame change that continues through exon 3 and the beginning of exon 4 to end in a premature stop codon. This results in a smaller protein (SsAqp1ab2_v2) of 221 amino acids missing most of exon 4 (figure 2C and F).

3.3.4.2. Functional Characterization of Aqp1ab1 and Aqp1ab2 Isoforms and Protein Subcellular Localization

The *in silico* three-dimensional structural analyses of the predicted Aqp1ab1 and Aqp1ab2 isoforms suggested that some of these variants had the general transmembrane helix structure intact (figure 2D, E and F). Therefore, we next investigated whether the different aquaporin isoforms could be functional using *Xenopus laevis* oocytes as an expression system. For this purpose, oocytes were injected separately with cRNAs coding for WT SaAqp1ab1, HhAqp1ab1 or SsAqp1ab2 channels, their splice isoforms, or with water as negative controls, and subsequently submitted them to swelling assays. Since Aqp1ab2 can only traffic to the frog oocyte plasma membrane when it is bound to the teleost-specific YwhazLb protein in the presence of the intracellular cAMP activator forskolin (FSK) (Ferré *et al*., 2023a), oocytes injected with SsAqp1ab2-WT or its isoforms were also coinjected with Atlantic halibut YwhazLb cRNA and exposed to FSK for 1 h prior to the determination of oocyte swelling. Oocytes expressing SaAqp1ab1-WT or HhAqp1ab1-WT showed a 5.2- and 5.6-fold increase in osmotic water permeability (P_f), respectively, with respect to the control oocytes after a hyposmotic challenge (figure 3A and B), whereas oocytes injected with SsAqp1ab2-WT showed a P_f increment of ~4 times (figure 3C). However, with respect to the controls, oocytes expressing each of the seabream and halibut Aqp1ab1 or sole Aqp1ab2 isoforms did not show an increment of the oocyte P_f (figure 3A-C).

To visualize the cellular distribution for each aquaporin isoform in *X. laevis* oocytes, and evaluate the possible mistargeting of these channels to the plasma membrane, oocytes were injected with untagged SaAqp1ab1-WT, FLAG-tagged HhAqp1ab1-WT or SsAqp1ab2-WT, or human influenza hemagglutinin (HA)-tagged splice variants. Previous experiments showed that the Flag tag does not affect the function of the HhAqp1ab1 and

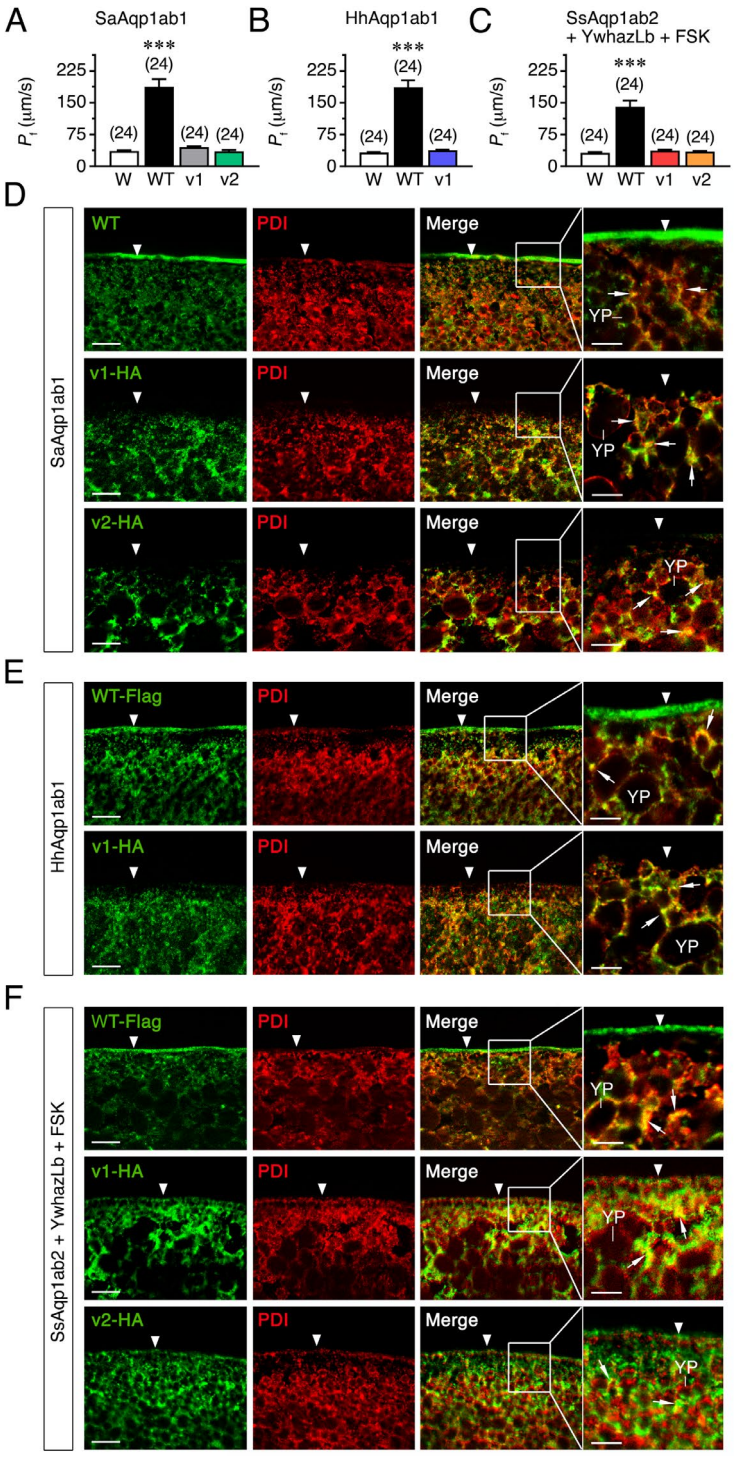

Figure 3. Functional characterization and subcellular localization of teleost wild-type Aqp1ab1 and -1ab2 and their splice variants. (**A-C**) P_f of *X. laevis* oocytes injected with water (W, controls) or expressing seabream SaAqp1ab1-WT, SaAqp1ab1_v1 or SaAqp1ab1_v2 (A), Atlantic halibut HhAqp1ab1-WT or HhAqp1ab1_v1 (B), or sole SsAqp1ab2-WT, SsAqp1ab2_v1 or SsAqp1ab2_v2 (C). Oocytes injected with SsAqp1ab2-WT or splice forms were co-injected with halibut YwhazLb and exposed to FSK for 1 h prior to the swelling assay. The data are the mean ± SEM (*n* indicated above each bar) and were statistically analyzed by an unpaired Student's *t*-test (***, $P < 0.001$; with respect to controls). (**D-F**) Double immunostaining of oocytes expressing untagged SaAqp1ab1-WT or HA-tagged SaAqp1ab1_v1 or HA-SaAqp1ab1_v2 (D), Flag-tagged HhAqp1ab1-WT or HA-tagged HhAqp1_v1 (E), or Flag-tagged SsAqp1ab2-WT or HA-tagged SsAqp1ab2_v1 or HA-SsAqp1ab2_v2 (F), and the ER marker protein disulfide isomerase (PDI). The plasma membrane is indicated by an arrowhead, whereas the co-localization of aquaporin channels and PDI in the cytoplasm is indicated by arrows. Scale bars, 10 µm (insets 5 µm).

SsAqp1ab2 channels (supplementary figure S1, see Annexes, page 279). Subsequently, we carried out double immunostaining using paralog-specific (SaAqp1ab1), or anti-FLAG (HhAqp1ab1 and SsAqp1ab2) or anti-HA (splice forms) antibodies, together with antibodies against the ER marker protein disulfide isomerase (PDI). These experiments showed that seabream and halibut Aqp1ab1-WT polypeptides were constitutively expressed at the oocyte plasma membrane, whereas their respective HA-SaAqp1ab1_v1, HA-SaAqp1ab1_v2 and HA-HhAqp1ab1_v1 isoforms only displayed intracellular staining (figure 3D and E). These channel isoforms colocalized with the PDI, suggesting their impaired sorting from the ER to the frog oocyte plasma membrane (figure 3D and E). In the presence of YwhazLb and FSK, the Flag-SsAqp1ab2-WT was also targeted to the plasma membrane, and most of the HA-SsAqp1ab2_v1 and HA-SsAqp1ab2_v2 signals colocalized with PDI in the cytoplasm (figure 3F), as observed for the seabream and halibut aquaporin isoforms. However, HA-SsAqp1ab1_v1 and HA-SsAqp1ab2_v2 staining was also detected in the oocyte plasma membrane (figure 3F), suggesting that the sole isoforms were not completely sequestered in the ER.

3.3.4.3. Aqp1ab-Type Protein Isoforms Display Different Mechanisms of Dominant-Negative Inhibition of the Canonical Channels

The previous immunolocalization data suggested that the identified aquaporin isoforms could have dominant-negative effects on cell surface expression of the full-length Aqp1ab proteins, and therefore impair channel function. To investigate this possibility, we expressed untagged SaAqp1ab1-WT, HhAqp1ab1-WT or SsAqp1ab2-WT, alone or in combination with different amounts of their respective non-tagged isoforms, in *X. laevis* oocytes, and subsequently determined the P_f. Water fluxes in oocytes expressing SaAqp1ab1-WT with increasing amounts of SaAqp1ab1_v1 or SaAqp1ab1_v2, in ratios from 0.5 to 50 (isoform:WT), were reduced in a dose-dependent manner up to 71 ± 3% and 57 ± 4%, respectively, with respect to oocytes expressing the SaAqp1ab1-WT alone (figure 4A). Similar coexpression results were observed for the HhAqp1ab1_v1 isoform, although in this case the P_f of oocytes coexpressing HhAqp1ab1_v1 and HhAqp1ab1-WT in ratios from 0.05 to 50 was inhibited up to 94 ± 4% with respect to oocytes injected with the canonical channel only (figure 4B). Finally, water permeability of oocytes expressing SsAqp1ab2-WT plus YwhazLb and treated with FSK was also disrupted by coexpression with the SsAqp1ab2_v1

or SsAqp1ab2_v2 isoforms, the P_f being highly inhibited (91 ± 3% and 84 ± 3%, respectively) already after injecting equal cRNA amounts of SsAqp1ab1-WT and channel variants (figure 4C). These data indicated that the SsAqp1ab2 variants were ~40 times more inhibitory than the Aqp1ab1-type isoforms on the respective canonical channels. However, when SaAqp1ab1 and HhAqp1ab1 were coexpressed with YwhazLa and exposed to FSK, which increases the trafficking of these channels to the oocyte plasma membrane (Ferré *et al.*, 2023a), the P_f of oocytes was incremented, resulting in the enhancement of the percentage of inhibition produced by their respective splice forms (figure 4D). Since in native seabream oocytes SaAqp1ab1 binds YwhazLa (Ferré *et al.*, 2023a), these observations suggest that Aqp1ab1-type channels are more sensitive to low levels of splice variant coexpression under *in vivo* conditions, as observed for SsAqp1ab2.

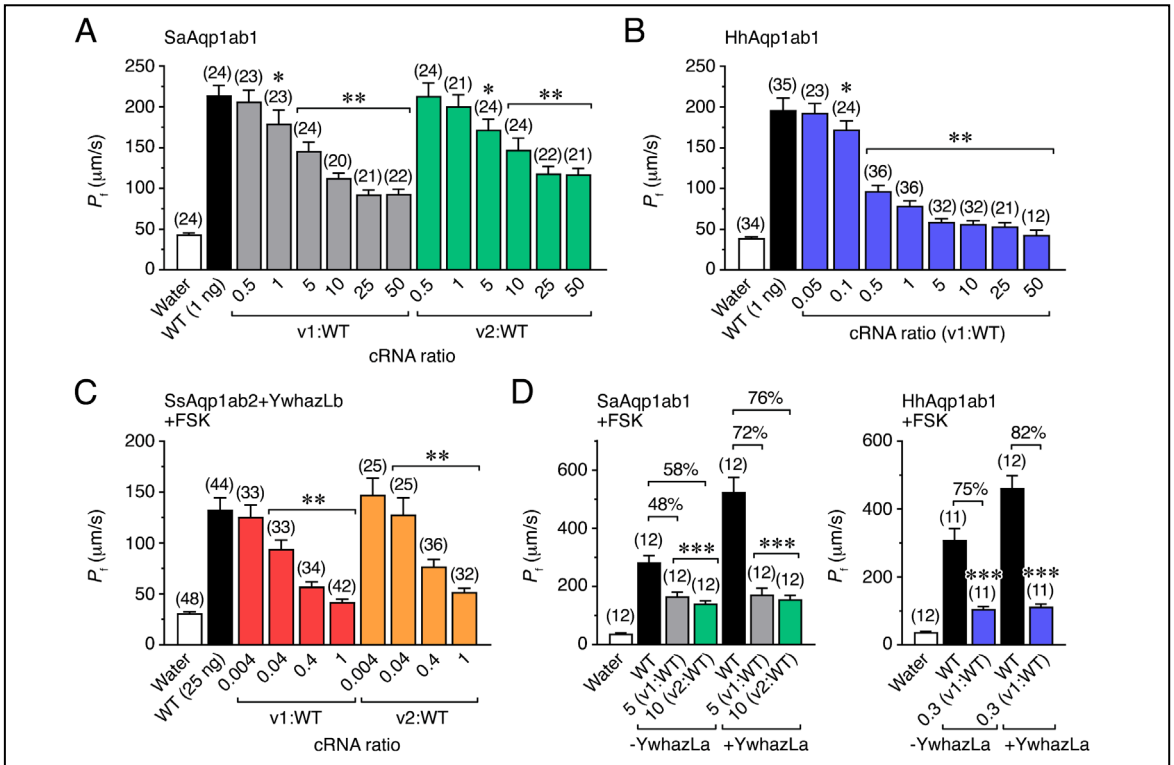

Figure 4. The dominant-negative activity of teleost Aqp1ab1 and -1ab2 splice forms. (**A-C**) Changes in P_f of *X. laevis* oocytes injected with water or expressing SaAqp1ab1-WT (A), HhAqp1ab1-WT (B) or SsAqp1ab2-WT (C) alone or in combination with different amounts of the isoforms of each paralog. For SsAqp1ab2-WT and splice forms, oocytes were co-injected with halibut YwhazLb and exposed to FSK. (**D**) Effect of the inhibition of the oocyte P_f by the different Aqp1ab1 splice forms, at a concentrations that produced approximately half-maximal reduction (as observed in A-C), in SaAqp1ab1 or HhAqp1ab1 expressing oocytes in the presence or absence of YwhazLa, and exposed to FSK. The percentage of P_f inhibition elicited by each isoform under the two conditions is indicated in each plot. In all panels, data are the mean ± SEM (*n* indicated above each bar) and were statistically analyzed by an unpaired Student's *t*-test (*, $P < 0.05$: **, $P < 0.01$; ***, $P < 0.001$; with respect to oocytes injected with the WT form alone).

To determine whether any of the Aqp1ab variants could physically interact with the respective canonical proteins and misroute their trafficking, we next performed double immunostaining of WT channels and their isoforms in oocytes expressing tagged constructs as above, followed by immunoblotting and co-immunoprecipitation experiments. Immunofluorescence analyses showed that SaAqp1ab1-WT and Flag-HhAqp1ab1-WT were both targeted to the plasma membrane, whereas in the presence of HA-SaAqp1ab1_v1 or HA-SaAqp1ab1_v2, or HA-HhAqp1ab1_v1, respectively, the expression of the WT channels was reduced in the oocyte surface, and the proteins colocalized with their respective isoforms within intracellular compartments (figure 5A and B) compatible with ER as seen in previous experiments. Immunoblotting of total and plasma membrane extracts of oocytes confirmed the absence of plasma membrane localization of the HA-SaAqp1ab1_v1 or HA-SaAqp1ab1_v2, and HA-HhAqp1ab1_v1 isoforms, as well as the reduction of the relative amounts of SaAqp1ab1-WT and Flag-HhAqp1ab1-WT in the oocyte surface when coexpressed with their respective channel variants (figure 5D and E). Co-immunoprecipitation trials using a SaAqp1ab1-specific antiserum and a FLAG antibody (for HhAqp1ab1-WT) corroborated the interaction of the WT channels with their respective isoforms in the intracellular compartments (figure 5G and H). These analyses also revealed that the interaction of SaAqp1ab1-WT with HA-SaAqp1ab1_v1, and that of Flag-HhAqp1ab1-WT with HA-HhAqp1ab1_v1, were associated with a decrease of the amount of the WT proteins in the oocyte total membrane fraction (figure 5D and E) This suggested that multimeric complexes formed by the full-length and truncated isoforms are probably retained in the ER because they are incorrectly assembled and rapidly targeted for degradation. However, the complex formed by SaAqp1ab1-WT and HA-SaAqp1ab1_v2 appeared to be more stable, since the expression of the WT channel in the total membrane fraction of oocytes was not clearly affected by this truncated variant (figure 5D).

In contrast to the seabream and halibut Aqp1ab1 channel variants, immunofluorescence and immunoblotting data indicated that the HA-SsAqp1ab2_v1 isoform with an extended extracellular E loop was targeted to the oocyte plasma membrane (figure 5C), and did not affect the protein expression levels of the canonical channel (figure 5F). However, the accumulation of the WT protein in the plasma membrane appeared to decline in the presence of high amounts of HA-SsAqp1ab2_v1 (figure 5F), suggesting the progressive substitution of the WT channel by the inactive variant in multimeric tetramers

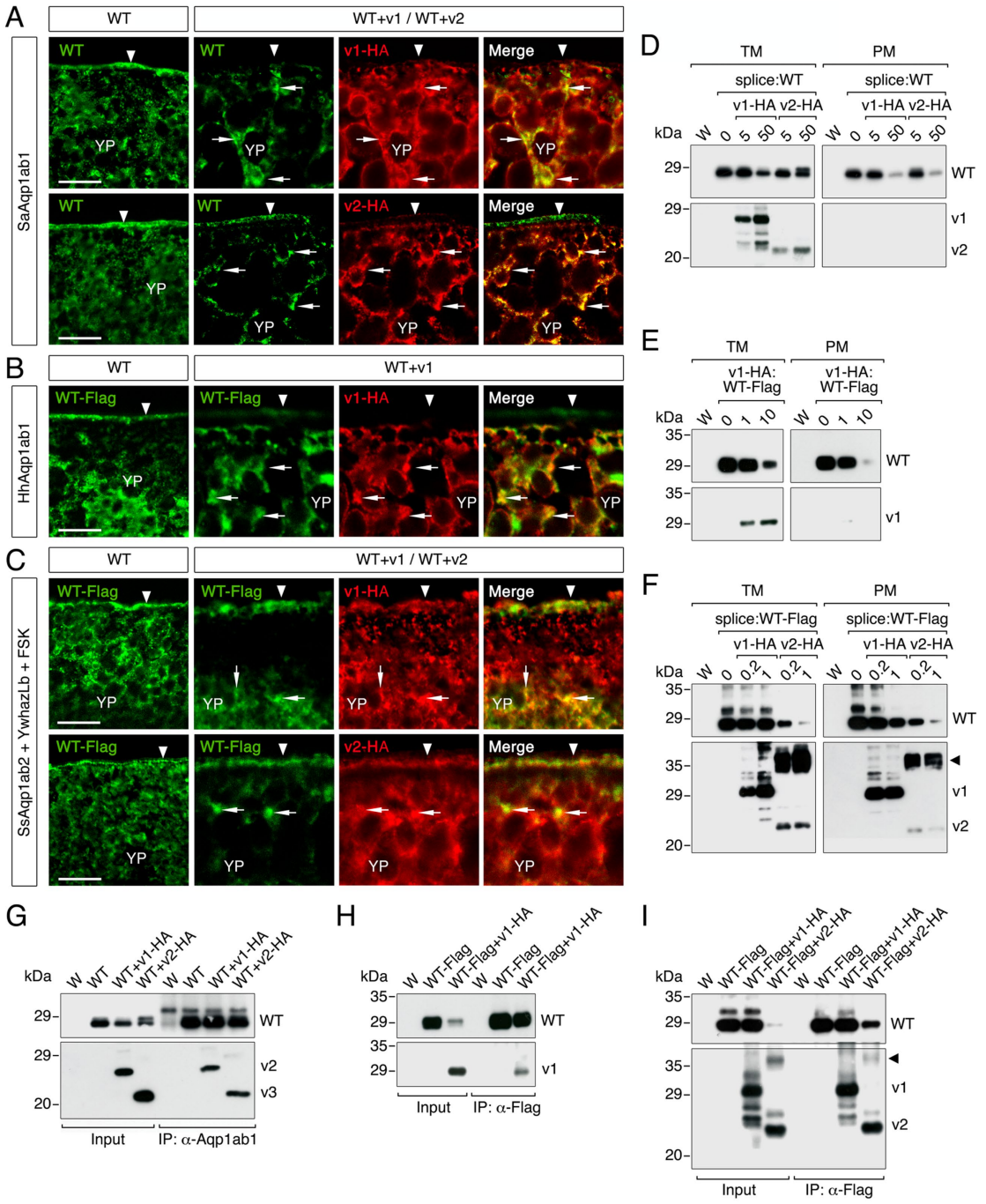

Figure 5. Teleost Aqp1ab1 and -1ab2 splice forms generate distinct mechanisms of dominant-negative repression. (**A-C**) Double immunolocalization of SaAqp1ab1-WT, Flag-tagged HhAqp1ab1-WT or Flag-tagged SsAqp1ab2-WT (green) with the respective HA-tagged splice forms in *X. laevis* oocytes as indicated. Oocytes expressing SsAqp1ab2-WT and splice forms were co-injected with halibut YwhazLb and exposed to FSK. In all panels, the plasma membrane is indicated by an arrowhead, whereas the co-localization of WT aquaporins and splice forms is indicated by arrows. Scale bars, 10 µm. (**D-F**) Representative immunoblots of total (TM) and plasma (PM) membrane protein extracts from oocytes injected with water (W) or co-expressing the different aquaporin WT channels with increasing amounts of the splice forms as indicated. (**G-I**) Illustrative immunoblots of precipitated proteins from oocytes treated as in A-C using anti-SaAqp1ab1 or anti-Flag (for HhAqp1ab1 and SsAqp1ab2) antibodies, and revealed with antibodies against SaAqp1ab1, Flag or HA. In D-I, upper blots were probed with SaAqp1ab1 (D and G) or Flag (E, F, H and I) antibodies, whereas in all panels the lower blots were probed with HA antibodies. Molecular mass markers (kDa) are on the left. The arrowhead in F and I indicate potential post-translational modifications of the SsAqp1ab1 v2 isoform.

(figure 5I), which remain correctly assembled and are thus targeted to the oocyte surface. Interestingly, the HA-SsAqp1ab2_v2 isoform was highly post-translationally modified and also targeted to the oocyte plasma membrane, despite the truncated nature of this variant compared to the canonical channel (figure 5C and F). In this case, however, interaction of HA-SsAqp1ab2_v2 with the Flag-SsAqp1ab2-WT induced the decrease of both the total and plasma membrane amounts of the WT channel (figure 5F and I), suggesting that these complexes can partially escape from the ER and traffic to the oocyte surface.

3.3.4.4. Expression Pattern of Senegalese sole Aqp1ab2 Isoforms during Ovarian Follicle Growth and Maturation *In Vivo*

To investigate the physiological relevance of the Aqp1ab2 variants in Senegalese sole, we determined the *in vivo* dynamics of the endogenous channels during oocyte growth and maturation. For this purpose, two affinity-purified antibodies were prepared by immunizing rabbits with two synthetic peptides, one corresponding to a region from loop A conserved amongst the three SsAqp1ab2 proteins (α-Aqp1ab2-Nt), and another to a specific sequence of the SsAqp1ab2_v1 variant in loop E (α-Aqp1ab2_v1) (figure 6A). The specificity of the antibodies was tested by Western blot analysis on total membrane protein extracts from *X. laevis* oocytes expressing SsAqp1ab2-WT, SsAqp1ab2_v1 or SsAqp1ab2_v2 separately. The results showed that the α-Aqp1ab2-Nt specifically recognized the three SsAqp1ab2 polypeptides, whereas the α-Aqp1ab2_v1 only reacted with the SsAqp1ab2_v1 protein product (figure 6B). The antibodies revealed immunoreactive bands of ~28 kDa, ~32 kDa and ~24 kDa, thus approximately of the same molecular masses of the SsAqp1ab2-WT, SsAqp1ab2_v1 or SsAqp1ab2_v2 monomers predicted *in silico* (28.5, 32.2 and 23.6 kDa, respectively).

The changes in protein expression of the three SsAqp1ab2 variants were estimated by immunoblotting in isolated ovarian follicles at different developmental stages using both of the generated antisera. The stages analyzed were: previtellogenic; follicles enclosing oocytes at the primary growth and cortical alveoli stages; vitellogenic follicles, with oocytes filled with yolk granules containing vitellogenin-derived yolk proteins; hydrating follicles, with oocytes undergoing meiotic maturation and hydration; mature, follicle-enclosed oocytes that resumed meiosis and hydration; and ovulated eggs, free of the surrounding follicle cells (figure 6C). The α-Aqp1ab2-Nt detected the protein products for all three SsAqp1ab2

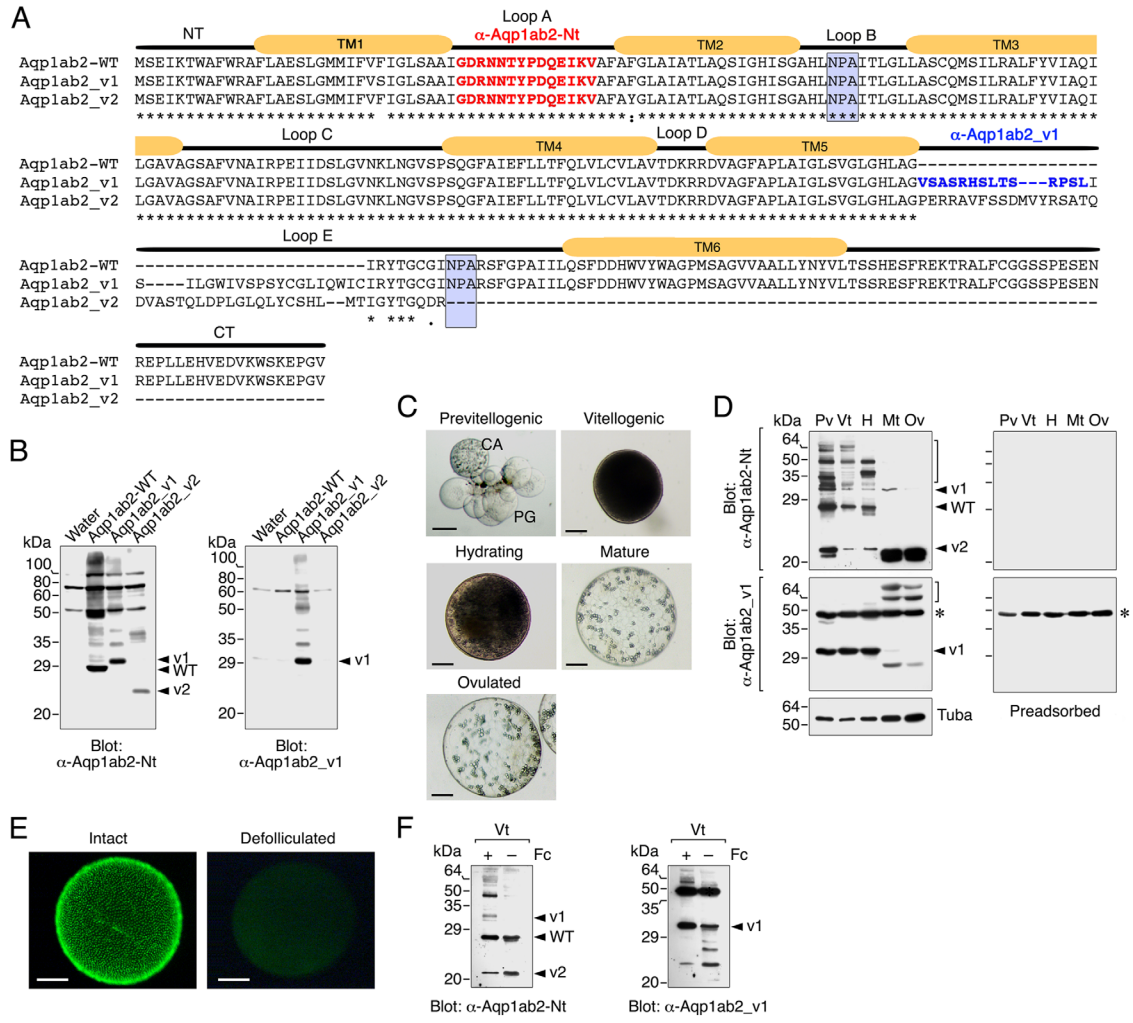

Figure 6. Production of Senegalese sole total Aqp1ab2 and Aqp1ab2_v1 specific antisera and immunoblot analysis of Aqp1ab2 splice variants protein expression in developing ovarian follicles. (**A**) Amino acid sequence alignment of SsAqp1ab2-WT, SsAqp1ab2_v1 and SsAqp1ab2_v2 splice forms highlighting the sequences employed for the production of the sole-specific Aqp1ab2 and Aqp1ab2_v1 antibodies (α-Aqp1ab2-Nt and α-Aqp1ab2_v1, in red and blue color, respectively). The N- and C-termini of the WT channel, the six transmembrane helices (TM1-TM6) and the two conserved NPA motifs are also indicated. (**B**) Immunoblots of *X. laevis* oocytes injected with water or expressing Aqp1ab2-WT, SsAqp1ab2_v1 or SsAqp1ab2_v2 and probed with the α-Aqp1ab2-Nt or α-Aqp1ab2_v1 antisera separately. (**C**) Representative photomicrographs of sole ovarian follicles at different developmental stages during oocyte growth and maturation. PG, primary growth stage; CA, cortical alveoli stage. Scale bars, 50 and 250 µm. (**D**) Immunoblots of Aqp1ab2-WT, Aqp1ab2_v1 and Aqp1ab2_v2 in protein extracts from previtellogenic (Pv), vitellogenic (Vt), hydrating (H) and mature (Mt) follicle-enclosed oocytes, as well as from ovulated oocytes (Ov), using the generated antisera. Alpha tubulin (Tuba) was used as loading control. Duplicated blots (right) were run in parallel and incubated with the primary antibodies preadsorbed by the antigenic peptide to test for specificity. The brackets indicate potential post-translational modifications. (**E**) Hoechst staining of intact vitellogenic follicles and defolliculated oocytes. Scale bar, 100 µm. (**F**) Immunoblots of Aqp1ab2 isoforms in total protein extracts from intact or defolliculated vitellogenic follicles (+/- follicle cells, Fc). In B, D and E, the arrowheads indicate aquaporin monomers, whereas the asterisks in D and E indicate cross-reactive polypeptides revealed with the Aqp1ab2_v1 antiserum. In all blots, molecular mass markers (kDa) are on the left.

variants in protein extracts from follicles in most developmental stages, which were identified by their apparent molecular mass (figure 6D, upper left panel). However, several higher molecular bands were also revealed at the previtellogenic, vitellogenic and hydrating stages, which could represent post-translational modifications of the channels, since these

bands, as well as those corresponding to the monomers, were no longer detected after the preadsorbtion of the antibody with the immunizing peptide (figure 6D, upper right panel). The relative amounts of the SsAqp1ab2-WT slightly decreased from the previtellogenic to the hydrating stage, whereas those of the SsAqp1ab2_v1 and SsAqp1ab2_v2 variants showed a more drastic reduction during the same developmental stages (figure 6D, upper left panel). In the mature and ovulated samples, SsAqp1ab2-WT immunoreactivity was no longer detected, while that of SsAqp1ab2_v1 also disappeared but only in ovulated eggs. In contrast, the SsAqp1ab2_v2 signal intensity strongly increased in both mature and ovulated eggs (figure 6D, upper left panel).

The α-Aqp1ab2_v1-specific antibody revealed two major immunoreactive bands, one of ~32 kDa, approximately matching the molecular mass of the SsAqp1ab2_v1 isoform, and another of ~49 kDa, the intensity of which did not change throughout the different follicular stages (figure 6D, lower left panel). The cross-adsorption of the antibody with its antigenic peptide eliminated the SsAqp1ab2_v2 corresponding band, but not the 49-kDa reactive band, indicating that the latter corresponds to a cross-reactive protein present in the sole ovarian follicles (figure 6D, lower right panel). The SsAqp1ab2_v1 immunoreactivity in the follicular extracts did not change from the previtellogenic to the hydrating stage, but it was no longer detected in mature and ovulated eggs (figure 6D, lower left panel). Instead, at these later stages, secondary reactive bands of higher and lower molecular masses than the predicted monomer were revealed (figure 6D, lower left panel). These new bands could correspond to complex post-translational modifications and degradation products of SsAqp1ab2, respectively.

In our recent studies, we found that the seabream Aqp1ab2 paralog is not only expressed in the oocyte but also in the surrounding follicle cells (Ferré *et al*., 2023a and b). To assess whether the sole Aqp1ab2 and channel variants are expressed in the oocyte, we carried out immunoblotting of protein extracts from isolated intact vitellogenic ovarian follicles and defolliculated oocytes using the α-Aqp1ab2-Nt and α-Aqp1ab2_v1 antisera (figure 6E). In agreement with the previous data, SsAqp1ab2-WT, SsAqp1ab2_v1 and SsAqp1ab2_v2 protein products were detected in extracts from intact follicles with the α-Aqp1ab2-Nt antibody, while in defolliculated oocytes the SsAqp1ab2_v1 isoform was not revealed (figure 6F, left panels). In contrast, using the α-Aqp1ab2_v1-specific antiserum, the SsAqp1ab2_v1 variant became visible in both intact follicles and defolliculated oocytes

(figure 6F, right panels), suggesting that this antiserum is able to detect lower amounts of the SsAqp1ab2_v1 isoform than the α-Aqp1ab2-Nt antibody. These data therefore corroborate that the sole Aqp1ab2 paralog and its splice variants are expressed in vitellogenic oocytes as observed for the seabream Aqp1ab2 channel.

To confirm the previous observations and investigate potential changes in the subcellular localization of SsAqp1ab2 and the SsAqp1ab2_v1 isoform in ovarian follicles during oocyte growth and maturation, we conducted immunofluorescence microscopy on sole ovarian sections containing follicles at different stages. In previtellogenic follicles containing primary growth oocytes, total SsAqp1ab2 and SsAqp1ab2_v1-specific staining was dispersed in the oocyte cytoplasm, but positive signals were also found in the developing follicle cells (figure 7A-C). When oocytes enter into secondary growth and reach the cortical

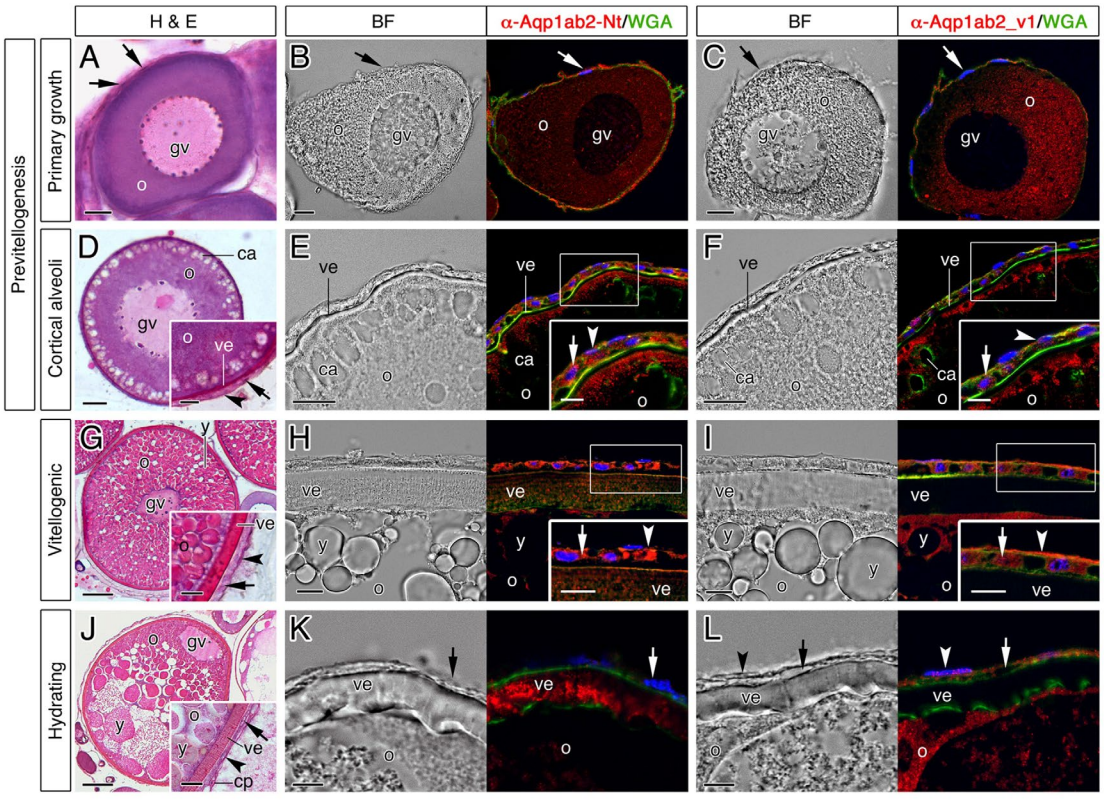

Figure 7. Immunolocalization of total Aqp1ab2 and the Aqp1ab2_v1 isoform in developing Senegalese sole ovarian follicles. (**A, D, G. J**) Representative histological sections of follicle-enclosed oocytes at previtellogenesis, including the primary growth (A) and cortical alveoli (D) stages, vitellogenic (G) and maturing and hydrating (J) stage stained with hematoxylin and eosin. (**B-C, E-F, H-I, K-L**) Bright field (BF) images and immunostaining of total Aqp1ab2 or Aqp1ab2_v1 (red) in follicles in each of the different stages using the sole-specific α-Aqp1ab2-Nt and α-Aqp1ab2_v1 antisera. Sections were counterstained with 4′,6-diamidino-2-phenylindole (DAPI; blue) and wheat germ agglutinin (WGA; green). Control sections incubated with preabsorbed antisera were negative (figure S1, see Annexes, page 279). The arrows and arrowheads, indicate granulosa and theca cells, respectively, surrounding the oocyte. Abbreviations: o, oocyte; y, yolk globule; gv, germinal vesicle; ve, vitelline envelope; cp, capillary; ca, cortical alveoli. Scale bars, 10 µm (A-D, H, I, L, K, and inset in I and L), 50 µm (G, J), 20 µm (E, F), 5 µm (inset in E and F).

alveoli stage, total SsAqp1ab2 and SsAqp1ab2_v1 immunoreactions become accumulated towards the cortical region of the oocyte just below the plasma membrane (figure 7D-F). At this stage, differentiated granulosa and theca cells also showed positive staining with both antibodies (figure 7D-F). However, in fully-grown vitellogenic follicles, while follicle cells remained labelled by either of the antisera (figure 7G-I), total SsAqp1ab2 immunostaining was observed in the oocyte plasma membrane and partially distributed along the microvilli crossing the vitelline envelope (figure 7H). In contrast, SsAqp1ab2_v1 signals remained accumulated in the oocyte cortex and plasma membrane (figure 7I). In hydrating follicles, follicle cells were either not or slightly stained with the α-Aqp1ab2 and α-Aqp1ab2_v1 antisera, respectively (figure 7J-L). In addition, total SsAqp1ab2 staining almost disappeared from the oocyte cytoplasm and became accumulated in the microvilli (figure 7K). On the contrary, that of SsAqp1ab2_v1 was detected in the cortical ooplasm but not in the oocyte plasma membrane (figure 7L). In all stages, the specificities of the immunoreactions were demonstrated by the lack of staining when the antisera were preincubated with their corresponding antigenic peptide (supplementary figure S2, see Annexes, page 280). These data therefore indicated that the expression of SsAqp1ab2 and SsAqp1ab2_v1 is not restricted to the oocyte but also occurs in follicle cells, and that the trafficking of these channels to the oocyte plasma membrane is differentially regulated during hydration.

3.3.4.5. Follicular Aqp1ab2 Isoforms Are Differentially Regulated during Sole Oocyte Maturation and Hydration *In Vivo*

To analyze whether the expression levels of the SsAqp1ab2_v1 and SsAqp1ab2_v2 isoforms in relation to those of the SsAqp1ab2-WT could be developmentally regulated, we evaluated protein abundance of the three channels in three different pools of ovarian follicles at previtellogenesis, vitellogenesis and hydration, and in mature follicles, by immunoblotting using the α-Aqp1ab2-Nt antisera. The results showed that the relative amount of SsAqp1ab2_v1 with respect to that of the WT channel progressively decreased from previtellogenesis to hydration, whereas this ratio increased by ~10 times at the maturation stage (figure 8A and B). The SsAqp1ab2_v2 to WT expression ratio also showed a decrease during vitellogenesis, but a small but significant increase was seen during hydration (figure 8A and C). However, a stronger increment (~10 times) of the amount of SsAqp1ab2_v2 with respect to that of the WT occurred at the maturation stage (figure 8A and C). Thus, low

protein expression levels of SsAqp1ab2_v1 and SsAqp1ab2_v2 during the hydration stage could facilitate SsAqp1ab2-WT trafficking to the oocyte plasma membrane and water influx, whereas the diminished SsAqp1ab2-WT protein levels in the mature follicles are likely to be the result of the negative effect of increased expression of SsAqp1ab2_v2.

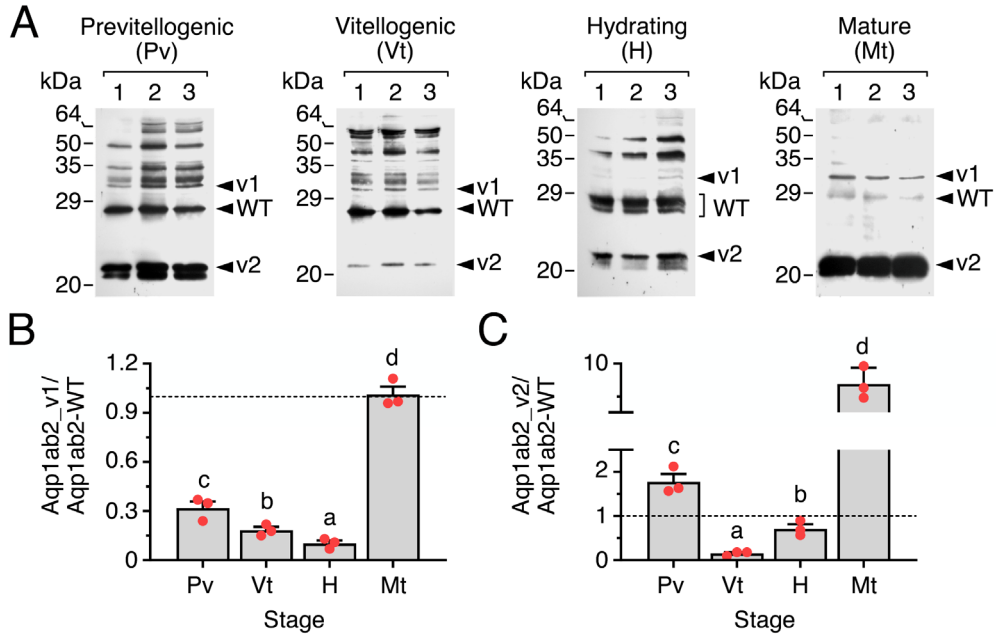

Figure 8. Differential regulation of Aqp1ab2 splice variants during ovarian follicle maturation and hydration *in vivo*. (**A**) Representative immunoblots of protein extracts from follicles at the previtellogenic, vitellogenic), hydrating, and mature stage (2.5 follicle equivalents/lane) using the α-Aqp1ab2-Nt antisera. The blots show extracts from three different pools of follicles collected from three different females. The arrowheads indicate the Aqp1ab2-WT, Aqp1ab2_v1 and Aqp1ab2_v2 proteins according to their apparent molecular masses. In all blots, molecular mass markers (kDa) are on the left. (**B**) Relative amount of the Aqp1ab2_v1 (left) and Aqp1ab2_v2 (right) isoforms with respect to the Aqp1ab2-WT at the different development stages based on the blots shown in A. Bars (mean ± SEM; $n = 3$ fish) with different superscript are statistically significant (one-way ANOVA; $P < 0.05$).

3.3.5. Discussion

In the present study, we identified five novel splice variants of *aqp1ab*-type genes from four species of marine pelagophil teleosts. For the Atlantic halibut and seabream, the splicing of intronic regions of the *aqp1ab1* genes introduces premature stop codons and thus C-terminally truncated proteins are translated. By contrast, in the Senegalese sole, the alternative in-frame splicing of the proximal second intronic region of the *aqp1ab2* gene generates an intact Aqp1ab2_v1 protein with an extended extracellular loop E, while the splicing of the distal region of the second intronic region leads to out-of-frame readthrough of exon 3 and 4 and the generation of a C-terminally truncated Aqp1ab2_v2 protein due to a premature stop codon. These *aqp1ab2_v1* and *-1ab2_v2* splice variants were also identified

in the ovary of the common sole indicating that the isoforms are at least conserved within the genera. However, in contrast to the WT Aqp1ab1 and Aqp1ab2 channels, none of the variants were found to function as water channels when expressed in *X. laevis* oocytes, indicating that their positive selection in the different species evolved for a different purpose.

An insight into this potential purpose arose from the observations that the WT channels are constitutively localized in the plasma membrane when heterologously expressed in *X. laevis* oocytes, while the seabream and halibut Aqp1ab1 splice variants are retained in the ER. Conversely, the sole Aqp1ab2 splice isoforms are targeted to the oocyte plasma membrane (Aqp1ab2_v1) or partially sequestered in the ER (Aqp1ab2_v2). By co-expressing each of the variants with the WTs and immunologically locating their proteins in the frog oocytes, it became evident that the splice variants elicit distinct mechanisms of dominant-negative inhibition of the WT channel function. Our double immunostaining and co-immunoprecipitation experiments suggest that one of these mechanisms, displayed by the three Aqp1ab1 variants and partially by the sole Aqp1ab2_v2 isoform, is gained by trapping the WT channels in the ER by hetero-oligomerization, thereby preventing their trafficking to the plasma membrane. This dominant-negative effect could be explained by the oligomeric structure of Aqp1ab1 and Aqp1ab2 tetramers, which are probably retained in the ER when they are formed by WT channels and truncated isoforms, because they are incorrectly assembled and thus targeted for degradation (De Bellis *et al*., 2014; Kamsteeg *et al*., 1999). Such a mechanism is therefore reminiscent of the dominant-negative effect caused by the truncated human AQP4-Δ4 and AQP0-Δ213 splice forms, which heterodimerize with the canonical channels to cause their retention in the ER (Varadaraj *et al*., 2008 ; De Bellis *et al*., 2014). However, our data also revealed that the sole Aqp1ab2 splice variants, which show high inhibitory efficiency, are also targeted to the plasma membrane together with the Aqp1ab2-WT channel. Due to the lack of functionality of these variants as water transporters, possibly because of altered structural domains that affect the water pore or impede the formation of functional homotetramers in the plasma membrane (Mathai and Agre, 1999), their increased trafficking to the plasma membrane results in dominant-negative repression of water permeation. These findings suggest that Aqp1ab-type splice variation in teleosts may have evolved to differentially and more efficiently regulate channel function in species that lost one of the *aqp1ab*-type genes, such as soleid fishes, which lost the *aqp1ab1* gene (Ferré *et al*., 2023a).

Currently, nothing is known concerning the physiological relevance of aquaporin splice variation in fishes. In the ovaries of seabream and halibut, the *aqp1ab1*-type variants are much lower expressed *in vivo* than the WTs, and therefore their biological significance is uncertain, although increased transcription and translation of these isoforms might occur due to stress associated with disease or in response to changes in the environment (Lee *et al*., 2021; Gómez-Redondo *et al*., 2021; Tian *et al*., 2022; Rogalska *et al*., 2023).

On the contrary, since the *aqp1ab2* splice variants are relatively highly expressed in the ovaries of soles, we aimed to determine their potential physiological significance *in vivo* during oocyte growth and maturation in the Senegalese sole. The immunological data show that sole Aqp1ab2-WT, Aqp1ab2_v1 and Aqp1ab2_v2 proteins are consistently expressed between previtellogenesis and oocyte hydration, but in fully mature and ovulated eggs the WT is strongly downregulated, while Aqp1ab2_v1 and Aqp1ab2_v2 expression continues, with levels of Aqp1ab2_v2 greatly increased. In terms of ratios to the WT, both of the splice variants show a general decrease as between previtellogenesis and hydration, but a substantial increase in the mature eggs. The immunostaining data also show that as for seabream Aqp1ab2-WT (Ferré *et al*., 2023a and b), the sole Aqp1ab2-WT and its splice variants are expressed both in the theca and granulosa cells as well as in the oocyte. However, in contrast to the Aqp1ab2-WT, which begins to enter the oocyte plasma membrane microvilli during vitellogenesis, and is almost completely translocated there during hydration, the Aqp1ab2_v1 never enters the microvillar membrane. It would thus seem apparent that the roles of the splice variants in the follicular cells would be to modulate the rate of water flow during oocyte growth via the observed dominant-negative repression mechanisms. During hydration, their presence in the oocyte is strongly reduced so as not to inhibit maximal water influx through the canonical channel, which can thus form homotetramers and be fully translocated to the membrane microvilli. For species that retain both Aqp1ab1 and Aqp1ab2 in the TSA1C, such a regulation may not be under the same selection pressure as the two channels evolved to occupy the distal and proximal regions of the oocyte microvilli, respectively, thereby avoid competitive membrane space occupancy to accelerate bulk water influx during oocyte maturation (Ferré *et al*., 2023a and b). In the seabream, the differential trafficking of the Aqp1ab-type paralogs in the oocyte is regulated via the luteinizing (Lh) hormone through a common Avp signaling pathway (Ferré *et al*., 2023b). In sole, although the downregulation of the Aqp1ab2 splice variants occurs mainly

during oocyte maturation and hydration, a process typically controlled by Lh in fishes (Lubzens *et al*., 2010), the endocrine pathway regulating the expression of these isoforms at this stage is unknown and should be investigated in the future.

In order for the hydration process to terminate and keep the acquired water within the mature egg, it has been shown that euacanthomorph teleosts evolved a C-terminal p38 MAPK site within the YwhazLa binding site of Aqp1ab1 that causes the channel to be recycled (Tingaud-Sequeira *et al*., 2008; Ferré *et al*., 2023a). However, since soleid flatfishes lack the *aqp1ab1* gene, the present data indicate that Aqp1ab2 recycling in mature oocytes is possibly promoted by increasing the levels of the Aqp1ab2_v1 and Aqp1ab2_v2 variants, which dominantly negatively enhance the degradation pathway.

Taken together, the present findings provide new evidence that euacanthomorph species of marine teleosts evolved an array of mechanisms to control aquaporin-mediated oocyte hydration. This includes the selective retention of the Aqp1ab-type channels which co-evolved subdomain phosphorylation sites with YwhazL binding proteins to differentially localize the channels in the oocyte membrane microvilli for maximal hydration (Ferré *et al*., 2023a and b). Here, we find that Aqp1ab-type splice variation adds a further layer of control through distinct mechanisms of dominant-negative regulation of channel function. This includes the inhibition of transmembrane water conductance due to the trafficking of non-functional variants to the plasma membrane, and the repression of the trafficking of the canonical channels, so that degradation pathways are enhanced. In marine pelagophil species that retain only one of the *aqp1ab*-type genes, the regulatory repression mechanisms achieved through splice variation may be relatively more important for the maintenance of hydration than in species that encode the complete TSA1C.

Author contributions

Conceptualization: Joan Cerdà.

Investigation: Alba Ferré, François Chauvigné, Cinta Zapater.

Formal analysis: Alba Ferré, François Chauvigné, Cinta Zapater, Roderick Nigel Finn, Joan Cerdà.

Supervision: Joan Cerdà.

Funding Acquisition: Joan Cerdà.

Writing-original draft: Alba Ferré.

Writing- review & editing: Joan Cerdà, Roderick Nigel Finn.

3.3.6. References

Ampah-Korsah H, Anderberg HI, Engfors A, Kirscht A, Norden K, Kjellstrom S, Kjellbom P, Johanson U. 2016. The aquaporin splice variant NbXIP1;1α is permeable to boric acid and is phosphorylated in the N-terminal domain. *Frontiers Plant Sci*. 7:862. doi:10.3389/fpls.2016.00862.

Catalán-García M, Chauvigné F, Stavang JA, Nilsen F, Cerdà J, Finn RN. 2021. Lineage-level divergence of copepod glycerol transporters and the emergence of isoform-specific trafficking regulation. *Commun Biol*. 4(1):643. doi: 10.1038/s42003-021-01921-9.

Cerdà J, Chauvigné F, Finn RN. 2017. The physiological role and regulation of aquaporins in teleost germ cells. *Adv Exp Med Biol*. 969:149-171. doi:10.1007/978-94-024-1057-0_10.

Cerdà J, Zapater C, Chauvigné F, Finn RN. 2013. Water homeostasis in the fish oocyte: New insights into the role and molecular regulation of a teleost-specific aquaporin. *Fish Physiol Biochem*. 39:19-27. doi:10.1007/s10695-012-9608-2.

Chauvigné F, Boj M, Vilella S, Finn RN, Cerdà J. 2013. Subcellular localization of selectively permeable aquaporins in the male germ line of a marine teleost reveals spatial redistribution in activated spermatozoa. *Biol Reprod*. 89(2):37. doi:10.1095/biolreprod.113.110783.

Chauvigné F, Fatsini E, Duncan N, Ollé J, Zanuy S, Gómez A, Cerdà J. 2016. Plasma levels of follicle-stimulating and luteinizing hormones during the reproductive cycle of wild and cultured Senegalese sole (*Solea senegalensis*). *Comp Biochem Physiol A Mol Integr Physiol*. 191:35-43. doi:10.1016/j.cbpa.2015.09.015.

Chauvigné F, Ferré A, Cerdà J. 2021. The Xenopus oocyte as an expression system for functional analyses of fish aquaporins. *Methods Mol Biol*. 2218:11-28. doi:10.1007/978-1-0716-0970-5_2.

De Bellis M, Pisani F, Mola MG, Basco D, Catalano F, Nicchia GP, Svelto M, Frigeri A. 2014. A novel human aquaporin-4 splice variant exhibits a dominant-negative activity: a new mechanism to regulate water permeability. *Mol Biol Cell*. 25(4):470-80. doi:10.1091/mbc.E13-06-0331.

De Bellis M, Pisani F, Mola MG, Rosito S, Simone L, Buccoliero C, Trojano M, Nicchia GP, Svelto M, Frigeri A. 2017. Translational readthrough generates new astrocyte AQP4 isoforms that modulate supramolecular clustering, glial endfeet localization, and water transport. *Glia*. 65(5):790-803. doi:10.1002/glia.23126.

Deen PM, Verdijk MA, Knoers NV, Wieringa B, Monnens LA, van Os CH, van Oost BA. 1994. Requirement of human renal water channel aquaporin-2 for vasopressin-dependent concentration of urine. *Science*. 264(5155):92-5. doi:10.1126/science.8140421.

Fabra M, Raldúa D, Power DM, Deen PM, Cerdà J. 2005. Marine fish egg hydration is aquaporin-mediated. *Science*. 307(5709):545. doi:10.1126/science.1106305.

Fabra M, Raldúa D, Bozzo MG, Deen PM, Lubzens E, Cerdà J. 2006. Yolk proteolysis and aquaporin-1o play essential roles to regulate fish oocyte hydration during meiosis resumption. *Dev Biol*. 295(1):250-62. doi:10.1016/j.ydbio.2006.03.034.

Ferré A, Chauvigné F, Vlasova A, Norberg B, Bargelloni L, Guigó R, Finn RN, Cerdà J. 2023a. Functional evolution of clustered aquaporin genes reveals insights into the oceanic success of teleost eggs. *Mol Biol Evol*. 4;40(4):msad071. doi:10.1093/molbev/msad071.

Ferré A, Chauvigné F, Gozdowska M, Kulczykowska E, Finn RN, Cerdà J. 2023b. Neurohypophysial and paracrine vasopressinergic signaling regulates aquaporin trafficking to hydrate marine teleost oocytes. *Front Endocrinol (Lausanne)*. 14:1222724. doi:10.3389/fendo.2023.1222724.

Finn RN, Østby GC, Norberg B, Fyhn HJ. 2002. *In vivo* oocyte hydration in Atlantic halibut (*Hippoglossus hippoglossus*); proteolytic liberation of free amino acids, and ion transport,

are driving forces for osmotic water influx. *J Exp Biol*. 205(Pt 2):211-24. doi:10.1242/jeb.205.2.211.

Finn RN, Cerdà J. 2011. Aquaporin evolution in fishes. *Front Physiol*. 2:44. doi:10.3389/fphys.2011.00044.

Finn RN, Chauvigné F, Hlidberg JB, Cutler CP, Cerdà J. 2014. The lineage-specific evolution of aquaporin gene clusters facilitated tetrapod terrestrial adaptation. *PLoS One*. 9(11):e113686. doi:10.1371/journal.pone.0113686.

Fyhn HJ, Finn RN, Reith M, Norberg B. 1999. Yolk protein hydrolysis and oocyte free amino acids as key features in the adaptive evolution of teleost fishes to seawater. *Sarsia*. 84:451-456. doi: 10.1080/00364827.1999.10807350.

Gao Y, Deng Q, Zhang Y, Zhang S, Zhu Y, Zhang J. 2014. The expression of the multiple splice variants of AQP8 in porcine testes at different developmental stages. *J Appl Genet*. 55(4):511-4. doi:10.1007/s13353-014-0219-8.

Gómez-Redondo I, Planells B, Navarrete P, Gutiérrez-Adán A. 2021. Role of alternative splicing in sex determination in vertebrates. *Sex Dev*. 15(5-6):381-391. doi:10.1159/000519218.

Jorgacevski J, Zorec R, Potokar M. 2020. Insights into cell surface expression, supramolecular organization, and functions of Aquaporin 4 isoforms in astrocytes. *Cells*. 9(12):2622. doi:10.3390/cells9122622.

Kamsteeg EJ, Deen PM. 2001. Detection of aquaporin-2 in the plasma membranes of oocytes: a novel isolation method with improved yield and purity. *Biochem Biophys Res Commun*. 282(3):683-90. doi:10.1006/bbrc.2001.4629.

Kamsteeg EJ, Wormhoudt TA, Rijss JP, van Os CH, Deen PM.1999. An impaired routing of wild-type aquaporin-2 after tetramerization with an aquaporin-2 mutant explains dominant nephrogenic diabetes insipidus. *Embo J*. 18(9):2394-400. doi:10.1093/emboj/18.9.2394.

Lee HJ, Lee SY, Kim YK. 2021. Molecular characterization of transient receptor potential vanilloid 4 (TRPV4) gene transcript variant mRNA of chum salmon Oncorhynchus keta

in response to salinity or temperature changes. *Gene*. 795:145779. doi:10.1016/j.gene.2021.145779.

Lind U, Järvå M, Alm Rosenblad M, Pingitore P, Karlsson E, Wrange AL, Kamdal E, Sundell K, André C, Jonsson PR, *et al*. 2017. Analysis of aquaporins from the euryhaline barnacle *Balanus improvisus* reveals differential expression in response to changes in salinity. *PLoS One*. 12(7):e0181192. doi:10.1371/journal.pone.0181192.

Lubzens E, Young G, Bobe J, Cerdà J. 2010. Oogenesis in teleosts: how eggs are formed. *Gen Comp Endocrinol*. 165(3):367-89. doi:10.1016/j.ygcen.2009.05.022.

Mathai JC, Agre P. 1999. Hourglass pore-forming domains restrict aquaporin-1 tetramer assembly. *Biochemistry*. 38(3):923-8. doi:10.1021/bi9823683.

Moe SE, Sorbo JG, Sogaard R, Zeuthen T, Petter Ottersen O, Holen T. 2008. New isoforms of rat Aquaporin-4. *Genomics*. 91(4):367-77. doi:10.1016/j.ygeno.2007.12.003.

Nagase H, Agren J, Saito A, Liu K, Agre P, Hazama A, Yasui M. 2007. Molecular cloning and characterization of mouse aquaporin 6. *Biochem Biophys Res Commun*. 352(1):12-6. doi:10.1016/j.bbrc.2006.10.110.

Rogalska ME, Vivori C, Valcárcel J. 2023. Regulation of pre-mRNA splicing: roles in physiology and disease, and therapeutic prospects. *Nat Rev Genet*. 24(4):251-269. doi:10.1038/s41576-022-00556-8.

Sievers F, Wilm A, Dineen D, Gibson TJ, Karplus K, Li W, Lopez R, McWilliam H, Remmert M, Söding J, Thompson JD, Higgins DG. 2011. Fast, scalable generation of high-quality protein multiple sequence alignments using Clustal Omega. *Mol Syst Biol*. 7:539. doi:10.1038/msb.2011.75.

Sohara E, Rai T, Yang SS, Uchida K, Nitta K, Horita S, Ohno M, Harada A, Sasaki S, Uchida S. 2006. Pathogenesis and treatment of autosomal-dominant nephrogenic diabetes insipidus caused by an aquaporin 2 mutation. *Proc Natl Acad Sci U S A*. 103(38):14217-22. doi:10.1073/pnas.0602331103.

Sorani MD, Zador Z, Hurowitz E, Yan D, Giacomini KM, Manley GT. 2008. Novel variants in human Aquaporin-4 reduce cellular water permeability. *Hum Mol Genet*. 17(15):2379-

89. doi:10.1093/hmg/ddn138.

Stavang JA, Chauvigné F, Kongshaug H, Cerdà J, Nilsen F, Finn RN. 2015. Phylogenomic and functional analyses of salmon lice aquaporins uncover the molecular diversity of the superfamily in Arthropoda. *BMC Genomics*. 16(1):618. doi:10.1186/s12864-015-1814-8.

Tajima T, Okuhara K, Satoh K, Nakae J, Fujieda K. 2003. Two novel aquaporin-2 mutations in a sporadic Japanese patient with autosomal recessive nephrogenic diabetes insipidus. *Endocr J*. 50(4):473-6. doi:10.1507/endocrj.50.473.

Tian Y, Gao Q, Dong S, Zhou Y, Yu H, Liu D, Yang W. 2022. Genome-wide analysis of alternative splicing (as) mechanism provides insights into salinity adaptation in the livers of three euryhaline teleosts, including *Scophthalmus maximus*, *Cynoglossus semilaevis* and *Oncorhynchus mykiss*. *Biology (Basel)*. 11(2):222. doi:10.3390/biology11020222.

Tingaud-Sequeira A, Chauvigné F, Fabra M, Lozano J, Raldúa D, Cerdà J. 2008. Structural and functional divergence of two fish aquaporin-1 water channels following teleost-specific gene duplication. *BMC Evol Biol*. 8:259. doi:10.1186/1471-2148-8-259.

Tsujimoto H, Liu K, Linser PJ, Agre P, Rasgon JL. 2013. Organ-specific splice variants of aquaporin water channel AgAQP1 in the malaria vector Anopheles gambiae. *PLoS One*. 8(9):e75888. https://doi:10.1371/journal.pone.0075888.

Varadaraj K, Kumari SS, Patil R, Wax MB, Mathias RT. 2008. Functional characterization of a human aquaporin 0 mutation that leads to a congenital dominant lens cataract. *Exp Eye Res*. 87(1):9-21. doi:10.1016/j.exer.2008.04.001.

Yilmaz O, Chauvigné F, Ferré A, Nilsen F, Fjelldal PG, Cerdà J, Finn RN. 2020 Unravelling the complex duplication history of deuterostome glycerol transporters. *Cells*. 9(7):1663. doi:10.3390/cells9071663.

Zapater C, Chauvigné F, Norberg B, Finn RN, Cerdà J. 2011. Dual neofunctionalization of a rapidly evolving aquaporin-1 paralog resulted in constrained and relaxed traits controlling channel function during meiosis resumption in teleosts. *Mol Biol Evol*. 28(11):3151-69. doi:10.1093/molbev/msr146.

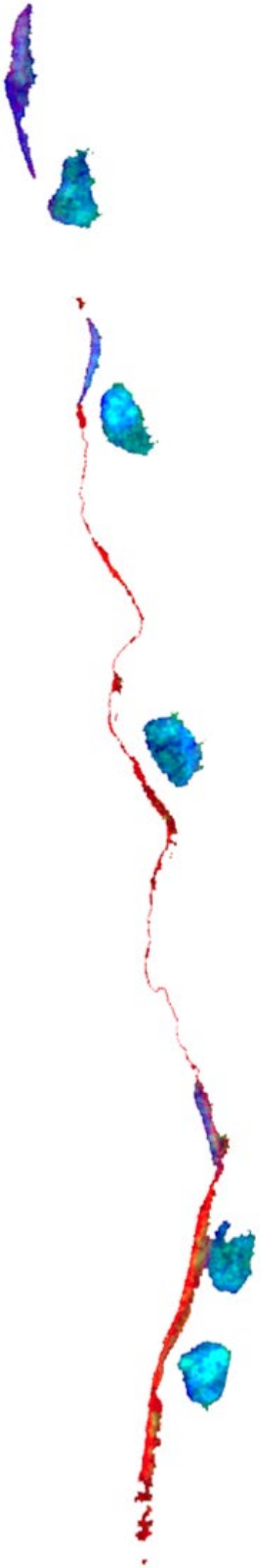

OVERALL DISCUSSION

The present thesis reports a comprehensive investigation of the evolution of *aqp1*-type genes in teleosts and the various molecular mechanisms underlying the regulation of the intracellular trafficking of these channels. The research has uncovered an ancient teleost-specific aquaporin-1 cluster (TSA1C), comprised of tandemly arranged *aqp1aa-aqp1ab2-aqp1ab1* genes, which shows ~300-million-year history of downstream *aqp1ab*-type gene loss, neofunctionalization, and subfunctionalization, but with marine species that spawn highly hydrated pelagic eggs almost exclusively retaining at least one of the downstream paralogs. Accordingly, the data shows the specific regulation of Aqp1ab-type channel trafficking during oocyte hydration, involving different protein kinases, binding proteins, endocrine signals and inhibitory alternative splice forms of the channels. These findings therefore provide new knowledge on the molecular mechanisms underlying egg formation in marine teleosts, and set the basis for the future development of biomarkers of egg quality in wild and cultured fish populations.

4.1. Evolution of the TSA1C and Selective Retention and Expression of *aqp1ab* Genes

Almost two decades ago, a specialized water-selective aquaporin (Aqp1o, now referred to as Aqp1ab) was discovered in teleosts, which facilitates water entry into oocytes (Fabra *et al*., 2005). This channel is temporarily inserted into the oocyte plasma membrane during meiotic maturation and maximal yolk proteolysis, playing a crucial role in developing the pelagic egg phenotype (Fabra *et al*., 2005 and 2006; Zapater *et al*., 2011 and 2013). The *aqp1ab* gene evolved and neofunctionalized as a downstream tandem duplicate of the *aqp1aa* paralog, which retains a more conserved protein structure to tetrapod AQP1 (Tingaud-Sequeira *et al*., 2008; Zapater *et al*., 2011). The teleost Aqp1ab thus belongs to a broader superfamily of aquaporins (Agre *et al*., 1993), which in jawed vertebrates currently comprise 17 subfamilies (Aqp0-16) (Finn *et al*., 2014; Chauvigné *et al*., 2019). The teleost repertoire of aquaporins (19-25 and 37-47 paralogs in diploid and tetraploid species, respectively) is larger than in mammals (14-15 paralogs), partly due to independent whole genome duplications and lineage-specific tandem duplications (Cerdà and Finn, 2010; Finn and Cerdà, 2011; Finn *et al*., 2014; Yilmaz *et al*., 2020). This has led to the presence of multiple aquaporin gene clusters in teleosts, such as the *aqp1aa-aqp1ab* cluster, which is

retained in all teleosts examined to date (Finn *et al*., 2014; Cerdà *et al*., 2017; Zhang *et al*., 2021).

In previous studies, a second *aqp1ab*-type gene flanking the *aqp1aa* and *aqp1ab* loci was noted in the gilthead seabream (*Sparus aurata*) and African cichlids, which may represent *aqp1ab*-type pseudogenes (Zapater *et al*., 2013; Finn *et al*., 2014). To investigate this observation further a gene-walking experiment was carried out in seabream, which uncovered an additional four exon aquaporin-like gene upstream of the previously identified *aqp1ab* channel, and downstream of the encoded *aqp1aa* gene. Phylogenetic analysis indicated that nonteleost species such as cartilaginous, chondrostean, and holostean fishes encode a single *aqp1* channel, while all teleosts have at least one *aqp1aa* gene, and different species have one or two copies of *aqp1ab* genes, which cocluster on a separate branch to the *aqp1aa* genes. In line with the convention of aquaporin nomenclature, which names genes in accordance with the chronology of their discovery, we named the second seabream *aqp1ab*-type channel and its orthologs in other species as *aqp1ab2*, and renamed the original seabream *aqp1ab* channel (Fabra *et al*., 2005 and 2006) and its orthologs in other species as *aqp1ab1*. These analyses thus uncovered a novel ternary TSA1C comprised of *aqp1aa-aqp1ab2-aqp1ab1*, in which the *aqp1ab2* and *aqp1ab1* genes, when present in teleost genomes, are closely juxtaposed downstream of the *aqp1aa* gene.

The comprehensive phylogenetic data revealed that the TSA1C likely evolved at the root of the crown clade of Teleostei, in the near aftermath of the R3 event ~300 Ma (Amores *et al*., 2011). The TSA1C is thus ancient but has until now been masked likely due to differential gene loss in various lineages. A systematic phylogenetic analysis of the *aqp1*-type genes and their syntenic loci assembled from >400 piscine genomes confirmed the asymmetric retention of the aqp1aa gene in all teleosts. The analysis also showed that many teleost lineages have lost or only retain fragmented pseudogenes of both *aqp1ab1* and *aqp1ab2* paralogs, while others have lost either the *aqp1ab1* or *-1ab2* gene, yet many species still retain both of the tandem duplicates. However, an overwhelming majority (95%) of species that spawn pelagic eggs in marine environments retain at least one of the duplicates, with a third of the species still harboring complete copies of both paralogs. Conversely, much higher levels of gene loss are seen in species that spawn benthic eggs (43%) or incubate their eggs internally (91%). In marine benthic eggs, oocytes hydrate to a significantly lower degree than pelagic eggs, reaching water contents of 68–82% of egg wet mass (Finn *et al*.,

2002a and 2002b). These data suggest that both Aqp1ab1 and Aqp1ab2 channels may be required for oocyte hydration in marine teleosts producing highly hydrated eggs. This notion is reinforced by the finding that *aqp1ab1* and -*1ab2* transcript enrichment within the ovaries of marine pelagophil species are orders of magnitude higher than in the somatic tissues.

4.2. Functional Evolution of Intracellular Trafficking Regulation of the TSA1C Channels

The functional characterization of the channels within the TSA1C using the *Xenopus laevis* oocyte expression system revealed that the trafficking of each paralog to the plasma membrane was differentially regulated. Thus, while the Aqp1aa was constitutively localized in the oocyte surface, the Aqp1ab1 and Aqp1ab2 channels were partially or completely retained in the endoplasmic reticulum (ER). Further experiments employing protein kinase A (PKA) and C (PKC) activators and a p38 mitogen-activated protein kinase (p38 MAPK) agonist in distantly related marine and freshwater teleosts, showed that the intracellular trafficking of the TSA1C is differentially regulated by PKA and PKC, and also by p38 MAPK in the case of Aqp1ab1. However, site-directed mutagenesis trials indicated that the specific residues involved in these regulations appear to have changed with the evolution of the different lineages. In addition, transcriptomic, phylogenetic and functional analyses uncovered the role of teleost-specific Ywhaz-like regulatory proteins (tyrosine 3-monooxygenase/tryptophan 5-monooxygenase activation proteins or 14-3-3ζ-like), YwhazLa and YwhazLb. which selectively interact with teleost Aqp1ab1 and Aqp1ab2 to regulate channel trafficking to the plasma membrane. The data suggest that Aqp1ab-type trafficking regulation evolved from a relatively relaxed, low-specificity YWHA-binding requirement that has been maintained in species that retain only one of the Aqp1ab-type channels, albeit with a slight binding preference for Aqp1ab1 to YwhazLa. However, a highly constrained binding requirement of Aqp1ab2 to YwhazLb evolved in euacanthomorph species that retain both of the Aqp1ab-type channels. In addition, the pre-euteleost Aqp1ab1 channels evolved YWHA-independent phosphorylation mechanisms for trafficking to the plasma membrane, while the euteleost channels evolved recycling mechanisms mediated by p38 MAPK-phosphorylation

The comparison of the subdomains of the teleost TSA1C channels to the Aqp1 orthologs of nonteleost vertebrates suggests that the regulatory sites in the Aqp1 and Aqp1aa orthologs have remained relatively fixed through time, while those of the Aqp1ab1 and Aqp1ab2 channels have selectively changed during teleost evolution. For example, PKC positively regulates the membrane trafficking of the Aqp1/Aqp1aa orthologs through phosphorylation of a conserved Thr in loop D in most vertebrate groups except some amphibians, Polypteriformes, Siluriformes, and Euteleostei, which encode a Val or Ala. The Thr/Val substitution in Euteleostei resulted in the loss of the positive PKC-mediated regulation and the emergence of a negative PKC-mediated regulation. Further, in contrast to Chondrichthyes and Sarcopterygii, many actinopterygian fishes evolved a C-terminal Ser for positive regulation via PKA-mediated phosphorylation. Nevertheless, even in euacanthomorph species in which the Aqp1aa C-terminal PKA site is conserved, as in Senegalese sole (*Solea senegalensis*), an alternative negative PKC-mediated regulation still exists, while the positive PKA-mediated regulation of the older lineages is also maintained.

In contrast to the Aqp1/Aqp1aa, the two Aqp1ab-type channels evolved PKA, PKC, and p38 MAPK regulatory sites that are both dependent and independent of the teleost-specific YwhazL binding proteins. The identification of the novel YwhazLa and -zLb paralogs in the present study extend recent findings reporting that ostariophysan teleosts encode duplicated *ywhaz* genes of the mammalian *YWHAZ* ortholog (Zhang *et al*., 2021). In this context, however, we note that the *ywhazLa* gene synteny is only conserved between Otophysi and osteoglossomorph teleosts, while the *ywhazLb* gene is only syntenic within the Ostariophysi, e.g., zebrafish (*Danio rerio*) and catfishes. The novel *ywhazLa* and *-zLb* genes identified cluster within the vertebrate *ywhaz* clade, but are polyphyletic and are not syntenic between euacanthomorph and the more basal teleost lineages. Their neofunctionalization can be inferred from the longer branch lengths, and the mutagenesis experiments show their specific functional requirement for plasma membrane trafficking of the Aqp1ab-type channels. For example, in the basal cohort of elopomorph teleosts, such as the European eel (*Anguilla anguilla*), which spawn pelagic eggs and only retain the Aqp1ab2 paralog, PKA-mediated positive regulation of membrane trafficking is dependent on C-terminal YwhazLa binding and two YwhazLa-independent PKC-regulated sites in loop D and the C-terminus, respectively. In modern lineages of euacanthomorph species that retain both the Aqp1ab2 and -1ab1 paralogs, the PKC-mediated regulation of Aqp1ab2 is lost, and membrane

trafficking became dependent on PKA-mediated phosphorylation of the same C-terminal Ser residues as in the elopomorph teleosts, but dependent on YwhazLb rather than YwhazLa binding.

A more intricate regulation of membrane trafficking evolved in the teleost Aqp1ab1 channels. Amongst cyprinid species, such as zebrafish, PKA-mediated phosphorylation of different Ser residues in the C-terminus positively regulates membrane trafficking, on both YwhaLa-dependent and independent manner, while PKC-mediated phosphorylation in loop D recycles the channel. In salmonids, only the positive PKA-mediated regulation in the C-terminus that is dependent on YwhazLa binding is maintained, while new C-terminal recycling sites emerge that are regulated by PKC (outside of the YwhazLa binding domain) and p38 MAPK (within the YwhazLa binding site). The p38 MAPK negative regulatory site in the YwhazLa binding region is maintained in euacanthomorph teleosts, such as seabream, together with a positive PKA-mediated YwhazLa-dependent site. However, two additional positive PKA-mediated regulation sites appear in loop D of Aqp1ab1 that depend on the binding of the channel to YwhazLa. The studies in *X. laevis* oocytes shows that it is this latter two-step regulation that generates a membrane trafficking shunt of Aqp1ab1 to the distal region of the microvilli, and thus the avoidance of competitive occupancy of the same membrane space with the Aqp1ab2 channel. In contrast, Aqp1ab2, which is strictly dependent on YwhazLb binding, lacks the loop D regulatory step, and thus remains in the proximal region of the microvilli.

4.3. Aqp1ab-type Channel Regulation by Alternative Splicing

In addition to kinase phosphorylation and YwhazL carrier proteins, the trafficking of Aqp1ab1 and Aqp1ab2 channels can also be regulated by alternative splice forms of the channels, which are expressed in the ovary and other tissues. In the Atlantic halibut (*Hippoglossus hippoglossus*) and seabream, the splicing of intronic regions of the *aqp1ab1* genes introduces premature stop codons and thus C-terminally truncated proteins are translated (Aqp1ab1_v1 and Aqp1ab1_v2). By contrast, in the Senegalese sole and common sole (*Solea solea*), the alternative in-frame splicing of the proximal second intronic region of the *aqp1ab2* gene generates an intact Aqp1ab2_v1 protein with an extended extracellular loop E, while the splicing of the distal region of the second intronic region leads to out-of-

frame readthrough of exon 3 and 4 and the generation of a C-terminally truncated Aqp1ab2_v2 protein due to a premature stop codon. However, in contrast to the canonical Aqp1ab1 and Aqp1ab2 channels, none of the variants were found to function as water channels when expressed in *X. laevis* oocytes. On the contrary, they all cause dominant-negative inhibition of the canonical channel function, but through different mechanisms.

The heterologous expression of seabream and halibut Aqp1ab1 splice variants in *X. laevis* oocytes showed that these isoforms are completely retained in the ER, unlike the canonical wild-type (WT) channel. Conversely, the Aqp1ab2 splice variants are targeted to the oocyte plasma membrane (Aqp1ab2_v1) or partially sequestered in the ER (Aqp1ab2_v2). By co-expressing each of the variants with the WTs and immunologically locating their proteins in the frog oocytes, it became evident that the splice variants elicit distinct mechanisms of dominant-negative inhibition of the WT channel function. The double immunostaining and co-immunoprecipitation experiments suggest that one of these mechanisms, displayed by the three Aqp1ab1 variants and partially by the sole Aqp1ab2_v2 isoform, is gained by trapping the WT channels in the ER by hetero-oligomerization, thereby preventing their trafficking to the plasma membrane. This dominant-negative effect could be explained by the oligomeric structure of Aqp1ab1 and Aqp1ab2 tetramers, which are probably retained in the ER when they are formed by WT channels and truncated isoforms, because they are incorrectly assembled and thus targeted for degradation (Kamsteeg *et al*., 1999; De Bellis *et al*., 2014). Such a mechanism is therefore reminiscent of the dominant-negative effect caused by the truncated human AQP4-Δ4 and AQP0-Δ213 splice forms, which heterodimerize with the canonical channels to cause their retention in the ER (Varadaraj *et al*., 2008; De Bellis *et al*., 2014). However, our data also revealed that the sole splice variants, which show the greatest inhibitory efficiency, are also targeted to the plasma membrane together with the Aqp1ab2-WT channel. Due to the lack of functionality of these variants as water transporters, possibly because of altered structural domains that affect the water pore or impede the formation of functional homotetramers in the plasma membrane (Mathai and Agre, 1999), their increased trafficking to the plasma membrane results in dominant-negative repression of water permeation. These findings thus indicate that Aqp1ab-type splice variation in teleosts may have evolved to differentially and more efficiently regulate channel function in species that lost one of the *aqp1ab*-type genes. In the present case, this is exemplified by the soleid fishes, which lost the *aqp1ab1* gene, while the

inhibitory efficiency of the Aqp1ab-type splice forms of euacanthomorph teleosts, such as halibut and seabream that retain intact TSA1Cs, is lower, perhaps because other p38 MAPK regulatory pathways controlling channel recycling remain in place.

4.4. Endocrine and Molecular Regulation of Aqp1ab1 and -1ab2 Intracellular Trafficking During Oocyte Hydration in Marine Euacanthomorph Teleosts

Immunolocalization of Aqp1ab1 and Aqp1ab2 channels in the seabream ovarian follicle employing paralog-specific antibodies, as well as co-immunoprecipitation experiments confirmed the regulation of the trafficking of these channels by PKA phosphorylation and YwhazL binding in hydrating oocytes. In addition, we found that both an hypophysial and paracrine vasopressinergic system exists in the ovary of the seabream that regulates Aqp1ab1 and Aqp1ab2 trafficking in the oocyte through the arginine vasopressin (Avp) receptor 2aa (Avpr2aa), which is highly expressed in the oocyte and activates the cAMP-PKA cascade.

By integrating the functional data *ex vivo*, *in vivo* and *in vitro* obtained for the seabream in the present thesis, a new model for the endocrine and molecular regulation of Aqp1ab1 and Aqp1ab2 intracellular trafficking during oocyte hydration can be proposed for marine euacanthomorph teleost that retain both paralogs (figure 1). During vitellogenesis, neurohypophysial secretion of Avp arrives at the capillary beds of the thecal layer. From there it diffuses to activate the Avpr2aa receptor, which is expressed in the plasma membrane of the theca and granulosa cells, to induce the PKA-mediated phosphorylation of Thr^{262} in the C-terminus of Aqp1ab2. This results in the coupling of the YwhazLb binding protein and the trafficking of the channel to the cell surface of the theca and granulosa cells. Meanwhile, in the oocyte Aqp1ab1, which is already expressed since the primary growth stage (Fabra *et al*., 2006) and phosphorylated at the C-terminal Ser^{253} by a PKA-mediated mechanism, preferentially couples with the YwhazLa binding protein and is trafficked close to the basal region of the oocyte microvilli during vitellogenesis. Some of Aqp1ab1 also enters the basal region of the oocyte microvilli, potentially to mediate water homeostasis during the vitellogenic growth phase. Concomitant with the preovulatory surge of the luteinizing hormone (Lh) (Gothilf *et al*., 1997; Meiri *et al*., 2002), the major endocrine signal controlling oocyte meiotic maturation and hydration (Lubzens *et al*., 2010), the circulating and ovarian

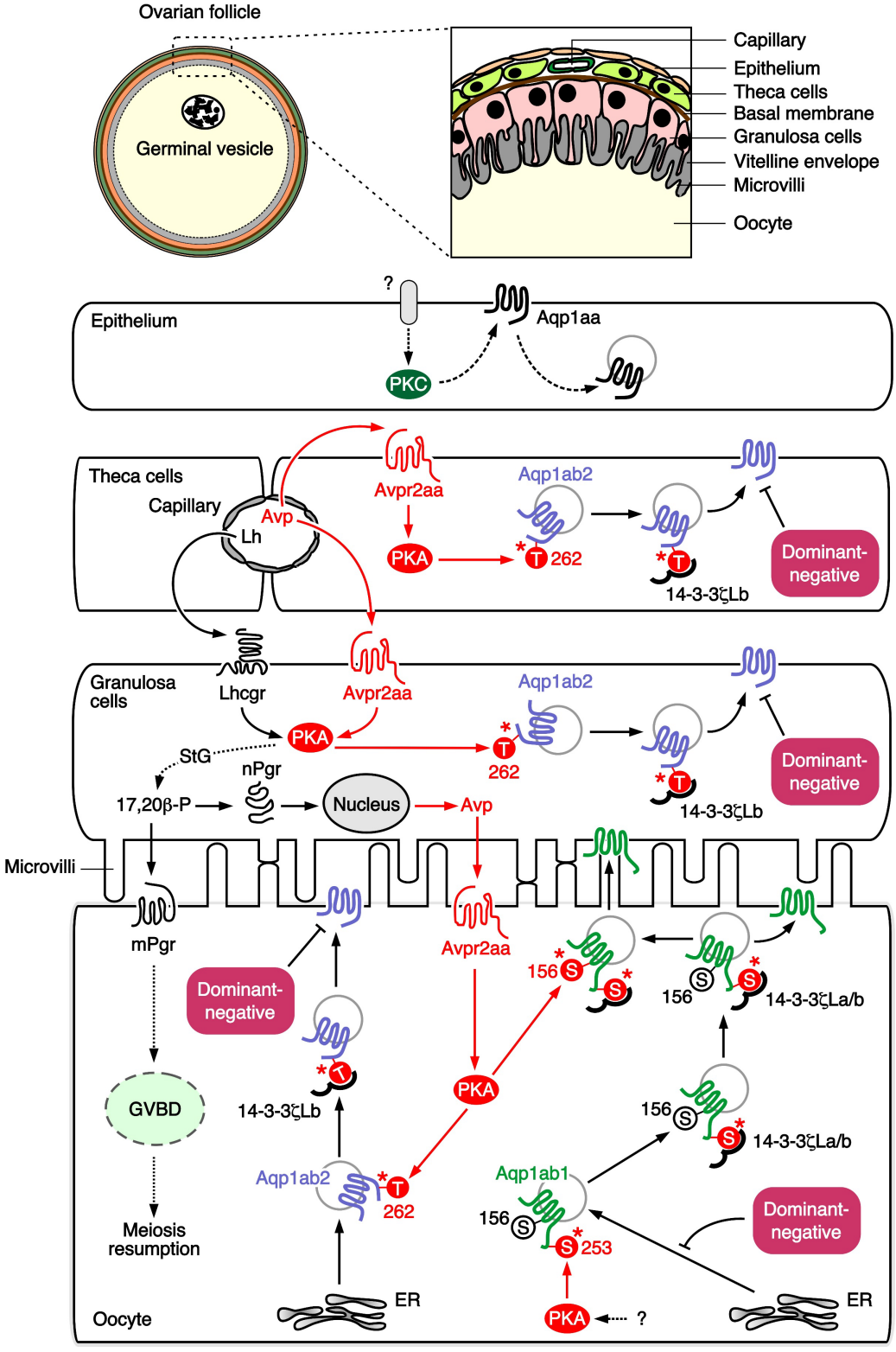

Figure 1. Proposed integrated model for the endocrine and molecular regulation of Aqp1ab1 and Aqp1ab2 intracellular trafficking during oocyte hydration in the marine euacanthomorph teleost gilthead seabream. In primary growth oocytes, Aqp1ab1 is phosphorylated at Ser^{253} by PKA, which is activated by a yet unknown signaling pathway, to bind YwhazLa and -zLb. The complex is then slowly transported to the oocyte cortical region during the vitellogenic period, where it is retained just below the oocyte plasma membrane in postvitellogenic oocytes, while

occupancy some of Aqp1ab1 enters the basal region of the oocyte microvilli. The release of systemic (circulating) hypohysial Avp and Lh from capillaries in the theca layer at the time of oocyte maturation activate the Avpr2aa in theca and granulosa cells, as well as the Lh/choriogonadotropin receptor (Lhcgr) in the granulosa cells. In the theca and granulosa, the Avp-stimulated Avpr2aa triggers PKA activation, which mediates the phosphorylation of Thr^{262} in Aqp1ab2 promoting the binding to YwhazLb and the trafficking of the channel to the plasma membrane of these cells. The activation of the Lhcgr-PKA pathway in granulosa cells drives the synthesis of the progestagen 17,20ß-P, through a switch in the steroidogenic (StG) pathway from estrogen to progestagen production. The 17,20ß-P, in turn stimulates the local synthesis of Avp through a genomic mechanism mediated by the nuclear progestin receptor (nPgr). The resulting release of Avp and 17,20ß-P from the granulosa cells respectively activates the Avpr2aa and the membrane progestin receptor (mPgr) in the oocyte surface. The mPr triggers meiosis resumption (oocyte maturation), whereas the Avpr2aa-PKA signaling regulates the trafficking of Aqp1ab2 as in follicle cells, and a secondary phosphorylation of Ser^{156} in the loop D of Aqp1ab1 channels already complexed with YwhazLa/b. The secondary phosphorylation of Aqp1ab1 further shuttles the channel to the most distal region of the oocyte microvilli. The systemic and/or local levels of Avp, or a possible Lh-mediated production of Oxt, may potentially activate the PKC signaling pathway in the epithelium, through a yet unidentified receptor, to recycle Aqp1aa. Finally, the trafficking of Aqp1ab1 and Aqp1ab2 in somatic cells and oocyte can be regulated by non-functional alternative splicing forms of Aqp1ab1 and Aqp1ab2, which can inhibit transmembrane water conductance by the canonical channels or induce their retention in the ER and further degradation. This model integrates both the systemic and paracrine vasopressinergic regulation of the intracellular trafficking of Aqp1ab-type paralogs in the seabream ovarian follicle, such that competitive plasma membrane spatial occupancy by both channels in the oocyte is avoided and bulk water influx is augmented during the hydration process.

levels of Avp are increased. Such an elevated systemic Avp further enhances the PKA-mediated trafficking of Aqp1ab2 channels in the theca and granulosa cells. However, as previously observed in the catfish (Singh *et al*., 2021), the combined activation of Lh on the Lh/choriogonadotropin receptor (Lhcgr) and Avp on Avpr2aa could also multiply the action of the PKA-mediated Lh induction of the steroidogenic shift from estrogen production to the synthesis of the maturation-inducing progestin 17α,20ß-dihydroxypregn-4-en-3-one (17,20ß-P) in granulosa cells (Lubzens *et al*., 2010). Thus, the 17,20ß-P could act as a master switch regulating the reciprocal genomic production of Avp via the nuclear progestin receptor in granulosa cells, and the non-genomic activation of germinal vesicle breackdown (GVBD) and meiosis resumption via the membrane progestin receptor that is expressed in the oocyte plasma membrane (Lubzens *et al*., 2010). It is the former reciprocal genomic production of Avp that would provide the paracrine signal between the granulosa cells and the Avpr2aa in the oocyte plasma membrane, which now activates the PKA-mediated phosphorylation of Thr^{262} in the Aqp1ab2 C-terminus and Ser^{156} in loop D of Aqp1ab1. The Thr^{262} phosphorylation promotes the coupling of the YwhazLb binding protein and the trafficking of Aqp1ab2 to the basal region of the oocyte microvilli, while the secondary phosphorylation of loop D Ser^{156} in Aqp1ab1 relocalizes the channel to the distal portion of the oocyte microvilli. In this way, the two Aqp1ab-type paralogs are co-regulated by the same Avp-Avpr2aa-PKA pathway to cooperatively enhance water influx while avoiding competitive occupancy of the same membrane space, and hence the bulk water flow is augmented during oocyte hydration.

In *X. laevis* oocytes, we observed that Aqp1aa is recycled when the channel is co-expressed with the Avp receptor 1aa (Avpr1aa) or the oxytocin (Oxt) receptor b (Oxtrb), which both activate the phospholipase C and PKC pathways. The proposed model, however, does not yet explain the signal transduction mechanism that may activate PKC-mediated recycling of Aqp1aa in the follicular epithelium. Nevertheless, we did observe that in vitellogenic ovarian follicles, both the mRNA and protein of Oxt are accumulated in the theca and granulosa cells, while those of Avp are only accumulated in the granulosa cells. These observations may suggest that trafficking of epithelial Aqp1aa could also be under Avp or Oxt regulation through receptors not characterized in our study, such as the Avpr1ab or the Oxtra, since in our *in situ* hybridization experiments neither *avpr1aa* nor *oxtrb* mRNA expression could not be detected in the follicular epithelial layer. In any event, the potential recycling of the Aqp1aa channel in the follicular epithelium may provide an important mechanism for the flow of water into the hydrating oocyte. The water path originates with the seawater imbibed by the mother and is delivered to the follicles through the thecal capillary beds. By simultaneously recycling epithelial Aqp1aa and driving Aqp1ab2 to the membranes of the theca and granulosa cells, water is only free to flow in one direction toward the oocyte. The differential proteolysis of primarily vitellogenin-Aa (VtgAa) type yolk proteins (Finn and Kristoffersen, 2007; Finn, 2007; Kolarevic *et al*., 2008) generates the osmotic driving force that converts the oocyte into the water sink, which then enters via the vasopressinergic induction of the Aqp1ab1 and Aqp1ab2 channels to the distal and proximal regions of the microvilli. The water finally becomes trapped within the highly hydrated oocyte due to the precipitous drop in the ovarian levels of Avp, thus ending the paracrine regulation of the trafficking of the Aqp1ab-type channels, and their resultant internalization in the oocyte. The subsequent cyclical increase in the level of circulating Oxt may thus prepare the oocytes for ovulation as in mammals (Gainer and Wray, 1994), leaving the eggs ready for fertilization and dispersal in the oceanic currents.

The trafficking of Aqp1a-type channels in the oocyte may also be regulated by alternative splicing isoforms encoding for non-functional channels (figure 1). In seabream and Atlantic halibut, the biological significance of this regulation is uncertain because the *aqp1ab1*-type variants are much lower expressed *in vivo* than the WTs. However, in soleids the *aqp1ab2* splice variants are relatively highly expressed in the ovary, and the data show that the protein ratios of the Aqp1ab2_v1 and Aqp1ab2_v2 to the WT generally decrease during previtellogenesis and hydration, and subsequently greatly increase in the mature eggs.

Immunostaining data also show that as for seabream Aqp1ab2-WT, the sole Aqp1ab2-WT and its splice variants are expressed both in the theca and granulosa cells as well as in the oocyte. However, in contrast to the Aqp1ab2-WT, which begins to enter the oocyte plasma membrane microvilli during vitellogenesis, and is almost completely translocated there during hydration, the Aqp1ab2_v1 never enters the microvillar membrane. It would thus seem apparent that the roles of the splice variants in the follicular cells would be to modulate the rate of water flow during oocyte growth via the observed dominant-negative repression mechanisms, while their presence in the oocyte is strongly reduced during hydration so as not to inhibit maximal water influx through the canonical channel, which can form homotetramers and be fully translocated to the membrane microvilli. For species that retain both Aqp1ab1 and Aqp1ab2 in the TSA1C, such a regulation may not be under the same selection pressure as the two channels evolved to occupy the distal and proximal regions of the oocyte microvilli, respectively, and thereby avoid competitive membrane space occupancy to accelerate bulk water influx. In the seabream, the differential trafficking of the Aqp1ab-type paralogs in the oocyte is regulated via Lh through a common Avp signaling pathway. However, in sole, although the downregulation of the Aqp1ab2 splice variants occurs mainly during oocyte maturation and hydration, the endocrine pathway regulating the expression of these isoforms at this stage is unknown and should be investigated in the future.

4.5. References

Agre P, Sasaki S, Chrispeels MJ. 1993. Aquaporins: a family of water channel proteins. *Am J Physiol.* 265(3 Pt 2):F461. doi: 10.1152/ajprenal.1993.265.3.F461.

Amores A, Catchen J, Ferrara A, Fontenot Q, Postlethwait JH. 2011. Genome evolution and meiotic maps by massively parallel DNA sequencing: Spotted gar, an outgroup for the teleost genome duplication. *Genetics*. 188(4):799-808. doi: 10.1534/genetics.111.127324.

Cerdà J, Chauvigné F, Finn RN. 2017. The physiological role and regulation of aquaporins in teleost germ cells. *Adv Exp Med Biol*. 969:149-171. doi: 10.1007/978-94-024-1057-0_10.

Cerdà J, Finn RN. 2010. Piscine aquaporins: an overview of recent advances. *J Exp Zool A Ecol Genet Physiol*. 313(10):623-50. doi: 10.1002/jez.634.

Chauvigné F, Yilmaz O, Ferré A, Fjelldal PG, Finn RN, Cerdà J. 2019. The vertebrate Aqp14 water channel is a neuropeptide-regulated polytransporter. *Comm Biol*. 2:462. doi: 10.1038/s42003-019-0713-y.

De Bellis M, Pisani F, Mola MG, Basco D, Catalano F, Nicchia GP, Svelto M, Frigeri A. 2014. A novel human aquaporin-4 splice variant exhibits a dominant-negative activity: a new mechanism to regulate water permeability. *Mol Biol Cell*. 25: 470-480.

Fabra M, Raldúa D, Bozzo MG, Deen PM, Lubzens E, Cerdà J. 2006. Yolk proteolysis and aquaporin-1o play essential roles to regulate fish oocyte hydration during meiosis resumption. *Dev Biol*. 295(1):250-62. doi: 10.1016/j.ydbio.2006.03.034.

Fabra M, Raldúa D, Power DM, Deen PM, Cerdà J. 2005. Marine fish egg hydration is aquaporin-mediated. *Science*. 307(5709):545. doi: 10.1126/science.1106305.

Finn RN, Cerdà J. 2011. Aquaporin evolution in fishes. *Front Physiol*. 2:44. doi: 10.3389/fphys.2011.00044.

Finn RN, Chauvigné F, Hlidberg JB, Cutler CP, Cerdà J. 2014. The lineage-specific evolution of aquaporin gene clusters facilitated tetrapod terrestrial adaptation. *PLoS One*. 9(11):e113686. doi: 10.1371/journal.pone.0113686.

Finn RN, Kristoffersen BA. 2007. Vertebrate vitellogenin gene duplication in relation to the ‘‘3R Hypothesis’’: Correlation to the pelagic egg and the oceanic radiation of teleosts. *PLoS One*. 2(1):e169. doi: 10.1371/journal.pone.0000169.

Finn RN, Østby G, Norberg B, Fyhn HJ. 2002a. *In vivo* oocyte hydration in Atlantic halibut (*Hippoglossus hippoglossus*); Proteolytic liberation of free amino acids, and ion transport are driving forces for osmotic water influx. *J Exp Biol*. 205(Pt 2):211-24. doi: 10.1242/jeb.205.2.211.

Finn RN, Wamboldt M, Fyhn HJ. 2002b. Differential processing of yolk proteins during oocyte hydration in fishes (Labridae) that spawn benthic and pelagic eggs. *Mar Ecol Prog Ser*. 237: 217-226. doi:10.3354/meps237217.

Finn RN. 2007. The maturational disassembly and differential proteolysis of paralogous vitellogenins in a marine pelagophil teleost: A conserved mechanism of oocyte hydration. *Biol Reprod*. 76(6):936-48. doi: 10.1095/biolreprod.106.055772.

Gainer H, Wray S. 1994. Cellular and molecular biology of oxytocin and vasopressin. In: Knobil E, Neill JD, editors. The Physiology of Reproduction. Vol 2. New York, Raven Press. p 1099-29.

Gothilf Y, Meiri I, Elizur A, Zohar Y. 1997. Preovulatory changes in the levels of three gonadotropin-releasing hormone-encoding messenger ribonucleic acids (mRNAs), gonadotropin beta-subunit mRNAs, plasma gonadotropin, and steroids in the female gilthead seabream, *Sparus aurata*. *Biol Reprod*. 57(5):1145-54. doi: 10.1095/biolreprod57.5.1145.

Kamsteeg EJ, Wormhoudt TA, Rijss JP, van Os CH, Deen PM.1999. An impaired routing of wild-type aquaporin-2 after tetramerization with an aquaporin-2 mutant explains dominant nephrogenic diabetes insipidus. *Embo J*. 18(9):2394-400. doi:10.1093/emboj/18.9.2394.

Kolarevic J, Nerland A, Nilsen, F, Finn RN. 2008 Goldsinny wrasse (*Ctenolabrus rupestris*) is an extreme *vtgAa*-type pelagophil teleost. *Mol Reprod Dev*. 75(6):1011-20. doi: 10.1002/mrd.20845.

Lubzens E, Young G, Bobe J, Cerdà J. 2010. Oogenesis in teleosts: how eggs are formed. *Gen Comp Endocrinol*. 165(3):367-89. doi: 10.1016/j.ygcen.2009.05.022.

Mathai JC, Agre P. 1999. Hourglass pore-forming domains restrict aquaporin-1 tetramer assembly. *Biochemistry*. 38(3):923-8. doi:10.1021/bi9823683.

Meiri I, Gothilf Y, Zohar Y, Elizur A. 2002. Physiological changes in the spawning gilthead seabream, *Sparus aurata*, succeeding the removal of males. *J Exp Zool*. 292(6):555-64. doi: 10.1002/jez.10072.

Singh V, Chaube R, Joy KP. 2021. Vasotocin stimulates maturation-inducing hormone, oocyte maturation and ovulation in the catfish *Heteropneustes fossilis*: Evidence for a preferential calcium involvement. *Theriogenology*. 167:51-60. doi: 10.1016/j.theriogenology.2021.03.001.

Tingaud-Sequeira A, Chauvigné F, Fabra M, Lozano J, Raldúa D, Cerdà J. 2008. Structural and functional divergence of two fish aquaporin-1 water channels following teleost-specific gene duplication. *BMC Evol Biol*. 8:259. doi: 10.1186/1471-2148-8-259.

Varadaraj K, Kumari SS, Patil R, Wax MB, Mathias RT. 2008. Functional characterization of a human aquaporin 0 mutation that leads to a congenital dominant lens cataract. *Exp Eye Res*.

87(1):9-21.

Yilmaz O, Chauvigné F, Ferré A, Nilsen F, Fjelldal PG, Cerdà J, Finn RN. 2020. Unravelling the complex duplication history of deuterostome glycerol transporters. *Cells*. 9(7):1663. doi: 10.3390/cells9071663.

Zapater C, Chauvigné F, Norberg B, Finn RN, Cerdà J. 2011. Dual neofunctionalization of a rapidly evolving aquaporin-1 paralog resulted in constrained and relaxed traits controlling channel function during meiosis resumption in teleosts. *Mol Biol Evol*. 28(11):3151-69. doi: 10.1093/molbev/msr146.

Zapater C, Chauvigné F, Tingaud-Sequeira A, Finn RN, Cerdà J. 2013. Primary oocyte transcriptional activation of Aqp1ab by the nuclear progestin receptor determines the pelagic egg phenotype of marine teleosts. *Dev Biol*. 377(2):345-62. doi: 10.1016/j.ydbio.2013.03.001.

Zhang X, Yu p, Wen H, Qi X, Tian Y, Zhang K, Fu Q, Li Y, Li C. 2021. Genome-wide characterization of aquaporins (aqps) in *Lateolabrax maculatus*: Evolution and expression patterns during freshwater acclimation. *Mar Biotechnol*. 23(5):696-709. doi: 10.1007/s10126-021-10057-0.

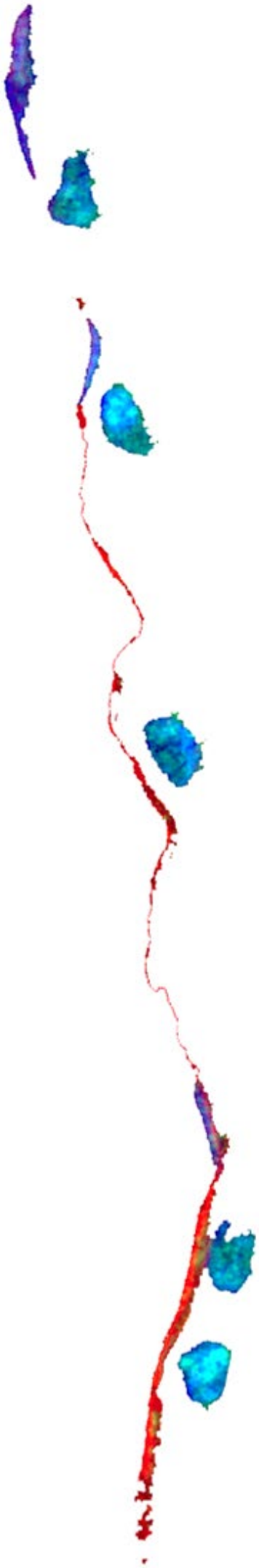

CONCLUSIONS

1. The analysis of >400 piscine genomes has uncovered a previously unknown teleost-specific aquaporin-1 cluster (TSA1C) comprised of tandemly arranged *aqp1aa-aqp1ab2-aqp1ab1* genes. Functional evolutionary analysis of the TSA1C reveals a ~300-million-year history of downstream *aqp1ab*-type gene loss, neofunctionalization, and subfunctionalization, but with marine species that spawn highly hydrated pelagic eggs almost exclusively retaining at least one of the downstream paralogs.

2. The phosphorylation of specific residues in the C-termini and intracellular loop D of the TSA1C channels by protein kinase A (PKA) and protein kinase C (PKC) plays a pivotal role in the regulation of their intracellular trafficking.

3. Teleost-specific Ywhaz-like (14-3-3ζ-like) binding proteins, YwhazLa and YwhazLb, are involved in the trafficking of Aqp1ab1 and Aqp1ab2. They can bind to these aquaporins in a PKA phosphorylation-dependent manner, facilitating their proper subcellular sorting to the plasma membrane. Each channel co-evolved with the YwhazL regulatory proteins, with Aqp1ab1 preferentially binding to YwhazLa, and Aqp1ab2 specifically requiring YwhazLb.

4. Immunolocalization and functional data suggest a novel mechanism during oocyte hydration in euacanthomorph marine teleosts such as the gilthead seabream (*Sparus aurata*) that retains both *aqp1ab*-type genes. During vitellogenesis in the seabream, Aqp1ab1 is phosphorylated at Ser^{253} by PKA (or by another kinase activated by PKA) to bind YwhazLa and -zLb, and the complex is transported to the oocyte cortical region, where it is retained just below the oocyte plasma membrane. At this stage, Aqp1ab2 is not bound to YwhazLb and remains in the cytoplasm. When meiosis resumption and yolk hydrolysis are activated in oocytes by hormonal signals, the Aqp1ab1 channel complexed with YwhazLa or -zLb is phosphorylated again by PKA at Ser^{156} in loop D, which further shuttles Aqp1ab1 to the most distal region of the oocyte microvilli. At this time, Aqp1ab2 is also phosphorylated by PKA at Thr^{262}, which drives the YwhazLb interaction and the trafficking of the channel to the proximal region of the oocyte microvilli. The hydration process is terminated though the evolution of p38 MAPK-mediated phosphorylation sites in the YwhazLa binding region of Aqp1ab1, which dissociates the interaction with YwhazLa, and through a different mechanism also resulting in the release of the YwhazLb from Aqp1ab2. This model may explain how marine euacanthomorph marine teleosts that retain a complete TSA1C evolved

subfunctionalized mechanisms involving protein kinases and specific YwhazL proteins for the trafficking regulation of the downstream Aqp1ab-type paralogs, such that competitive plasma membrane spatial occupancy is avoided and the bulk water flow is augmented during oocyte hydration.

5. We show that, concomitant with an increased systemic production of the nonapeptides arginine vasopressin (Avp, formerly vasotocin) and oxytocin (Oxt, formerly isotocin) during oocyte maturation and hydration, the nonapeptides are also produced and accumulated locally in the ovarian follicles.

6. In addition, functional characterization of representative Avp and Oxt receptor subtypes indicates that Avpr1aa and Oxtrb are expressed in the postvitellogenic oocyte and activate phospholipase C and PKC pathways, while Avpr2aa, which is highly expressed in the oocyte and in the follicular theca and granulosa cells, activates the cAMP-PKA cascade.

7. The data suggest that the ovarian vasopressinergic system represents the endocrine signal that regulates oocyte hydration during meiosis resumption in the gilthead seabream. In this model, the ovarian vasopressinergic system is possibly activated via systemic neuroendocrine signaling to multiply the luteinizing hormone induction of progestin which generates Avp for the paracrine signaling. Thus, the oocyte Avpr2aa paralog, which activates PKA, plays a vital role in the transduction of the paracrine signals and the co-ordinated trafficking of the Aqp1ab-type channels, so that they avoid competitive occupancy of the same membrane space and maximize the hydration of the oocyte.

8. In species that encode the full TSA1C, such as the gilthead seabream and Atlantic halibut (*Hippoglossus hippoglossus*), we found ovarian expression of different in-frame intronic splice variants of Aqp1ab1 that result in truncated proteins. Conversely, in species that only encode the Aqp1ab2 channel, such as the Senegalese sole (*Solea senegalensis*) and common sole (*S. solea*), we found an in-frame intronic splice variant that results in an intact protein with an extended extracellular loop E, and an out-of frame intronic splice variant with exon readthrough that results in a truncated protein.

9. None of the Aqp1ab1 or Aqp1ab2 variants identified are functional when expressed in *Xenopus laevis oocytes*. On the contrary, they all cause dominant-negative inhibition of

the canonical channel function, but through different mechanisms. For some of the splice forms the inhibition likely occurs through hetero-oligomerization with the canonical channel and retention in the endoplasmic reticulum (ER), which will rapidly be targeted for degradation, whereas others can partially escape from the ER to reach the oocyte plasma membrane, where they dominantly-negatively inhibit water flux.

10. In the Senegalese sole, the ovarian follicular protein expression ratios of the Aqp1ab2 isoforms in relation to the canonical channel are lowest during oocyte hydration, but subsequently highest when the canonical channel is recycled, thus leaving the eggs endowed with >90% water. Therefore, in marine pelagophil species that retain only one of the *aqp1ab*-type genes, such as soleids, our data suggest that regulatory repression mechanisms achieved through splice variation may be relatively more important for the maintenance of hydration than in species that encode the complete TSA1C.

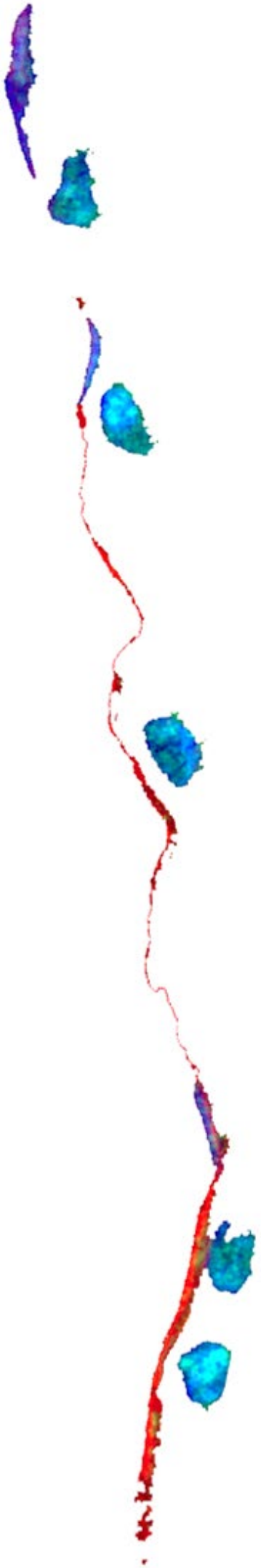

ANNEXES

Table of Contents:

6.1. Supplementary Material Chapter I

6.1.1. Supplementary Figures S1-S4

https://drive.google.com/file/d/114fbHZLAEAPHN3fYuhvYWMSMiCaWV8-X/view?usp=share_link

6.1.2. Supplementary Data SD1-SD5

https://drive.google.com/file/d/14U5Q0_0pDtQmRIelYFvuc6sT-hOlnJ2k/view?usp=share_link

6.1.3. Supplementary Data SD6-SD11

https://drive.google.com/file/d/1OUb2j_FxImdjxOUdRNSlvx4ppcPNWaLe/view?usp=share_link

6.1.4. Supplementary Figure S5

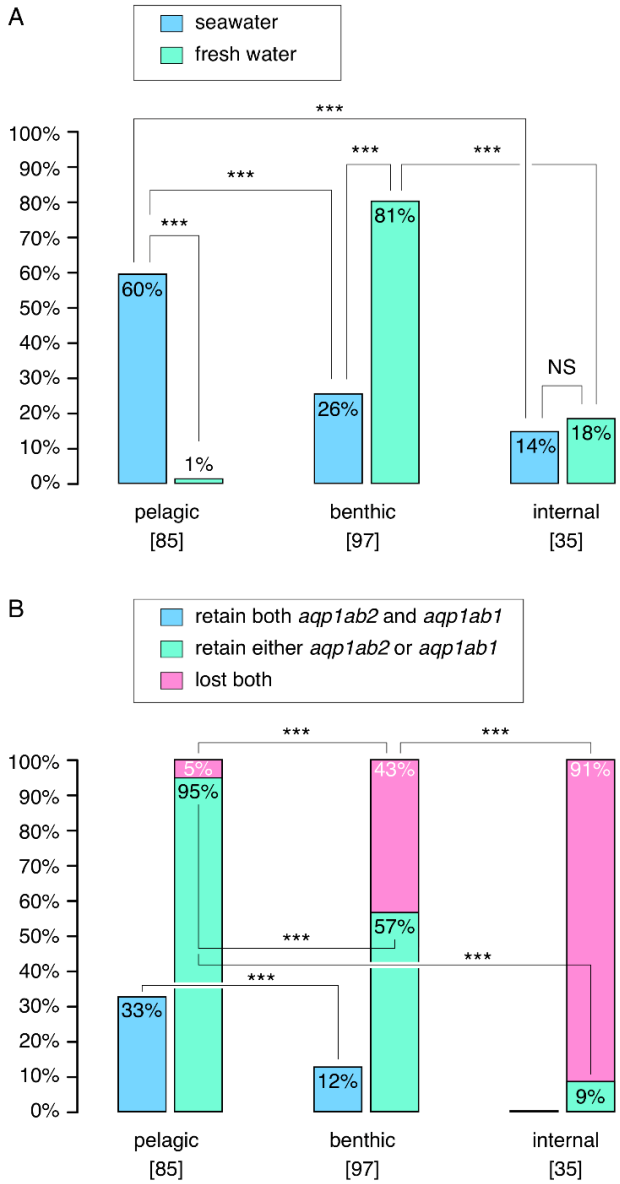

Figure S5. Relationship between egg type and the retention of *aqp1ab*-type genes in Euacanthomorphacea. (**A**) The relative fraction of species spawning pelagic or benthic eggs, or incubating their eggs internally in relation to their marine and freshwater spawning habitats. The number of species analyzed from 217 genomes is indicated in square brackets. Statistical differences were analyzed via the critical z-value approach ($P < 0.001$ ***; with NS indicating no significant difference). (**B**) The relative fraction of species that retain both *aqp1ab*-type paralogs, either one of the *aqp1ab*-type paralogs or have lost both paralogs in relation to the pelagic, benthic or internal nature of their eggs. The number of species analyzed and statistical differences as in (A).

6.1.5. Supplementary Figure S6

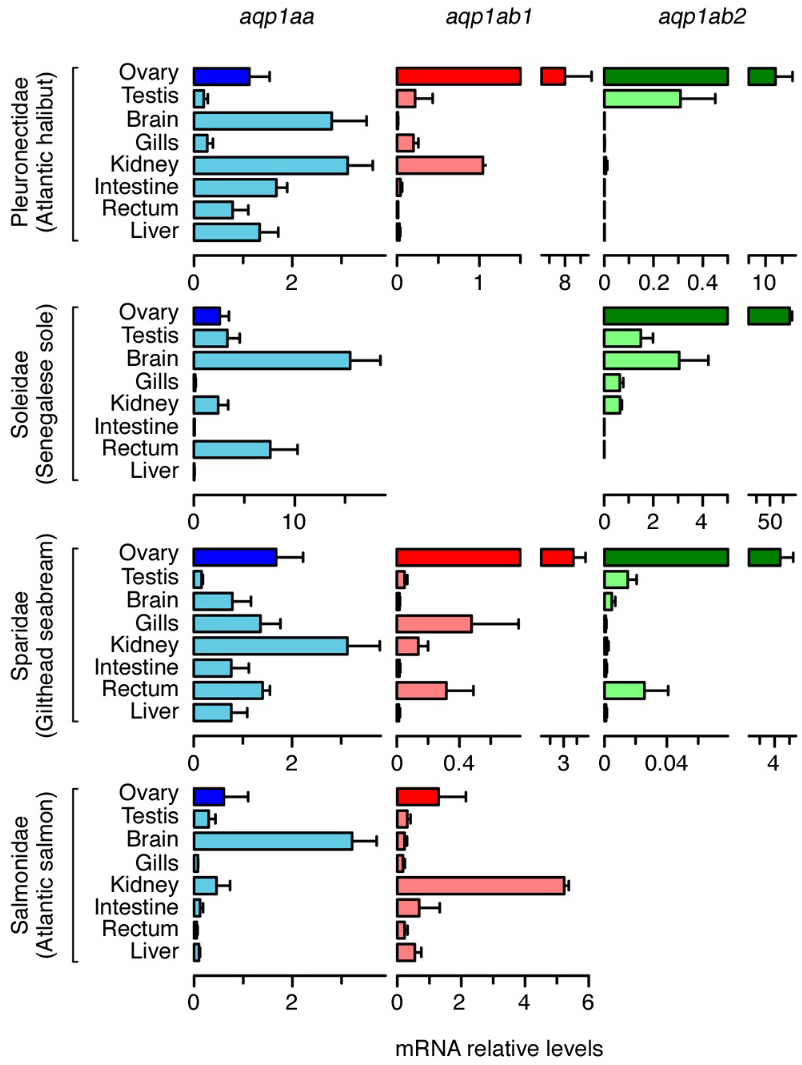

Figure S6. Tissue distribution of *aqp1*-like mRNA expression in representative teleosts. Relative mean expression levels of *aqp1aa*, *aqp1ab1* and *aqp1ab2*, normalized to the expression of the *b-actin* gene, in different adult tissues from distantly related teleosts determined by qRT-PCR. Data are means ± SEM (n = 3 fish).

Extraction of total RNA and qRT-PCR analyses were carried out as previously described (Zapater *et al*., 2011). The relative transcript levels were calculated by using a standard curve generated for each primer pair from 10-fold serial dilutions of a pool of first-stranded cDNA template from ovary samples. All calibration curves exhibited correlation coefficients higher than 0.98. Primer sequences and amplification efficiencies are listed in (supplementary table S4; see Annexes, page 260). The 18S ribosomal RNA (*rps18*) was used as reference gene.

6.1.6. Supplementary Figure S7

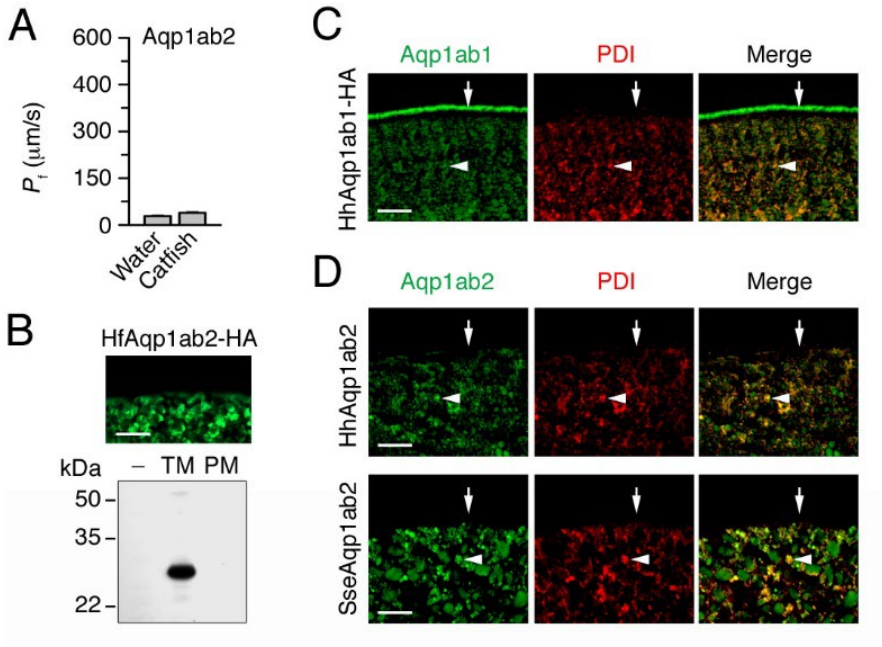

Figure S7. Functional characterization of Aqp1ab1 and Aqp1ab2 in additional teleosts. (**A**) P_f of *X. laevis* oocytes injected with water or expressing wild-type Aqp1ab2 from the stinging catfish (*Heteropneustes fossilis*). Data are the mean ± SEM (n = 22 oocytes). (**B**) Immunolocalization (upper panel) and immunoblot of total and plasma membrane (TM and PM) protein extracts (lower panel) of wild-type catfish HA-tagged Aqp1ab2 in oocytes expressing the channel. Molecular mass markers (kDa) are on the left. (**C**, **D**) Double immunostaining of oocytes expressing HhAqp1ab1 or -1ab2, or SseAqp1ab2, and the protein disulfide isomerase (PDI) endoplasmic reticulum (ER) marker. The PM of oocytes is indicated by arrows, whereas the arrowheads indicate colocalization of the channels with the PDI in the oocyte cytoplasm. In B, C and D, scale bars, 25 µm.

6.1.7. Supplementary Figure S8

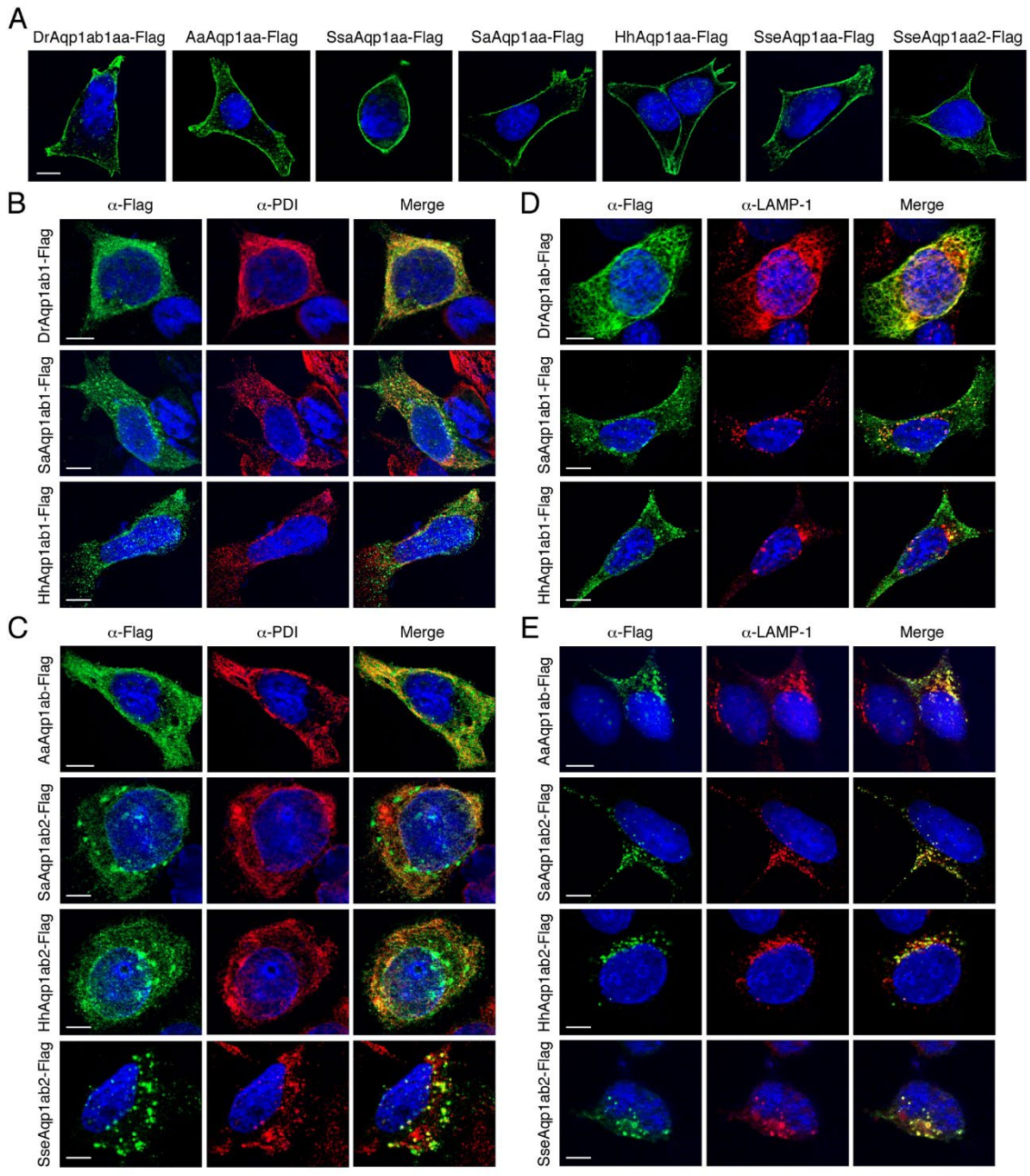

Figure S8. Expression of teleost Aqp1aa, -1ab1 and -1ab2 channels in cultured mammalian cells. (**A**) Immunostaining of MCF-7 cells transiently transfected with Flag-tagged Aqp1aa from different teleosts. (**B**-**E**) Double immunostaining of Flag-tagged Aqp1ab1 or Aqp1ab2 from different teleosts with the ER marker PDI (B and C) or the lysosomal marker LAMP-1 (D and E) in MCF-7 cells transiently transfected with each channel. Scale bars, 10 µm.

The breast cancer Michigan Cancer Foundation-7 (MCF-7, ATCC # HTB-22^{TM}) cells were grown at 37°C in an atmosphere of air/CO_2 [95:5 (v/v)] in Dulbecco's modified Eagle's medium (DMEM) supplemented with 10% v/v fetal bovine serum (FBS), 260 U/ml of

penicillin and streptomycin, and 2 mM L-glutamine in 12 wells plate containing 15 mm-diameter round coverslips (Electron microscopy Sciences, 72196-15). At 70% of confluence, cells were transiently transfected with 2.5 µg of pcDNA3-aquaporin constructs using Lipofectamine 3000 (Invitrogen). The following day, the medium was replaced with fresh medium and cells were processed for immunofluorescence microscopy 48 h after transfection.

For immunofluorescence of MCF-7 cells, transfected cells attached to round coverslips were fixed in methanol during 6 min at -20ºC, and subsequently permeabilized in cold acetone for 30 s. Cells were washed twice in PBS and then permeabilized again with PBS plus 0.2% Triton X-100 for 10 min. The blocking step and incubation with primary and secondary antibodies was carried out as described for ovarian samples.

6.1.8. Supplementary Figure S9

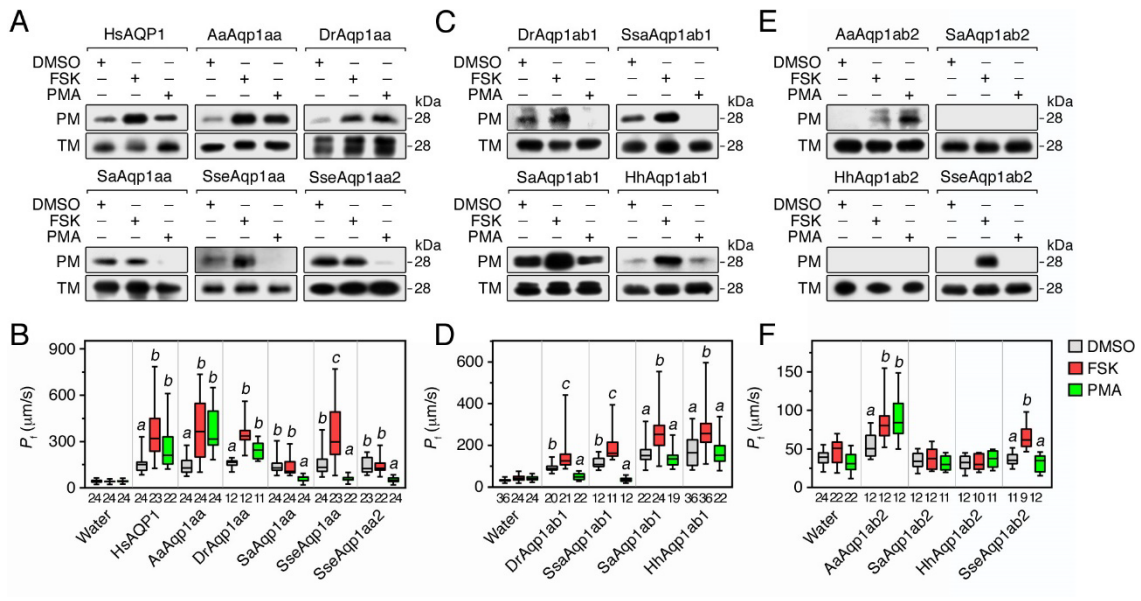

Figure S9. Regulation of teleost Aqp1-like channel trafficking by PKA and PKC. (**A**, **C** and **E**) Immunoblots of total (TM) and plasma (PM) membrane protein extracts from *X. laevis* oocytes expressing HsAQP1 (A), or each Aqp1aa (A), -1ab1 (C) or -1ab2 (E) paralog from different teleosts, and exposed or not to IBMX/FSK or PMA as indicated. Molecular mass markers (kDa) are on the right. (**B**, **D** and **F**) Effect of IBMX/FSK and PMA on the P_f of oocytes expressing wild-type (WT) HsAQP1 or teleost Aqp1aa (B), -1ab1 (D) and -1ab2 (E) channels. Data are presented as box and whisker plots with the number of oocytes in each group indicated below each plot, and were analyzed by one-way ANOVA ($P < 0.05$; bars with different superscript are statistically significant) for each control or construct.

The Aqp1aa, -1ab1 and -1ab2 paralogs from different teleosts, as well as the human AQP1 (HsAQP1) as a positive control, were heterologously expressed in *X. laevis* oocytes, which were exposed to either the PKC activator phorbol 12-myristate 13-acetate (PMA) or the cAMP-PKA activator, forskolin (FSK), respectively. In the latter instance, the FSK-exposed oocytes were pre-incubated with the phosphodiesterase inhibitor 3-isobutyl-1-methylxanthine (IBMX) to prevent rapid cAMP degradation. We then determined the changes in plasma membrane channel content via Western blots of the total and plasma membrane extracts of oocytes, and corroborated the observations by oocyte P_f quantification. Injection of HsAQP1 and exposure of the oocytes to PMA or FSK consistently resulted in an increase of the channel in the plasma membrane fraction and of the P_f compared to the controls treated with the DMSO vehicle (figure S9A and B), thus confirming previous observations (Nesverova and Törnroth-Horsefield, 2019). Similarly, in oocytes expressing Aqp1aa from elopomorph and cyprinid teleosts (AaAqp1aa and DrAqp1aa) both FSK and PMA also increase membrane channel trafficking and oocyte P_f,

but in oocytes injected with Aqp1aa orthologs from the euacanthomorph teleosts (SaAqp1aa, SseAqp1aa or -1aa2) only FSK stimulated channel trafficking of SseAqp1aa, while PMA was inhibitory for each of the three channels (figure S9A and B). For oocytes expressing teleost-specific Aqp1ab1, FSK triggered plasma membrane transport and an increase in the P_f of all the channels investigated (DrAqp1a1, SsaAqp1ab1, SaAqp1ab1 and HhAqp1ab1), whereas PMA reduced the trafficking of DrAqp1ab1 and SsaAqp1ab1, but had no effect on SaAqp1ab1 and HhAqp1ab1 (figure S9C and D). In contrast, in oocytes expressing teleost Aqp1ab2 (AaAqp1ab2, SaAqp1b2, HhAqp1ab2 or SseAqp1ab2) each channel was retained in the cytoplasm, and only trafficked to the plasma membrane in response to FSK or PMA in the case of AaAqp1ab2, or with only FSK for SseAqp1ab2, whereas in other species this channel did not respond to either of the two drugs (figure S9E and F). Altogether, these data suggest that HsAQP1 and Aqp1aa from older teleost lineages share a similar pattern of trafficking regulation, while the control of the Aqp1aa orthologs of euacanthomorph species, as well as of the teleost-specific Aqp1ab1 and -1ab2, appears to be more divergent.

6.1.9. Supplementary Figure S10

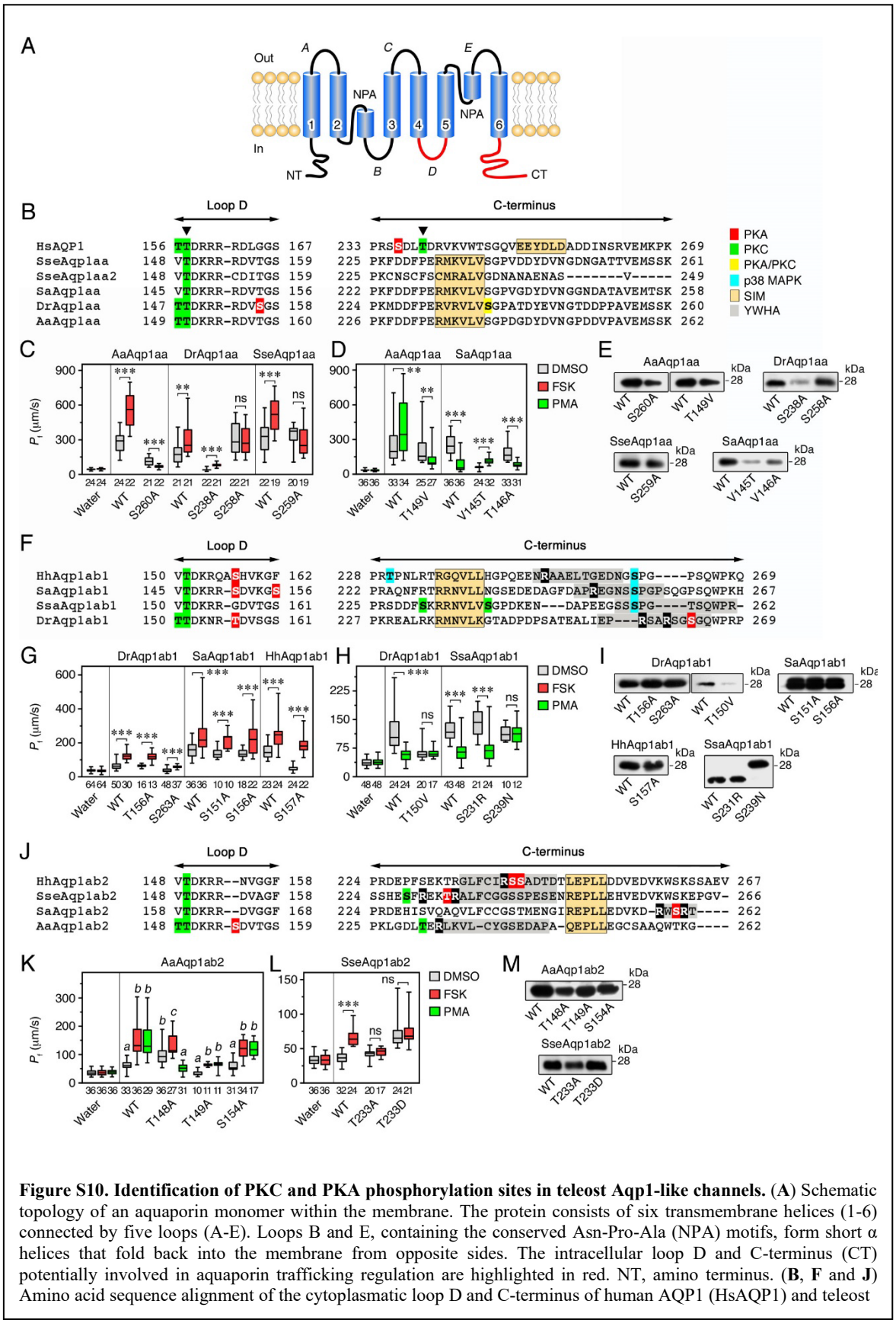

Figure S10. Identification of PKC and PKA phosphorylation sites in teleost Aqp1-like channels. (**A**) Schematic topology of an aquaporin monomer within the membrane. The protein consists of six transmembrane helices (1-6) connected by five loops (A-E). Loops B and E, containing the conserved Asn-Pro-Ala (NPA) motifs, form short α helices that fold back into the membrane from opposite sides. The intracellular loop D and C-terminus (CT) potentially involved in aquaporin trafficking regulation are highlighted in red. NT, amino terminus. (**B**, **F** and **J**) Amino acid sequence alignment of the cytoplasmatic loop D and C-terminus of human AQP1 (HsAQP1) and teleost

Aqp1aa (B), -1ab1 (F) and -1ab2 (J). Predicted phosphorylation sites by PKA (red), PKC (green), PKA and PKC (yellow) and p38 MAPK (blue), as well as sorting and internalization motifs (SIM, orange), are indicated. The specific residues involved in PKC-mediated HsAQP1 trafficking previously identified are indicated by arrowheads. For Aqp1ab1 and -1ab2, putative YWHA binding regions, showing the typical Arg residue shaded in black, are indicated by grey color. (**C**-**D**, **G**-**H** and **K**-**L**) Mutagenesis analysis of potential sites involved in the PKA or PKC trafficking regulation of teleost Aqp1-like channels. In all panels, data are presented as box and whisker plots with the number of oocytes in each group indicated below each plot. Data in G, H and L were analyzed by the unpaired Student's *t*-test (**, $P < 0.01$; ***, $P < 0.001$; as indicated in brackets), whereas data in K were analyzed by one-way ANOVA ($P < 0.05$; bars with different superscript are statistically significant) for each construct. ns, statistically not significant. (**E**, **I** and **M**) Immunoblots of total membrane (TM) protein extracts from oocytes expressing the wild-type (WT) or mutant Aqp1aa, -1ab1 or -1ab2 channels shown in C-D, G-H and K-L. Molecular mass markers (kDa) are on the right

In order to identify the regulatory sites involved in the intracellular trafficking of the TSA1C gene products, we conducted *in silico* searches for putative PKA- or PKC-mediated phosphorylation sites in the intracellular loop D and C-terminus of each channel (figure S10A), followed by site-directed mutagenesis experiments. For Aqp1aa, *in silico* data indicated DrAqp1aa Ser^{156} and Ser^{238} were the only predicted residues for PKA phosphorylation (figure S10B). This would be consistent with the previously observed positive effect of FSK on channel trafficking to the plasma membrane of *X. laevis* oocytes expressing this paralog. However, these sites are not conserved in AaAqp1aa or SseAqp1aa, which are also stimulated by FSK to traffic to the plasma membrane (figure S9A and B). Further inspection of the amino acid sequences in the C-termini of AaAqp1aa, DrAqp1aa and SseAqp1aa, respectively, identified several conserved Ser residues (Ser^{260}, Ser^{258} and Ser^{259}), which are not predicted as putative phosphorylation sites. However, mutation of these sites into an Ala blocked the stimulatory effect of FSK on oocyte P_f observed in *X. laevis* oocytes expressing the wild-type channels (figure S10B and C). These C-terminal Ser residues were thus identified as the likely PKA-mediated phosphorylation targets that stimulate AaAqp1aa, DrAqp1aa and SseAqp1aa trafficking.

The double Thr residues in loop D of AaAqp1aa and DrAqp1aa, $Thr^{149,150}$ and $Thr^{147,148}$, respectively, are conserved with respect to HsAQP1, and are both predicted as PKC phosphorylation sites, (figure S10B). In HsAQP1, however, only Thr^{157} is involved in the PKC-mediated positive regulation of channel trafficking (Nesverova and Törnroth-Horsefield, 2019; figure S10B). In eel AaAqp1aa, mutation of Thr^{149} into an Ala reversed the effect of PMA on oocyte P_f (figure S10D). This suggests that the first Thr in loop D of Aqp1aa of elopomorph, and possibly of cyprinid teleosts, determines the positive or negative directional effect that PKC has on channel transport. In contrast, in the Aqp1aa orthologs of the euacanthomorph teleosts (SaAqp1aa, SseAqp1aa and -1aa2), the first Thr

in loop D is naturally substituted by a Val, and PMA inhibits rather than stimulates channel trafficking (figures S9B and S10D). However, when Thr^{146} in loop D of seabream SaAqp1aa was substituted by an Ala, PMA still elicited an inhibitory effect on oocyte P_f (figure S10D), indicating that alternative residues, outside of loop D, are likely involved in the PKC inhibition of Aqp1aa trafficking in euacanthomorph teleosts.

Activation of PKA stimulated plasma membrane Aqp1ab1 trafficking in all species analyzed (figure S9D). Accordingly, amino acid sequence alignment of teleost Aqp1ab1 paralogs and searches for putative phosphorylation sites identified loop D Thr^{156} and Ser^{263} in DrAqp1ab1, Ser^{151} and Ser^{156} in SaAqp1ab1, and Ser^{157} in HhAqp1ab1, as predicted PKA phosphorylation sites that could mediate this regulation (figure S10F). However, mutation of these residues into Ala did not prevent the positive effect of FSK (figure S10G), indicating that the *in silico* predicted sites are not functional. The alignment did not reveal any other conserved residue predicted to be phosphorylated by PKA, and therefore the residues involved in the PKA-mediated positive effect on teleost Aqp1ab1 trafficking were not identified.

In the Aqp1ab1 channels we also found that the conserved C-terminal Ser^{254}, Ser^{250} and Ser^{254} residues in SsaAqp1ab1, SaAqp1ab1 and HhAqp1ab1, respectively, are each predicted to be p38 mitogen-activated protein kinase (p38 MAPK) phosphorylation sites (figure S10F). Phosphorylation by p38 MAPK has previously been shown to reduce plasma membrane trafficking in frog oocytes expressing SaAqp1ab1 (Tingaud-Sequeira *et al*., 2008). The identified p38MAPK sites are conserved in the C-termini of most (74%) of the euteleost species examined, but are not found in the otophysan lineages of siluriform and clupeiform teleosts that also retain intact *aqp1ab1* genes. In contrast to the evolution of inhibitory p38 MAPK sites in euteleosts, PMA-activation of PKC only inhibited the trafficking of the Aqp1ab1 from more basal lineages of ostariophysan and protacanthopterygian teleosts, such as DrAqp1ab1 and SsaAqp1ab1 (figure S9D and 5H; see Chapter I, page 99). However, mutagenesis experiments revealed that the residues involved in this mechanism are different for each channel. Thus, in DrAqp1ab1 Thr^{150} in loop D is the functional PKC site, whereas Ser^{239} in the C-terminus of SsaAqp1ab1 appears to be the residue involved, since mutations in these sites abolished the negative effect of PMA on oocyte P_f (figure S10H).

Altogether, these observations suggest that PKA-mediated phosphorylation pathways evolved to promote the trafficking of Aqp1ab1 channels to the plasma membrane, although the specific residues were not yet identified. Conversely, an evolutionary switch between PKC-mediated phosphorylation pathways and those of p38 MAPK respectively occurred between the pre-euteleostean and euteleostean lineages to regulate Aqp1ab1 recycling from the membrane. Interestingly, in salmonids, which represent some of the earliest euteleosts to evolve, the SsaAqp1ab1 channel retain both of the inhibitory PKC and p38 MAPK sites respectively identified in the older pre-euteleostean channels and modern euacanthomorph channels, which reaffirms the notion of an evolutionary switch between the inhibitory pathways.

For the Aqp1ab2 paralogs, the PKA and/or PKC activation of *X. laevis* oocytes expressing elopomorph AaAqp1ab2 and euacanthomorph SseAqp1ab2 stimulated channel trafficking (figure S9F). Mutagenesis experiments showed that, as in AaAqp1aa, the predicted loop D PKC phosphorylation site at Thr^{148} of AaAqp1ab2 (figure S10J) is the functional site promoting trafficking to the plasma membrane (figure S10K). However, mutation of the only predicted PKA phosphorylation site identified in loop D of AaAqp1ab2 (Ser^{154}) (figure S10J) did not affect the stimulatory effect of FSK on the oocyte P_f (figure S10K), as observed for the Aqp1ab1-expressing oocytes. By contrast, in the euacanthomorph SseAqp1ab2 the C-terminal Thr^{233} appears to be the site for the PKA-mediated activation of channel trafficking since mutation of this site into an Ala prevented the effect of FSK, while its substitution by an Asp, which mimics constitutive phosphorylation, resulted in an increased P_f of oocytes with respect to those expressing the wild-type regardless of FSK treatment (figure S10L).

Finally, for most of the aquaporins tested, immunoblotting experiments showed that the frog oocytes expressed equivalent amounts of the wild-type and mutants (figure S10E, I and M), indicating that the observed effects were not caused by differential expression mechanisms. These experiments thus show that the intracellular trafficking of the TSA1C is differentially regulated by PKA and PKC, and also by p38 MAPK in the case of Aqp1ab1, but that the specific residues involved in these regulations appear to have changed with the evolution of the different lineages, and in most cases not detected by prediction softwares currently available.

6.1.10. Supplementary Figure S11

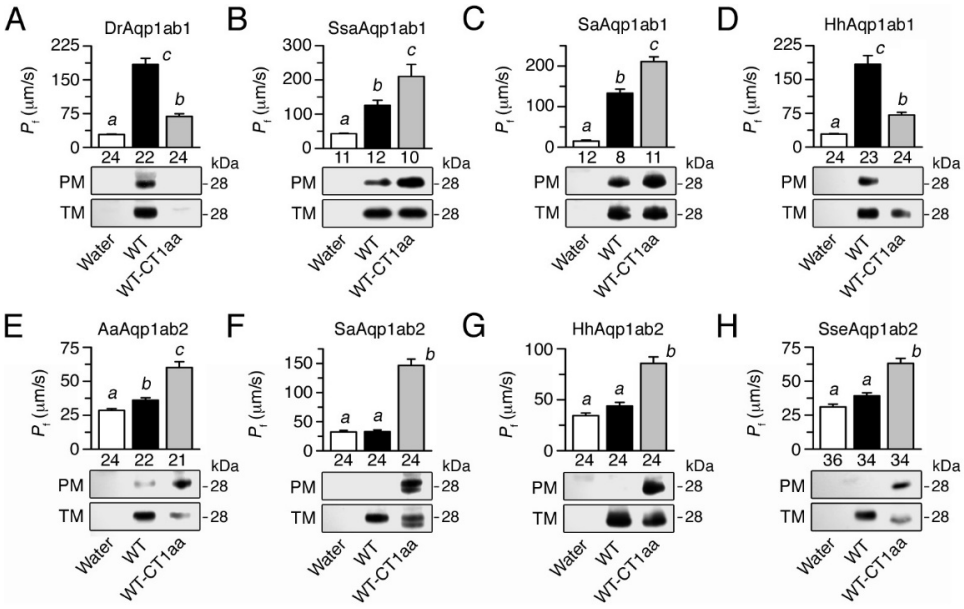

Figure S11. Functional properties and subcellular accumulation of teleost Aqp1-like channels and chimeric proteins. (**A-D**) P_f (upper panels) and immunoblot of total and plasma membrane (TM and PM, respectively) protein extracts (lower panels) of *X. laevis* oocytes expressing Aqp1ab1-wild-type (WT), or chimeric channels in which the C-terminus of Aqp1ab1 was exchanged with that of Aqp1aa, from different teleosts as indicated. (**E-H**) The same analyses were carried out for both distantly, and closely related teleost Aqp1ab2 channels. For each plot, the numbers below the bars indicate the number of oocytes analyzed. In all panels, data were statistically analyzed by one-way ANOVA ($P < 0.05$; bars with different superscript are statistically significant). In the blots, molecular mass markers (kDa) are on the right.

Expression vectors were constructed in which the C-terminal domain of the Aqp1ab1 (DrAqp1ab1, SsaAqp1ab1, SaAqp1ab1, HhAqp1ab1) and the Aqp1ab2 (AaAqp1ab2, SaAqp1ab2, HhAqp1ab2 and SseAqp1ab2) channels was exchanged with that of Aqp1aa for each species. These chimeras, as well as the wild-type Aqp1ab1 or -1ab2 channels, were expressed in *X. laevis* oocytes and the P_f and protein abundance at the oocyte plasma membrane monitored. The P_f of oocytes expressing chimeric SsaAqp1ab1-1aaCT and SaAqp1ab1-1aaCT was increased with respect to wild-type Aqp1ab1-expressing oocytes, which was correlated with a higher accumulation of the chimeras in the plasma membrane (figure S11A-D). However, chimeric DrAqp1ab1-1aaCT and HhAqp1ab1-1aaCT were not well expressed in oocytes, as the oocytes showed a decreased P_f and lower protein levels of these channels with respect to the wild-types (figure S11A and D). In contrast, oocytes injected with any of the chimeric Aqp1ab2-1aaCT channels showed increased protein levels in the plasma membrane and water permeabilities when compared to oocytes expressing the wild-types (figure S11E-H).

6.1.11. Supplementary Figure S12

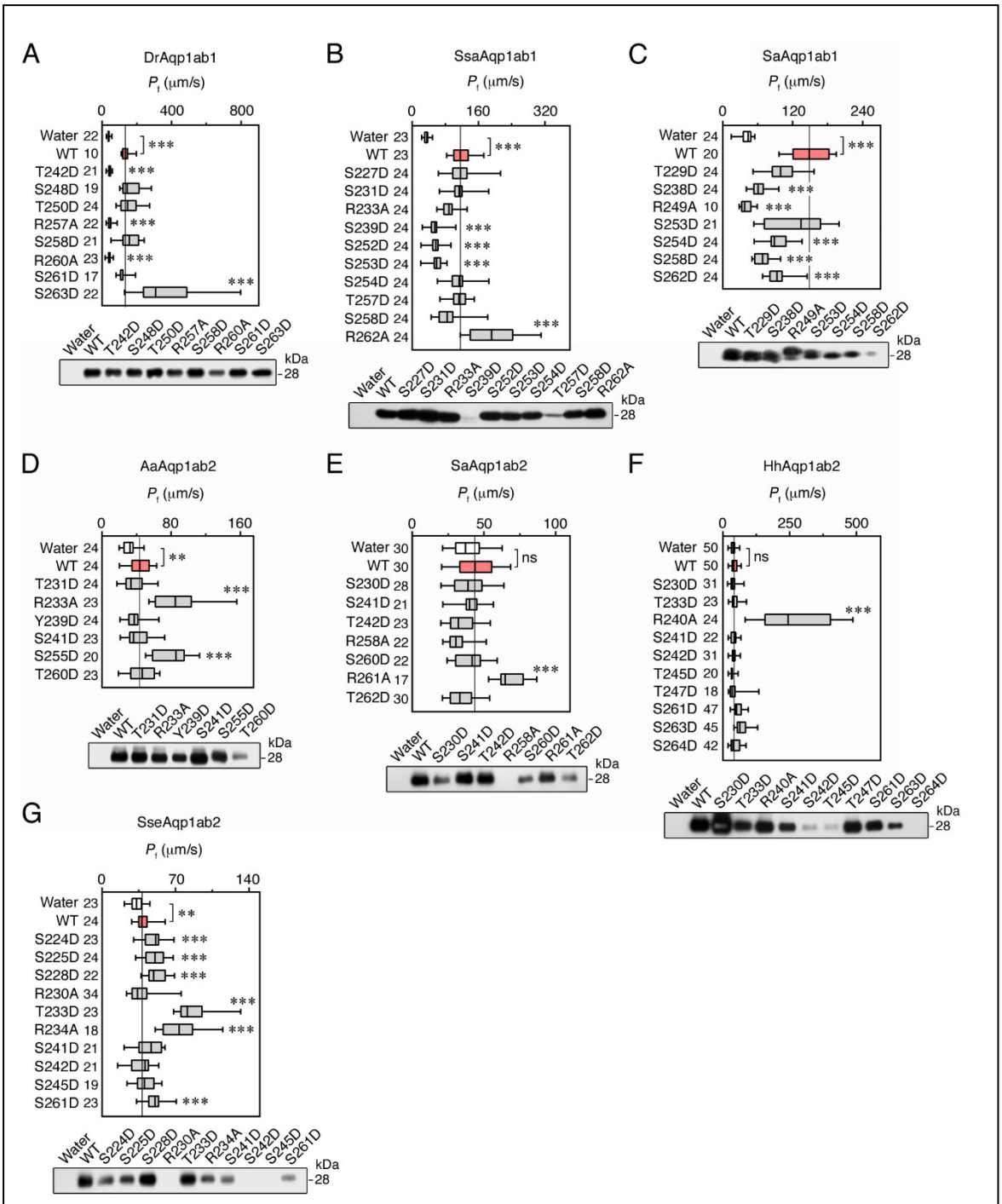

Figure S12. Effects of Aqp1ab1 and -1ab2 C-terminal single mutants on oocyte P_f. (**A-G**) P_f of *X. laevis* oocytes injected with water or expressing Aqp1ab1-wild-type (WT) (A-C) or Aqp1ab2-WT (D-G) from different teleosts, or channel mutants carrying single point mutations in the C-terminus as indicated. The line indicates the level of P_f of oocytes expressing the WT channels (red boxes). The numbers on the left of the plots indicate the number of oocytes analyzed. Below the plots are the immunoblots showing the expression levels of the WT and mutant channels in total membrane protein extracts. The P_f data were analyzed by the unpaired Student's *t*-test (**, $P < 0.01$; ***, $P < 0.001$; with respect to the WT or as indicated in brackets). ns, statistically not significant.

To further identify which specific residues could be involved in these mechanisms, we carried out a mutagenesis screen in which all potential phosphorylation sites in the C-terminus of DrAqp1ab1, SsaAqp1ab1, SaAqp1ab1, AaAqp1ab2, SaAqp1ab2, HhAqp1ab2 and SseAqp1ab2 were independently substituted by Asp to mimic a phosphorylation state. The wild-type and mutants were then expressed in *X. laevis* oocytes and the P_f determined. *In silico* analysis of the C-termini of these channels also revealed the presence of potential binding motifs for YWHA (14-3-3) regulatory proteins (figure S10F and J), which can bind various signaling and membrane proteins, including plant and animal aquaporins, in a PKA-mediated Ser/Thr phosphorylation-dependent manner (Fu *et al*., 2000; Moeller *et al*., 2016; Prado *et al*., 2019). The YWHA interaction motif usually contains an Arg residue in the target protein that increases binding affinity (Rajan *et al*. 2002; Shikano *et al*., 2005), and therefore some additional Aqp1ab1 and -1ab2 mutants were constructed in which this residue was replaced by an Ala. Oocytes expressing the different DrAqp1ab1 mutants did not show an elevated P_f with respect to those injected with the wild-type, except for the DrAqp1ab1-S263D mutant (figure S12A,), which suggested that this paralog has an additional PKA phosphorylation site, since previous mutation of this site into an Ala did not prevent the positive effect of FSK on the oocyte P_f (figure S10G). For salmonid SsaAqp1ab1, the only mutant which showed an increase in the P_f with respect to the wild-type was the SsaAqp1ab1-R262A (figure S12B), in which the Arg located within the putative YWHA binding site was replaced by an Ala (figure S10F). In contrast, none of the mutations in the euacanthomorph SaAqp1ab1 C-terminus had a positive effect on the wild-type-induced oocyte P_f, rather most of the mutations resulted in the degradation of the channels as judged by immunoblot analysis of protein expression (figure S12C).

For the Aqp1ab2 channels (AaAqp1ab2-R233A, SaAqp1ab2-R261A, HhAqp1ab2-R240A and SseAqp1ab2-R234A), we observed a consistent increase of the oocyte P_f with respect to that induced by the wild-type when the Arg residue within the putative C-terminal YWHA binding region was mutated (figure S10J and S12D-G). These results suggested that binding of teleost Aqp1ab2 to a teleost-specific YWHA carrier protein might be involved in the channel trafficking regulation. However, in some species, which only retain the Aqp1ab2 and not the Aqp1ab1 channel, mutations of single C-terminal residues into Asp outside of the potential YWHA binding region, such as Ser^{255} in AaAqp1ab2, and Thr^{233} in SseAqp1ab2 (figure S10J), clearly incremented the P_f of

oocytes with respect to that of oocytes injected with the wild-type (figure S12D and G). This type of regulation reflected that observed for DrAqp1ab1. Taken together, the data suggested that in species retaining only one Aqp1ab-type paralog, such as the zebrafish (DrAqp1ab1), European eel (AaAqp1ab2) and sole (SseAqp1ab2), phosphorylation mechanisms that are both dependent and independent of YWHA binding might regulate channel trafficking.

6.1.12. Supplementary Figures S13-S14

https://drive.google.com/file/d/1Bb31veSy7JH5rKBndJ3cd-Ni7B1SGKx0/view?usp=share_link

6.1.13. Supplementary Figure S15

Binding of YwhazL Proteins Regulates Aqp1ab1 and -1ab2 Trafficking in *X. laevis* Oocytes

Full-length cDNAs encoding seabream YwhazLa and -zLb were isolated and the corresponding HA- or Flag-tagged cRNAs co-expressed in *X. laevis* oocytes with HA-tagged DrAqp1ab1 or untagged SaAqp1ab1 (figure S15; see below). The P_f of oocytes, the trafficking of the channels to the oocyte plasma membrane, and their interaction with YwhazLa or -zLb carrier proteins assessed by co-immunoprecipitation experiments, was further investigated in response to FSK. Oocytes expressing DrAqp1ab1 or SaAqp1ab1 alone, or together with YwhazLb, showed the same increment in P_f in response to FSK (figure S15A and B). However, when YwhazLa was co-expressed with each of the channels a higher increment of oocyte permeability was detected after FSK treatment, which correlated with more accumulation of the channels in the plasma membrane (figure S15C and D). The YwhazLa, but not YwhazLb, could be detected in immunoprecipitated extracts from oocytes stimulated with FSK using either an HA antibody (for DrAqp1ab1) or a specific SaAqp1ab1 antibody (figure S15E and F), thus indicating that DrAqp1ab1 and SaAqp1ab1 preferentially bind YwhazLa in response to PKA phsophorylation. A similar higher increment of P_f was observed in FSK treated oocytes expressing SsaAqp1ab1 and seabream YwhazLa, or HhAqp1ab1 and halibut YwhazLa, with respect to oocytes injected with the channels alone or together with the corresponding YwhazLb proteins (figure S17A). These findings suggested that plasma membrane trafficking of teleost Aqp1ab1 channels can be partially regulated by heterologous frog YWHA proteins, but that this mechanism is more efficiently controlled by the binding to the teleost-specific YwhazLa paralogs.

Further mutagenesis experiments revealed that the YwhazLa interaction is likely initiated by the PKA-mediated phosphorlation of Ser^{261} within the YWHA binding region of the DrAqp1ab1 C-terminus. This conclusion was based on observations that the P_f of oocytes co-expressing the DrAqp1ab1-S261A or -S261D mutants with seabream YwhazLa was only partially stimulated by FSK exposure (figure S15G), and co-immunoprecipitation experiments showed that these mutated channels were no longer able to interact with YwhazLa (figure S15H). These data therefore confirmed the presence of two PKA

mechanisms regulating DrAqp1ab1 trafficking, one dependent on the phosphorylation status of Ser^{261} for YwhazLa binding, and another independent of YwhazLa interaction and controlled by Ser^{263} phosphorylation. In contrast, similar experiments using the seabream SaAqp1ab1 showed that in this case only one mechanism based on PKA phosphorylation of Ser^{253} and YwhazLa interaction regulates channel trafficking, since both Ala and Asp mutations of this site prevented YwhazLa binding and completely abolished the positive effect of FSK on the oocyte P_f (figure S15I and J). Similarly, the trafficking of salmonid SsaAqp1ab1 is only regulated by PKA Ser^{258} phosphorylation-dependent interaction with YwhazLa (figure S17B), which indicates that even though salmonids retain only one Aqp1ab paralog (SsaAqp1ab1) as do cyprinids such as the zebrafish (DrAqp1ab1), the salmonid Aqp1ab1s have lost the second PKA regulatory mechanism for channel trafficking that is independent of YwhazLa interaction. Interestingly, however, we also found that when seabream SaAqp1ab1 Ser^{254} and salmonid SsaAqp1ab1 Ser^{252}-Ser^{253} are phosphorylated by the activator of the p38 MAPK pathway anisomycin, plasma membrane targeting of the channel is inhibited (figure S15I and S17C). Co-immunopreciptation shows that the trafficking inhibition of SaAqp1ab1 by p38 MAPK-mediated phosphorylation of Ser^{254} is caused by preventing the YwhazLa interaction (figure S15J). Altogether, these observations suggest that the Aqp1ab1 paralog from euteleosts (euacanthomorphs and salmonids) have retained the PKA-mediated mechanism dependent on the YwhazLa interaction to trigger channel trafficking to the plasma membrane, and have acquired an additional recycling mechanism controlled by p38 MAPK-mediated phosphorylation of residues in the YWHA binding region, which prevents the YwhazLa interaction and consequently Aqp1ab1 plasma membrane trafficking.

To investigate the role of YwhazLa and -zLb proteins in the regulation of teleost Aqp1ab2, we initially selected the channel from the most basal lineage of elopomorph teleosts (AaAqp1ab2), in which only the Aqp1ab2 paralog from the TSA1C is retained, and the ortholog from a modern euacanthomorph (SaAqp1ab2), in which the complete TSA1C is expressed (figure S16). The results showed that the P_f of *X. laevis* oocytes expressing AaAqp1ab2 with or without seabream YwhazLa or -zLb co-expression was equally stimulated by PMA, whereas the positive effect on channel trafficking to the plasma membrane and oocyte permeability elicited by FSK treatment was the highest when AaAqp1ab2 was co-expressed with YwhazLa (figure S16A and C). In addition,

immunoprecipitation experiments indicated that FSK, but not PMA, induced AaAqp1ab2-YwhazLa interaction (figure S16E), as observed for the Aqp1ab1 paralogs. By contrast, an increase in plasma membrane targeting of SaAqp1ab2 and oocyte P_f was only observed in the presence of seabream YwhazLb and after FSK stimulation (figure S16B and D), which also triggered the YwhazLb interaction (figure S16F). A strong increment of P_f was also observed in oocytes expressing the Aqp1ab2 channel from other euacanthomorphs (HhAqp1ab2 and SseAqp1ab2) together with halibut YwhazLb, and subsequently treated with FSK, although in the case of sole, which has lost the Aqp1ab1 paralog, FSK also induced a slight increase of the permeability of oocytes expressing the Aqp1ab2 paralog alone or when co-expressed with the YwhazLa (figure S17D).

The subsequent mutagenesis trials revealed that C-terminal Ser^{241} in AaAqp1ab2 and Thr^{262} in SaAqp1ab2, both of which reside within the predicted YWHA interaction motifs, are the important residues for the PKA-mediated YwhazLa and -zLb interaction, respectively (figure S16G-J). In HhAqp1ab2 and SseAqp1ab2 these respective sites are Ser^{241}-Ser^{242} and Ser^{242} (figure S17E and F). In the AaAqp1ab2 C-terminus, we also identified Ser^{255} as a site for PKC phosphorylation, which drives channel trafficking to the plasma membrane independently of YwhazL regulation (figure S16G and H). This mechanism, however, appears to depend on the PKC-mediated phosphorylation status of Thr^{148} in loop D, since the absence of phosphorylation of this residue seems to cause channel retention in the cytoplasm regardless of whether the C-terminal Ser^{255} is phosphorylated (figure S10K). In SseAqp1ab2, we also confirmed Thr^{233} outside of the predicted YWHA interacting region as an additional PKA phosphorylation site for positive plasma membrane targeting (figure S17F). Interestingly, however, SseAqp1ab2 trafficking mediated by phosphorylation of this site still depends on the YwhazLb interaction, since when Ser^{242} in the YWHA binding site is mutated into an Ala, FSK treatment can no longer insert the channel into the plasma membrane (figure S17F).

To finally confirm that teleost Aqp1ab1 and -1ab2 trafficking is specifically regulated by the YwhazL carrier proteins we tested whether Ywhaqb, which is highly expressed in the halibut ovarian follicle transcriptome, could mimic the effects of YwhazL on channel transport. The results showed that the P_f of oocytes expressing SaAqp1ab1 alone or co-expressed with seabream Ywhaqb, and further stimulated with FSK or PMA, did not differ significantly, while water permeability of oocytes expressing SaAqp1ab2

plus seabream Ywhaqb was not induced after FSK treatment (figure S18). These data therefore suggest that teleost Aqp1ab1 and -1ab2 channels selectively interact with teleost-specific YwhazLa and -zLb proteins to regulate channel trafficking.

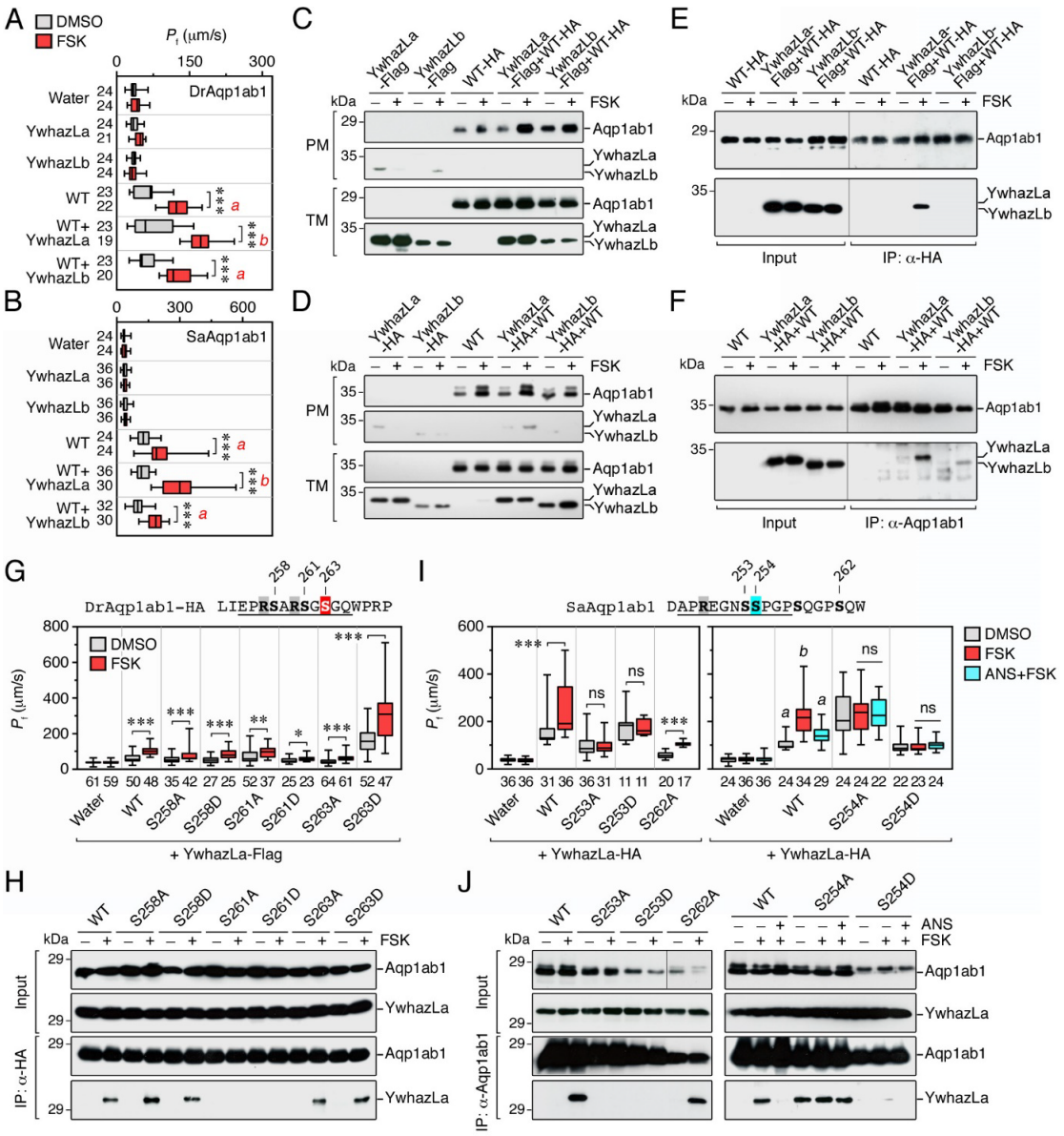

Figure S15. Binding of teleost Aqp1ab1 to YwhazLa increases channel trafficking in *X. laevis* oocytes. (**A**, **B**) P_f of *X. laevis* oocytes injected with water or expressing HA-tagged wild-type (WT) DrAqp1ab1 (A) or SaAqp1ab1 (B), with or without co-injection of seabream HA- or Flag-tagged YwhazLa or -zLb, and treated with DMSO or IBMX/FSK. (**C**, **D**) Immunoblots of total (TM) and plasma (PM) membrane protein extracts from oocytes

expressing WT DrAqp1ab1-HA (C) or SaAqp1ab1 (D), together with Flag- or HA-tagged YwhazLa or -zLb (as indicated), and treated or not with IBMX/FSK. (**E**, **F**) Co-immunoprecipitation of Aqp1ab1 and YwhazLa or -zLb in oocytes treated as in C and D. The immunoprecipitated products (IP) using an anti-HA or anti-SaAqp1ab1 specific antibodies (in E and F, respectively) were immunoblotted with appropriate antibodies (as indicated). (**G**, **I**) Partial amino acid sequences of WT DrAqp1ab1 (G) and SaAqp1ab1 (I) C-termini showing the predicted YWHA binding regions underlined with the Arg residue shaded in grey, and the PKA and p38 MAPK phosphorylation sites shaded in red or blue, respectively. Below each sequence is shown the P_f of oocytes injected with water or expressing WT DrAqp1ab1-HA (G) or WT SaAqp1ab1 (I), or mutant channels at specific residues potentially involved in YwhazLa binding (indicated on each sequence), and treated with IBMX/FSK alone or in the presence of anisomycin (ANS). Control and aquaporin expressing oocytes were also co-injected with YwhazLa-Flag or -HA. (**H**, **J**) Co-immunoprecipitation of WT and mutant Aqp1ab1 channels and YwhazLa or -zLb in oocytes treated as in G and I. In A, B, G and I, data are presented as box and whisker plots with the number of oocytes in each group indicated on the left or below of each plot. Data were analyzed by the unpaired Student's *t*-test (*, $P < 0.05$; **, $P < 0.01$; ***, $P < 0.001$; as indicated in brackets). In A and B, letters indicate significant differences in one-way ANOVA ($P < 0.05$). ns, statistically not significant.

6.1.14. Supplementary Figure S16

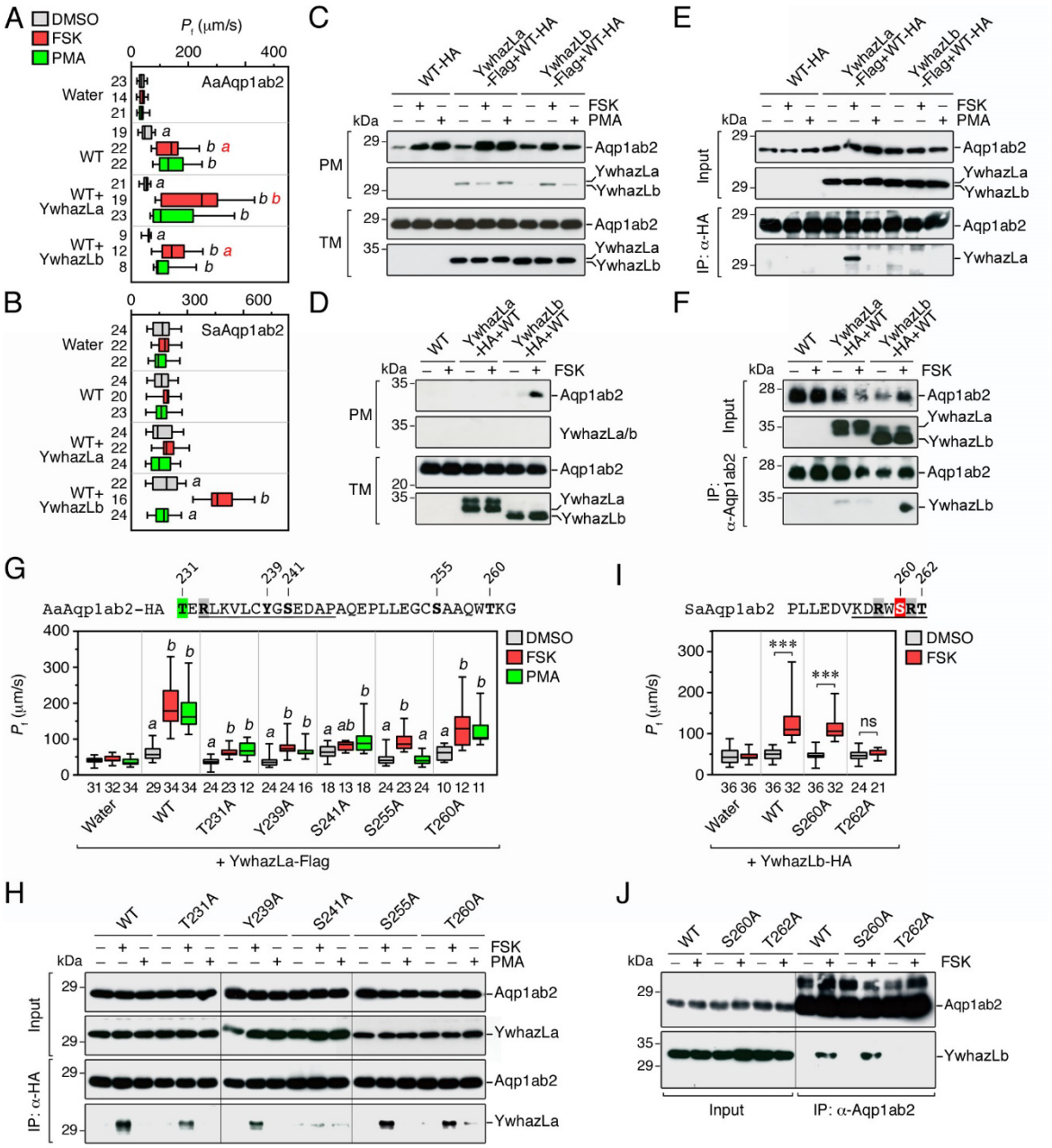

Figure S16. Binding of Aqp1ab2 to YwhazLa or -zLb differentially increases channel trafficking in ancient and modern lineages of teleosts, respectively, in *X. laevis* oocytes. (**A**, **B**) P_f of *X. laevis* oocytes injected with water or expressing HA-tagged wild-type (WT) AaAqp1ab2 (A) or SaAqp1ab2 (B), with or without co-injection of seabream HA- or Flag-tagged YwhazLa or -zLb, and treated with DMSO, IBMX/FSK or PMA. (**C**, **D**) Immunoblot of protein extracts of total (TM) and plasma (PM) membrane from oocytes expressing WT AaAqp1ab2-HA (C) or SaAqp1ab2 (D), together with Flag- or HA-tagged (as indicated) YwhazLa or -zLb, and treated or not with IBMX/FSK or PMA. (**E**, **F**) Co-immunoprecipitation of Aqp1ab2 and YwhazLa or -zLb in oocytes treated as in C and D. The immunoprecipitated products (IP) using an anti-HA or anti-SaAqp1ab2 specific antibodies (in E and F, respectively) were immunoblotted with appropriate antibodies (as indicated). (**G**, **I**) Partial amino acid sequences of WT AaAqp1ab2 (G) and SaAqp1ab2 (I) C-termini showing the putative YwhazLa or -zLb binding regions underlined with the Arg residue shaded in grey, and the PKA and PKC phosphorylation sites shaded in red or green, respectively. Below each sequence is shown the P_f of oocytes expressing WT AaAqp1ab2-HA (G) or WT SaAqp1ab2 (I), or mutant channels at specific residues potentially involved in YwhazL binding (indicated on each sequence), and treated with IBMX/FSK or PMA. Control

and aquaporin expressing oocytes were also co-injected with YwhazLa-Flag (G) or YwhazLb-HA (I). (**H**, **J**) Co-immunoprecipitation of WT and mutant Aqp1ab2 channels and YwhazLa or -zLb in oocytes treated as in G and I. In A, B, G and I, data are presented as box and whisker plots with the number of oocytes in each group indicated on the left or below each plot. For each construct in A, B and G, data were analyzed by one-way ANOVA ($P < 0.05$; different letters indicate significant differences). In I, data were analyzed by the unpaired Student's *t*-test (***, $P < 0.001$; as indicated in brackets). ns, statistically not significant.

6.1.15. Supplementary Figure S17

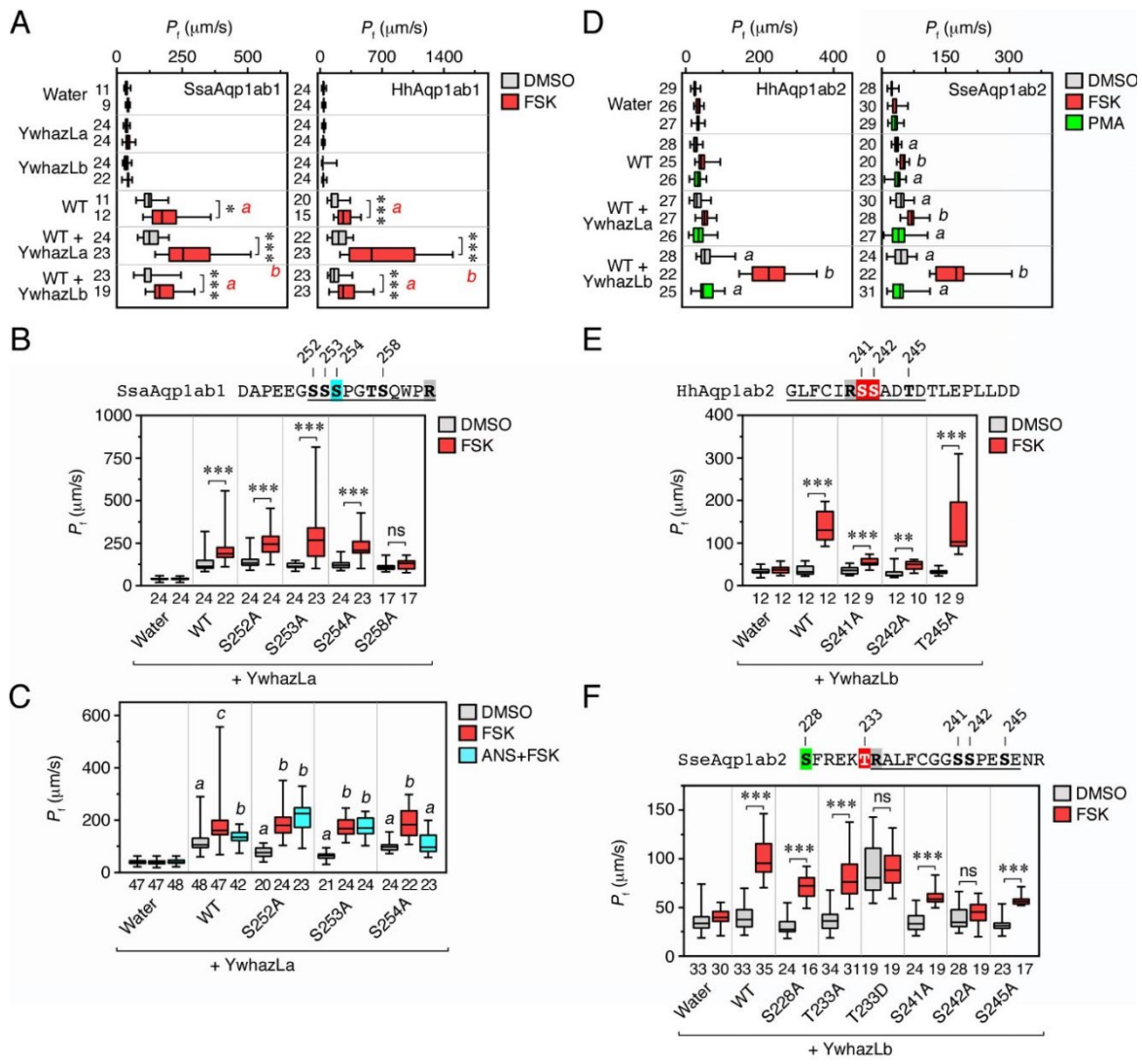

Figure S17. YwhazLa and -zLb regulate Aqp1ab1 and -1ab2 trafficking in distantly related teleosts. (**A**) P_f of *X. laevis* oocytes injected with water or expressing wild-type (WT) SsaAqp1ab1 or HhAqp1ab1, with or without co-injection of seabream YwhazLa or -zLb, or Atlantic halibut YwhazLa or -zLb, respectively, and treated with DMSO or IBMX/FSK. (**B**, **C**) Partial amino acid sequence of SsaAqp1ab1 C-terminus showing the predicted YWHA binding region underlined with the Arg residue shaded in grey, and the predicted p38 MAPK phosphorylationsite shaded in blue. Below the sequence is the P_f of oocytes injected with water or expressing SsaAqp1ab1-WT, or channels mutated at specific residues (indicated on the sequence), and treated with IBMX/FSK alone (B) or in the presence of anisomycin (ANS) (C). Control and aquaporin expressing oocytes were also co-injected with seabream YwhazLa. (**D**) P_f of oocytes injected with water or expressing wild-type WT HhAqp1ab2 or SseAqp1ab2, with or without co-injection of halibut YwhazLa or -zLb, and treated with DMSO, IBMX/FSK or PMA. (**E**, **F**) Partial C-terminal amino acid sequence of HhAqp1ab2 (E) and SseAqp1ab2 (F) showing the predicted YWHA binding regions underlined with the Arg residue shaded in grey, and the predicted PKA and PKC phosphorylation sites shaded in red and green, respectively. Below each sequence is the P_f of oocytes injected with water or expressing HhAqp1ab2-WT or SseAqp1ab2-WT, or channels mutated at specific residues (indicated on each sequence), and treated with DMSO or IBMX/FSK. Control and aquaporin expressing oocytes were also co-injected with halibut YwhazLb. Data are presented as box and whisker plots with the number of oocytes in each group indicated on the left or below of each plot. Data, except in C, were analyzed by the unpaired Student's *t*-test (*, $P < 0.05$; **, $P < 0.01$; ***, $P < 0.001$; as indicated in brackets), whereas in C letters indicate significant differences in one-way ANOVA ($P < 0.05$). ns, statistically not significant.

6.1.16. Supplementary Figure S18

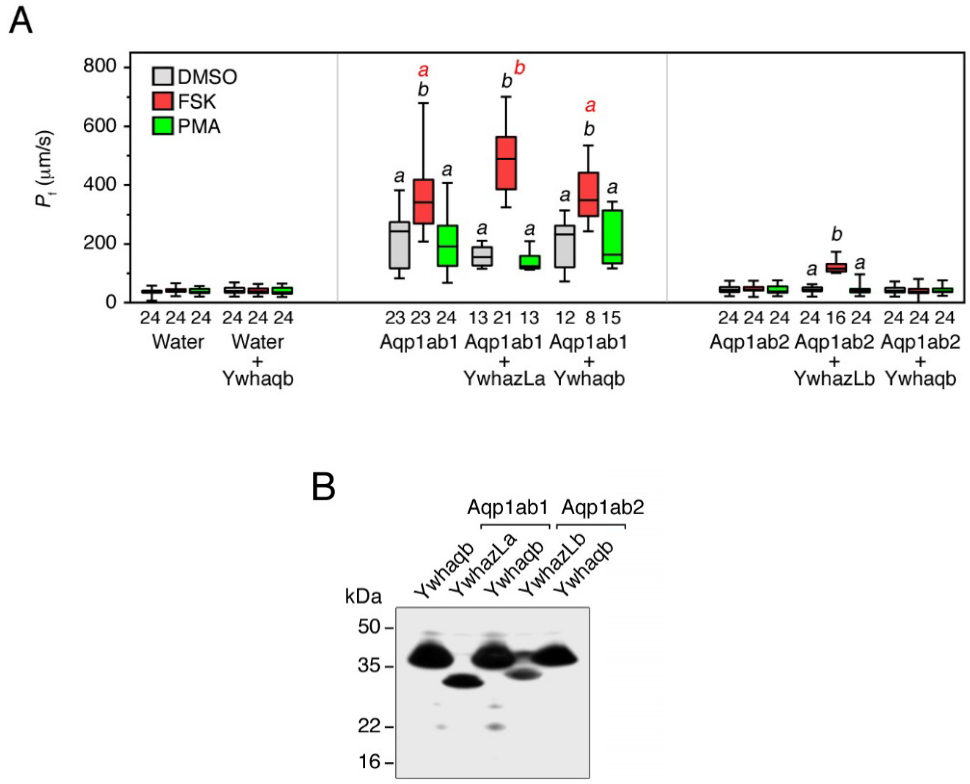

Figure S18. The teleost-specific Ywhaqb does not regulate seabream Aqp1ab1 or -1ab2 trafficking. (**A**) P_f of *X. laevis* oocytes injected with water of expressing SaAqp1ab1 or -1ab2, with or without co-injection of seabream HA-tagged YwhazLa, -zLb or -qb, and treated with DMSO, IBMX/FSK or PMA. Data are presented as box and whisker plots with the number of oocytes in each group indicated below the plot. For each construct, letters on top of the boxes indicate significant differences in one-way ANOVA ($P < 0.05$). Letters in red indicate statistical differences among groups treated with FSK (one-way ANOVA; $P < 0.05$). (**B**) Immunoblot of oocytes injected with HA-tagged Ywha proteins, with or without Aqp1ab1 or -1ab2 coexpression, confirming that YwhazLa, -zLb and -qb are translated. Molecular mass markers are on the left.

6.1.17. Supplementary Figure S19

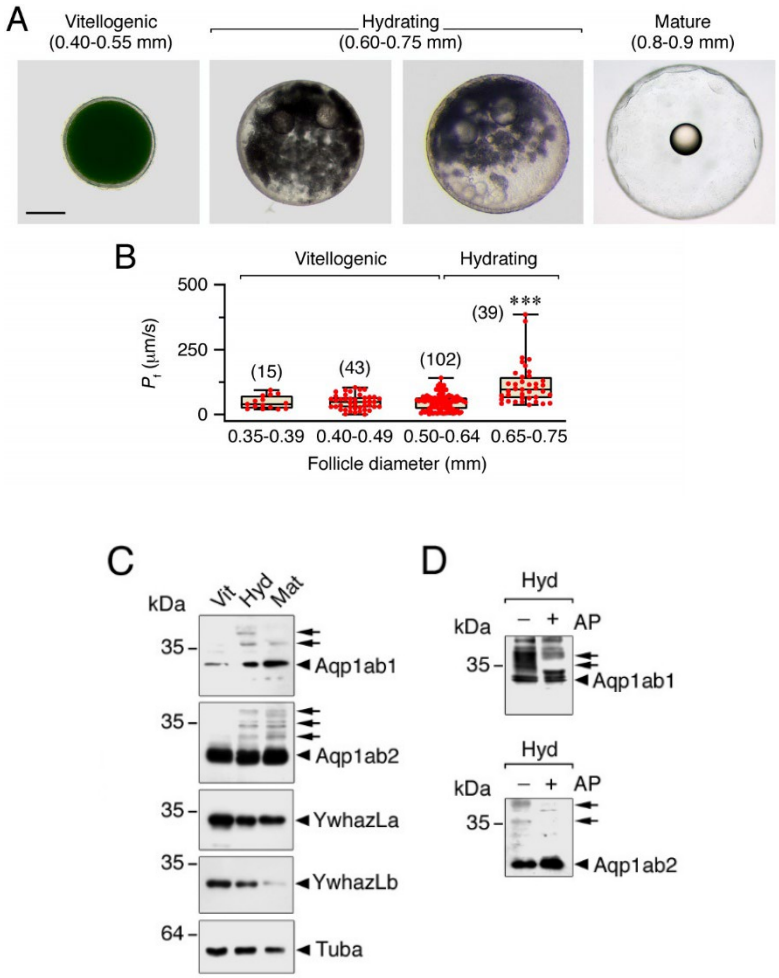

Figure S19. Ovarian follicle water permeability and phosphorylation of Aqp1a1 and -1ab2 channels increase during oocyte hydration in vivo. (**A**) Photomicrographs of isolated seabream ovarian follicles undergoing meiosis resumption and hydration *in vivo*. Scale bar, 250 µm. (**B**) P_f of vitellogenic and hydrating follicles collected *in vivo*. (**C**) Immunoblot of Aqp1ab1 and -1ab2 channels, YwhazLa and -zLb, and α-tubulin (Tuba) as loading control, during seabream oocyte hydration. (**D**) Dephosphorylation of Aqp1ab1 and -1ab2 in follicles at the hydration stage by alkaline phosphatase (AP) treatment prior to immunoblotting. In both C and D, phosphorylated forms of the channels are indicated by arrows, whereas aquaporin and YwhazL monomers are indicated by arrowheads. Molecular mass markers (kDa) are on the left.

As previously reported (Fabra *et al*., 2006), seabream ovarian follicles undergoing meiotic maturation and hydration swell by a factor of ~4, which coincides with fusion of yolk globules, a progressive ‘‘clearing’’ of the oocyte cytoplasm (figure S21A), and the differential hydrolysis of vitellogenin-derived yolk proteins. This latter proteolysis liberates free amino acids to generate an inward osmotic gradient at the same time that Aqp1ab1 is inserted into the oocyte plasma membrane (Fabra *et al*., 2005 and 2006). As a

result, the water permeability of hydrating follicles increases by ~3-fold with respect to that of vitellogenic follicles (figure S21B; Fabra *et al*., 2006), leading to a ~30% increment in water content in the final mature oocyte (Fabra *et al*., 2006).

Immunoblotting confirmed that Aqp1ab1, -1ab2, YwhazLa and -zLb monomer proteins were expressed in ovarian follicles from vitellogenesis to maturation (figure S21C). However, increased phosphorylation of Aqp1ab1 and -1ab2 was observed in follicles enclosing hydrating oocytes, while no post-translational modifications were noted in YwhazLa or -zLb (figure S21C and D).

6.1.18. Supplementary Figure S20

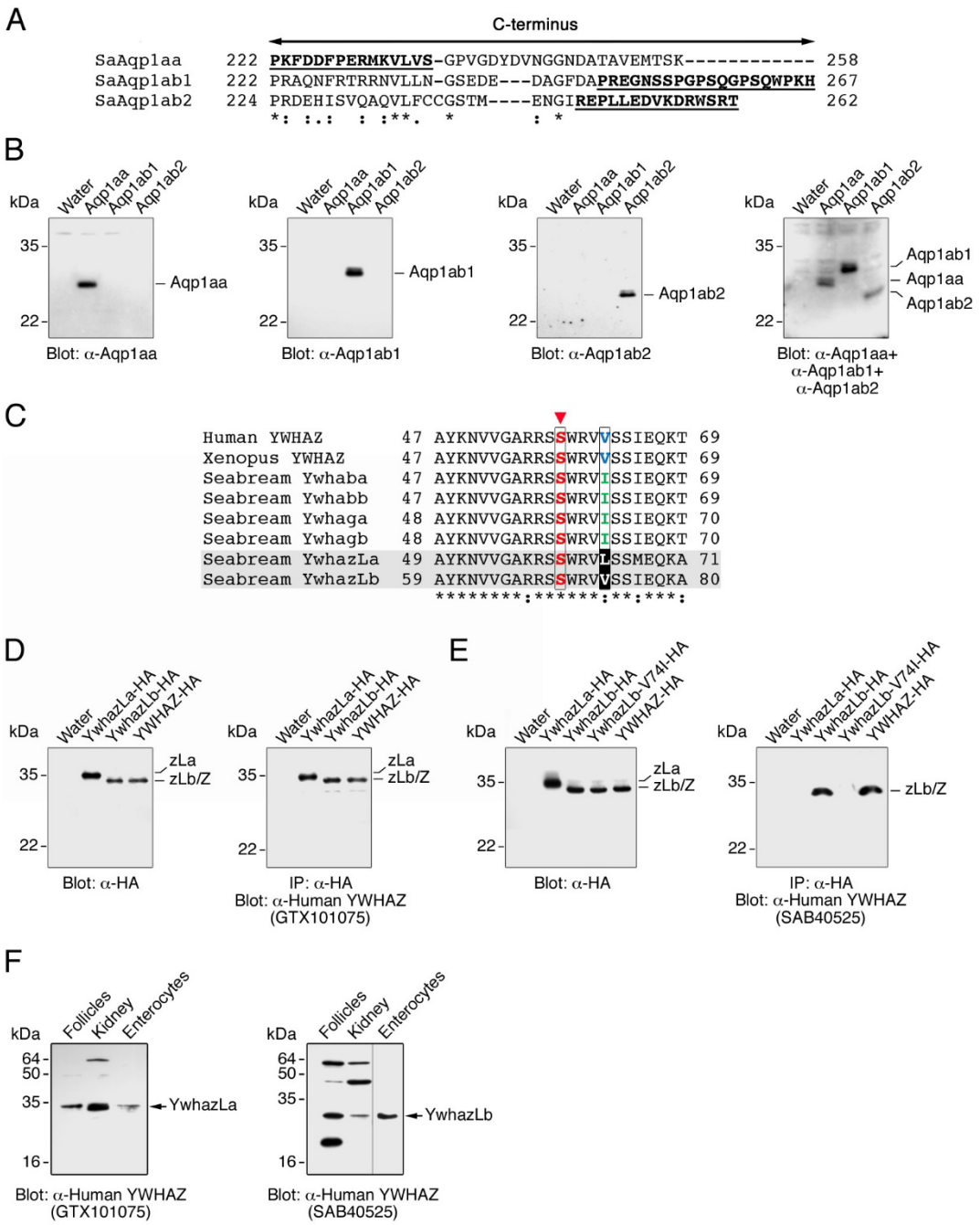

Figure S20. Validation of seabream Aqp1aa, -1ab1 and -1ab2 specific antisera and YWHAZ commercial antibodies. (**A**) Amino acid sequence alignment of the seabream Aqp1aa, -1ab1 and -1ab2 C-termini showing the sequences (underlined) used to raise paralog-specific antibodies in rabbits. (**B**) Immunoblots of *X. laevis* oocytes injected with water or expressing Aqp1aa, -1ab1 or -1ab2 and probed with custom made paralog-specific antibodies separately or with the three antibodies combined, demonstrating that none of the three antisera showed cross-reactivity with another aquaporin. (**C**) Alignment of the region from human YWHAZ around the non-phosphorylation site of Ser^{58} employed for immunization to raise the SAB40525 antibody (Signalway Antibody LLC) with the orthologous regions from *X. laevis* YWHAZ and seabream Ywhaba, -bb, -ga, -gb, -zLa and -zLb. The Ser^{58} of human YWHAZ is indicated by a red arrowhead, whereas amino acid substitutions in the residue at position +4 from Ser^{58} are boxed. The GTX101075 antibody (GeneTex) was raised against a recombinant protein encompassing a sequence within the center region of human YWHAZ, which is not publicly available. (**D**) Immunoblots of *X. laevis* oocytes injected with water or expressing HA-tagged seabream YwhazLa, YwhazLb or *X. laevis* YWHAZ using an anti-HA antibody (left panel), or

after immunoprecipitation with the HA antibody and probed with the GTX101075 antibody (right panel). (**E**) Immunoblots of oocytes injected with water or HA-tagged seabream YwhazLa, YwhazLb, YwhazLb-V74I mutant or *X. laevis* YWHAZ and probed with the HA antibody (left panel), or immunoprecipitated with the same antibody and subsequently exposed to the SAB40525 antibody (right panel). The data shows that the GTX101075 antibody can recognize both seabream YwhazLa and YwhazLb, whereas the SAB40525 antibody cross-reacts specifically with the seabream YwhazLb. The specificity of the SAB40525 antibody towards the seabream YwhazLb is conferred by a Val residue at position +4 from Ser^{58} in this protein, as in human and *X. laevis* YWHAZ, as demonstrated with the YwhazLb-V74I mutant, which is no longer recognized by this antibody. (**F**) Immunoblot of YwhazLa and -zLb in protein extracts from seabream ovarian follicles, kidney and enterocytes using the GTX101075 and SAB40525 commercial antibodies as indicated. The YwhazLa/b and -zLb antibodies detect immunoreactive bands of approximately the same molecular mass as the seabream YwhazLa and -zLb predicted monomers (28.4 and 28 kDa, respectively) in all samples. Additional secondary bands of higher or lower molecular masses than the predicted monomers are also revealed, particularly with the YwhazLb antibody, which could correspond to dimerization products and/or complex posttranslational modifications. The lack of detection of the YwhazLb protein in the samples using the YwhazLa/b antibody may be caused by a higher specificity of this antibody for seabream YwhazLa than for YwhazLb, or by a lower relative amount of the latter protein in the samples analyzed. In B, D and F, molecular mass markers (kDa) are on the left.

6.1.19. Supplementary Figure S21

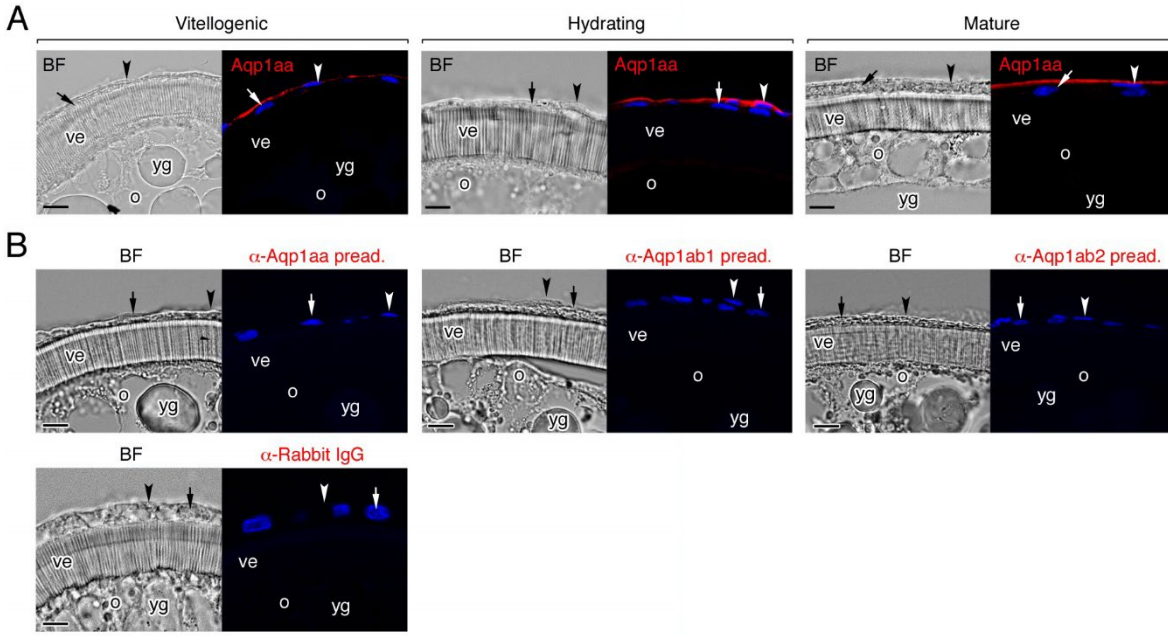

Figure S21. Immunolocalization of Aqp1aa in seabream ovarian follicles and control sections for Aqp1ab1 and -1ab2 immunostaining. (**A**) Representative bright field (BF, left) and immunostaining (right) images showing Aqp1aa reaction (red) exclusively in the external epithelium of ovarian follicles at different developmental stage. (**B**) Control sections from seabream ovary incubated with Aqp1aa, -1ab1 or -1ab2 antisera preabsorbed with the immunizing peptides, or probed only with the anti-rabbit secondary antibody, are negative, indicating the specificity of the antibodies. In all panels, the cell nuclei were counterstained with DAPI (blue). The arrows indicate the granulosa cells, whereas the arrowheads indicate the theca cells. Scale bars, 10 µm.

6.1.20. Supplementary Figure S22

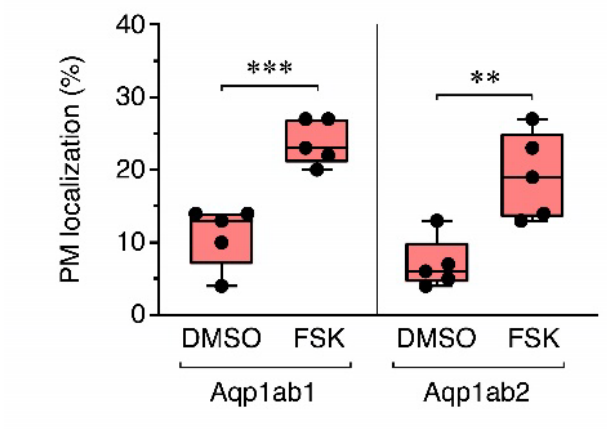

Figure S22. Quantitative estimation of the amount of Aqp1ab1 and -1ab2 in the plasma membrane of oocytes after IBMX/FSK treatment. Data are presented as box and whisker plots with the number of follicles indicated by dots, and were analyzed by an unpaired Student's *t*-test (**, $P < 0.01$; ***; $P < 0.001$, as indicated in brackets).

6.1.21. Supplementary Table S1

https://drive.google.com/file/d/19B2wove8svFFp55C94bt8FIlAyAgQPAy/view?usp=share_link

6.1.22. Supplementary Table S2

Table S2. De novo assembly of the Atlantic halibut and *X. laevis* transcriptomes.

	Atlantic halibut	***Xenopus laevis***
# Contigs	179,617	345,439
Assembly length	129,380,318 bp	184,370,001 bp
N25	3260 bp	1614 bp
N50	1145 bp	613 bp
N75	442 bp	345 bp
Min length	200 bp	200 bp
Max length	22,125 bp	14,281 bp
Mean length	720.31 bp	533.73 bp

6.1.23. Supplementary Table S3

Table S3. Antibodies used in this study.

				Working dilution[a]		
Antibody	**Host species**	**Origin/Vendor**	**Ref. no.**	**IB**	**IF**	**IP[b]**
Seabream Aqp1aa	Rabbit	Custom made [(1)]	-	1:1000	1:500	
Seabream Aqp1ab1	Rabbit	Custom made, this study[c]	-	1:1000	1:500	0.2
Seabream Aqp1ab2	Chicken	Custom made, this study[c]	-	1:1000	1:500	0.5
Halibut Aqp1ab2	Rabbit	Custom made [(2)]	-	1:1000	1:500	-
Bovine PDI	Rabbit	Merck	P7496	1:2000	1:500	-
Chicken Na^+/K^+-ATPase	Mouse	DSHB	A5	-	1:1000	-
Human LAMP-1	Mouse	DSHB	H4A3	-	1:250	-
Human YWHAZ	Rabbit	Signalway Antibody	SAB40525	1:1000	1:400	-
Human YWHAZ	Rabbit	GeneTex	GTX101075	1:1000	1:400	-
α-Tubulin	mouse	Merck	T9026	1:25000	-	-
HA tag	Rabbit	Invitrogen	PA1-985	1:1000	1:500	0.2
HA tag	Goat	Genscript	A00168-40	1:1000	1:500	-

Flag	Rabbit	Merck	F7425	1:1000	1:500	0.2
Flag, clone M2	Mouse	Merck	F3165	1:500	1:250	-
Rabbit IgG HRP	Goat	Bio-Rad	172-1019	1:5000	-	-
Mouse IgG HRP	Goat	Bio-Rad	172-1011	1:5000	-	-
Chicken IgY HRP	Goat	Thermo-Fisher	A16054	1:5000	-	-
Goat IgG HRP	Rabbit	Merck	A8919	1:5000	-	-
Rabbit IgG Cy3	Sheep	Merck	C2306	-	1:1000	-
Rabbit IgG Alexa Fluor 488	Goat	Invitrogen	A-11008	-	1:1000	-
Mouse IgG Alexa Fluor 488	Goat	Invitrogen	A-11001	-	1:1000	-
Chicken IgY Alexa Fluor 488	Goat	Invitrogen	A-11039	-	1:1000	-
Goat IgG Alexa Fluor 488	Donkey	Invitrogen	A-11055	-	1:1000	-

[a] IB: immunoblotting; IF: immunofluorescence; IP: immunoprecipitation.

[b] Indicates µg of antibody per µl of beads.

[c] Rabbit polyclonal antisera for Aqp1ab1 and -1ab2 were raised against synthetic peptides, PREGNSSPGPSQGPSQWPKH and REPLLEDVKDRWSRT, respectively, located in the C-terminal regions of the corresponding predicted proteins (Agrisera AB, Vännäs, Sweden). The antisera were purified by affinity chromatography against the synthetic peptides, and their specificity was confirmed by ELISA and heterologous expression of the corresponding protein in *Xenopus laevis* oocytes followed by immunoblotting.

(1) Raldúa *et al*., 2008.

(2) Zapater *et al*., 2011.

6.1.24. Supplementary Table S4

Table S4. Oligonucleotide sequences used for qRT-PCR.

Species	Gene	GenBank #	Forward/Reverse (5'-3')[1]	Efficiency
Sparus aurata	*aqp1aa*	AY626939	TCCTGAACAATTTCACGAACC/CTACAGCTGTGGCGTCATTG	2.17
	aqp1ab1	AY626938	TTAACCCTGCTCGCTCTTTC/GCCTTCTCTAGGTGCGTCAA	2.14
	aqp1ab2	MW960021	GATCCTTTGGTCCTGCAGTC/CGAATGCCATTTTCCATTGT	2.23
Hippoglossus hippoglossus	*aqp1aa*	HQ185294	TCCTGAACAATTTTGAGAACCA/CGTCATCTCCACGTTTGTG	2.14
	aqp1ab1	MW960022	TCACTGGATGTGGCATCAAC/AGTTCAGCTGCACGGTTTTC	1.94
	aqp1ab2	HQ185295	TGATGATCATTGGGTATTCTGG/CTGCCGAACTCTTTGACCAT	1.99
Solea senegalensis	*aqp1aa*	MW960023	TTGGTCCAGCTTTGATCCTT/TCCCCGTTAACATCATAGTCG	2.06

	aqp1ab2	AY626941	ATCAACCCAGCTCGATCCTT/CTCTGAAGGACTCGTGACTGG	2.02
Salmo salar	*aqp1aa1*	BT046625	CCGATCCTTTGGACCTGCT/ACTGACCAGGACCCTCATGC	1.84
	aqp1ab1	MW960026	GGGCCAGCTGTAATCTACAAAC/CCAGAACATTCCTCCGCTTA	1.86
Multispecies	*rps18*	AY587263	ACTAAGAACGGCCATGCACCACCAC/GAATTGACGGAAGGGCACCACC	2.20

[1]All primers are flanking at least one intron for each gene.

6.1.25. Supplementary Text S1

Materials and Methods

Animals and Sampling

Adult seabream, Senegalese sole and European eels were obtained from the Institut de Recerca i Tecnologia Agroalimentàries (IRTA, Spain) aquaculture facilities, whereas Atlantic halibut and Atlantic salmon were maintained at the Austevoll and Matredal Aquaculture Research Stations (Institute of Marine Research, Norway), respectively. Biological samples were collected from sacrificed fish as previously described (Zapater *et al*., 2011; Chauvigné *et al*., 2013). Procedures relating to the care and use of fish and sample collection were approved by the Ethics Committee of IRTA, following the European Union Council Guidelines (86/609/EU), or in accordance with the regulations approved by the governmental Norwegian Animal Research Authority (http://www.fdu.no/fdu/).

Adult *X. laevis* were purchased from the Centre de Ressources Biologiques Xénopes (University of Rennes, France) and maintained at the AQUAB facilities of the Universitat Autònoma de Barcelona (Spain). Oocytes were collected by surgical laparotomy from anesthetized females following a procedure approved by the Ethics Committee for Animal and Human Experimentation (CEEAH) from Universitat Autònoma de Barcelona (Spain) and the Catalan Government (Direcció General de Polítiques Ambientals i Medi Natural; Project no. 10985).

Gene Walking

The 23.7-kb upstream genomic region of seabream *aqp1ab1* gene was sequenced by four rounds of overlapping PCR-based directional genome walking using the Universal GenomeWalker™ 2.0 kit (Clontech) on DNA extracted from erythrocytes following the manufacturer's instructions. The DNA was ligated into the pGEM-T Easy plasmid vector (Promega) and Sanger sequenced. The sequences were confirmed by available genome sequence data from seabream (Pauletto *et al*. 2018).

Phylogenetic, Syntenic and Structural Analyses

For the aquaporin analyses, Aqp1aa or Aqp1ab-type proteins from our previous analysis (Zapater *et al*., 2011) were used as tblastn queries of open-source whole genome shotgun (WGS), transcriptome shotgun (TSA) and nucleotide databases (NCBI, https://blast.ncbi.nlm.nih.gov), GenomeArk (https://vgp.github.io/) and Ensembl (https://www.ensembl.org). Contiguous peptides identified with the BLOSUM62 matrix and other default parameters were assembled into >1000 proteins using the alignment of Zapater *et al*., 2011, as reference. Corresponding nucleotide sequences were then retrieved from the respective databases and trimmed to match each peptide fragment and concatenated to construct a CDS for each gene or transcript as described previously (Chauvigné *et al*., 2019; Yilmaz *et al*., 2020). For the analyses of the Ywha regulatory proteins, complete repertoires of Ywha-type proteins together with their corresponding nucleotide CDS were initially retrieved from Ensembl and further sequences subsequently obtained using blastp queries (BLOSUM62 matrix and other default parameters) of either open-source protein and nucleotide databases (NCBI), or the Atlantic halibut and *X. laevis* oocyte transcriptomes (from the present study).

For phylogenetic analyses, the deduced amino acids were aligned using the L-INS-I algorithm of MAFFT v7.490 (Katoh & Toh, 2008), and converted to codon alignments using Pal2Nal (Suyama *et al*., 2006). Bayesian inference (Mr Bayes v3.2.2) (Ronquist & Huelsenbeck, 2003) with model parameters nucmodel = 4by4, nst = 2, rates = gamma was performed on each of the codon alignments following removal of gapped regions containing less than three sequences. Depending upon the number of taxa in the alignment, different iterations (1 million to 100 million) of Markov chain Monte Carlo (MCMC) algorithms were run with three heated and one cold chain with resulting posterior distributions examined for convergence and an effective sample size >200 using Tracer version 1.7 (Rambaut *et al*., 2018). Majority rule consensus trees were summarized with a burnin of 25%. All trees generated were processed with Archaeopteryx (Han and Zmasek, 2009) and rendered with Geneious v9.1.8 (Biomatters Ltd, New Zealand). Alignment files for aquaporin and Ywha codons are provided in supplementary data SD1-5 (see Annexe, page 223) and SD 6-11 (see Annexe, page 224), respectively.

In silico prediction of kinase-specific phosphorylation residues in the amino acid sequence of aquaporin paralogs was carried out using the NetPhos 3.1 Server (http://www.cbs.dtu.dk/services/NetPhos/) (Blom *et al*., 2004) and The Eukaryotic Linear

Motif resource (http://elm.eu.org/) (Gouw *et al*. 2018). Prediction of YWHA-binding sites was carried out using the 14-3-3-Pred webserver (http://www.compbio.dundee.ac.uk/1433pred/) (Madeira *et al*., 2015).

Transcriptome Shotgun Sequencing and Data Processing

Total RNA from Atlantic halibut postvitellogenic and *X. laevis* stage IV follicle-enclosed oocytes was isolated using the RNeasy Maxi Kit (Qiagen), and polyA$^+$ mRNA was further purified using the Oligotex mRNA MiniKit (Qiagen). Illumina RNA sequencing (RNA-seq) library construction (150-750 bp inserts) and HiSeq2500 sequencing were carried out at ZF-Genomics (The Netherlands). A total of ~161 and ~149 million paired-end 2 x 150 nt reads were generated for Atlantic halibut and *X. laevis* follicles, respectively, which were used in two *de novo* assemblies to generate cDNA sequences corresponding to the expressed mRNAs. The quality of the reads was evaluated with the FastQC v. 0.11.5, no quality trimming was performed prior to the assembly. Trinity v.2.3.2 was used to assemble paired-end reads with the default parameters and k-mer size of 25. Scaffolded transcriptome assembly consisted of 179,617 contigs for Atlantic halibut and 345,439 for *X. laevis* (supplementary table S2, see Annexe, page 257). Functional annotation of assembled scaffold and contigs was performed using blastx search against NCBI non-redundant (NR) collection of protein sequences and KEGG pathway annotation. KEGG orthology (KO) groups were assigned by KAAS server (Moriya *et al*., 2007; Kanehisa *et al*., 2012) using bi-directional best hit (BBH) method against a representative gene set, including genomes of *X. tropicalis* and *D. rerio*. The *X. laevis* and Atlantic halibut transcriptome shotgun assembly projects have been deposited at DDBJ/EMBL/GenBank under accession nos. GJQV00000000 and GJQU00000000, respectively (the versions described in this paper are the first versions, GJQV01000000 and GJQU01000000, respectively).

The *X, tropicalis* YWHA transcripts proteins were initially downloaded from ensembl and used as BLASPp enquires for the *X. laevis* follicle transcriptome and open source NCBI protein and TSA databases. Following Bayesian inference to identify the teleost orthologs, the obtained flatfish Ywha proteins were used as BLASTp queries of the Atlantic halibut follicle transcriptome. Reads were aligned to the identified *X. laevis* and halibut transcripts using BWA v. 0.7.17 (Li and Durbin, 2009) and quantified using HTSeq

v.0.11.0 (Anders *et al*., 2015). The expression levels are given in read counts and in reads per kilobase per million mapped reads (RPKM) (Mortazavi *et al*., 2008).

Cloning of Aquaporin-1-like Channels and YWHAZ cDNAs

Full-length cDNAs encoding Aqp1 and YwhazL paralogs from different teoleosts were isolated by RT-PCR using ovary or kidney total RNA as previously described (Zapater *et al*., 2011). Oligonucleotide primers were designed based on the Atlantic halibut ovarian follicle transcriptome sequenced in this study, the seabream gene-walking and genome sequence data (Pauletto *et al*., 2018), and genomic information available for Atlantic salmon (Lien *et al*. 2016) and Senegalese sole (Guerrero-Cózar *et al*., 2021). Full-length AaAqp1aa, SsaAqp1aa and *X. laevis* YWHAZ were cloned from cDNA sequences previously deposited in GenBank (accession nos. AJ564420, BT046625, and NM_001086648, respectively). The newly isolated cDNAs were submitted to GenBank under the following accession numbers: SaAqp1ab2 (MW960021), SaYwhazLa (OK572451), SaYwhazLb (OK572452), SaYwhaqb (OK572453), HhAqp1ab1 (MW960022), HhYwhazLa (OK572454), HhYwhazLb (OK572455), SseAqp1aa (MW960023), SseAqp1aa2 (MW960024), and SsaAqp1ab1 (MW960026).

In addition to the cloned cDNAs indicated above, the following aquaporin cDNAs previously isolated (Fabra *et al*., 2005; Tingaud-Sequeira *et al*., 2008, 2010; Zapater *et al*., 2011) were also employed (GenBank accession nos. in parenthesis): DrAqp1aa (AY626937), SaAqp1aa (AY626939), HhAqp1aa (HQ185294), DrAqp1ab1 (EU327345), SaAqp1ab1 (AY626938), AaAqp1ab2 (EF011738), HhAqp1ab2 (HQ185295) and SseAqp1ab2 (DQ889223).

6.1.26. Supplementary References

Anders S, Pyl PT, Huber W. 2015. HTSeq--a Python framework to work with high-throughput sequencing data. *Bioinformatics.* 31(2):166-9. doi: 10.1093/bioinformatics/btu638.

Blom N, Sicheritz-Pontén T, Gupta R, Gammeltoft S, Brunak S. 2004. Prediction of post-translational glycosylation and phosphorylation of proteins from the amino acid sequence. *Proteomics*. 4(6):1633-49. doi: 10.1002/pmic.200300771.

Chauvigné F, Boj M, Vilella S, Finn RN, Cerdà J. 2013. Subcellular localization of selectively permeable aquaporins in the male germ line of a marine teleost reveals spatial redistribution in activated spermatozoa. *Biol Reprod*. 89(2):37. doi: 10.1095/biolreprod.113.110783.

Chauvigné F, Yilmaz O, Ferré A, Fjelldal PG, Finn RN, Cerdà J. 2019. The vertebrate Aqp14 water channel is a neuropeptide-regulated polytransporter. *Comm Biol*. 2:462. doi: 10.1038/s42003-019-0713-y.

Fabra M, Raldúa D, Power DM, Deen PM, Cerdà J. 2005. Marine fish egg hydration is aquaporin-mediated. *Science*. 307(5709):545. doi: 10.1126/science.1106305.

Fabra M, Raldúa D, Bozzo MG, Deen PM, Lubzens E, Cerdà J. 2006. Yolk proteolysis and aquaporin-1o play essential roles to regulate fish oocyte hydration during meiosis resumption. *Dev Biol*. 295(1):250-62. doi: 10.1016/j.ydbio.2006.03.034.

Fu H, Subramanian RR, Masters SC. 2000. 14-3-3 proteins: Structure, function, and regulation. *Annu Rev Pharmacol Toxicol*. 40:617-47. doi: 10.1146/annurev.pharmtox.40.1.617.

Gouw M, Michael S, Sámano-Sánchez H, Kumar M, Zeke A, Lang B, Bely B, Chemes LB, Davey NE, Deng Z, *et al*. 2018. The eukaryotic linear motif resource - 2018 update. *Nucleic Acids Res*. 46:D428-D434.

Guerrero-Cózar I, Gomez-Garrido J, Berbel C, Martinez-Blanch JF, Alioto T, Claros MG, Gagnaire PA, Manchado M. 2021. Chromosome anchoring in Senegalese sole (*Solea*

senegalensis) reveals sex-associated markers and genome rearrangements in flatfish. *Sci Rep*. 11(1):13460. doi: 10.1038/s41598-021-92601-5.

Han, M. V. & Zmasek, C. M. 2009. phyloXML: XML for evolutionary biology and comparative genomics. *BMC Bioinformatics*. 10:356. doi: 10.1186/1471-2105-10-356.

Kanehisa M., Goto S., Sato Y., Furumichi M., Tanabe M. 2012. KEGG for integration and interpretation of large-scale molecular datasets. *Nucleic Acids Res*. 40**:**D109-D114.

Katoh K, Toh H. 2008. Recent developments in the MAFFT multiple sequence alignment program. *Brief Bioinform*. 9(4):286-98. doi: 10.1093/bib/bbn013.

Li H, Durbin R. 2009. Fast and accurate short read alignment with Burrows-Wheeler transform. *Bioinformatics*. 25(14):1754-60. doi: 10.1093/bioinformatics/btp324.

Madeira F, Tinti M, Murugesan G, Berrett E, Stafford M, Toth R, Cole C, MacKintosh C, Barton GJ. 2015. 14-3-3-Pred: improved methods to predict 14-3-3-binding phosphopeptides. *Bioinformatics*. 31(14):2276-83. doi: 10.1093/bioinformatics/btv133.

Moeller HB, Slengerik-Hansen J, Aroankins T, Assentoft M, MacAulay N, Moestrup SK, Bhalla V, Fenton RA. 2016. Regulation of the water channel aquaporin-2 via 14-3-3q and -z. *J Biol Chem*. 291**:**2469-2484.

Moriya Y., Itoh M., Okuda S., Yoshizawa A., Kanehisa M. 2007. KAAS: an automatic genome annotation and pathway reconstruction server. *Nucleic Acids Res*. 35:W182-5. doi: 10.1093/nar/gkm321.

Mortazavi A, Williams BA, McCue K, Schaeffer L, Wold B. 2008. Mapping and quantifying mammalian transcriptomes by RNA-Seq. *Nat Methods*. 5(7):621-8. doi: 10.1038/nmeth.1226.

Nesverova V, Törnroth-Horsefield S. 2019. Phosphorylation-dependent regulation of mammalian aquaporins. *Cells*. 8(2):82. doi: 10.3390/cells8020082.

Pauletto M, Manousaki T, Ferraresso S, Babbucci M, Tsakogiannis A, Louro B, Vitulo N, Quoc VH, Carraro R, Bertotto D, *et al*. 2018. Genomic analysis of *Sparus aurata*

reveals the evolutionary dynamics of sex-biased genes in a sequential hermaphrodite fish. *Commun Biol*. 1:119. doi: 10.1038/s42003-018-0122-7.

Prado K, Cotelle V, Li G, Bellati J, Tang N, Tournaire-Roux C, Martinière A, Santoni V, Maurel C. 2019. Oscillating aquaporin phosphorylation and 14-3-3 proteins mediate the circadian regulation of leaf hydraulics. *Plant Cell*. 31(2):417-429. doi: 10.1105/tpc.18.00804.

Rajan S, Preisig-Müller R, Wischmeyer E, Nehring R, Hanley PJ, Renigunta V, Musset B, Schlichthörl G, Derst C, Karschin A, Daut J. 2002. Interaction with 14-3-3 proteins promotes functional expression of the potassium channels TASK-1 and TASK-3. *J Physiol*. 545(1):13-26. doi: 10.1113/jphysiol.2002.027052.

Raldúa D, Otero D, Fabra M, Cerdà J. 2008. Differential localization and regulation of two aquaporin-1 homologs in the intestinal epithelia of the marine teleost *Sparus aurata*. *Am J Physiol Regul Integr Comp Physiol*. 294(3):R993-1003. doi: 10.1152/ajpregu.00695.2007.

Rambaut A, Drummond AJ, Xie D, Baele G, Suchard MA. 2018. Posterior summarization in Bayesian phylogenetics using Tracer 1.7. *Syst Biol*. 67(5):901-904. doi: 10.1093/sysbio/syy032.

Ronquist F, Huelsenbeck JP. 2003. MrBayes 3: Bayesian phylogenetic inference under mixed models. *Bioinformatics*. 19(12):1572-4. doi: 10.1093/bioinformatics/btg180.

Shikano S, Coblitz B, Sun H, Li M. 2005. Genetic isolation of transport signals directing cell surface expression. *Nat Cell Biol*. 7(10):985-92. doi: 10.1038/ncb1297.

Suyama M, Torrents D, Bork P. 2006. PAL2NAL: robust conversion of protein sequence alignments into the corresponding codon alignments. *Nucleic Acids Res*. 34:W609-12. doi: 10.1093/nar/gkl315.

Tingaud-Sequeira A, Calusinska M, Finn RN, Chauvigné F, Lozano J, Cerdà J. 2010. The zebrafish genome encodes the largest vertebrate repertoire of functional aquaporins with dual paralogy and substrate specificities similar to mammals. *BMC Evol Biol*. 10:38. doi: 10.1186/1471-2148-10-38.

Tingaud-Sequeira A, Chauvigné F, Fabra M, Lozano J, Raldúa D, Cerdà J. 2008. Structural and functional divergence of two fish aquaporin-1 water channels following teleost-specific gene duplication. *BMC Evol Biol*. 8:259. doi: 10.1186/1471-2148-8-259.

Yilmaz O, Chauvigné F, Ferré A, Nilsen F, Fjelldal PG, Cerdà J, Finn RN. 2020. Unravelling the complex duplication history of deuterostome glycerol transporters. *Cells*. 9(7):1663. doi: 10.3390/cells9071663.

Zapater C, Chauvigné F, Norberg B, Finn RN, Cerdà J. 2011. Dual neofunctionalization of a rapidly evolving aquaporin-1 paralog resulted in constrained and relaxed traits controlling channel function during meiosis resumption in teleosts. *Mol Biol Evol*. 28(11):3151-69. doi: 10.1093/molbev/msr146.

6.2. Supplementary Material Chapter II

6.2.1. Supplementary Table S1

Table S1. Primers used to amplify the seabream mRNAs encoding Avp, Oxt and corresponding receptors.

Transcript	GenBank accession no.	Direction	Primer sequence (5' to 3')	Purpose
pro-avp	FR851924	Forward	TGAACATCATCCCTGTTCCA	RT-PCR
		Reverse	ACTTTTGCAAAGCCGTCATC	
		Forward	TGAACATCATCCCTGTTCCA	ISH probe
		Reverse	TTTTGGCAGCGATTCAGTCT	
pro-oxt	FR851925	Forward	ATGACCAAAGCAGCCAATTC	RT-PCR
		Reverse	GGCATCAGATGATGACAAACA	
		Forward	CTGCTGACGCAATGGGACTA	ISH probe
		Reverse	TCAAAACTTTATTTCAACATGCAG	
avpr1aa	KC195974	Forward	ACTATGCGCTTGTCCTGAGC	Cloning of Full-length cDNA and RT-PCR
		Reverse	TGTGTACCTTGATGCCAGACA	
		Forward	TCACCTTCTCCAGGATTTCG	
		Forward	AGAAGGAGGACTCAGACAGCA	ISH probe
		Reverse	TGTGTACCTTGATGCCAGACA	
avpr2aa	KC960488	Forward	AAAGGACACGCGTGAGAAAG	Cloning of Full-length cDNA and RT-PCR
		Reverse	CCGTGCATGTCTTTTCAAAC	
		Forward	CCAAGGAGTAGCCTTCACCA	
		Forward	ACGGCTTCAAGAAGGAGGAC	ISH probe
		Reverse	GGAGAGGGGGTGCGTAGT	
oxtrb	KC195973	Forward	GACCCGGACTCTTGTGTTGT	Cloning of Full-length cDNA and RT-PCR
		Reverse	GGGATTGCCAGGTTACTCAA	
		Forward	ATCCTGGCTCTGACTGCAAG	

		Forward	GTACCTGACAGCCTCCACCT	ISH probe
		Reverse	TTGGGATTGCCAGGTTACTC	
rps18	AY587263	Forward	ACTAAGAACGGCCATGCACCACCAC	RT-PCR
		Reverse	GAATTGACGGAAGGGCACCACC	

6.2.2. Supplementary Figure S1

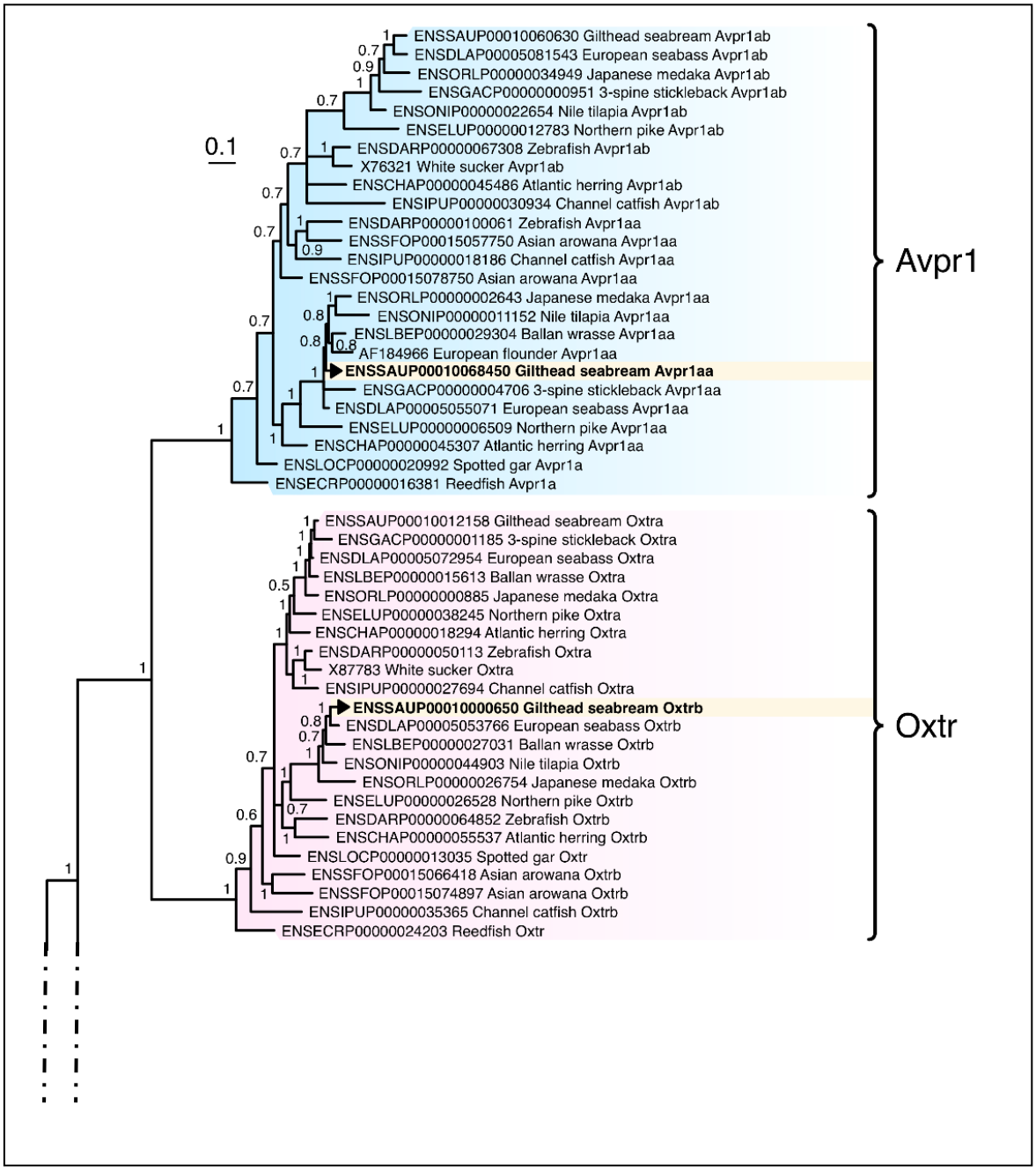

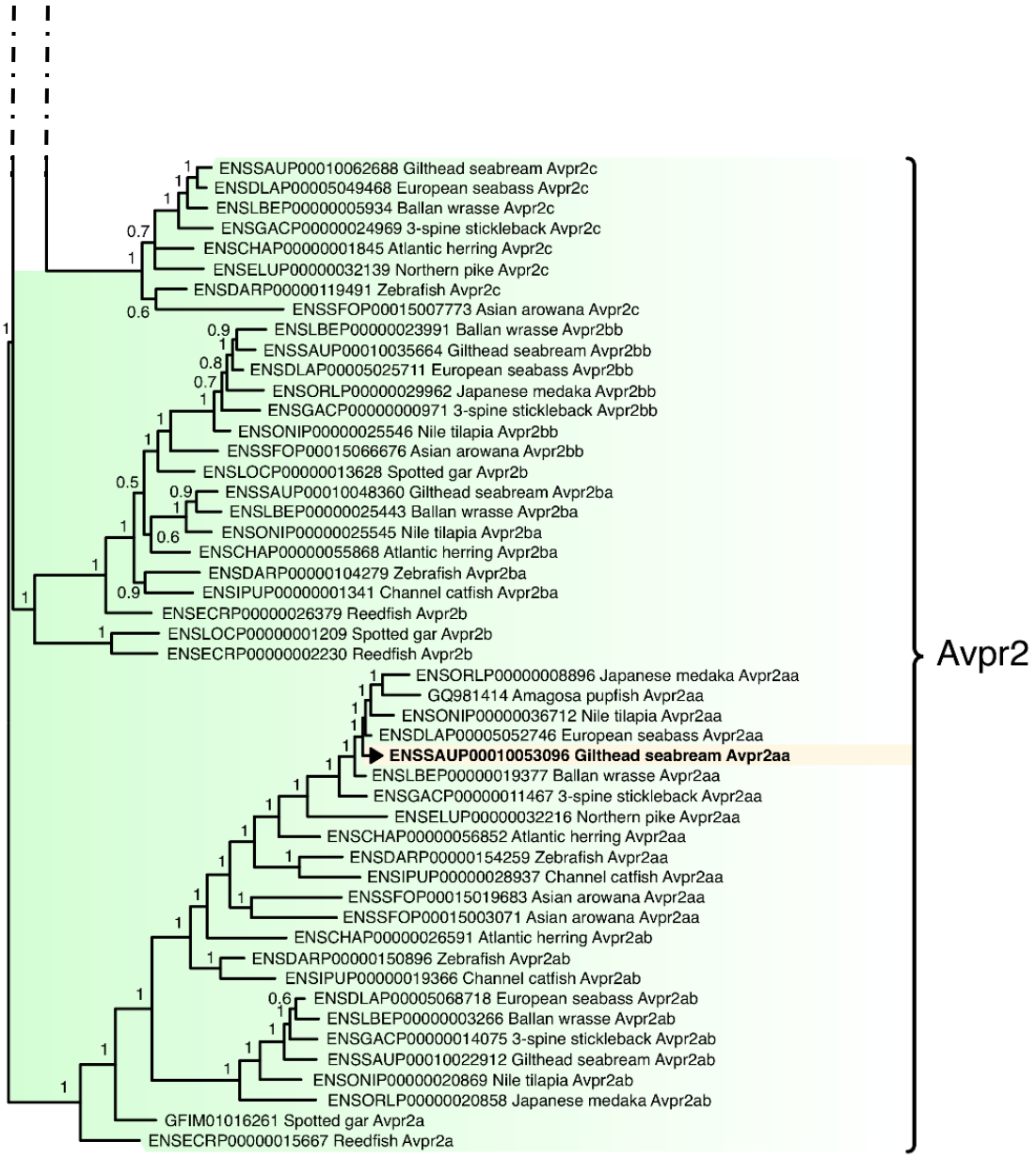

Figure S1. Molecular phylogeny of piscine vasopressinergic and oxytocinergic receptors. Bayesian majority rule midpoint rooted consensus tree inferred from 2 million MCMC generations (aamodel = mixed4; burnin = 25%) of a ClustalX amino acid alignment of 97 receptors downloaded from Ensembl (v109). Bayesian posterior probabilities are shown at each node with the scale bar indicating the expected rate of amino acid substitution per site. The seabream paralogs used for functional experiments in the present study are highlighted (orange) with arrows in bold. The tree topology matches that computed by maximum likelihood (Daza *et al*., 2022) with the exception that the zebrafish Avpr2ba and Avpr2bb receptors are named in accordance with the Ensembl (v109) nomenclature. Daza DO, Bergqvist CA, Larhammar D. 2022. The evolution of oxytocin and vasotocin receptor genes in jawed vertebrates: A clear case for gene duplications through ancestral whole-genome duplications. Front Endocrinol 12: 792644.

6.2.3. Supplementary Figure S2

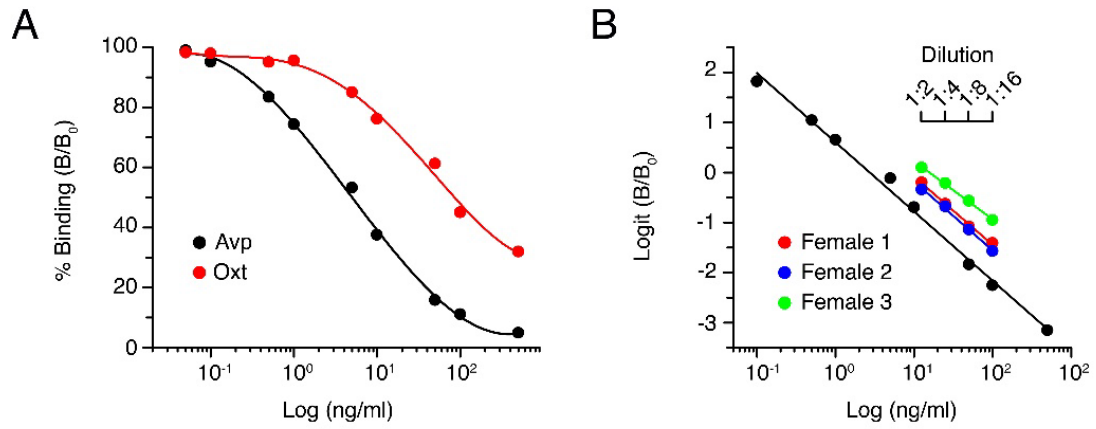

Figure S2. Development of an ELISA for Avp. (**A**) Competitive binding curves for arginine vasopressin (Avp) standard, and cross-reactivity with serial dilutions of oxytocin (Oxt), using the anti-Avp antiserum. Data are the mean of 3 replicates. The optimal concentration for coating the wells with Avp was 50 ng/ml using a 1:15000 dilution of the antibody, whereas the Avp used to generate the standard curves ranged from 10 pg to 500 ng/ml. The sensitivity of the assay was 10 pg/ml (B/B0 > 95%) with the optical density decreasing as a linear function of Avp concentration (r^2 =0.9945). The intra- and inter-assay coefficient of variation was 4.64% and 8.35%, respectively. The evaluation of the cross-reactivity of the assay with Oxt showed that the displacement of the B/B0 dilution curve obtained with Avp was only seen when using high doses of Oxt (>10 ng/ml), the cross-reaction being 8.4%. (**B**) Parallelism between the standard curve of ELISA using Avp and displacement curves obtained with serial dilutions of the ovary from three different females. Each point is the mean of two replicates. The slope obtained for Avp (slope ± SEM) was of −0.588 ± 0.025 , and not significantly different from that obtained for ovarian samples from 3 different females (-0.566 ± 0.029).

6.2.4. Supplementary Figure S3

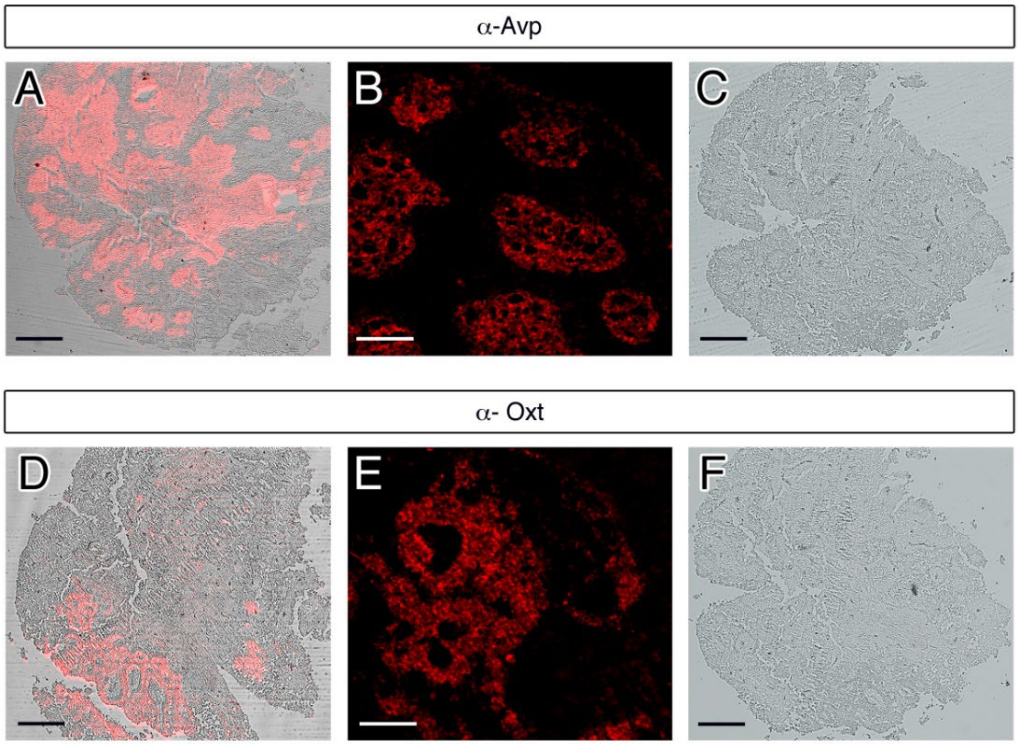

Figure S3. Immunolocalization of Avp and Oxt in the seabream pituitary gland. (**A-E**) Immunostaining of Avp (A-C) and Oxt (D-F) in paraffin sections of the posterior pituitary (neurohypophysis). In A and C and D and F, the epifluorescence image (red color) is merged with the brightfield image. (**C-F**) Control sections incubated with preabsorbed antisera. Scale bars, 200 µm (A, D, C and F); 50 µm (B and E).

6.2.5. Supplementary Figure S4

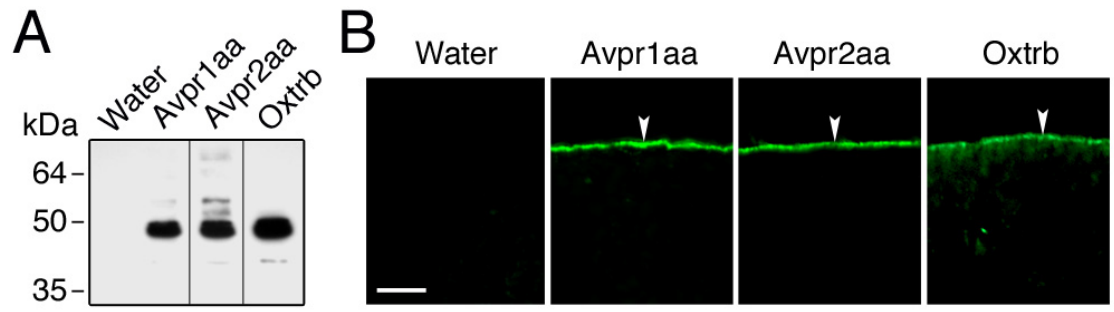

Figure S4. Expression of seabream Avp and Oxt receptors in *X. laevis* oocytes. (**A**) Immunoblots of total membranes of oocytes injected with water or expressing HA-tagged Avpr1aa, Avpr2aa or Oxtrb. Molecular mass markers (kilodaltons) are on the left. (**B**) Immunofluoresence microscopy of water-injected and Avpr1aa-, Avpr2aa- or Oxtrb-expressing oocytes. The arrowhead points the oocyte plasma membrane. Scale bar, 50 µm.

6.2.6. Supplementary Figure S5

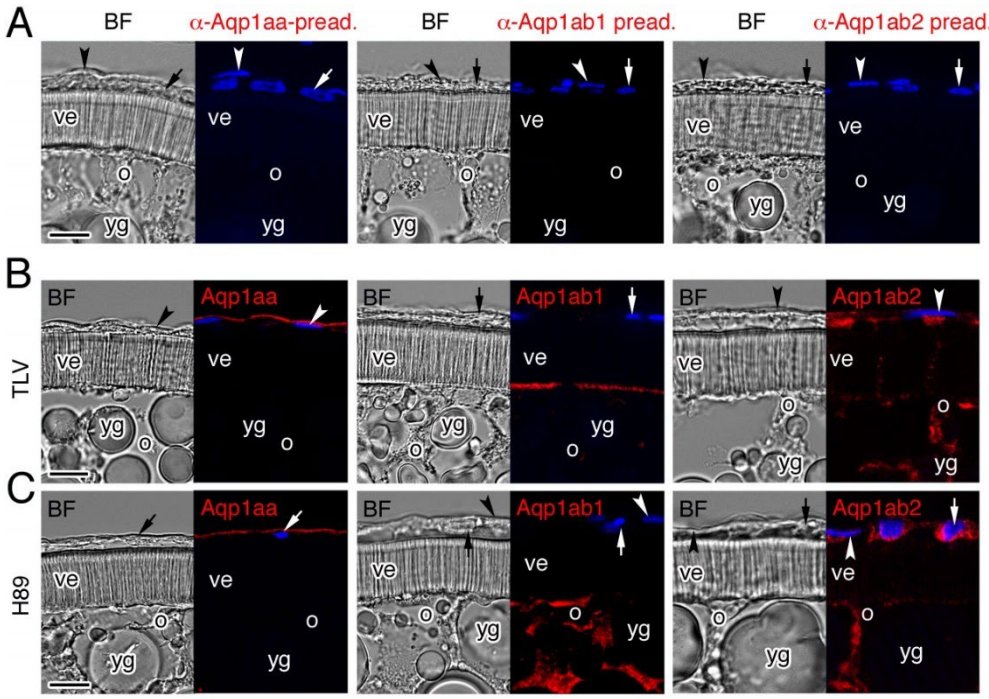

Figure S5. Immunostaining of the TSA1C channels in the seabream ovarian follicle. (**A**) Control paraffin sections incubated with preabsorbed antisera specific for Aqp1aa, Aqp1ab1 and Aqp1ab2. (**B-C**) Representative immunostaining of Aqp1aa, Aqp1ab1 and Aqp1ab2 (red color) in follicles exposed only to 10 µM of the Avpr2aa antagonist tolvaptan (TLV) or the PKA inhibitor H89. In all panels, brightfield (BF) and epifluprescence images are shown on the left and right, respectively, and nuclei were counterstained with DAPI (blue). The theca and granulosa cells are indicated by arrows and arrowheads, respectively. ve, vitelline envelope; o, oocyte; yg, yolk globules. Scale bars, 10 µm.

6.3. Supplementary Material Chapter III

6.3.1. Supplementary Table S1

Table S1. Oligonucleotide primers employed for the RT-PCR screening of splice forms expression of *aqp1ab*-type genes in teleosts.

Species	Gene	GenBank accession	Forward (F) / Reverse (R)	Amplicon (bp)
Sparus aurata	*aqp1ab1*	AY626938	F: CTGGCTATTGGGCTGTCAGT R: AGCCATATTGAAAGCTTTTC TGC	375
	aqp1ab2	MW960021	F: TTTGGCGTAGAATTCCTGCT R: CGAATGGCCATTTTCCATTG T	356
Hippoglossus hippoglossus	*aqp1ab1*	MW960022	F: CGAGTCATGTCAAGGGCTTT R: GCCGACAGCCAGAAAAGTT A	380
	aqp1ab2	HQ185295	F: GCCATTGAATTCCTGCTCAC R: TTCACATCCTCAACGTCGTC	383
Solea senegalensis / Solea solea	*aqp1ab2*	AY626941	F: CGCAGTCACTGACAAACGAC R: CTCTGAAGGACTCGTGACTG G	254

6.3.2. Supplementary Figures S1

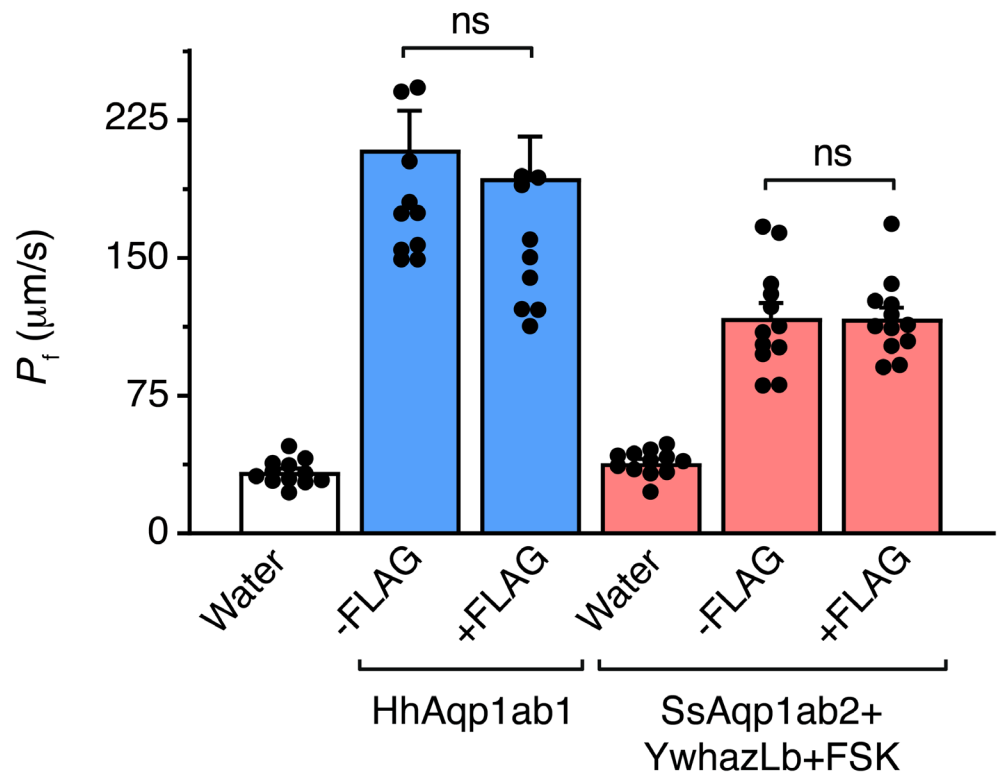

Figure S1. Tagging HhAqp1ab1 and SsAqp1ab2 constructs do not affect channel function. P_f of *X. laevis* oocytes injected with water (W, controls), or expressing non-tagged or Flag-tagged Atlantic halibut HhAqp1ab1-WT or sole SsAqp1ab2-WT. Oocytes injected with SsAqp1ab2-WT were co-injected with non-tagged halibut YwhazLb and exposed to FSK. The data are the mean ± SEM (n = 12 oocytes per treatment, indicated with dots above each bar).

6.3.3. Supplementary Figures S2

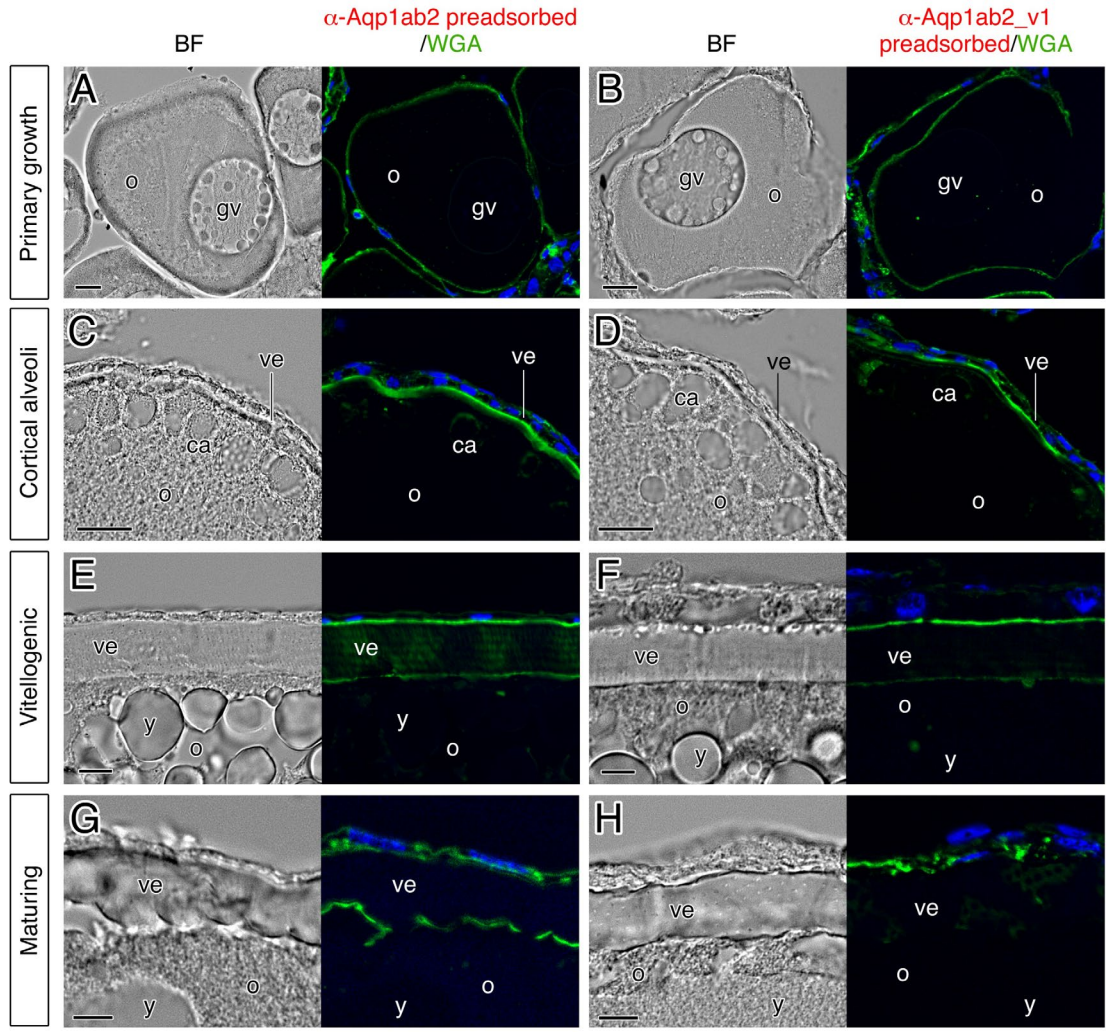

Figure S2. Immunostaining controls of Senegalese sole ovarian follicles at different developmental stage. Histological sections were incubated with Aqp1ab2-Nt and Aqp1ab2_v1 antisera preabsorbed with the immunizing peptides, indicating the specificity of the antibodies. Abbreviations: o, oocyte; y, yolk globule; gv, germinal vesicle; ve, vitelline envelope; cp, capillary; ca, cortical alveoli. Scale bars, 10 µm.